

**SCHOOL OF  
CIVIL ENGINEERING**

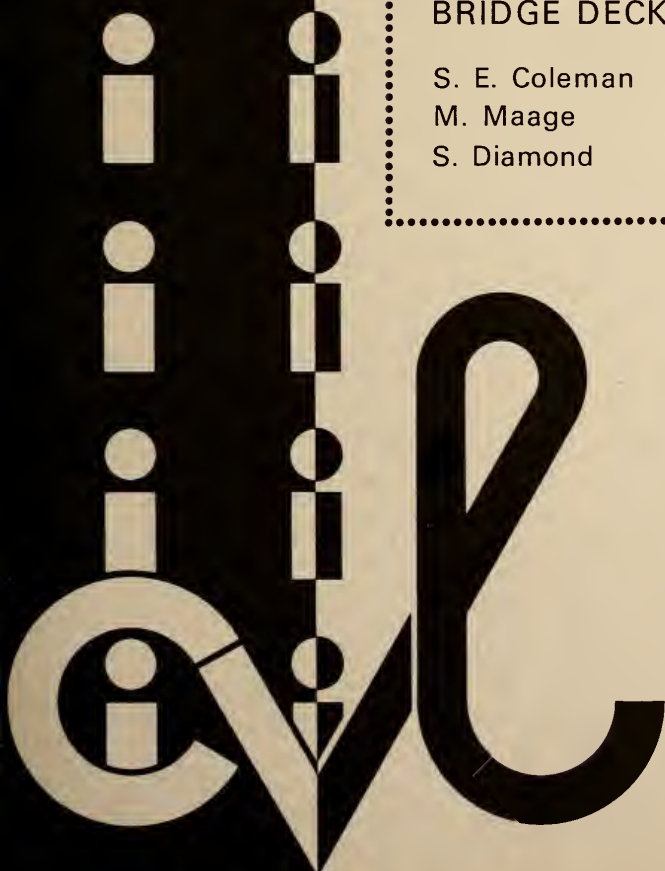
**INDIANA**

**DEPARTMENT OF HIGHWAYS**

JOINT HIGHWAY  
RESEARCH PROJECT  
FHWA/IN/JHRP-82/2

LOW POROSITY HIGH STRENGTH  
CONCRETE FOR HIGHWAY  
BRIDGE DECKS

S. E. Coleman  
M. Maage  
S. Diamond



**PURDUE UNIVERSITY**



## Final Report

## LOW POROSITY HIGH STRENGTH CONCRETE FOR HIGHWAY BRIDGE DECKS

TO: H. L. Michael, Director  
Joint Highway Research Project

February 2, 1982  
Revised August 1982  
Project: C-36-61H

FROM: Sidney Diamond, Research Associate  
Joint Highway Research Project

File: 5-14-8

Attached is the Final Report on the HPR Part II Study titled "Low Porosity High Strength Concrete for Highway Bridge Decks". The Report authors are S. E. Coleman, M. Maage and Sidney Diamond, each a researcher for the Joint Highway Research Project.

The project findings indicate clearly that characteristics of the low porosity concrete resulted in excellent freezing resistance, reduced drying shrinkage, reduced carbonation and a tight pore structure. The resistance to penetration of chloride was good. Equally important passivation appeared to be maintained even in the presence of large chloride concentrations.

The findings appear promising and should lend at least to consideration of use in an experimental bridge deck.

It has been a pleasure to conduct this research.

Sincerely,



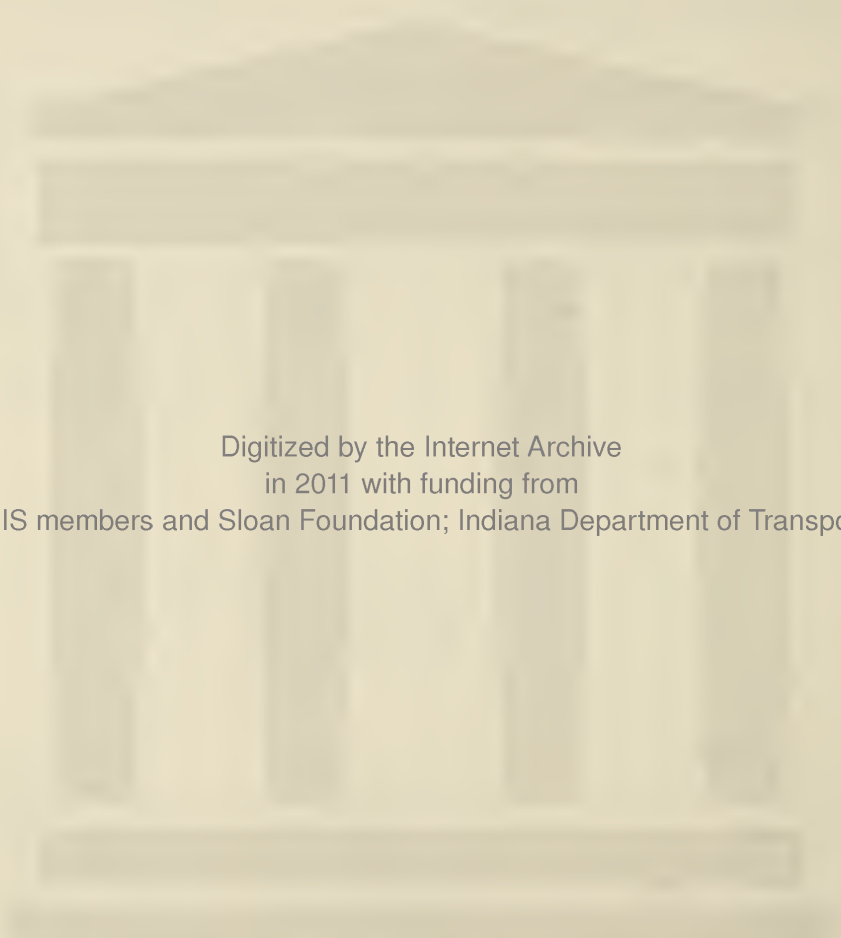
Sidney Diamond  
Research Associate

SD:ms

cc: A. G. Altschaeffl  
J. M. Bell  
W. L. Dolch  
R. L. Eskew  
J. D. Fricker  
G. D. Gibson  
W. H. Goetz

M. J. Gutzwiller  
G. K. Hallock  
J. F. McLaughlin  
R. D. Miles  
P. L. Owens  
B. K. Partridge  
G. T. Satterly

C. F. Scholer  
R. M. Shanteau  
K. C. Sinha  
C. A. Venable  
L. E. Wood  
E. J. Yoder  
S. R. Yoder



Digitized by the Internet Archive  
in 2011 with funding from  
LYRASIS members and Sloan Foundation; Indiana Department of Transportation



Final Report  
LOW POROSITY HIGH STRENGTH CONCRETE FOR HIGHWAY BRIDGE DECKS

by

S. E. Coleman, Graduate Instructor in Research  
M. Maage, Visiting Research Associate  
and  
S. Diamond, Research Associate

Joint Highway Research Project

Project No.: C-36-61H

File No.: 5-14-8

Prepared as Part of an Investigation

Conducted by

Joint Highway Research Project  
Engineering Experiment Station  
Purdue University

in cooperation with the

Indiana Department of Highways  
and the

U.S. Department of Transportation  
Federal Highway Administration

The contents of this report reflect the views of the authors who are responsible for the facts and the accuracy of the data presented herein. The contents do not necessarily reflect the official views or policies of the Federal Highway Administration. This report does not constitute a standard, specification, or regulation.

Purdue University  
West Lafayette, Indiana  
February 2, 1982  
Revised August 1982



1. Report No. FHWA/IN/JHRP-82/2		2. Government Accession No.		3. Recipient's Catalog No.	
4. Title and Subtitle LOW POROSITY HIGH STRENGTH CONCRETE FOR HIGHWAY BRIDGE DECKS		5. Report Date February 2, 1982 Revised August 1982		6. Performing Organization Code	
7. Author(s) S. E. Coleman, M. Maage, and S. Diamond		8. Performing Organization Report No. JHRP-82-2		10. Work Unit No.	
9. Performing Organization Name and Address Joint Highway Research Project Civil Engineering Building Purdue University West Lafayette, IN 47907		11. Contract or Grant No. HPR-1(19) Part II		13. Type of Report and Period Covered Final Report	
12. Sponsoring Agency Name and Address Indiana Department of Highways State Office Building 100 North Senate Avenue Indianapolis, IN 46204		14. Sponsoring Agency Code		15. Supplementary Notes Prepared in cooperation with the U. S. Department of Transportation, Federal Highway Administration as part of project titled "Low Porosity High Strength Concrete for Highway Bridge Decks".	
16. Abstract Premature failure of concrete bridge decks stemming from chloride-induced corrosion of reinforcing steel constitutes a major problem. This study relates to the possibility of substituting "low porosity" concrete (made with gypsum-free portland cement) for conventional concrete on bridge decks. Relevant properties of certain experimental low-porosity concretes, formulated with and without flyash, were determined experimentally and compared with the corresponding properties of conventional bridge deck concrete formulations and also with those of Iowa-type dense concrete mixtures. Conventional concrete was shown to be deficient in terms of long-term resistance to the penetration of chloride ions, and in terms of maintaining steel passivation once the chloride had penetrated. Measured characteristics of the dense concretes were generally superior to the conventional bridge deck mixes, but grossly inferior to the low porosity concretes. Low porosity concretes could be formulated to produce flowing concrete of good workability at w:c 0.28. Strengths developed were in the range 10,000-13,000 psi, and these concretes showed excellent freezing resistance, reduced drying shrinkage, reduced carbonation, and a tight pore structure. The resistance to penetration of chloride was good. Equally important, because of the high inherent alkalinity of the concrete pore solutions of low porosity concrete, passivation appeared to be maintained throughout the monitoring period, even in the presence of large chloride concentrations. Low porosity concrete showed the brittle behavior expected of any high strength concrete, but this should be no practical problem in view of the ductility provided by the considerable percentage of steel in most bridge deck designs.					
17. Key Words concrete, bridge decks, steel corrosion, low porosity cement, low porosity concrete			18. Distribution Statement No restrictions. This document is available to the public through the National Technical Information Service, Springfield, VA 22161		
19. Security Classif. (of this report) Unclassified		20. Security Classif. (of this page) Unclassified		21. No. of Pages 306	
				22. Price	



## ACKNOWLEDGMENTS

The authors acknowledge the assistance and advice of Professors W. L. Dolch, L. E. Wood and T. R. West in the conduct of this research. They are also grateful to Mrs. Janet Lovell for her fine work in preparation of some of the laboratory specimens for various studies in this research.

The untiring efforts of Dennis Eliassen and Paul Tourney, undergraduate student assistants, in preparing concrete specimens and the diverse help provided during the course of this study is very much appreciated. The work done by the staff at the Chemistry Laboratory of the Materials and Testing Division, Indiana State Department of Highways (ISDH), Indianapolis, in analyzing some samples is very much appreciated. Special thanks to Mr. Jackson and Mr. Richardson of that organization.

Loan of certain equipment by the Research and Training Center, ISDH, West Lafayette, and suggestions provided by Mr. Barry Partridge of that organization are much appreciated.

The financial support of the Indiana Department of Highways is also gratefully acknowledged as is the advice provided by personnel of the DOH and FHWA through individual contact and the Study Advisory Committee.



## TABLE OF CONTENTS

	Page
LIST OF TABLES.....	ix
LIST OF FIGURES.....	xiii
HIGHLIGHT SUMMARY.....	xxi
 PART ONE: INTRODUCTION AND LITERATURE REVIEW	
1.1 INTRODUCTION.....	1
1.1.1 Statement of the Problem.....	1
1.1.2 Objectives of the Present Study.....	4
1.2 LITERATURE REVIEW.....	8
1.2.1 Background.....	8
1.2.2 Development of Low Porosity Cement, Paste and Concrete.....	9
1.2.3 Low Porosity Cement.....	10
1.2.4 Properties and Mechanism of Hydration in Paste and Concrete.....	10
1.2.5 Potential Uses of Low Porosity Concretes	14
1.2.6 Durability of Concrete Bridge Decks.....	15
1.2.7 Fly Ash in Concrete.....	26
 PART TWO: MATERIALS AND EXPERIMENTAL METHODS	
2.1 MATERIALS.....	30
2.1.1 Cementitious Materials.....	30
2.1.2 Aggregates.....	33
2.1.3 Admixtures.....	36
2.2 EXPERIMENTAL METHODS.....	38
2.2.1 Types of Concrete, Methods of Preparation and Fresh Concrete Properties.....	38





2.2.2 Instrumental Methods.....	43
PART THREE: PRELIMINARY STUDIES	
3.1 INTRODUCTION.....	60
3.2 WORKABILITY OF LOW POROSITY CONCRETES.....	61
3.2.1 Effect of Mixing Time on Slump and Workability.....	61
3.2.2 Proportioning of Fly Ash in Low Porosity Concrete.....	63
3.3 USE OF AN AIR ENTRAINING AGENT IN LOW POROSITY CONCRETES.....	71
3.3.1 Effect of An Air Entraining Agent in Low Porosity Concrettes Without Fly Ash..	71
3.3.2 Effects of An Air Entraining Agent in Fly Ash-Bearing Low Porosity Concrettes..	72
3.3.3 Air Content of Hardened Low Porosity Concrettes.....	76
3.3.4 Results and Discussion.....	76
3.4 HEAT EVOLUTION OF PASTES.....	82
3.5 STUDIES ON CHARACTERISTICS OF THE FLY ASH USED.....	87
3.5.1 Preparation of Calibration Chart for $\text{Ca}(\text{OH})_2$ Analysis.....	87
3.5.2 Reaction in Fly Ash-Water Paste.....	88
3.5.3 Fly Ash - $\text{CaO}$ Paste.....	88
3.5.4 Study of Pastes of Fly Ash-Bearing Low Porosity Cement.....	91
3.5.5 Study of Pastes of Fly Ash-Bearing Low Porosity Cement Without Admixtures..	95
3.5.6 Results and Discussion.....	99
3.6 STRENGTH CHARACTERISTICS OF LOW POROSITY CONCRETES.....	102
3.6.1 Materials and Mixes.....	102
3.6.2 Test for Hardened Concrete.....	104



3.6.3	Results and Discussion.....	107
PART FOUR: PROPERTIES RELATING TO THE COMPACT NATURE OF CONCRETES		
4.1	PORE SIZE DISTRIBUTION AND POROSITY OF CONCRETES.....	110
4.1.1	Introduction.....	110
4.1.2	Materials, Sampling and Testing for Pore Size Distribution Study.....	110
4.1.3	Results.....	113
4.1.4	Discussion.....	113
4.2	MEASURED SHRINKAGE CHARACTERISTICS OF THE VARIOUS CONCRETES.....	129
4.2.1	Materials, Specimens and Test.....	129
4.2.2	Results and Discussion.....	130
4.3	CHLORIDE ION PENETRATION INTO CONCRETES.....	134
4.3.1	Introduction.....	134
4.3.2	Materials, Samples and Tests.....	134
4.3.3	Results and Discussion.....	143
4.4	CARBONATION OF CONCRETES.....	148
4.4.1	Introduction.....	148
4.4.2	Materials, Samples and Tests.....	148
4.4.3	Differential Thermal Analysis of Mortar Pieces from Concrete.....	151
4.4.4	Results and Discussion.....	153
4.5	WATER PERMEABILITY OF CONCRETES.....	159
4.5.1	Materials, Samples and Test.....	159
4.5.2	Results and Discussion.....	161
4.6	MICROSTRUCTURE OF CONCRETES.....	165
4.6.1	Materials, Samples and Test.....	165
4.6.2	Results and Discussion.....	167
PART FIVE: EVALUATION OF CONCRETES FOR FREEZE-THAW DURABILITY AND DE-ICER SCALING		
5.1	INTRODUCTION.....	183



5.2	FREEZE-THAW DURABILITY.....	185
5.2.1	Materials, Mixes and Tests.....	186
5.2.2	Results and Discussion.....	189
5.3	RESISTANCE TO DE-ICER SCALING.....	216
5.3.1	Materials, Mixes and Test.....	216
5.3.2	Results and Discussion.....	218
PART SIX: CORROSION OF EMBEDDED STEEL IN CONCRETE		
6.1	INTRODUCTION.....	227
6.2	STUDY OF PORE FLUID OF FLY ASH-BEARING LOW POROSITY PASTE.....	230
6.2.1	Materials, Methods and Tests.....	230
6.2.2	Results and Discussion.....	231
6.3	VISUAL EVALUATION OF CORROSION OF STEEL EMBEDDED IN CONCRETE.....	235
6.3.1	Steel Mats Embedded in Concrete Specimens Kept Indoors.....	235
6.3.2	Steel Mats Embedded in Concrete Specimens Kept Outdoors.....	236
6.3.3	Results and Discussion.....	239
6.4	ELECTROCHEMICAL MEASUREMENTS OF ONGOING CORROSION.....	246
6.4.1	Introduction.....	246
6.4.2	Equipment, Concrete Mixes and Voltage Measurements.....	248
6.4.3	Results and Discussion.....	258



PART SEVEN: BRITTLE FAILURE BEHAVIOR OF LOW  
POROSITY CONCRETE

7.1	INTRODUCTION.....	268
7.2	CONCRETES.....	270
7.3	INSTRUMENTATION AND TESTING PROCEDURE.....	270
7.4	RESULTS.....	272
7.4.1	Compressive Strength Levels.....	272
7.4.2	Strain at Maximum Load.....	272
7.4.3	Young's Modulus.....	272
7.4.4	Brittle Behavior.....	278
7.4.5	Relationship Between Strength and Brittleness.....	280
7.5	DISCUSSION.....	280
7.6	REFERENCES.....	282

PART EIGHT: COST COMPARISONS

8.1	INTRODUCTION.....	283
8.2	COST ESTIMATES.....	285
8.3	EVALUATION OF COST COMPARISONS.....	291

PART NINE: TECHNICAL FINDINGS, CONCLUSIONS,  
AND RECOMMENDATION

9.1	TECHNICAL FINDINGS.....	293
9.2	CONCLUSIONS.....	297
9.3	RECOMMENDATION AND PROPOSED FIELD TRIAL.....	299
	BIBLIOGRAPHY.....	301
	APPENDIX.....	309





## LIST OF TABLES

<u>Table</u>		<u>Page</u>
2.1.1	Analysis of Cements Used.....	31
2.1.2	Chemical Analysis of Fly Ash by Energy Dispersive X-Ray Analysis.....	34
2.1.3	Sieve Analysis of Fine Aggregates.....	35
3.2.1	Trial Mixes with Varying Proportions of Fly Ash in Low Porosity Concrete.....	64
3.2.2	Workability of Plastic Fly Ash-Bearing Low Porosity Concretes with Time as Measured by Slump and Vebe Time.....	65
3.3.1	Amount of Entrained Air vs. Dosage of Air Entraining Agent in a Low Porosity Concrete Without Fly Ash.....	73
3.3.2	Comparison of Air Content Determination in Fresh and Hardened Concrete.....	77
3.5.1	Estimation of $\text{Ca(OH)}_2$ Contents in Various Fly Ash-Bearing Paste Using DTA.....	90
3.6.1	Mix Proportions of Low Porosity Concretes for Strength Test.....	103
3.6.2	Compressive Strength of Low Porosity Concretes.....	105
4.1.1	Mix Proportions of Concretes Used for Pore Size Distribution, Porosity, Ingress of Chloride Ions and Shrinkage Studies.....	112



<u>Table</u>		<u>Page</u>
4.1.2	Measured Specific Surface Areas and Densities of Mortars from Various Concretes.....	123
4.1.3	Measured Porosities of Mortars from Various Concretes, in Per Cent by Volume.....	125
4.3.1	Average Chloride Content (% by weight) of Concrete Ponded with 3% NaCl Solution.....	138
4.3.2	Mix Proportions Used in the Second Chloride Ion Penetration Study.....	140
4.3.3	Average Chloride Content (% by weight) of Concrete in Outdoor Exposed Concretes Ponded for 12 Months Using 4% CaCl <sub>2</sub> Solution.....	144
4.4.1	Mix Proportion of Concretes Used in the Initial Carbonation Test.....	150
4.4.2	Second Mix Proportions of Concretes Used in the Carbonation Test Series.....	152
4.5.1	Concrete Mix Proportions Used in Permeability Studies.....	160
4.5.2	Measured Permeability of Different Types of Concretes.....	163
4.6.1	Concretes Used in SEM Study to Study Structure of Mortar Matrix.....	166
5.2.1	Mix Proportions of Different Types of Concretes Used for Freeze- Thaw Studies.....	187
5.2.2A-E	Average Dynamic Modulus and Relative Dynamic Modulus at Different Freeze- Thaw Cycles Using the Resonance Frequency Method.....	190



<u>Table</u>		<u>Page</u>
5.2.3A-E	Average Weight and Relative Weight at Different Freeze-Thaw Cycles.....	196
5.2.4	Dynamic Modulus and Relative Dynamic Modulus at Different Cycles - Using the Pulse Velocity Method.....	201
5.3.1	Mix Proportions of Different Types of Concretes Used for De-Icing Scaling Resistance Study.....	217
5.3.2	Rating of Condition of Specimen Surface Per Number of Freeze- Thaw Cycles.....	219
6.2.1	Mix Proportion of Fly Ash-Bearing Low Porosity Paste Used in Pore Fluid Study.....	233
6.2.2	pH Values and Ion Concentrations in Pore Fluids of LPF Paste.....	233
6.2.3	Non-Evaporable Water in Fly Ash- Bearing Low Porosity Paste.....	234
6.3.1	Mix Proportions of Different Types of Concretes Used in Indoor Corrosion Study.....	234
6.3.2-A	Details of Rating Scheme for Recording Corrosion Extent on Individual Segments of Steel Bars as Delineated in Sketch Below.....	237
6.3.2-B	Results of Visual Estimation of Corrosion on Steel Bars Embedded in Different Types of Concretes After 12 Months Ponding with 3% NaCl Solution.....	238



<u>Table</u>		<u>Page</u>
6.3.3	Physical Condition of Concrete Specimens and the Corrosion of Steel Mats in the Different Types of Concretes Pondered for 12 Months in Outdoor Condition.....	241
6.4.1	Mix Proportions of Different Types of Concretes Used in Outdoor Corrosion Study.....	251
6.4.2A-B	Average Weekly Voltage Readings of Embedded Steel Mats in Different Concretes.....	254
6.4.3	Voltage Readings With Respect to $\text{Cu/CuSO}_4$ Half Cell of Steel Mats Embedded in Different Concretes.....	259
7.2.1	Mix Proportions of Concrete.....	271
7.4.1	Measured Properties of the Concrete Specimens.....	277
8.2.1	Cost Calculations for Conventional BD Concrete.....	286
8.2.2	Cost Calculations for Flyash-Bearing Low Porosity Concrete (LPF).....	288
8.2.3	Cost Calculations Low Porosity Concrete Without Flyash (LPN).....	290





## LIST OF FIGURES

<u>Figure</u>		<u>Page</u>
2.2.1	Permeability Test Assembly (Schematic).....	53
2.2.2	Permeability Apparatus.....	54
3.2.1	Effect of Initial Mixing Time on Initial Slump.....	62
3.2.2	Changes in Vebe Time on Standing for Mixes with Various Percentages of Fly Ash.....	70
3.3.1	Effect of Type of Mixer on Entrained Air at Several Dosages of Vinsol Resin.....	75
3.4.1	Temperature Evolution Curve of LP Cement Paste and OPC Paste.....	83
3.5.1	Calibration Curve for $\text{Ca(OH)}_2$ Analysis by DTA.....	89
3.5.2	Reduction of $\text{Ca(OH)}_2$ with Time in a Fly Ash-CaO Paste.....	92
3.5.3	SEM Micrograph of Fly Ash-CaO Paste, w:s = 0.5, at 3 Days (1500X).....	93
3.5.4	SEM Micrograph of Fly Ash-CaO Paste, w:s = 0.5, at 3 Days (10,000X).....	93
3.5.5	SEM Micrograph of Fly Ash-CaO Paste, w:s = 0.5, at 33 Weeks (1500X).....	94
3.5.6	SEM Micrograph of Fly Ash-CaO Paste. w:s = 0.50, at 33 Weeks (3000X).....	94



<u>Figure</u>		<u>Page</u>
3.5.7	SEM Micrograph of FALP Paste, w:s = 0.24, at 7 Days (150X).....	96
3.5.8	SEM Micrograph of FALP Paste, w:s = 0.24, at 7 Days (2000X).....	96
3.5.9	Generation of $\text{Ca(OH)}_2$ in Fly Ash- Low Porosity Cement Pastes (With and Without The Usual Admixtures).....	97
3.5.10	SEM Micrograph of FALPN Paste, w:s = 0.30, at 7 Days (2000X).....	98
3.5.11	SEM Micrograph of FALPN Paste, w:s = 0.30, at 7 Days (2000X).....	98
3.6.1	Compressive Strengths of Low Porosity Concretes at Various Ages.....	106
3.6.2	Strengths of Low Porosity Concetes of Different Compositions at Increasing Ages Relative to Strength of Reference Concrete Without Fly Ash or Admixture at the Same Age.....	106
3.6.3	Strengths at Increasing Age of Fly Ash- Bearing Low Porosity Concretes With an Air Entraining Agent Relative to Strength of Reference Concrete Without Air Entraining Agent at the Same Time.....	108
4.1.1	Pore Size Distribution Curves (By Mercury Porosimetry) of Replicate Mortar Pieces From IWA Concrete.....	114
4.1.2	Pore Size Distribution Curves (By Mercury Porosimetry) of Replicate Mortar Pieces From BD Concrete.....	115



<u>Figure</u>		<u>Page</u>
4.1.3	Pore Size Distribution Curves (By Mercury Porosimetry) of Replicate Mortar Pieces From Fly Ash-Bearing Low Porosity Concrete...	116
4.1.4	Pore Size Distribution Curves (By Mercury Porosimetry) of Replicate Mortar Pieces From Low Porosity Concrete Without Fly Ash.....	117
4.1.5	Pore Size Distribution Curves (By Mercury Porosimetry) of Replicate Mortar Pieces From Low Porosity Concrete Without Fly Ash (Special Sand Gradation).....	118
4.1.6	Pore Size Distribution Curves (By Mercury Porosimetry) of Replicate Mortar Pieces From Top Portion of 6 x 12 in. LPN Concrete Cylinder.....	119
4.1.7	Pore Size Distribution Curves (By Mercury Porosimetry) of Replicate Mortar Pieces From Bottom Portion of 6 x 12 in. LPN Concrete Cylinder.....	120
4.1.8	Pore Size Distribution Curves (By Mercury Porosimetry) of Replicate Mortar Pieces From Bottom Portion of 6 x 12 in. BD Concrete Cylinder.....	121
4.1.9	Pore Size Distribution Curves (By Mercury Porosimetry) of Replicate Mortar Pieces From Top Portion of 6 x 12 in. BD Concrete Cylinder.....	122



<u>Figure</u>		<u>Page</u>
4.2.1	Shrinkage of Different Concretes at Increasing Ages.....	131
4.2.2	Shrinkage of Different Concretes at Various Ages Relative to that of IWA-Concrete at the Same Age.....	132
4.3.1	Sketch of Steel Mat Embedded in Concretes.....	142
4.3.2	Chloride Content As a Function of Depth For Different Concretes.....	147
4.4.1	Differential Thermograms of Powdered Mortar Pieces From Different Concretes Kept in Open Air and in Enhanced CO <sub>2</sub> Atmosphere for 9 Months.....	154
4.4.2	Extent of Carbonation of Four Different Concretes As Indicated by Phenolphthalein Test.....	156
4.4.3	Extent of Carbonation of Three Different Concretes As Indicated by Phenolphthalein Test.....	156
4.6.1	SEM Micrograph of Mortar From IWA Concrete, w:c = 0.33, at 28 Days (2000X).	168
4.6.2	SEM Micrograph of Mortar From IWA Concrete, w:c = 0.33, at 28 Days (2000X).....	168
4.6.3	SEM Micrograph of Mortar From IWA Concrete, w:c = 0.33, at 28 Days (2000X).....	169
4.6.4	SEM Micrograph of Mortar From BD Concrete, w:c = 0.43, at 28 Days (2000X).....	169





<u>Figure</u>		<u>Page</u>
4.6.5	SEM Micrograph of Mortar From BD Concrete, w:c = 0.43, at 28 Days (2000X).....	171
4.6.6	SEM Micrograph of Mortar From LPF Concrete, w:c = 0.26, at 28 Days (2000X).....	171
4.6.7	SEM Micrograph of Mortar From LPF Concrete, w:c = 0.26, at 28 Days (2000X).....	172
4.6.8	SEM Micrograph of Mortar From LPN Concrete, w:c = 0.26, at 28 Days (2000X).....	172
4.6.9	SEM Micrograph of Mortar From LPN Concrete, w:c = 0.28, at 28 Days (2000X).....	174
4.6.10	SEM Micrograph of Mortar From LPF Concrete, w:c = 0.28, at 28 Days (2000X).....	174
4.6.11	SEM Micrograph of Mortar From LPF Concrete, w:c = 0.26, at 1 Year (1000 and 10,000X).....	175
4.6.12	SEM Micrograph of Mortar From LPF Concrete, w:c = 0.26, at 1 Year (2000X).....	175
4.6.13	SEM Micrograph of Mortar From LPF Concrete, w:c = 0.26, at 1 Year (2000X).....	177
4.6.14	SEM Micrograph of Mortar From LPN Concrete, w:c = 0.28, at 1 year (2000X).....	177
4.6.15	SEM Micrograph of Mortar from LPN Concrete, w:c = 0.28, at 1 Year (30 and 300X).....	178



<u>Figure</u>		<u>Page</u>
4.6.16	SEM Micrograph of Mortar from LPN Concrete, w:c = 0.28, at 1 Year (2000X).....	178
4.6.17	SEM Micrograph of Mortar from LPN Concrete, w:c = 0.28, at 1 Year (10,000X).....	180
4.6.18	SEM Micrograph of Mortar from LPN Concrete, w:c = 0.28, at 1 Year (30 and 300X).....	180
5.2.1	Physical Appearance of Concrete Specimens After 400 Freeze-Thaw Cycles.....	205
5.2.2	Physical Appearance of Another Set of Concrete Specimens After 400 Freeze-Thaw Cycles.....	205
5.2.3	Physical Appearance of Horizontal Cast Surface of Different Concretes After 400 Cycles of Freezing and Thawing.....	207
5.3.1	Appearance of Surface of BD Concrete Specimens Before Scaling Test.....	221
5.3.2	Appearance of Surface of Air-Entrained BD Concrete After Scaling Test.....	221
5.3.3	Appearance of Surface of Non-Air Entrained BD Concrete After Scaling Test.....	222
5.3.4	Appearance of Surface of LP Concrete Before Scaling Test.....	222
5.3.5	Appearance of Surface of LPNS-1 Specimens at the End of Scaling Test....	223
5.3.6	Appearance of Surface of LPNS-2 Specimens at the End of Scaling Test....	223



<u>Figure</u>		<u>Page</u>
5.3.7	Appearance of Surface of LPNS-4 Specimens at the End of Scaling Test....	225
5.3.8	Appearance of Surface of LPNS-3 Specimens at the End of Scaling Test....	225
5.3.9	Appearance of Surface of LPFS-1 Specimens at the End of Scaling Test....	226
6.3.1	Appearance of Concrete Specimens Ponded with 4% $\text{CaCl}_2$ Solution After Being Exposed Outdoors for 12 Months....	242
6.3.2	Close-Up Picture of Damaged BD Concrete Specimen.....	242
6.3.3	Sketch Showing Physical Layout of Steel Mat.....	244
6.4.1	Photograph of Steel Mat of the Kind Embedded in 18 x 18 x 6 in. Concrete Specimens.....	249
6.4.2	Scheme For Measuring Electrical Potential of Embedded Steel Using Cooper/Copper Sulfate Half Cell.....	257
6.4.3	Appearance of Surface Condition of BD Concrete Ponded With 4% $\text{CaCl}_2$ Solution After Being Exposed Outdoors for 56 Weeks.....	265
6.4.4	Appearance of Surface Condition of IWA Concrete Ponded With 4% $\text{CaCl}_2$ Solution After Being Exposed Outdoors for 56 Weeks.....	265



<u>Figure</u>		<u>Page</u>
6.4.5	Appearance of Surface Condition of LPF Concrete Ponded With 4% $\text{CaCl}_2$ Solution After Being Exposed Outdoors for 56 Weeks.....	266
6.4.6	Appearance of Surface Condition of LPN Concrete Ponded With 4% $\text{CaCl}_2$ Solution After Being Exposed Outdoors for 56 Weeks.....	266
7.4.1	Stress-Strain Curve for LPN-8 Low Porosity Concrete Specimens (Originally Coded LPW8).....	273
7.4.2	Stress-Strain Curve for LPF-1 Flyash-Bearing Low Porosity Concrete Specimens (Originally Coded LP1).....	274
7.4.3	Stress-Strain Curves for BD-11 Conventional Bridge Deck Concrete.....	275
7.4.4	Stress-Strain Curves for IWA-4 Iowa Dense Concrete.....	276
7.4.5	Linear Regression Between Ductility Ratio and Compressive Strength.....	281





## HIGHLIGHT SUMMARY

The early deterioration of concrete bridge decks in most areas of North America where de-icing salts are used is a major concern. Corrosion of reinforcing steel in the concrete has generally been singled out as the major cause of this problem. The corrosion is a consequence of penetration of chloride from the de-icing salt through the concrete to the vicinity of the reinforcing steel. This study is based on the idea that low porosity concrete prepared from so-called "low porosity cement" may provide an appropriate preventative measure against such difficulties.

The thrust of the study was first to prepare and characterize appropriate mix design for this purpose using low porosity cement with and without fly ash additions. Subsequently, the durability-related characteristics of low porosity concretes were compared with those of conventional bridge deck concrete as normally specified. A further comparison was made with a special high density low slump mix design incorporating conventional cement



and used successfully in bridge deck rehabilitation. Low porosity concretes prepared at water:cement ratios of 0.24 to 0.30 were found to have high slump (6-10 in.) but were difficult to work in the fresh state and had a relatively short working life. Fly ash incorporation was found to remove both these difficulties. Measurements of the resistance of concretes to freeze-thaw action, the resistance to de-icer scaling, the ingress of chloride ions into the concretes, the water permeability, the extent of carbonation, the development of compressive strength, the rates of drying shrinkage, the pore size distribution of the concrete mortar, and the apparent corrosion rates of reinforcing steel embedded in test concrete specimens were secured.

The performance of the low porosity concrete formulations was found to be highly superior to conventional bridge deck concrete mixes in essentially all the laboratory tests carried out, and to the special high-density mixes as well. Incorporation of fly ash resulted in only modest reduction in the overall superiority of the hardened low porosity concrete while markedly improving workability and handling characteristics.



PART ONE

INTRODUCTION AND LITERATURE REVIEW



## 1.1 INTRODUCTION

### 1.1.1 Statement of the Problem

One of the most severe problems facing the highway engineering profession is currently that of early deterioration of concrete bridge decks in areas where salts are routinely applied for winter de-icing.

There is a large body of evidence that traditional concrete, designed and conventionally placed for highway bridge decks, is not adequate to provide satisfactory service for the design life of the structure under these conditions of exposure. ▲

While there is a consensus among investigators that several factors contribute to early deterioration of bridge decks the primary problem is electrochemical in nature and involves corrosion of reinforcing steel under the influence of chloride ions penetrating to the level of the upper steel mat.

Usually steel embedded in concrete is passivated electrically under the influence of the alkaline environment maintained within the concrete. However, it is well established that under the influence of a sufficiently high chloride ion concentration maintenance of this passivating film becomes difficult. Electrochemical corrosion cells are set up by differences in local electrical potentials in





different areas of steel, and accelerated corrosion occurs. This leads to extensive formation of rust (ferric hydroxide) surrounding the steel within the concrete. The pressure developed by the voluminous ferric hydroxide thus formed eventually delaminates areas of concrete above the steel mat and results in widespread spalling and eventual failure. The process is favored by a number of factors including:

- a) A thin depth of concrete cover over the steel.
- b) extensive usage of salt, leading to high chloride ion concentrations occurring around the steel.
- c) high permeability of concrete to water and chloride ions.
- d) low alkalinity of the concrete pore solution, either due to use of cement with low alkali contents or to carbonation.
- e) the presence of cracks in the concrete induced by excessive shrinkage or inadequate resistance to freezing and thawing.
- f) the presence of bleeding channels within the concrete when placed at improperly high water contents, providing an almost direct access of water and chloride ions to the steel.
- g) the dislodging effect of repeated vibration and impact under high traffic densities and heavy wheel loads once delamination and spalling have begun.
- h) inadequate construction practice on the part of the contractor, especially inadequate mixing and ineffective consolidation of fresh concrete in



restricted spaces within and around the steel mat.

A number of prospective methods have been proposed to mitigate and arrest the problem on new or replacement bridge decks. At least six general approaches have been taken, including:

- a) pre-coating the reinforcing steel with a special epoxy coating applied in an electrospray process.
- b) galvanizing the reinforcing steel.
- c) incorporating special wax beads in the fresh concrete mix which, after setting and some strength gain, is then heated to melt the beads to attempt to render the concrete impermeable.
- d) use of latex-modified concrete.
- e) use of conventional concrete components formulated in a special mix design to produce high density concrete.
- f) use of overlays of various types to retard the penetration of the chloride ion into the concrete.

Most of these have been at least partly successful, but all of them except (e) are expensive and some require special equipment and special contracting crews.

A somewhat more practical approach to the problem may be that of altering the nature of the concrete cover itself so as to provide a concrete layer above the steel that is:

- a) easily flowable and self consolidating even in the restricted spaces provided in bridge deck courses.
- b) highly resistant to the penetration of water and chloride ions.



- c) highly resistant to cracking due to freezing and thawing effects.
- d) highly resistant to shrinkage cracking.
- e) possessed of the potential for developing and retaining high alkalinity so as to properly maintain steel passivation.
- f) strong enough to hold together under traffic load, impact, vibration, etc.

There is now sufficient laboratory data to suggest that these requirements can be met simultaneously and economically by substituting so-called "low porosity" cement for ordinary portland cement of an appropriate mix design which may incorporate fly ash.

"Low porosity" cement (LP Cement) is ordinary portland cement clinker ground finer than usual ( $4500-5500 \text{ cm}^2/\text{g}$  Blaine as compared to normal cement which is  $2700-3500 \text{ cm}^2/\text{g}$  Blaine), and to which no gypsum is added. The set control and rheological characteristics are regulated by addition of a special sulfonated lignin retarder and an alkali carbonate or bicarbonate. The effects of these departures from normal portland cement are to provide flowing concrete of superior rheological character at low water content in the fresh state, rapid rates of hydration and of strength gain, and superior properties in the final hardened concrete product.

#### 1.1.2 Objectives of the Present Study

The overall objectives of this work are to determine the potential suitability of LP concrete for bridge deck



applications and at the same time to study its characteristics and behavior from a scientific and technical point of view.

The thrust of the study then is to attempt to compare appropriate formulations of LP concrete with conventional bridge deck concrete in terms of characteristics pertinent to the bridge deck problems outlined previously. In pursuit of these objectives a series of tests were performed in parallel for LP and conventional concretes, with the results compared and integrated in an overall evaluation of suitability for this specific concrete use.

The actual scope of the comparisons was somewhat wider than simple LP concrete-conventional concrete comparisons. To begin with, two distinct general formulations of LP concrete were evaluated through all of the test program. In the first formulation, designated LPN concrete throughout this work, LP cement was used as the sole cementitious component, in concrete mixes which ranged from 8 to 10 bags per cubic yard. In a second general formulation, a high-lime fly ash was used in the mix design and the LP cement content correspondingly reduced. These concrete mixes, designated LPF concretes throughout this work, generally contained between 10 to 13 bags of total cementitious component, that is, LP cement plus fly ash, per cubic yard. The LP cement component itself ranged between 7 to 9.5 bags per cubic yard.

The primary formulation representing conventional bridge deck concrete used in this work is the current concrete mix design used by the Indiana State Department of





Highways as its normal specification for highway bridge decks. This is a mix containing 6 bags per cubic yard of ordinary Type I portland cement, and in this work is designated as BD concrete. In addition, a second formulation representing a much higher quality of conventional concrete made with ordinary portland cement was used. This was a dense, low slump mix design developed by the Iowa State Highway Department having a Type I portland cement content of 8.5 bags per cubic yard. In this work such mixes are designated as IWA concretes.

In early work on this project still another portland cement-based mix design was used, this one a 5.5 bags/cubic yard mix as specified by the Illinois State DOT. In tests of freezing and thawing resistance the extent of damage was about the same with this design as with the BD mix, and it was decided to eliminate this formulation in the main test sequence.

Initially, a number of preliminary studies were conducted with LP concretes to determine the most suitable mixing time, slump loss with time, and the amount of entrained air with and without an air entraining agent. The effect of type of mixer used in relation to entrained air was also investigated, and the effect of aging of the cement and lignosulfonate was observed. Tests were performed to establish a suitable mix proportion consistent with suitable characteristics of the fresh concrete, e.g. workability, air content, and setting time. Further tests



were done to determine suitable amount of fly ash to be incorporated in the mix.

After completion of these preliminary studies, parallel determinations of the following characteristics were performed for each of four general concrete formulations mentioned above, namely:

- a) heat evolution of pastes
- b) strength and failure behavior under compressive load
- c) freezing and thawing resistance
- d) scaling resistance
- e) shrinkage
- f) carbonation
- g) ingress of chloride ions into concretes
- h) apparent corrosion rates of reinforcing steel embedded in concretes
- i) pore fluid chemistry
- j) pore size distribution
- k) hydraulic conductivity (water permeability)



## 1.2 LITERATURE REVIEW

### 1.2.1 Background

The literature on low porosity concrete is not extensive since active work on it started only a little over a decade ago. The origins of low porosity cement rests with the work of Rehbinder and associates in the Soviet Union in the late 1950's (1). Brunauer started work on low porosity cement while at the Portland Cement Association in the 1960's and continued his research at Clarkson College of Technology, New York, between the period 1965-72 (2-9). Subsequent development work on low porosity cements was carried out by industrial laboratories, notably the American Cement Company, Riverside, California in the period 1972-74; the Martin Marietta Laboratories, 1975-77; and the Aalborg Portland A/S, Denmark in the period 1974-76. Superior low porosity additives were developed and considerable low porosity concrete research was carried out by Westvaco Corporation, North Charleston, S. Carolina. U.S. patents for various aspects of low porosity cement and concrete technology have been awarded to Brunauer (10), to Stryker (11) Ball, Braddon and Stryker (12) of Westvaco, and to Wills (13) of Martin Marietta Cement Company. Other workers have carried out further work on low porosity pastes and concretes. The results of these works have been reported (14-26).



### 1.2.2 Development of Low Porosity Cement, Paste and Concrete

The hydraulic binder, portland cement paste, is essentially the system: clinker - gypsum -  $H_2O$ . The idea of replacing the gypsum, to reduce the amount of water needed to produce a workable paste, in this classical system was initially expressed by Reh binder and associates (1). Their first system was clinker - lignosulfonate -  $H_2O$ . This mix was characterized by rapid setting and high initial strength gain. In their subsequent work (27), the initial setting was controlled by addition of potassium carbonate, thus employing the system: clinker - (lignosulfonate -  $K_2CO_3$ ) -  $H_2O$ . The combination of alkali carbonate and calcium lignosulfonate as a substitute for gypsum in cement resulted in considerable delay of initial set and high strength gain.

Research work carried out in Czechoslovakia in the late 1960's (25) led essentially to the same system as the second of Reh binder and associates. This system was called Modified Quick Binding High Strength Pastes.

In an extensive research carried out by Brunauer and co-workers (2-9) use was made of cements ground to between 6000 and 9000  $cm^2/g$ , obtained by extensive grinding in the presence of grinding aids. A system chemically similar to Reh binder's second system was produced by Brunauer and co-workers, except that their clinker was ground much finer. This system produced excellent results in laboratory pastes, mortars and concretes, in that all could be produced at a low water: cement ratio. Brunauer and co-workers called the resulting





low water contents pastes and concretes "low porosity" pastes or concretes, and the fine cement - lignosulfonate -  $K_2CO_3$  system "low porosity" cement.

### 1.2.3 Low Porosity Cement

A "low porosity" cement as the term is presently understood is essentially an ordinary Type I or II portland cement clinker ground to a fineness of  $4500 \text{ cm}^2/\text{g}$  or more (Blaine method) without any interground gypsum or anhydrite. Grinding aids can be used to assist in achieving the required surface area and these were used extensively by Brunauer and co-workers (3). However, compatibility between specific grinding aids and the low porosity system is not assured and some grinding aids must be used with caution. Subsequent work (16, 17, 21, 26) indicates that lower surface area low porosity cements can be used without detrimental effect to the characteristics of either the fresh and hardened paste or concrete. Originally, the admixtures, lignosulfonate and alkali carbonate, were interground with the cement clinker. In some later work (21) the admixtures are added at the time of mixing the paste or concrete.

### 1.2.4 Properties and Mechanism of Hydration in Paste and Concrete

The results of Brunauer et al (2-9) can be briefly summarized as follows:

(i) Paste prepared from Type I or II clinkers ground to a Blaine fineness ranging from 6000 to  $9000 \text{ cm}^2/\text{g}$  with the



help of grinding aids, and with added calcium lignosulfonate and potassium carbonate, produced excellent workability and satisfactory setting time with as low water:cement ratio as 0.20

(ii) Hardened low porosity pastes suffered less shrinkage on drying than conventional hardened cement pastes.

(iii) High compressive strengths of low porosity pastes were reported, and a correlation found between the strength and the degree of hydration. An inverse correlation was found between the strength and total porosity.

Skalny and associates (14) showed that concretes made with low porosity cements not only had higher strengths than conventional concretes but had better freeze-thaw resistance and other engineering properties. However, they called attention to a number of unsolved problems with their low porosity concretes. Notable among them was the high sensitivity to fluctuations in water content and admixture type and dosage. They also found difficulties in using water:cement ratio of 0.30 or less so far as workability was concerned. Some of these problems have been resolved in subsequent work by other workers (17, 18, 21) using somewhat different low porosity admixtures.

Skalny et al (14) have provided a suggested explanation for the effect of the lignosulfonate and potassium carbonate admixtures in low porosity concrete. Their notion was that the lignosulfonate forms a coating on the unhydrated cement particles (and hydration products) thus preventing fast



hydration. The potassium in the alkali carbonate is considered to form potassium hydroxide, the presence of which decreases the concentration of calcium ions in the mix solution. The decreased concentration of calcium ions was thought to prevent the precipitation of the lignosulfonate as calcium lignosulfonate, thus prolonging its dispersing action. The carbonate ion was also thought to form a carboaluminate which prevents flash settings of  $C_3A$  and  $C_4AF$ . Odler and associates (17) agreed on the possible formation of calcium carboaluminate. In their analysis of fluid phase of low porosity paste in the first few minutes after mixing, they observed significant amounts of calcium ions which did not form calcium carbonate, in spite of the presence of dissolved carbonate. They speculated that calcium ions may be loosely bound to the lignosulfonate as poorly dissociated calcium lignosulfonate instead of being in the form of free calcium ions in solution.

Significant attractive forces exist between particles in ordinary portland cement-water suspensions, and the particles are linked together as floccules or agglomerations. Water-reducing admixtures, such as lignosulfonates are somewhat effective in breaking the cement floccules and dispersing them, thus reducing the amount of water required to suspend the particles and render the mix workable. This fact had been noted many years ago by Scripture (28) and various other workers (29, 30).

A similar effect but more effective dispersion also takes



place with the use of superplasticizers, permitting the use of water:cement ratios of almost the same low values as can be secured with low porosity cements. However, there are a number of differences in the fresh state between pastes or concretes made with conventional portland cement and superplasticizers on the one hand and those made with low porosity cements and the LP admixtures on the other. The former has a high rate of stiffening (slump loss) with respect to time, tending to be workable only for a comparatively short period of time, especially at elevated temperatures. This seems to be not the case with low porosity concretes, since the admixtures control the forces between particles and increase the fluidity of the mix for a long time.

Of the three known phenomena that may be responsible for maintaining a stable colloid, solid-liquid affinity, steric hindrance, and interparticle repulsion due to a high zeta potential, the latter is responsible for the condition as it obtains in the cement pastes and concretes (31).

Collepardi and co-workers (24) in their study of the combined effect of lignosulfonate and alkali carbonate on tetracalcium aluminoferrite hydration noted a strong negative charge in the zeta potential caused by the simultaneous addition of lignosulfonate and alkali carbonate. They speculated that both the strong retarding action and the dispersing effect caused by the negative charge in the zeta potential could explain the liquefying effect of the admixtures. The amounts of lignosulfonate and alkali carbonate





or bicarbonate needed to produce the desired dispersing effect and to control setting behavior depend among other things on the fineness of the clinker, or whether any grinding aid is used, and or whether any gypsum is present.

There exist threshold values for the amounts of lignosulfonate and alkali carbonate or bicarbonate required to produce the dispersing effect for a particular clinker of a given fineness. In a study by Odler et al (16), it was shown that a minimum of 0.50% of calcium lignosulfonate and 0.25% of sodium carbonate (by weight of the cement) was required to produce a flowing paste at w:c 0.25 using cement clinker of fineness  $3400 \text{ cm}^2/\text{g}$ . Skalny et al (14) have reported similar threshold values. They further reported that the paste setting behavior may be accurately controlled by the dosage of the additives employed, particularly the lignosulfonate. Diamond and Gomez-Toledo (21) ascertained from their studies that for sodium lignosulfonate an optimum value of 0.75% existed, and percentages of the order of 0.8 to 1.4% by weight of cement of sodium bicarbonate was required to produce a flowing paste using clinker of fineness  $5400 \text{ cm}^2/\text{g}$  at water:cement ratios of 0.22-0.24.

#### 1.2.5 Potential Uses of Low Porosity Concretes

Increasing data in the literature (3-9, 14, 21, 32, 33) suggest that uses of LP concrete for highway purposes may be anticipated. High strength concrete made with conventional cement has been reported to provide good durability of highway pavement in the severe freeze-thaw cycle region of Utah



(34). This concrete, with a design strength of 5200 psi is doing substantially better than 3500 psi concrete placed at the same time. With strengths of substantially over 8,000 psi recorded at 28 days (21), the performance of low porosity concrete for highway pavement may be anticipated to be equally good or better. Škvára and associates (32) have shown that a low porosity concrete is capable of setting and hardening at temperatures substantially below 0°C. This has led to the suggestion of the use of low porosity concrete in construction under winter conditions.

Higher strengths, greater dimensional stability, better freeze-thaw resistance and better resistance to corrosion of steel embedded in concrete have been reported in the literature (4, 14, 21, 35) to be some of the qualities characteristic of the low porosity concretes.

#### 1.2.6 Durability of Concrete Bridge Decks

##### (i) Background

The incidence of deterioration in large numbers of concrete bridge decks in the last two decades in the U.S.A. (36) has caused major concern to the various state highway authorities and the Federal Highway Administration. A large increase in the number of highway bridges resulting from the building of Interstate Highway System and an increase in the use of de-icing salts to ensure safer roads during the winter have contributed tremendously to this problem. It was estimated that 1/2 million tons of salt were used throughout



the U.S. for de-icing highways in 1947; and by 1976 the figure had risen to about 12 million tons (36). The cost associated with maintenance and repair of deteriorating concrete bridge decks are extremely high. It has been reported (36) that in 1975 the Federal Highway Administration estimated the annual cost for bridge deck repairs in the United States at \$200 million. The cost is expected to be much higher by now (1981).

Bridges are normally designed to last 30 years or more but there have been reported cases where signs of distress have appeared in less than 5 years (37). While several factors are known to contribute to the early deterioration of concrete bridge decks, it is clear that the paramount factor is the use of de-icing salts. The salts dissolve and chloride ions penetrate the concrete to the level of steel rod and initiate corrosion of the reinforcing steel. This corrosion results in spalling off of the concrete cover over the steel and eventual breakup of the bridge deck.

#### (ii) Corrosion of Steel Embedded in Concrete

Moisture and dissolved oxygen are essential in initiating corrosion of steel embedded in concrete; but even in their presence, with the high pH (13 and above) - normally found in the pore liquid in well placed and well cured concretes, passivation is usually maintained. This appears to be accomplished by the formation of a gamma iron



oxide layer, about  $30\text{\AA}$  thick, on the metal surface (38). Other factors, such as carbonation of the concrete leading to a lowering of the pH, and the presence of cracks which provide easy access of moisture, dissolved oxygen, and chloride ions to the rebars initiate and accelerate corrosion. Chloride ions are known to accelerate corrosion of steel in general and this is specifically true in the case of steel embedded in concrete (39, 40).

The quantity of chloride ions associated with the incidence of active corrosion of the reinforcing steel is given by Stratfull (41) as 1 lb. per cubic yard (i.e. 0.025% Cl by weight of concrete). Clear (42) suggests a figure of 0.20 per cent Cl by weight of cement. For a concrete with a cement factor of 700 lb. per  $\text{yd}^3$ , this corresponds to approximately 0.035% Cl by weight of concrete or 1.4 lb. Cl per  $\text{yd}^3$ .

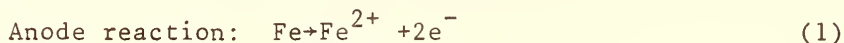
A typical highway pavement in the snow belt receives about  $1/4$  lb. of salt per cubic foot during the course of a winter (36). Even more damaging levels of application have been reported in some areas. For example, chloride tests performed on several bridges in the State of Pennsylvania revealed that decks with only one winter's salting already had chloride levels as high as  $2 \text{ lb/yd}^3$  of concrete within the concrete deck at the depth of the rebars. Older decks had chloride concentrations ranging from  $2 \text{ lb/yd}^3$  to as high as  $15 \text{ lb/yd}^3$  of concrete (43).





Gjørsv and Vennesland (44) suggest that the porosity or permeability mainly influences chloride penetration near the surface; diffusion into the interior of the concrete is more affected by other controlling factors such as chloride binding and ion exchange.

A brief summary of the mechanism of electrochemical corrosion is as follows. Corrosion occurs as a result of the development of coupled anodic and cathodic areas on the metal surface, with oxidation occurring at the anode and reduction at the cathode.



Cathode reaction (in moist, aerated medium):



These half cell reactions are coupled by transfer of electrons from the anodic to the cathodic regions of the steel. The end-product of the corrosion is ferrous hydroxide which precipitate from solution as can be deduced by adding equations (1) and (2). Subsequent oxidation of the ferrous hydroxide results in formation of ferric hydroxide or hydrous ferric oxide. The corrosion product occupies as variously reported between 2.2 to approximately 13 times as much space as the metal which it replaces (45). This increase in solid volume within the confines of the concrete produces mechanical pressures. Expansive pressures as high as 4700 psi (46) have been reported. This is many times greater than the tensile strength of most concretes and in consequence failure occurs.



Clear (40) has suggested the following limits of chloride ion content at the level of the rebars as a guideline in the rehabilitation of concrete bridge decks. For less than 1.0 lb. Cl/yd<sup>3</sup> concrete may be considered to be in good shape, and should be left without rehabilitation since no corrosion is expected. If chloride contents greater than 2.0 lb. Cl/yd<sup>3</sup> of concrete at the level of the rebars are found, the concrete should be removed or the entire deck replaced. Chloride ion contents between 1.0 and 2.0 lb/yd<sup>3</sup> of concrete constitute a questionable level with appropriate remedial measures not certain.

(iii) Influence of Physical and Environmental  
Factors on Corrosion

The provision of a cover of well-compacted, dense concrete of low permeability and sufficient thickness in good contact with the steel is necessary in preventing corrosion. In the absence of cracking, the ingress of water, oxygen, carbon dioxide, and chloride ions all depend on the permeability of the concrete. This in turn depends on the mix design, specifically the cement content, the water:cement ratio, the aggregate type, size and grading; on the placing, especially the degree of compaction; and on the curing conditions.

Of the several physical factors that promote corrosion in concrete, the presence of cracks is of major importance. Cracks are caused by several mechanisms. Most surface cracking seems to be due primarily to concrete volume



changes caused by poor construction practices, including concrete that is too wet, placed too slowly, poorly finished and improperly cured (47).

Excessive shrinkage in concrete is known to cause cracks which adversely affect the service performance of the concrete structure. In their work on low porosity pastes Brunauer and co-workers (4) observed that low porosity pastes exhibited less shrinkage than those of conventional portland cement paste. This effect is due in part to the low water content used, and likely also to be the absence of gypsum, which results on hydration with  $C_3A$ , to form calcium sulfoaluminate hydrate (ettringite). The latter is known to exhibit great shrinkages on drying (48).

Shrinkage in concrete is also associated with carbonation, i.e., reaction of the cement paste with atmospheric  $CO_2$ . Carbonation of concretes occur even at low concentrations of carbon dioxide, e.g. at partial pressures of  $3 \times 10^{-4}$  atmospheres (48) in the presence of moisture. Opinion is divided as to exactly what happens when carbonation occurs (44, 50, 51). However, there seems to be agreement that strength gain often accompanies carbonation of pastes and concretes. Verbeck (51) has observed reduced permeability in carbonated samples, possibly due to the fact that water released by carbonation may aid in the process of further hydration. At the same time the calcium carbonate produced may reduce some of the voids in the cement paste. These effects which would be seemingly favorable to durability



of the bridge decks are negated by the more important effect of carbonation in lowering of the pH in the concrete cover, thus increasing the likelihood of failure to maintain passivity of the steel.

The depth of carbonation depends on the quality of the concrete cover. If carbonation does extend close to the rebars it makes them susceptible to corrosion. Pihlajavaara and Pihlman (52) have shown that the amount of carbon dioxide intake into pastes and concretes is dependent on the water:cement ratio. Their results indicate that in  $w:c = 0.45$  paste the maximum amount of carbon dioxide taken up was about 50 per cent higher than in  $w:c = 0.30$  paste. From this standpoint it can be expected the low porosity concretes made at low water contents will perform better under carbonation. It was further shown that carbon dioxide intake depends on the relative humidity of the storage air, being at a maximum at approximately 50% R.H. The effect of carbonation on the porosity or microstructure of the hardened cement paste was shown to be significant.

One of the effects of freezing and thawing on concrete is to cause cracking in the concrete, and this adversely affects concrete performance in service. Air entrainment has been used successfully to counter this effect, but there are some reported cases (53, 54) where concretes have suffered damage even with proper level of entrained air. Low water:cement ratio concretes have often been used to limit possible damage due to freezing and thawing action (14). Concretes mixed at low water:cement ratios tend to





have smaller pores in the paste system, thus reducing the amount of water that remains freezeable. Such concretes have low permeability and imbibe less water when wetted after drying.

Low permeability is an essential characteristic of a durable concrete. Ease of penetration of fluids has a generally adverse effect on durability. Calcium hydroxide may be leached out of readily permeable concrete by aggressive liquids.

The use of low porosity concrete has been shown to give rise to a more compact, dense concrete compared with conventional concretes (14, 21). An insight into the compact nature of low porosity paste can be gained by observing the microstructure of pastes cured for different periods of time at high magnification in a scanning electron microscope. Diamond and Gomez-Toledo (22) have shown that about the second day the hydration products in hardened low porosity pastes have partly fused into a massive structure. At later stages the structure consolidates further, with individual particles becoming barely separable. A similar structure was shown by Odler and associates (17) in Figure 9 of their work. This microstructural picture is different from that of conventional pastes with higher water contents. Here a more open microstructural arrangement is found where the individual product particles or clusters of them can be identified even at later ages, far in excess of 28 days.



In their study of the pore structure of the paste matrix as it relates to corrosion of steel reinforcement, Mikhail et al (35) showed that the pore size distribution as well as the total porosity, affect the corrosion behavior of steel reinforcement. Their study revealed that increasing the fineness of the cement effects a better passivity of the steel, due apparently to favorable changes brought about in the pore structure. These authors further revealed that the presence of  $\text{CaCl}_2$  in fresh concrete causes significant changes in the pore structure causing the formation of more open structure in the hardened product. This facilitates later entry of chlorides or other aggressive agents.

Concrete may also crack due to rapid evaporation of moisture during the early stages of hardening. If the evaporation rate is much greater than 0.1 lb. of water per square foot per hour, cracking is almost certain to occur (47). Local differences in distribution of moisture on a bridge deck can cause formation of electrochemical cells on the surfaces of the embedded steel, and this enhance corrosion. It has been observed (47) that poorly drained bridge decks deteriorate more rapidly than those that are well drained, and the cause could well be due to the formation of such cells. Details of a number of additional physical factors that affect durability of bridge decks are well documented by Carrier and Cady (47).



(iv) Influence of Chemical Factors  
on Corrosion

The chemical composition and type of cement used in making concrete is an important factor with regard to corrosion resistance of the embedded steel. Differences in the amount of sodium, potassium and calcium hydroxide derived from different cements account for the differences in the degree and reserve of alkalinity provided in the concrete. Higher levels of alkalinity are required to maintain the passivation that produces the resistance of the embedded steel to corrosion.

It had been widely believed that pore fluid in concrete was a saturated solution of calcium hydroxide. This is misleading. Diamond (55) has shown by direct analysis of pore fluid expressed from hardened pastes and mortars that pore fluids contain substantial amounts of alkali hydroxides. The presence of these stronger alkalis raises the pH and suppresses the amount of calcium in solution. A saturated solution of calcium hydroxide prepared in the laboratory has a pH of 12.6 and contains approximately 1 gram of calcium ions per liter. This is approximately 0.02 molar in concentration level. The pore fluid in a paste or mortar made from medium to high alkali cement was shown to be roughly 0.6 molar or greater with respect to alkali (potassium and sodium) hydroxide but only 0.002 molar or less with respect to calcium. The pH of this solution was 13.6.



The use of sodium lignosulfonate and especially sodium bicarbonate as admixtures in low porosity concrete is likely to substantially increase the pH of the resulting concrete. Due to other induced characteristics such as low porosity and permeability, such concrete is likely to maintain such high alkalinity indefinitely.

High amounts of tricalcium aluminate in cement may afford increased protection against corrosion in the presence of chloride ions (44) through formation of chloroaluminates. Though high alkalinity is a necessary condition for the protection of steel in concrete, its benefits are reduced by the presence of free chloride ions. In sufficient concentration, chloride ions destroy the protective passivating film of iron oxide on the steel surface (38, 39). At pH 12.6, it has been observed that passivity can be destroyed by concentrations of free chloride ions between 35 ppm and 700 ppm (39). Evidence also exists of a threshold chloride-hydroxide ion ratio which must be exceeded before corrosion can occur. The threshold ratio of chloride ion activity to hydroxide ion activity has been observed to be 0.6 in the pH range from 11.6 to 12.4 (39).

#### (v) Corrosion Measurement in Concrete

The use of electrochemical measurements to monitor corrosion behavior of steel in concrete was pioneered by Stratful using potential scan techniques (56). This potential measurement only gives a qualitative measure of the





corrosion of the reinforcing steel. A method which allows quantification to be made in most systems is known as the linear polarization technique (38); however, it appears that results of this technique are not reproducible in concretes (57).

A method of measuring electrical potential between steel reinforcement and the deck surface has been developed in California and accepted by the Federal Highway Administration (58). It consists of comparing the differences in potential between embedded steel and a standard reference cell on the deck surface. Copper-copper sulfate cells have replaced standard calomel electrodes in field work since the former are sturdier, less sensitive and generally more adaptable to field uses. Recent work by the FHWA (59) on exposed concrete slabs indicates that when the measured electrical potential is less than  $-0.20V$  the probability is very high (greater than 95 per cent) that corrosion is not occurring.. When the measured electrical potential is greater than  $-0.35V$  the probability is high (greater than 95 per cent) that corrosion is occurring.

#### 1.2.7 Fly Ash in Concrete

Since fly ash has been used in some of the low porosity concretes in this study, it is appropriate that a brief review be given of fly ash properties and their effects in concretes.



### (i) Fly Ash: Source and Composition

Fly ash is obtained as a by-product of the burning of pulverized coal in thermal or electric power plants. One of the many materials loosely classed as "artificial pozzolanas", fly ash has recently engaged considerable attention of concrete technologists, both because of the improved characteristics it imparts to fresh and hardened concrete and because of increases in its availability.

Fly ash particles are typically spherical and range in diameter from 1  $\mu\text{m}$  to sometimes as much as 100  $\mu\text{m}$  or more. The range of particle sizes in a given fly ash is largely determined by the type of dust collection equipment used (60). The chemical composition of fly ash is determined by the types and relative amounts of mineral matter in the coal burned. More than 85% of most fly ashes are composed of chemical compounds and glasses formed from  $\text{SiO}_2$ ,  $\text{Al}_2\text{O}_3$ ,  $\text{Fe}_2\text{O}_3$ ,  $\text{CaO}$  and  $\text{MgO}$ . From the mineralogical point of view fly ash consists mostly of alumino-silicate glass. Crystalline phases commonly present are quartz, mullite and hematite in low  $\text{CaO}$  content ashes, and these plus crystalline  $\text{CaO}$ , anhydrite,  $\text{C}_3\text{A}$ , and other phases in high  $\text{CaO}$  - content fly ash. The latter often have significant contents of alkali sulfates as well.

### (ii) Effects of Fly Ash on Properties of Fresh and Hardened Concrete

The inclusion of fly ash in concrete mixes affect both fresh and hardened concrete properties. Fly ash may perform



a dual function in concrete mixes acting in part as a fine aggregate and in part as a cementitious material. It influences the rheological properties of the plastic concrete as well as the strength, porosity and durability of the hardened mass.

Most workers (61, 62, 63) report a reduction in the amount of water required for a given workability compared to an equivalent paste without fly ash, but others have observed the opposite effect (64, 65). Concrete mixes which include fly ash generally show reduced segregation and bleeding.

It is widely believed that fly ash used in concrete causes a drop in the early temperature evolution compared with comparative plain concrete. The work of Elfert (66), and of Compton and MacInnis (63) confirm this. This effect is particularly desirable in mass concrete since it substantially lessens the risk of cracking.

The results of Davis et al (64) and Elfert (66) support the generally-held expectation of lower shrinkage for fly ash bearing concretes as compared with otherwise similar plain concretes. The most adverse effect of fly ash in concrete is found in its use on pavements under frost conditions. Concretes in frost environments are subjected to scaling on its surface much more than a comparable concrete without fly ash (67). It has further been shown that mortar and concrete cured for a longer time, 2 to 3 months, offer a better resistance than those cured for a shorter period (67).



There seem to be indicated some benefits of concretes containing fly ash on corrosion protection of steel in concrete. Some workers (65, 68) indicate that fly ash does not decrease the corrosion protection of steel reinforcing when compared to normal concrete, and a study by Larsen et al. (69) indicates that corrosion protection is increased by the inclusion of fly ash in concrete.





PART TWO

MATERIALS AND EXPERIMENTAL METHODS



## 2.1 MATERIALS

The following is a description of the materials used in the present work.

### 2.1.1 Cementitious Materials

#### (i) Low Porosity Cement

The cement used for low porosity concrete was a standard type I clinker ground to a measured Blaine fineness of  $5400 \text{ cm}^2/\text{g}$  without added gypsum. That used in the initial part of the study was produced at the Holly Hill, South Carolina plant of the Giant Cement Company in December 1974, and supplied through the courtesy of Westvaco Corporation. A second supply of cement of the same type (Type I clinker) and two grades of fineness, namely  $4500 \text{ cm}^2/\text{g}$  and  $3200 \text{ cm}^2/\text{g}$  was delivered by the same company in August 1979. The finer of the two ground clinkers delivered in the second supply, was used for most mixes of the low porosity concrete in this study. A typical plant analysis of the clinker is given in Table 2.1.1. Its chemical composition is that of an ordinary Type I clinker but one of unusually low alkali content.

#### (ii) Ordinary Portland Cement

Two Type I Portland cements meeting the requirements of ASTM Designation: C 150-75 were used for the conventional



Table 2.1.1 Analysis of Cements Used

ITEM	LP Cement	Type I	Type I
<u>Chemical Analysis</u>			
SiO <sub>2</sub>	22.17	20.95	21.12
Al <sub>2</sub> O <sub>3</sub>	6.18	4.98	5.40
Fe <sub>2</sub> O <sub>3</sub>	2.63	2.42	2.27
CaO	67.57	64.47	65.24
MgO	1.06	1.19	1.22
SO <sub>3</sub>	0.13	2.96	2.97
Na <sub>2</sub> O	0.07	-	-
K <sub>2</sub> O	0.17	0.69	0.78
Total Alkali as Na <sub>2</sub> O	0.18	0.45	0.51
Ignition Loss	0.35	2.15	0.80
Insoluble Residue		-	
Soluble K <sub>2</sub> O	0.04		
Soluble Na <sub>2</sub> O	0.01		
Free CaO	0.69		

Potential Compound Composition

C <sub>3</sub> S	58.20	57.81	57.02
C <sub>2</sub> S	19.70	16.54	17.62
C <sub>3</sub> A	11.90	9.11	10.47
C <sub>4</sub> Af	8.00	7.36	6.90

Physical Test

Fineness, Blaine cm <sup>2</sup> /g	5,400*	3,760	3,335
-------------------------------------	--------	-------	-------



Table 2.1.1, continued

- \* Low porosity cement of this fineness was used for the major part of this work. Cement of the same chemical composition but different fineness values of 4,500 and 3,200  $\text{cm}^2/\text{g}$  respectively were used for preparing some specimens in the study.





concretes. They both were produced by the Lone Star Industries, Inc., Greencastle, Indiana. The chemical composition and physical properties of these cements are also given in Table 2.1.1.

### (iii) Fly Ash

A fly ash supplied by the Otter Tail Power Company of Fergus Falls, Minn., was used. A typical analysis of this fly ash is given in Table 2.1.2. This is a fly ash of unusually high calcium oxide content, and would be classified as an ASTM Type C fly ash according to ASTM Designation: C 618-80. The sulfate content of this fly ash is higher than most fly ashes.

## 2.1.2 Aggregates

### (i) Fine Aggregates

The fine aggregate used was obtained locally and was composed of clean siliceous sand. A sieve analysis is given in Table 2.1.3; the fineness modulus was 2.71. The sand has a water absorption coefficient of 2.27 percent and a bulk specific gravity, saturated surface dry (SSD) of 2.53, both determined in accordance with ASTM Designation: C 128-73. The dry rodded unit weight was 110 lb/ft<sup>3</sup>, as measured in accordance with ANSI/ASTM Designation: C 29-78. The sand was oven dried prior to batching the concrete mix.

### (ii) Coarse Aggregate

The coarse aggregate used for the initial part of the study was hard clean dolomite rock obtained from Delphi



Table 2.1.2 Chemical Analysis of Fly Ash by Energy Dispersive X-ray Analysis\*

<u>Component Determined</u>	<u>%</u>
SiO <sub>2</sub>	30.7
Al <sub>2</sub> O <sub>3</sub>	8.2
Fe <sub>2</sub> O <sub>3</sub>	8.9
TiO <sub>2</sub>	1.8
CaO	30.2
MgO	2.6
K <sub>2</sub> O	0.9
Na <sub>2</sub> O	4.1
<u>SO<sub>3</sub>**</u>	<u>12.6</u>
LOI	1.65

\* Analysis courtesy of Martin Marietta Laboratories, Baltimore, MD. Values normalized to 100% without regard to loss on ignition.

\*\*Laboratory determination of SO<sub>3</sub> by barium sulfate precipitation yielded a value averaging 5.7%. The discrepancy has not been resolved.



Table 2.1.3 Sieve Analysis of Fine Aggregate

Sieve Size		Percentage by Weight
Passing through	Retained On	
1/2 in.	No. 4	1.80
No. 4	No. 8	10.05
No. 8	No. 16	13.20
No. 16	No. 30	22.50
No. 30	No. 50	39.65
No. 50	No. 100	10.65
No. 100	No. 200	1.90
No. 200	Pan	0.25
Fineness Modulus: 2.71		



Limestone, Inc. at its quarry located at Delphi, Indiana. The bulk specific gravity (SSD) was 2.74 and the absorption was 0.67 per cent.

For the major portion of this work the coarse aggregate used was a hard clean limestone obtained from Kentland Stone, Inc. at its quarry in Kentland, Indiana. The bulk specific gravity (SSD) of this aggregate was 2.62 and its absorption was 1.2 per cent. The coarse aggregate was oven dried and graded before use, the size separations being  $3/4 - 1/2$  in.,  $1/2 - 3/8$  in.,  $3/8 - \text{No. 4}$  and  $\text{No. 4} - \text{No. 8}$ . Portions passing No. 8 sieve were rejected. In general the ratio of the sizes used were 1.5:1.2:1 for the size groups  $3/4 - 1/2$  in.;  $1/2 - 3/8$  in.;  $3/8 - \text{No. 4}$  respectively.

### 2.1.3 Admixtures

#### (i) Sodium Lignosulfonate

The lignosulfonate (actually a sulfonated lignin) used as part of the admixture for the low porosity concrete was a material produced in experimental quantities by the Westvaco Corporation, North Charleston, South Carolina. The lignosulfonate is prepared from purified Kraft-process pine lignin and is said to be completely free of sugars and other carbohydrates. It is supplied as the sodium salt. Two separate batches were used in this work, the second being supplied after the initial batch was exhausted.





(ii) Sodium Bicarbonate

Laboratory reagent grade sodium bicarbonate (MCB Inc.) was used in conjunction with the lignosulfonate as admixtures for the low porosity concretes.

(iii) Air Entraining Agent

The air entraining admixture used in the conventional concrete and in some of the low porosity concrete was a neutralized vinsol resin supplied by Master Builders Division of Martin Marietta Corporation.

(iv) Water-Reducing and Retarding Agent

The water reducing and retarding admixture used with the conventional concrete was Pozzolith 122-R, also supplied by Master Builders.



## 2.2 EXPERIMENTAL METHODS

General details concerning the methods and procedures followed to investigate properties of cement paste and concretes in this study have been outlined in this section, along with details of equipment used, techniques for obtaining samples, and other pertinent information.

### 2.2.1 Types of Concrete, Methods of Preparation and Fresh Concrete Properties

#### (i) Types of Concrete

Two basic types of concrete mixes were investigated in this study, i.e. low porosity concrete and conventional concrete. Two distinct formulations of low porosity concretes were prepared. In the first formulation, designated LPN concrete throughout this work, low porosity cement was used as the sole cementitious component. Its content in the various concrete mixes ranged from 8 to 10 bags per cubic yard. In the second type of formulation, a high-lime fly ash was used in the mix design and the low porosity cement content accordingly reduced. These concrete mixes, designated LPF concretes throughout this work, contained between 10 to 13 bags of total cementitious component (that is, low porosity cement plus fly ash) per cubic yard. The low porosity cement component varied from 7 to 9.5 bags per cubic yard.



The lignosulfonate content used in the various mixes ranged from 0.28 to 0.7 per cent of the weight of cement, with the second batch of lignosulfonate being more effective and requiring smaller dosages than the first. The sodium bicarbonate content ranged from 0.88 to 1.2 per cent by weight of cement.

An air entraining agent, vinsol resin, was used in some of the low porosity concretes, notably the type without fly ash. When used, the dosage was either 2.5 or 5.0 oz/100 lb. of cement. The low porosity concretes made with fly ash were found to entrain sufficient air so that in general air entraining agents were not needed. Air entraining agent was used in the fly ash bearing low porosity concretes only in the preliminary studies, and only at low dosages i.e. 1 or 2 oz/100 lb. of cement.

Two distinct formulations of concrete made with conventional portland cement were also used in this study.

The primary formulation representing conventional bridge deck concrete in this work follows the standard mix design specified by the Indiana State Department of Highways as its normal specification for highway bridge decks. The mix, designated in this work as BD concrete, contains 6 bags per cubic yard of ordinary Type I portland cement. In addition, a second portland cement formulation was used representing a much higher quality conventional concrete made with ordinary portland cement. This was a dense, low-slump mix design developed by the Iowa State Highway Department having



a Type I portland cement content of 8.5 bags per cubic yard. In this work such mixes are designated as IWA concretes.

A water-reducing and retarding admixture and the air entraining agent were used in all the conventional concrete mixes prepared in this study except in samples where entrained air was specifically deleted for a special study.

Two types of mixers were used in this work - a Lancaster SKG horizontal pan mixer of 4.2 cu. ft. capacity, manufactured by Posey Iron Inc., Lancaster, Pa., and a 2 cu. ft. utility drum mixer. In the main study the Lancaster pan mixer was used in preparing all the conventional concretes and the drum mixer in preparing the low porosity concrete mixes. This arrangement was resorted to because the horizontal pan mixer was not well suited to the unusual characteristics of the low porosity mixes.

#### (ii) Mixing of Concrete

The ANSI/ASTM Designation: C 192-76 procedure was followed in making the concrete mixes except for minor variations. A Lancaster pan mixer was used in the preliminary study for preparing both the low porosity and conventional concretes. Later in the main study the Lancaster pan mixer was used only for the conventional concretes. The mixing procedure described below is applicable to both mixers used. The first step in each mix operation consisted of "buttering" the mixing bowl. This was done by making a mortar having approximately the same proportions





of that of the batch to be mixed and spreading it over the mixer bowl and paddles. Excess mortar was removed and the ingredients of the mix were added to the mixer in the order: coarse aggregate, sand, absorption water, cement, fly ash (where applicable) and mix water. In the low porosity concretes, the mix water contained the dissolved sodium bicarbonate and sodium lignosulfonate, and also vinsol resin where the latter was to be used. In the conventional concretes the mix water was divided into three portions: one part was clear water, the second contained dissolved Pozzolith 122-R water reducing retarder, and the third contained dissolved vinsol resin.

After the coarse aggregate and sand had been introduced to the mixer, mixing was started and the calculated amount of water was added to bring the aggregates to the saturated surface dry (SSD) condition. Mixing was continued for about a minute to allow for absorption of water by the aggregates. The cement was then added, followed by the fly ash if it was to be included in the mix. The mixing water containing the appropriate admixture was then added and timing started. In the case of conventional concretes the divided mix water was added separately in the order: clear water, mix water containing dissolved water reducer, and mix water containing dissolved vinsol resin. Timing was started when the first portion of mix water was introduced to the mixing bowl; the remaining portions were added within the first two minutes of mixing. In both



types of concrete mixing was done for 3 minutes, followed by 2 minutes rest, followed by 2 minutes of further mixing.

The fresh concrete was transferred to the appropriate molds, and consolidated in two or three layers as required. Hand rodding was used throughout. After mixing, a number of tests were performed on the fresh concrete, as described below.

#### (iii) Slump

The slump test was run following the ANSI/ASTM Designation: C 143-78.

#### (iv) Vebe Time

The Vebe time of the concrete was determined in accordance with the usual procedure as designated by the manufacturer. No ASTM Standard is prescribed.

#### (v) Air Content

The air content in the freshly mixed concrete was measured following the procedure prescribed by ASTM Designation: C 173-15 (the volumetric method). In preliminary work the pressure method according to ASTM Designation: C 231-75 and the gravimetric method according to ASTM Designation: C 138-75 were also used.

#### (vi) Unit Weight

The unit weight of the freshly prepared concrete was determined according to the procedure prescribed by ASTM Designation: C 138-75.



### (vii) Curing of Concrete

Curing of the concrete was done following ANSI/ASTM Designation: C 192-76. Some specimens were cured in the fog room; others in saturated lime water. The curing environment used for specimens for each individual test will be stated in the description of that test procedure.

### 2.2.2 Instrumental Methods

#### (i) Heat Evolution Measurement

The method used in this study involved a measurement of temperature elevation in hydrating pastes kept under quasi-adiabatic conditions. This measurement was made by means of the electrical potential difference developed in a pair of thermistors, one of which was placed in the hydrating paste and the other in an inert mix kept at constant temperature. The potential difference reflecting a corresponding temperature difference was measured with a Wheatstone bridge circuit and continuously recorded on a strip chart recorder.

Mixing of Paste. The pastes used in temperature evolution studies were mixed in a Standard Hobart Mixer (Type N-50, capacity  $4.73 \text{ dm}^3$ ).

The mix water containing the appropriate admixture was poured into the mixer bowl, cement was added, and a period of 30 seconds was allowed for the cement to absorb the mix water. Mixing was done at low-speed setting for 60 seconds followed by a 45 seconds rest, followed by a mixing at medium-speed setting for 60 seconds. Immediately



after the completion of this mixing procedure, the paste was poured into the appropriate container, consolidated by striking on the laboratory bench a few times and immediately placed in the temperature evolution test apparatus.

The mixing procedure described is similar to that given by ASTM Designation: C 305-65, but differs from it in that the time for mixing at low-speed setting was 60 seconds in this work instead of the recommended 30 seconds and the resting time was 45 seconds, instead of the recommended 15 seconds. These modifications were required because of the unusual mixing response of the low porosity cement paste.

Apparatus. The apparatus consisted of a styrofoam insulating system, two disposable plastic containers of 120 ml. capacity (one for the paste under study, and the other for the inert reference material), a pair of matched thermistors, a Wheatstone bridge and a recorder. Contact between the paste and the thermistors was maintained through mercury enclosed in crimped copper sleeves. Cement paste, made as described in the section above, was cast in one single layer in one of the plastic containers. The inert reference material placed in the other container was Ottawa sand (20-30 mesh) mixed with water, having the same water:sand ratio as the water:cement ratio of the paste under test. Immediately after casting the containers were sealed and placed in the device and temperature measurement started.





## (ii) Differential Thermal Analysis

Introduction. Differential thermal analysis is a technique in which temporary differences in temperature between thermally active substance under test and an inert reference material are recorded and plotted against either time or temperature as the system is heated at a controlled rate of temperature increase. The analysis involves placing small amounts of the sample and reference material into two matched specimen holders and heating these in a specially designed furnace. The measurement involves monitoring any temperature difference developed between sample and reference by thermocouples in contact with the two powders.

Apparatus. A D-600 Deltatherm III DTA apparatus (manufactured by Technical Equipment Corporation, Denver, CO) was used along with a Sargent SRG recorder. The sample size was approximately 50 mg. The parameters used throughout all the analytical measurements were: heating rate,  $10^{\circ}\text{C}$  per minute; recorder differential temperature sensitivity, 2 in. per  $^{\circ}\text{C}$ ; upper heating limit,  $1000^{\circ}\text{C}$ . Fired kaolinite was used as the reference material. Samples under investigation were dried in an oven at  $105^{\circ}\text{C}$  overnight. The dried samples were powdered in a porcelain mortar and screened until all of it passed a No. 100 sieve.

## (iii) Scanning Electron Microscopy

Background. The technique of scanning electron microscopy (SEM) was developed in the early 1960's and its use



has extended into many fields involving the study of solids.

Scanning electron microscopes differ from transmission electron microscopes in the method of image formation employed. In the SEM, the lens system is designed to focus the incident beam of electrons to a very fine spot, about 100 Å in diameter, before the incident beam interacts with the specimen. The fine spot is dynamically scanned across an area of the specimen surface. Secondary electrons emitted from the surface are collected by a collecting device and the resulting electrical signal, after amplification, is used to modulate the brightness of a cathode ray tube (CRT) display. The CRT is scanned synchronously with the incident beam to generate a one-to-one image of the surface. Coating the sample surface with a thin layer, typically 200 Å thick, of carbon or gold-palladium alloy improves the image obtained on the screen by minimizing the buildup of electrical charge on the surface being observed.

Apparatus. The equipment used was an ISI Super III A scanning electron microscope manufactured by ISI Inc., Santa Clara, California.

An accelerating voltage of 15 kV was used throughout, and the specimens were examined at magnifications ranging from 100x to 10,000x. Micrographs were obtained using Polaroid type 52 film.

Dried specimens were fractured and mounted on aluminum stubs with the fresh fracture surfaces facing upward. Electrical conductivity between the specimen and the stub was



achieved by mixing silver clay with Duco cement to mount the specimen. The specimens were then coated to a nominal coating thickness of 200 Å of gold-palladium alloy, using a sputter-type coater (Hummer I model manufactured by Technics, Inc., Alexandria, VA).

#### (iv) X-ray Diffractometry

Background. The technique of X-ray diffractometry is used in various fields of study involving the analysis of crystalline phases. Its use extends to the qualitative identification of crystalline compounds in the pure state and in mixtures. The sample to be analyzed is prepared and analyzed generally in the powdered form. Polymorphic forms of a single compound can be distinguished; e.g. the three forms of  $\text{SiO}_2$  (quartz, tridymite and cristobalite) or the three forms of  $\text{CaCO}_3$  (calcite, vaterite and aragonite). Furthermore, different hydrates of a given compound have different crystal structures, and therefore give different X-ray patterns.

Apparatus and Methods. A Siemens X-ray Diffractometer, Type D500 was used. The diffractometer angle range covered was from  $10^\circ$  to  $60^\circ$ ,  $2\theta$ . The X-ray runs were performed under the following conditions:  $\text{CuK}\alpha$  radiation; monochromator; voltage - 50 kV; amperage - 20 ma; slits -  $1^\circ$  -  $1^\circ$  -  $1^\circ$  -  $0.15^\circ$  -  $0.15^\circ$ ; time constant; 4 seconds; goniometer speed -  $2^\circ$ /minute. Appropriate amounts of dried samples to be analyzed were powdered in a porcelain mortar until all



material passed a No. 200 sieve. The sample was then homogenized using a laboratory Spex homogenizer, and mounted in an aluminum sample holder using the McCreery technique to ensure random orientation.

#### (v) Pore-Size Distribution Measurement

Background. The method used in this study to measure the pore-size distributions of the mortar pieces picked from concretes was mercury intrusion porosimetry. The pore diameter range measurable by mercury porosimetry runs from 400 microns or more to as little as 25 Å, depending on the pressure capacity of the instrument. The pressure required to force a non-wetting liquid such as mercury into a pore of a sample is a function of the surface properties of the liquid and the solid, and the geometry of the pore. The usual relationship assumes cylindrical pores, and was given by Washburn (70) as:

$$p = \frac{-4\gamma\cos\theta}{d}$$

where  $p$  = required external pressure

$\gamma$  = surface energy of the liquid

$\theta$  = contact angle between the liquid and the solid

$d$  = diameter of the pore.

Apparatus. The instrument used was a commercial unit (Catalog No. J5-712 5D. American Instrument Company, Silver Springs, Md.), modified in certain respects, and has a maximum capacity of 60,000 psi.

The porosimeter consists of a low pressure penetrometer capable only of one atmosphere pressure and a separate high





pressure vessel, pressure generating pump, and measurement systems for monitoring pressure and intrusion. The hydraulic fluid used was a mixture of two parts of a transformer oil and one part kerosene. Compressing the hydraulic fluid generates heat. To minimize the resulting temperature rise an air circulation fan was attached to the side of the wall of the cabinet to cool the pressure vessel. The commercial unit has two pressure gages, 0-5000 psi and 0-60,000 psi; a 0-500 psi was added to increase the accuracy in the coarse pore diameter range. The intrusion volume capacity is 0.2 ml.

Method. The sample under investigation was broken in such a way as to obtain a small piece having fresh surfaces and a suitable shape for the penetrometer space. This specimen was inserted into the penetrometer, evacuated to approximately 20 mm Hg pressure, and the penetrometer was flooded with mercury to completely surround the specimen. The penetrometer was then inserted first into the low pressure portion of the system, and subsequently into the high pressure chamber for high pressure mercury intrusion. Intrusion was carried out following a preset time and pressure schedule. At each pressure stop the pressure was held long enough to allow intrusion equilibrium in the sample. Correction factors obtained by a blank test were applied to the actual intrusion readings.



## (vi) Permeability Testing

Introduction. Information about permeability of concrete is of basic importance for evaluation and control of performance under service conditions. This is especially true for highway bridge deck concrete. In fact, GjØrv and Loland (71) suggested that specifications for concrete durability should be based on permeability rather than on detailed specification of factors of only indirect importance such as cement content, water:cement ratio, maximum aggregate size, etc.

Basic data on permeability in the literature is extremely limited and existing methods are considered by most workers to be unreliable and difficult to reproduce. A variety of methods have been used, and the testing conditions are so different that it may be difficult to compare test results.

Many parameters must be carefully controlled to make permeability results meaningful. For example, a rise in water temperature from 10 to 20°C will increase the rate of water flow by approximately 30 per cent (71). Variations in the degree of saturation of air dissolved in the water in the system may produce wide variations in the measured value of permeability of concrete. The use of different applied hydraulic pressures may also have significant effects on the measured permeability.

Robson (72), commenting on the reproducibility of permeability tests stated, "Nearly all permeability



experiments on cemented materials have shown a wide dispersion of results when conducted with the greatest care on apparently identical specimens." These difficulties are compounded with low porosity concretes and other cement-rich concretes where low permeabilities obtain. Despite these prospective difficulties and uncertainties, a sustained effort was made to study permeability of concretes prepared in this study. Equipment in use by the U.S. Army Corps of Engineers (73), for lean concretes was adapted for use in this study.

Theoretical Background. For water-saturated concrete the rate of water flow can be calculated on the basis of Darcy's law. The treatment below is based on that given by GjØrv and Loland (71).

Considering the equilibrium of all forces acting on a small volume of fine grains when water is flowing through, the following equation for the rate of apparent water flow is obtained:

$$q = cd^2 \frac{\rho_w \cdot g}{\mu} \cdot \frac{\Delta h}{z}$$

where

$c$  = a constant, depending on the pore geometry.

$d$  = diameter of the grains filling up the element

$\rho_w$  = density of liquid

$g$  = gravitation constant

$\mu$  = dynamic viscosity coefficient

$\Delta h/z$  = pressure gradient

By definition the product  $cd^2$  is called the internal



permeability  $k$ . If this permeability is multiplied by the factor  $\frac{\rho_w \cdot g}{\mu}$  the hydraulic conductivity, ( $K$ ) of the material is obtained.

$$K = k \cdot (\rho_w \cdot g) / \mu \quad \text{m/sec.}$$

If both  $\rho_w$  and  $\mu$  are assumed to be constant, the following expression for Darcy's law can be written:

$$q = -K \cdot \Delta h / z$$

The permeability measured is designed to provide a numerical value for  $K$ , in units of feet/sec. or meters/sec.

Apparatus and Method of Measurement. The permeability equipment was fabricated at Purdue University and was based on the apparatus used by the U.S. Army Corps of Engineers (73). The test apparatus is schematically diagrammed in Figure 2.2.1 and a picture of the equipment is shown in Figure 2.2.2. Cylindrical concrete specimens of dimensions of 6 in. in diameter and 12 in. in length were prepared and cured as described in Section 2.2. The samples were cured in saturated lime solution for ages between one to six months before testing. In preparing the actual specimens, after curing, both ends of concrete cylinders were sawn off to a depth of 1 in. The actual specimens, 2 in. in height, were sawn off from either end of the remaining cylinder. Both specimens from the same cylinder were tested at the same time in the two test compartments available in the equipment. The inside diameter of the sample container was 7/8 in. greater than the outside diameter of the specimen. Both the cylindrical surface





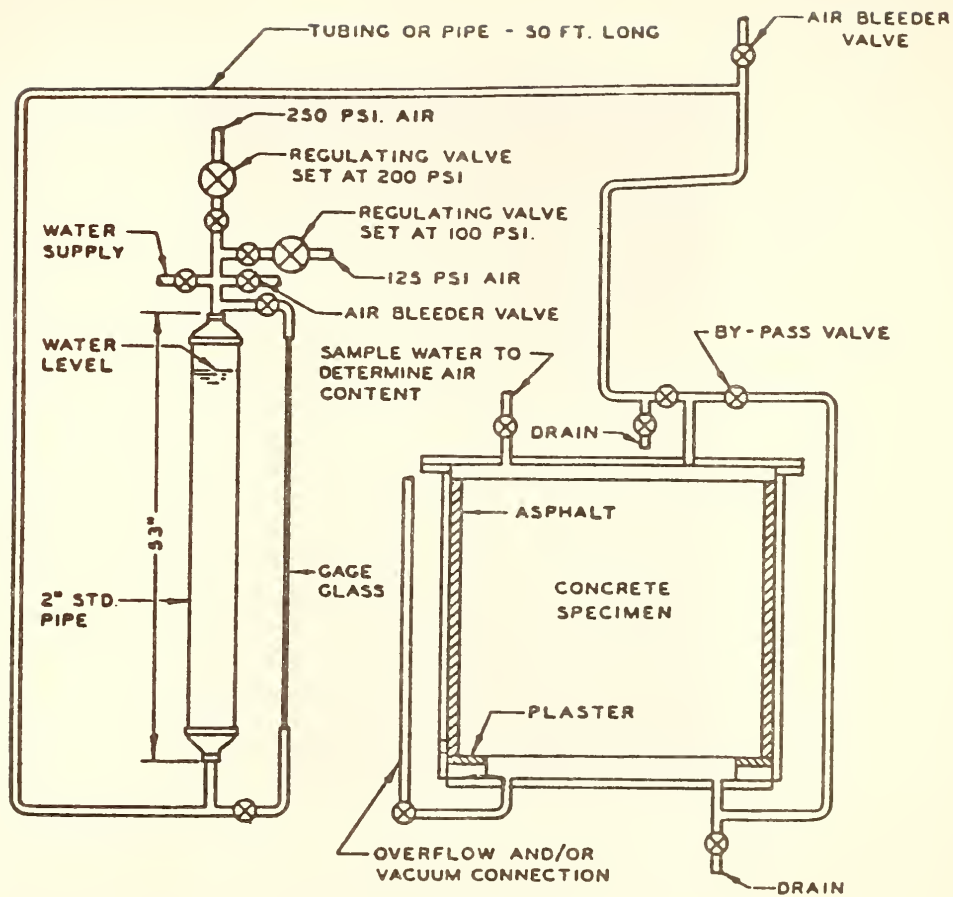


Figure 2.2.1 Permeability Test Assembly (Schematic)



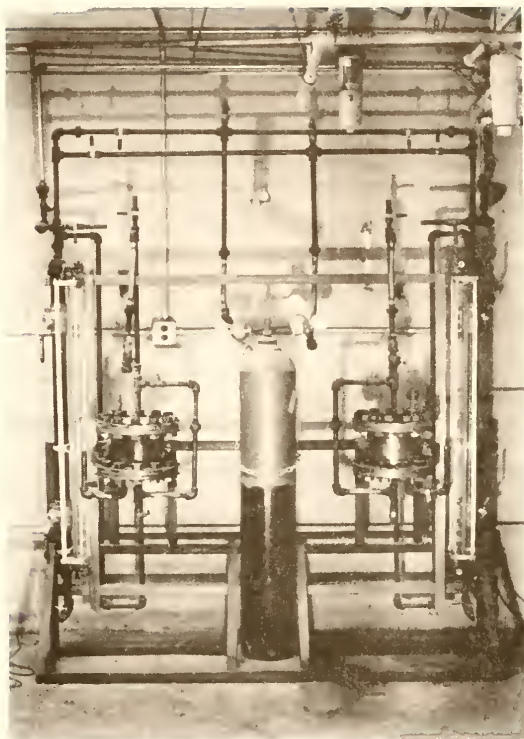


Figure 2.2.2 Permeability Apparatus



of the specimens and the inside cylindrical surface of the container were painted with a hot paraffin-rosin compound before each specimen was placed in the container. Each specimen was bedded on a retainer ring, at the lower end of the container, using hydrostone, a gypsum product of high porosity as compared with that of concrete. After each specimen had been bedded, and the hydrostone had hardened, a seal layer of about 1/2 in. in thickness composed of paraffin-rosin sealing compound was poured on top of the hydrostone. The remaining annular space between the specimen and the side of the container was filled with hot 200-300 penetration grade asphalt up to about 1/2 in. from top level of sample. After the asphalt had cooled down and shrunk, the depression formed and the remaining space was filled with paraffin-rosin compound to prevent the oil in the asphalt from mixing with the water during the test. The top and bottom of each container was bolted with a gasket, and all pipe connections made. The desired water pressures were produced by applying compressed air to the water surface in a calibrated reservoir of standard 2 in. pipe and the inflow was periodically measured by the fall in level of the water surface as indicated by a glass gage connected to the reservoir.

In pressure testing, the system was exhausted to a residual pressure of no more than 2 in. of mercury (i.e. 28 in. of "vacuum"). It was then filled with water at  $23 \pm 2^{\circ}\text{C}$  until the vacuum gage showed an abrupt decrease to about 20 in. of "vacuum" at which time the vacuum



valve was closed. Trapped air was flushed out by repeatedly opening the bleeder valve until water flow appeared, upon which the bleeder valve was closed. With the bleeder and bypass valves closed 100 psi air pressure was applied to the water reservoir. The overflow standpipe was opened and after 5 minutes the air pressure was increased to the working pressure of 200 psi. This started the test. The glass gage level was observed and recorded daily with the time of observation recorded to the nearest 0.1 hr. Observation was continued until after the flow became essentially constant, normally 14-20 days. The water in each assembly was replaced at frequent intervals - about once a week - so that the air content did not exceed 0.2 per cent.

The differences of readings of water reservoir level were converted to volume flow in milliliters by multiplying it by the reservoir calibration constant, previously obtained by a calibration procedure. The rate of flow in ml per day was obtained by dividing the volume by the elapsed time between readings. The apparent permeability constant was calculated from the following formula:

$$K = \frac{Q}{A \times \frac{d\phi}{dx}} \quad \text{or} \quad K = 1.772 \times 10^{-10} \frac{Q \times L}{A \times P} \text{ ft/sec}$$

where  $K$  = apparent permeability in ft/sec

$Q$  = flow rate in ml per day

$L$  = height of sample, in ft.

$P$  = pressure in psi.

and  $A$  = surface area of specimen in  $\text{ft}^2$ .

The time taken to measure permeability of a concrete specimen in this test was approximately four weeks.





About two weeks were allocated in attempts to obtain constant flow in the concrete samples. The subsequent actual readings normally were secured over a two week additional period. The average flow rate for the final two weeks of the test is used in estimating the permeability of the concrete (as compared to 5 days described by the method in (73)). In an attempt to check the source of the severe daily fluctuations observed, it was thought desirable to check that the through-put indicated in the calibrated glass tube was actually passing through the concrete sample. To do this, a glass tube of the same inside diameter as the calibrated glass tube was attached to the overflow pipe. The drop of water level in the calibrated glass tube and the rise of level in the glass tube attached to the overflow pipe mostly did not correspond on daily basis, but over an extended period, the correspondence was reasonably good.

Prior to establishing controlled operation, a considerable amount of time was spent eliminating leaks in the pipe connections and valves. However, once these difficulties were overcome, very little trouble was experienced in the operation of the equipment, per se. However, the measurement of flow on a day to day basis was not consistent even though the apparatus appeared to be functioning well and without leaks. Some of the variation is probably associated with temperature fluctuations. The equipment was not thermostatted and was by necessity



mounted in a non-air conditioned room. The room temperatures were recorded throughout the entire period of the permeability measurement, and ranged from 18-26°C.

(vii) Rapid Freezing and Thawing Test

The rapid freezing and thawing test in water was performed on varying mixes of the four basic concrete types under investigation in accordance with ANSI/ASTM Designation: C 666-77.

Test Procedure. The rapid freezing and thawing test was carried out in one or the other of two freeze-thaw cabinets (Catalog No. CT-110, supplied by Soil Test Inc., Evanston, IL). Each has a capacity for holding fifteen 3 x 3 x 15 in. standard concrete beams.

The ANSI/ASTM Designation: C 666-77, Procedure A, rapid freezing and thawing in water, was chosen because this procedure is said to give a better correlation with field performance (74). The samples were prepared and cured as described in section 2.2.1 (ii). Curing was carried out in saturated lime solution for 14 days for most samples except that longer times of curing was resorted to for special studies. These specimens from each mix were subjected to the freezing and thawing cycles and were tested at approximately 30 cycle intervals for weight change, and for change in fundamental dynamic resonance frequency. Additionally, pulse velocity measurement was used for selected samples. Almost all specimens were exposed to at least 400 freezing and thawing cycles



because after the 300 cycles recommended by the ANSI-ASTM procedure there was no significant damage done to the low porosity concrete specimen.

The change in Young's modulus of elasticity was determined from the fundamental transverse frequency readings as described in ANSI/ASTM Designation: C 215-76. The pulse velocity through the concrete specimens was measured according to the procedure recommended by ASTM Designation: C 597-79, using a "V-meter" supplied by James Electronics Inc. The modulus of elasticity was determined using the relationship:

$$E_d = \rho V^2 \frac{(1+\mu)(1-2\mu)}{1-\mu} \times 1.45 \times 10^{-5} \text{ psi}$$

where  $\rho$  = density of concrete, g/cc

$\mu$  = Poisson's ratio (assumed to be 0.16)

$V$  = longitudinal wave velocity, in cm/sec.

$E_d$  = dynamic modulus of elasticity



PART THREE  
PRELIMINARY STUDIES





### 3.1 INTRODUCTION

Preliminary studies were conducted to investigate certain characteristics of the low porosity concretes, and some mix design features from the standpoint of handling the fresh concrete. Specifically, the latter included the ability to retain workability over extended periods of time (a property associated with but not always controlled by slump loss with time); the appropriate amount of fly ash to be incorporated into the mix; the dosage of air entraining agent required to give a suitable level of entrained air; and the effect of using different mixers on workability and entrained air. The strength characteristics of low porosity concrete both with and without fly ash were determined for a period up to one year. Additionally, the heat evolution characteristics of cement pastes and certain characteristics of the fly ash used in this work were also studied.



## 3.2 WORKABILITY OF LOW POROSITY CONCRETES

### 3.2.1 Effect of Mixing Time on Slump and Workability

Trial mixes were made to observe the loss of slump with respect to time of a 0.25 cu. ft. batch of low porosity concrete mix (without fly ash - LPN concrete), using different mixing times but the same water:cement ratio of 0.32. In these trials, mixing was carried out using the Lancaster pan mixer, with no cover, and the initial mixing time was independently varied, mixing times of 3 , 6 and 9 minutes being used. The initial slump and slump readings at 30 minute intervals were taken. In between slump measurements, the mix was mounded up and covered with a wet burlap cloth to minimize evaporation. The relationship between initial slump and initial mixing time is given in Figure 3.2.1. There is a strong decrease in slump with time of mixing.

In all mixes the slump was zero after 30 minutes (after discharge from the mixer) and all mixes were unworkable after 60 minutes. Batches with initial mixing time of more than 3 minutes lost their cohesiveness and seemed to become dry much earlier than batches mixed initially for 3 minutes. A second batch with the same mix proportions was subsequently mixed in a second Lancaster pan mixer equipped with a built-in cover to prevent evaporation. The same mixing times of



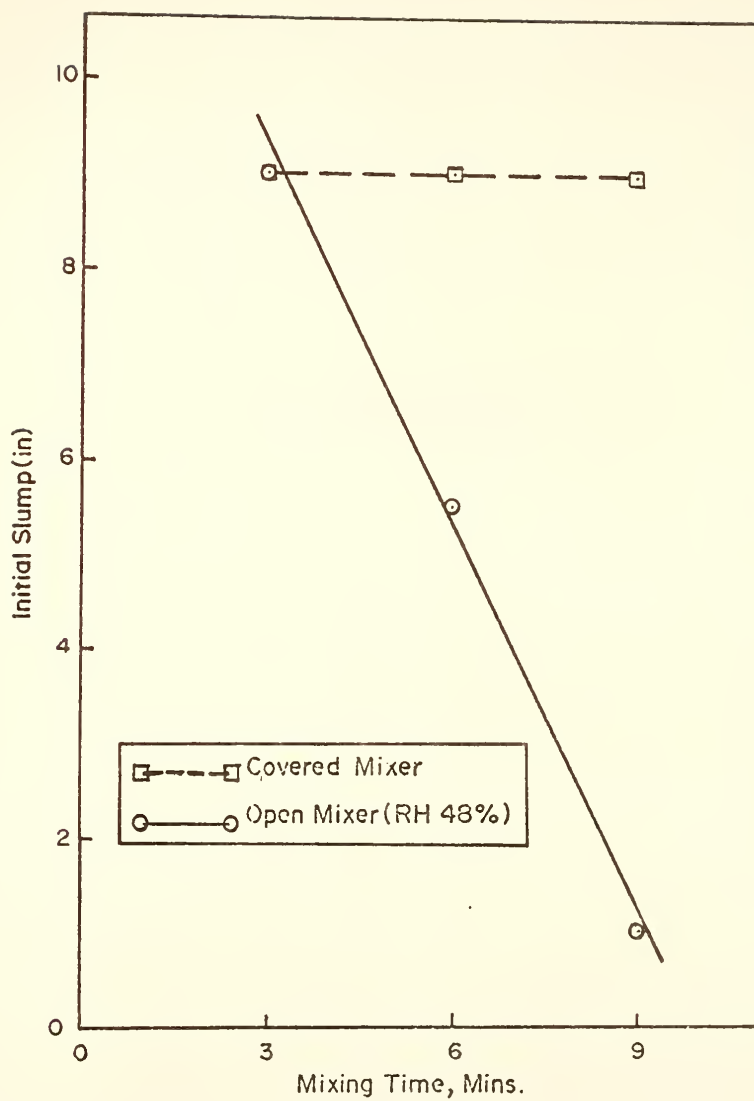


Figure 3.2.1 Effect of Initial Mixing Time on Initial Slump



3, 6 and 9 minutes were independently used. As indicated in Figure 3.2.1, an initial slump of about  $9\frac{1}{2}$  in. was recorded for all of these concretes prepared with the covered mixer at the 3 different mixing times. Thus, the effect of extended mixing observed in the original mixes was due to evaporative loss of water, which seems to produce a major effect on workability in these very low water content mixes.

### 3.2.2 Proportioning of Fly Ash in Low Porosity Concrete

Various proportions of fly ash by weight of low porosity cement (namely; 7, 10, 13, 20, 30, 35 and 40 per cent) were separately incorporated in low porosity concrete mixes, and the low porosity admixture contents were also independently varied. Details of the various trial mixes batched are given in Table 3.2.1. In this table, the water contents are given as ratios of the water to cementitious solids (cement plus fly ash). All batches were mixed in a Lancaster pan mixer and the procedure used is as described in 2.2.1 (ii).

Measurements were made of the slump-time characteristics and also the Vebe time measurements with respect to time of all of these mixes. The results of these measurements are given in Table 3.2.2. In this table, the elapsed time measured is the time between the first contact of water to the ingredients in the mixer and the time the measurement was taken. A plot of the Vebe measurements with





Table 3.2.1 Trial Mixes with Varying Proportions of Fly Ash in Low Porosity Concrete

Mix Design	% Fly Ash	% Lignosulfonate	% Sodium Bicarbonate	*Water:Cementitious Solids Ratio
1	7	0.7	1.2	0.30
2	7	0.6	1.1	0.30
3	7	0.7	1.2	0.32
4	7	0.7	1.2	0.34
5	10	0.7	1.2	0.30
6	10	0.7	1.2	0.32
7	10	0.7	1.2	0.34
8	13	0.6	1.1	0.29
9	13	0.7	1.2	0.32
10	13	0.7	1.2	0.32
11	13	0.7	1.1	0.34
12	20	0.58	1.0	0.30
13	30	0.54	0.9	0.30
14	35	0.52	1.2	0.30
15	35	0.52	0.88	0.28
16	40	0.5	0.88	0.30

\* Percentage by weight based on weight of cement.



Table 3.2.2 Workability of Plastic Fly Ash-Bearing Low Porosity Concretes with Time as Measured by Slump and Vebe Time

Fly Ash % by Weight of Cement	Water: Cementitious Solids Ratio	Elapsed Time (min.)	Slump (in.)	Vebe Time (sec.)	Ambient Relative Humidity, %
7	0.30	9	5-1/2	2.5	
		30	0	14	47
		60	0	19	
	0.30	8	Flowing*	1.5	
		30	0	13	40
		60	0	18	
	0.32	8	Flow	1	
		30	2	8	48
		60	0	14	
		90	0	22	
	0.34	8	Flowing*	0	
		30	2	5	
		60	0	13	47
		90	0	12	
		180	0	20	

\* Flowing: Concrete having an initial slump of about 7 in. to 9 in. and collapsing to almost floor level in less than 30 sec. after the cone has been removed.



Table 3.2.2 continued

Fly Ash % by Weight of Cement	Water: Cementitious Solids Ratio	Elapsed Time (min.)	Slump (in.)	Vebe Time (sec.)	Ambient Relative Humidity, %
10	0.30	7	Flowing	0	45
		30	0	17	
	0.32	4	Flowing	1	58
		30	0	11	
		60	0	15	
		90	0	22	
	0.34	7	Flowing	2	47
		30	1-1/2	7	
		60	0	13	
		90	0	16	



Table 3.2.2 continued

Fly Ash % by Weight of Cement	Water: Cementitious Solids Ratio	Elapsed Time (min.)	Slump (in.)	Vebe Time (sec.)	Ambient Relative Humidity, %
13	0.29	3	3	7	46
		30	0	15	
	0.30	5	5-3/4	4	39
		30	0	12	
		60	0	15	
		75	0	15	
	0.32	6	6-1/2	1	71
		30	0	13	
		60	0	21	
	0.34	5	Flowing	2	39
		30	2-3/4	5	
		60	0	11	
		90	0	16	
20	0.30	3	Flowing	1	61
		30	0	10	
		60	0	16	
30	0.30	4	6	1	54
		30	3-1/4	2	
		60	0	10	
		90	0	15	





Table 3.2.2 continued

Fly Ash % by Weight of Cement	Water: Cementitious Solids Ratio	Elapsed Time (min.)	Slump (in.)	Vebe Time (sec.)	Ambient Relative Humidity, %
35	0.30	5	6	1	
		30	5-1/4	1	
		60	1/4	4	69
		90	0	10	
		120	0	19	
	0.28	5	5	1	
		30	3	2	
		60	1/4	9	61
		90	0	16	
		4	6-1/4	<1	
40	0.30	30	5-1/2	1	63
		60	0	6	
		90	0	12	

\* Flowing: Concrete having an initial slump of about 7 in. to 9 in. and collapsing to almost floor level in less than 30 sec. after the cone has been removed.



respect to time for each percentage addition of fly ash at  $w/c = 0.30$  is given in Figure 3.2.2.



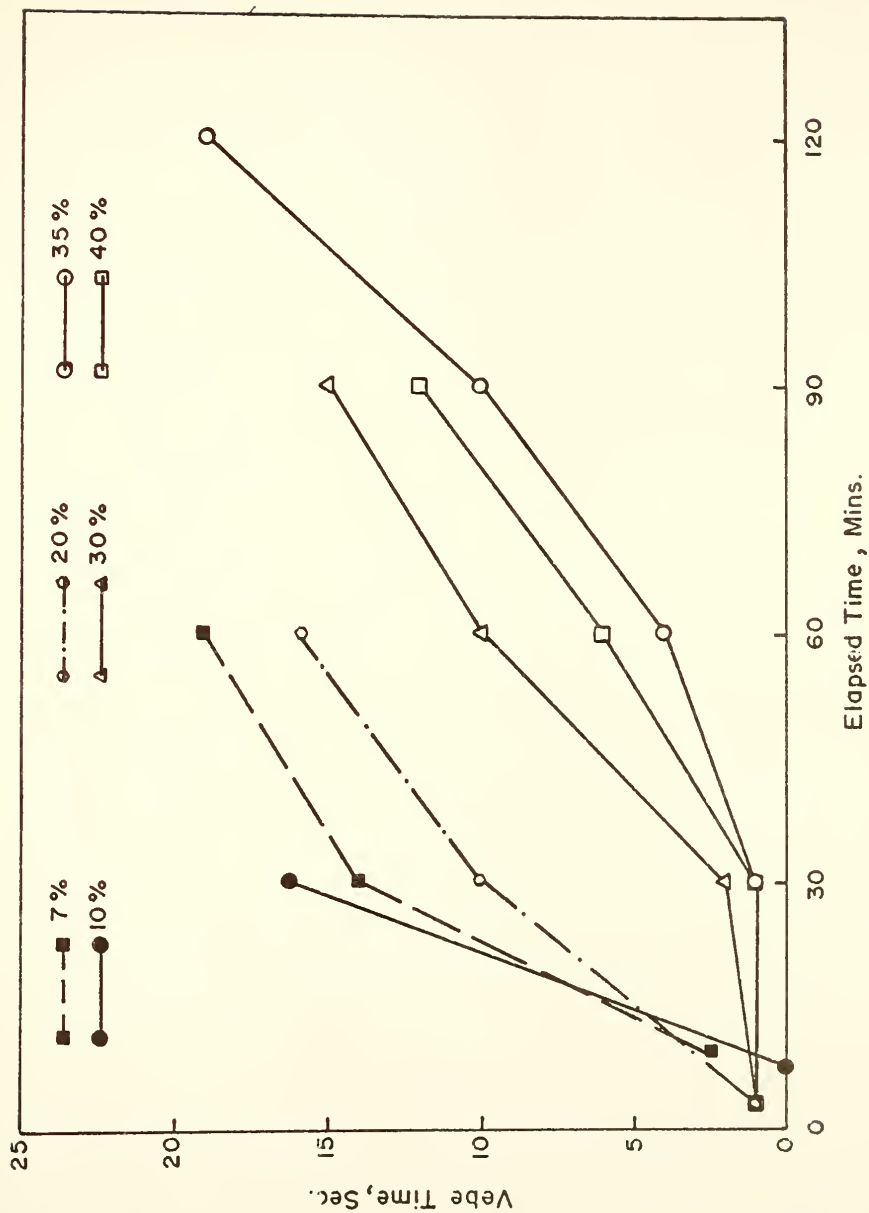


Figure 3.2.2 Changes of Vebe Time on Standing for Mixes with Various Percentages of Fly Ash



### 3.3 USE OF AN AIR ENTRAINING AGENT IN LOW POROSITY CONCRETES

#### 3.3.1 Effect of an Air Entraining Agent in Low Porosity Concretos Without Fly Ash

Two air-entrained concrete mixes were prepared of the same mix ingredients, with vinsol resin being used as the air entraining agent. Two different dosages, namely 2.5 and 5.0 oz/100 lb. of cement were used. In addition, a reference mix with no air entraining agent was prepared and subjected to the same observations.

The concretes were mixed using a drum mixer as described in section 2.2.1 (ii). The air contents were determined by both the pressure method and the volumetric method. The results were not concordant, the pressure determinations giving higher and more variable readings than the volumetric method. Typical values for the concrete without air entraining agent were 1.5% for the volumetric method and 6.0% for the pressure method. It appeared that the pressure method was not very well adapted to low porosity concrete, the tenacity of the material tending to result in high and variable readings.

To check on the amount of air in the fresh concrete, a modified point count determination of air content of the hardened concrete was determined using the recommended procedure of ASTM Designation: C 457-71. As





indicated in Section 3.3.3, this showed closer agreement with the value obtained by the volumetric method, which was then considered correct.

Results of entrained air for the air-entrained concretes and the reference concrete are given in Table 3.3.1. The air content increased only slightly by use of the air entraining agent, to a maximum of 3.0 per cent. Subsequently, an additional trial with dosages of 5 oz/100 lb. of cement, air contents of slightly higher values, up to 4 per cent, were obtained. It thus appears that vinsol resin could not serve satisfactorily as an air entraining agent in low porosity concrete without fly ash.

### 3.3.2 Effects of An Air Entraining Agent in Fly Ash-Bearing Low Porosity Concretes

#### (i) Mixing with Pan Mixer

Several batches of fly ash-bearing low porosity concrete with the same mix proportion of 35 per cent fly ash by weight of cement were mixed using the Lancaster pan mixer. Different doses of vinsol resin (1, 2 or 3 oz/100 lb. of cement) were separately added to each mix at the same water:cement ratio. A reference mix of the same composition but without an air entraining agent was also prepared. Two different mixing sequences were used in this section.

In the first procedure the mix water was divided into two portions, and the sodium bicarbonate and sodium lignosulfonate dissolved in one of them. The



Table 3.3.1 Amount of Entrained Air vs. Dosage of Air  
Entraining Agent in a Low Porosity Concrete\*  
without Fly Ash

Mix Designation	Vinsol Resin oz/100 lb. of cement	% Air Content (Volumetric Method)	w/c	Slump
LPN-1	0.0	1.5	0.26	6.0
LPN-2	2.5	3.0	0.28	9.5
LPN-3	5.0	3.0	0.27	9.0

\* Concrete design parameters:

1 fl. oz. = 28.4 ml.

Cement content: 8.2 bags/cu. yd.

% Sodium lignosulfonate by weight of cement: 0.56

% Sodium bicarbonate by weight of cement: 1.2



other portion contained vinsol resin. The dissolved sodium bicarbonate and sodium lignosulfonate mix portion was first added, and after a minute of mixing, the portion containing vinsol resin was added. Mixing for a further 2 minutes then took place, mixing was stopped for 2 minutes, and final mixing of 2 minutes was then done as described in section 2.2.1 (ii).

In the second mixing procedure all the admixtures were dissolved in the same mix water and mixing was done as described in section 2.2.1 (ii). There was no difference in the measured air content resulting from the two mixing procedures. The results of the air content measurements by the volumetric method are plotted in Figure 3.3.1.

#### (ii) Mixing with Drum Mixer

The same mix proportions and procedures for mixing as used earlier with the Lancaster pan mixer were also applied using a 2 cu. ft. drum mixer. The speed of the rotating drum mixer was 20 revolutions per minute. Air content determination was made using the volumetric method. The dosage of vinsol resin used were the same as used previously. Results of the measurements are plotted in Figure 3.3.1.

The results indicate that using the pan mixer entrained a consistently higher air content at a given dosage of air entraining agent, the difference in each case being about 2-1/2 per cent air. Increasing dosage of air entraining agent increases the air content as might be expected. However, even without an air entraining agent, an air content



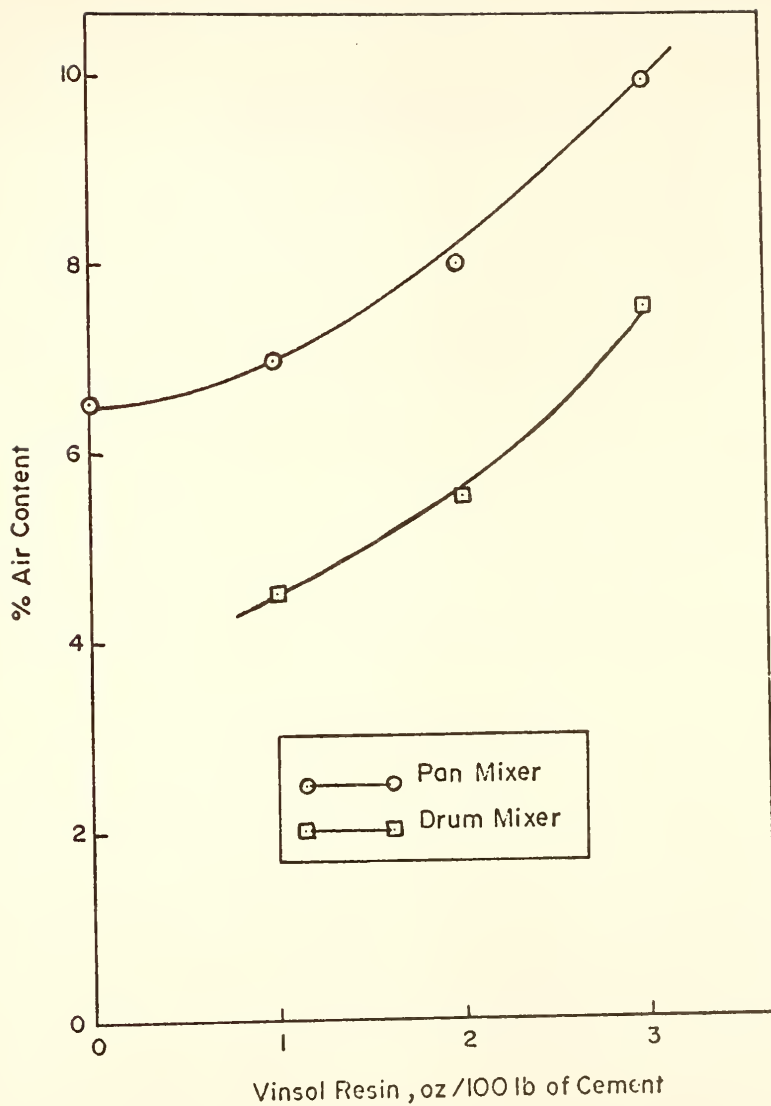


Figure 3.3.1 Effect of Type of Mixer on Entrained Air at Several Dosages of Vinsol Resin





in the range of 6-1/2 per cent was obtained using the pan mixer.

### 3.3.3 Air Content of Hardened Low Porosity Concretes

Using the modified point count method as described by ASTM Designation: C 457-71, the air content of the two formulations of low porosity concretes in the hardened state were measured and the results compared with the volumetric method of air determination of the fresh concrete.

Results of the two methods of air content determination are shown in Table 3.3.2. In both cases the results for the hardened state determination are slightly less than the corresponding results measured in the fresh state by the volumetric method. This is in accord with expectations.

### 3.3.4 Results and Discussion

Previously it has been mentioned that several different batches of ground clinker (low porosity cement) have been used in this study. There was a noticeable difference in the fresh concrete prepared from cement used in the initial part of the study - the old batch - and in the latter part of the study - the new batch, being of measured fineness  $5400 \text{ cm}^2/\text{g}$  and  $4500 \text{ cm}^2/\text{g}$  respectively.

The new batch used in a concrete mix required a smaller amount of water to produce the same consistency. The old batch had been stored for four years prior to use, and it seems likely that this is responsible for the difference. The



Table 3.3.2 Comparison of Air Content Determinations in Fresh and Hardened Concrete

Sample	% Air Content of Fresh Concrete (Volumetric Method)		Modified Point Count Method	
	% Air Content	Specific Surface $\alpha$ (in. <sup>-1</sup> )	Spacing Factor L (in.)	
LPF-6	8.0	7.5	811	$4.7 \times 10^{-3}$
LPN-3	1.5	0.6	480	0.025



same pattern was observed for the lignosulfonate. Here also two batches of lignosulfonate were used. It required a smaller dosage of the new batch to produce a given consistency. It was observed that the old batch had partly caked but was easily amenable to being powdered.

In general, with all materials, mixing times of three minutes followed by a two minute rest period and a further two minutes of mixing yielded good workable concretes. Longer initial mixing times produced concretes which appeared to become dry quickly.

The study confirmed an earlier observation (21) that the fresh low porosity concrete (without fly ash) had a short working life, and generally becomes unworkable after about 60 minutes. This characteristic of the fresh concrete needs to be improved for obvious reasons of transporting concrete over some distance from mix sites and to allow for possible on-site delays.

It was thought that fly ash might improve this behavior. Trials were made with several proportions of fly ash by weight of the cement in the concrete mix. The results of these trials are given in Table 3.2.2 and Figure 3.2.2. A treatment of 35 per cent of fly ash by weight of cement yielded optimum results in terms of a longer working time for fresh concrete at a low water:cement ratio of 0.30. Concretes containing smaller additions of fly ash showed progressively less working time. A good workable mix with long working life could be obtained for as little as a 7



percent proportion of fly ash by weight of cement. This was achieved, however, only at a higher water:cement ratio, 0.34.

A seemingly anomalous situation was observed with concretes prepared using a 13 percent of fly ash by weight addition. Such concrete appeared to segregate to an unusual extent, and also to lose workability unusually quickly in comparison with concretes mixed with 10, 20 or 30 percent fly ash additions.

The following observations were made with the various formulations of low porosity concretes:

(i) Low Porosity Concrete Prepared  
Without Fly Ash:

a) A water:cement ratio of between 0.24 to 0.30 gave concrete of high slump (between 6 and 10 in.). However, even with such a high slump, the concrete was difficult to work, seeming to resist rapid movement or displacement. For example, it was difficult to push a trowel through it rapidly.

b) High doses of air entraining agent did not help in entraining acceptable levels of air. For example, using vinsol resin, a dose of 5 oz/100 lb. of cement entrained only 4% air, while a 1.5 oz/100 lb. of cement dose of the same admixture entrains about 6% air in a conventional concrete.

c) Despite the low water:cement ratio, bleeding occurred with this concrete. Lowering the sodium lignosulfonate content helped reduce it considerably, but workability became poorer.





d) There is some tendency to segregate with this concrete, again in spite of the low water:cement ratio.

e) The unit weight of the fresh concrete was unusually high - about  $155 \text{ lb/ft}^3$ .

f) As stated earlier, the fresh concrete had a limited working time, i.e., it became unworkable after about 60 minutes.

(ii) Low Porosity Concrete Prepared  
With Fly Ash:

a) With the same water:cement ratio range used in (i) above, about the same high slump was recorded for this concrete. However, this concrete was very workable, and could be deformed and remolded readily.

b) The addition of fly ash helped entrain an appropriate level of air without an air entraining agent. The amount of air entrained was dependent on the sodium lignosulfonate used.

c) No bleeding occurred for this type of concrete.

d) The unit weight of the fresh concrete was about  $150 \text{ lb/ft}^3$ , slightly lower than that of the low porosity concrete without fly ash.

e) The fresh concrete retained its workability for periods generally of at least 90 minutes.

f) In contrast to the strong influence of mixing time on the initial slump of non-fly ash-bearing low porosity concretes mixed in an open mixer for 3, 6 or 9 minutes as shown previously (Figure 3.2.1), the initial slump for the



fly ash-bearing concretes were almost the same for mixing times of 3, 6 or 9 minutes in both the covered and the open pan mixers. The initial slump was about 8-1/2 in. for all measured concretes at the indicated mixing times and with both mixers.

g) Both types of concretes assumed a mirror finish when cast against a plastic sheet.

h) For both types of concretes, the fresh concrete with slumps higher than 6 in. were observed to flow along inclined surfaces when the slope is 1 in. to 1 ft. ( $4.8^\circ$ ) or more.

A special outdoor trial was carried out to check the suitability of fly ash-bearing low porosity concrete under field conditions. This was carried out on a sunny day in August 1980. The ambient temperature was  $85^\circ\text{F}$ . Concrete with a water:cement ratio of 0.28 and a fly ash addition of 35% by weight of cement was mixed in a drum mixer. The initial slump was 10 in. - a flowing concrete. The concrete was allowed to remain in the drum mixer and was mixed for one minute at 30 minute intervals. At one hour the measured slump was 8-1/2 in. After 90 minutes the slump dropped to 3-1/2 in. At this point a small amount of plain water was added to raise the water:content ratio from 0.28 to 0.29. The concrete was remixed for a minute. After 30 additional minutes the concrete was again mixed for one minute. The measured slump was 4-1/2 in. Thus, the ability of such concrete to remain workable for a long period under high temperature conditions was clearly demonstrated.



### 3.4 HEAT EVOLUTION OF PASTES

It was felt desirable to investigate the heat of evolution behavior of pastes corresponding to the various concretes whose properties are being investigated in this study, since this gives an indication of the course of hydration reactions occurring in the cement paste. The method for preparing the pastes used in the heat evolution studies has already been described in section 2.2.2 (i) together with the apparatus used. The pastes studied were:

- (i) a low porosity cement-fly ash paste (fly ash added was 35% by weight of cement) containing the usual low porosity admixtures. The water: cement ratio was 0.25.
- (ii) a low porosity cement paste, without fly ash, containing the usual low porosity admixtures. The water: cement ratio was 0.27.
- (iii) an ordinary portland cement paste with a water: cement ratio of 0.40.

These water: cement ratios were selected because they provided about the same paste consistency and were reasonably close to the water: cement ratios used in the concretes. The temperature evolution graphs for the above pastes are given in Figure 3.4.1.



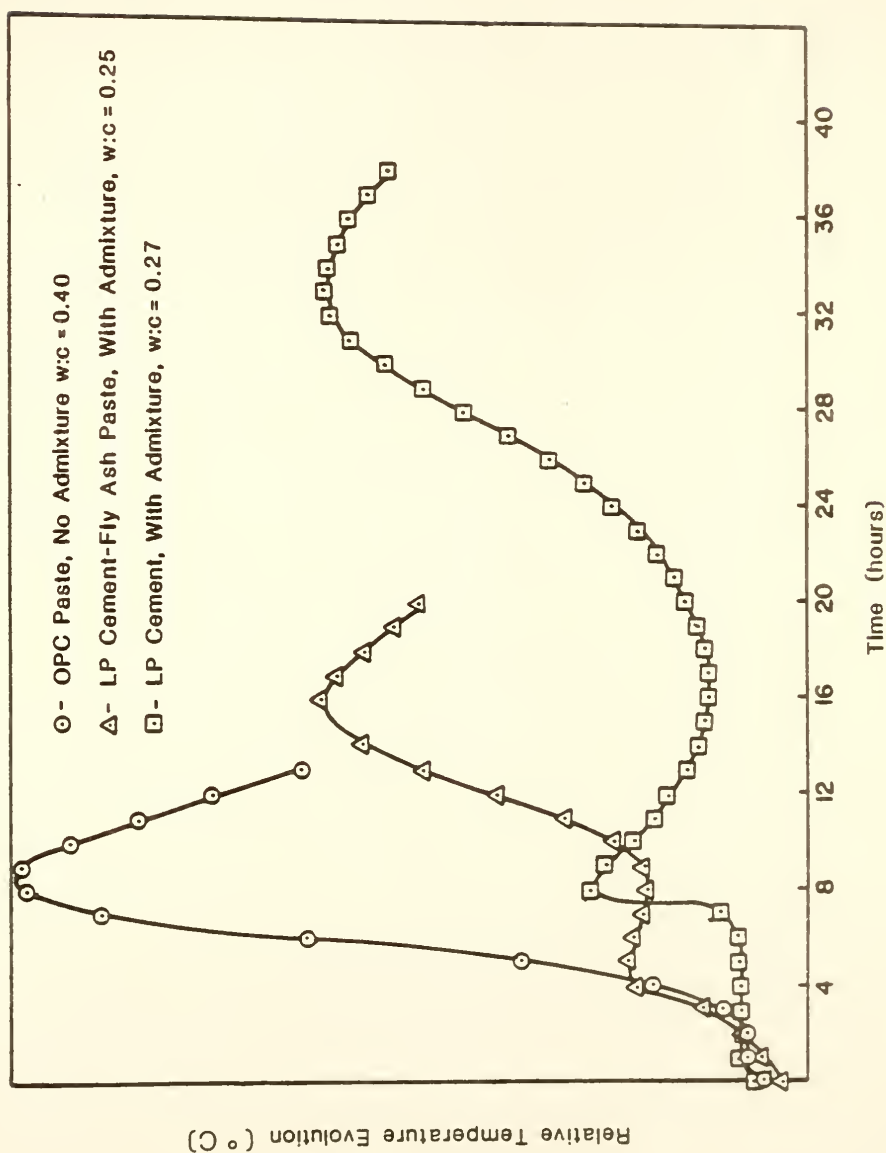


Figure 3.4.1 Temperature Evolution Curve of LP Cement Paste and OPC Paste





From these graphs the following observations can be made. Both the low porosity pastes exhibit a two-peak pattern which is unusual for ordinary portland cement paste. The latter paste shows one major peak following the dormant period. The first peak in the low porosity pastes is relatively small, and is followed by a second dormant period. The major peak follows the second dormant period.

In the low porosity cement paste with the usual admixtures and at a water:cement ratio of 0.27, the first dormant period lasts about 7 hours, and is followed by the first heat spike which lasts for about an hour. Then there is a gradual temperature drop, indicating the second dormant period until about 21 hours. The temperature then increases, gradually reaching a maximum at 33 hours and then slowly dropping. This peak is the second and major one.

The low porosity - fly ash paste with the usual admixtures and at a water:cement ratio of 0.25 follows the same general pattern typical of low porosity cement pastes (21) but is different in some significant respects. Here there is an initial dormant period of only 3 hours (cf. 7 hours for companion paste) followed by a small heat spike reaching a maximum at about an hour later. This heat level is maintained with only a slight drop in temperature over the next 5 hours, this corresponding to the second dormant period (cf. 13 hours for the companion paste). At about 9 hours of hydration, a temperature increase begins, and slowly rises to a maximum at about 15 hours (c.f. 33 hours for the companion paste).



Thus, the addition of fly ash changes the course of hydration reaction as seen from the heat evolution curves. Significantly, the two dormant periods for the low porosity cement - fly ash paste are much shorter than those of the companion paste. Also, the first heat spike for the former paste is lower than that of the companion paste. Furthermore, the time at which the maximum heat peak occur is about 15 hours for the fly ash-bearing low porosity cement paste and 33 hours for the companion paste. The maximum temperature reached is about the same for both pastes.

From the above observations it can be concluded that the early hydration of the low porosity cement is greatly influenced by the addition of fly ash, and it is clearly accelerated in time.

The ordinary portland cement paste prepared without any admixtures and at a water:cement ratio of 0.40 showed the typical major peak following a 2 hour dormant period. The rise in temperature started at about the third hour. The temperature rose to a maximum at about the ninth hour, and quickly dropped off. The maximum temperature reached in the apparatus for the ordinary portland cement paste at a higher water content is high, about one third higher than that for the low porosity pastes. Since water has a higher specific heat than the other constituents present, pastes of higher water:cement ratios require more evolved heat to achieve a given temperature increase. Despite this, the ordinary portland cement paste showed a much higher temperature increase than the low porosity pastes prepared



at much lower water:cement ratios. Thus, the heat evolution was much greater for the ordinary portland cement paste than for either of the low porosity cement pastes.

The temperature maximum occurs much earlier in the ordinary cement paste. The second maximum for the fly ash-bearing low porosity cement paste is delayed until at about 15 hours and it required about 33 hours for the low porosity paste without fly ash. In contrast, the maximum for the ordinary portland cement paste occurs about 9 hours.

The time at which the maximum heat occurs together with the maximum heat evolved at the time are significant parameters in the hardening of the fresh paste, and also may influence the cracking tendency of the paste or concrete.

It is obvious from the heat evolution curves that the kinetics of the hydration reactions occurring in ordinary portland cement paste are different from those occurring in low porosity cement paste. Addition of fly ash to the low porosity cement paste significantly modifies and accelerates the course of its hydration reaction.



### 3.5 STUDIES ON CHARACTERISTICS OF THE FLY ASH USED

#### 3.5.1 Preparation of Calibration Chart for $\text{Ca(OH)}_2$ Analysis

In this portion of the work, interest was focused on the reactivity of fly ash in the hydrating cement systems, especially its reaction with  $\text{Ca(OH)}_2$ . Determination of  $\text{Ca(OH)}_2$  in various hydrating systems was carried out by a DTA method, using a calibration chart prepared as follows.

A laboratory analytical reagent grade calcium hydroxide (Mallenckrodt, AR) and fired kaolin were oven dried overnight at  $105^\circ\text{C}$ . Mixtures of calcium hydroxide and the fired kaolin were prepared at proportions of 10, 25 and 50 per cent of  $\text{Ca(OH)}_2$  by weight. The mixtures were separately mixed for one minute in a laboratory homogenizer (Spex Mill) to ensure homogeneity of sample.

The areas under the curve corresponding to the  $\text{Ca(OH)}_2$  endotherm between  $400$  and  $500^\circ\text{C}$  were measured using a planimeter. The DTA runs were made in duplicate and the area under each was measured three times. The average areas measured for the duplicates in turn were averaged to provide the final area corresponding to the designated percentage of free  $\text{Ca(OH)}_2$  in the particular sample. A calibration chart prepared from these determinations is





shown in Figure 3.5.1. The relationship is accurately linear but does not quite go through the origin.

### 3.5.2 Reaction in Fly Ash-Water Pastes

A fly ash paste was made using the procedure described in section 2.2.2 (i), using a water-solid ratio of 0.50. The resulting paste was sealed in a plastic envelope for 24 hours. The hardened, but fragile paste was removed, placed in an open plastic container and cured in a fog room for periods of 3, 7, and 28 days. Samples were taken at the stipulated ages and differential thermal analysis performed on them as described in section 2.2.2 (i). No peak was found for  $\text{Ca(OH)}_2$  at any of the indicated ages, indicating that despite the high CaO content of the fly ash it does not itself liberate  $\text{Ca(OH)}_2$  when mixed with water in pastes.

### 3.5.3 Reaction in Fly Ash - CaO Pastes

Equal weights of fly ash and of analytical reagent grade calcium oxide were mixed in a Hobart mixer as described in section 2.2.2 (i); the water-solids ratio was 0.50. The resulting paste was sealed in a plastic envelope for 24 hours and the hardened paste removed, placed in an open plastic container, and stored in the fog room for periods of 3, 7, 28, 90 days, and 33 weeks. Differential thermal analyses were performed on portions of the sample removed at the indicated ages. The resulting measured areas of the  $\text{Ca(OH)}_2$  endotherm at the indicated ages are given in Table 3.5.1. The corresponding  $\text{Ca(OH)}_2$  content is plotted versus time



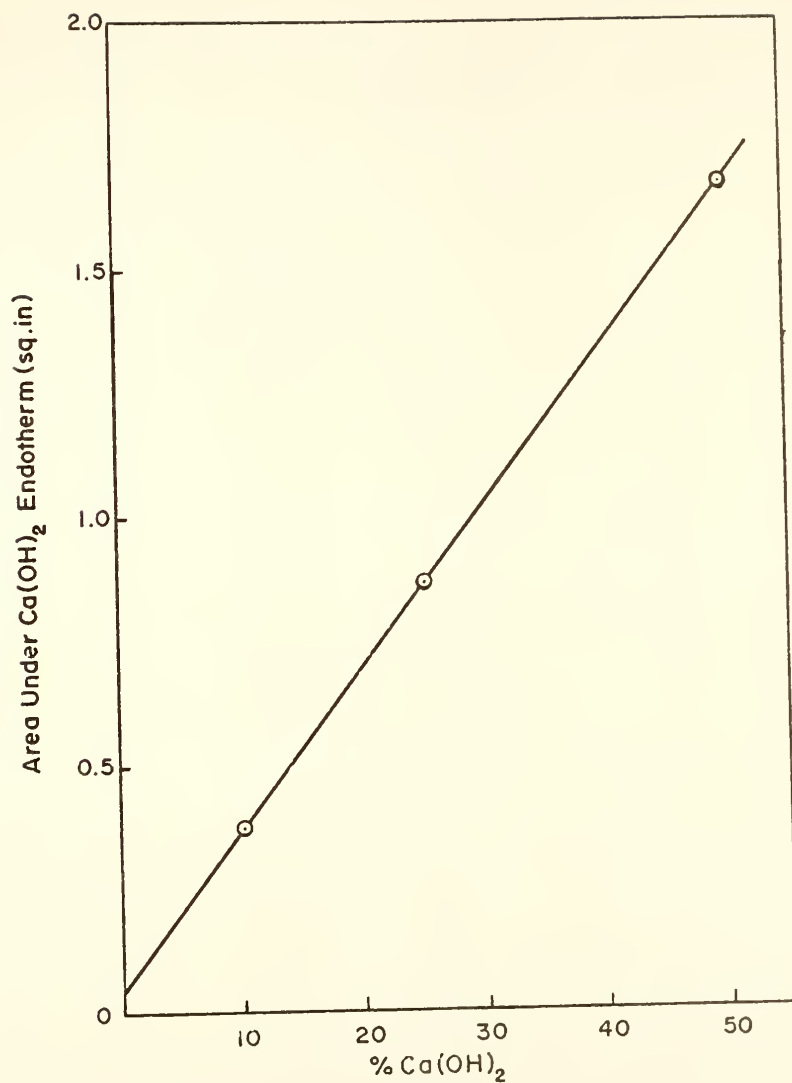


Figure 3.5.1 Calibration Curve for  $\text{Ca(OH)}_2$  Analysis by DTA



Table 3.5.1 Estimation of  $\text{Ca(OH)}_2$  Contents in Various Fly Ash-Bearing Pastes Using DTA

Type of Paste	Pattern	Average Area Under Curve (sq. in.)	Estimated Amount of $\text{Ca(OH)}_2^*$ , %
Fly Ash-Water Paste	FAP-3	0	-
	FAP-7	0	-
	FAP-28	0	-
Fly Ash-CaO Paste	FCP-3	1.40	41.5
	FCP-7	1.00	29.0
	FCP-28	0.73	21.0
	FCP-90	0.50	14.0
	FCP-33W	0.05	~ 0
Fly Ash-Low Porosity Cement Paste With Admixtures	FALPA-3	0.20	7.5
	FALPA-7	0.36	9.5
	FALPA-28	0.38	10.5
	FALPA-196	0.36	9.5
Fly Ash-Low Porosity Cement Paste Without Admixture	FALPN-3	0.35	9.5
	FALPN-7	0.50	14.0
	FALPN-28	0.48	13.5
	FALPN-196	0.55	14.5

\* Values obtained from calibration curve (See Figure 3.5.1)



in Figure 3.5.2. As expected, the CaO rapidly hydrated to produce  $\text{Ca(OH)}_2$ . There was a rapid drop in  $\text{Ca(OH)}_2$  over the first 28 days followed by a slower reduction which is approximately linear with time thereafter. Essentially all of the  $\text{Ca(OH)}_2$  was depleted by 9 months. Microstructural examination of fracture surfaces broken after drying was made using the scanning electron microscope. Micrographs of the 3 day old sample are shown in Figures 3.5.3 and 3.5.4. Typical micrographs of the 33 week old sample are shown in Figures 3.5.5 and 3.5.6. Interpretation of these micrographs are provided later in Section 3.5.6.

#### 3.5.4 Study of Pastes of Fly Ash-Bearing Low Porosity Cement

A fly ash-bearing low porosity cement paste was prepared using the Hobart mixer as described in section 2.2.2 (i). The percentage of fly ash by weight of cement was 35; that of sodium lignosulfonate and sodium bicarbonate were 0.42 and 1.2 respectively. The water-solid ratio was 0.24. The resulting paste was treated as described in section 3.5.2 and stored in a fog room for 3, 7, and 28 days.

A portion of the sample was broken off at each of the indicated ages and appropriately treated for DTA study as described in section 2.2.2 (ii). The amount of calcium hydroxide produced in the paste is given in Table 3.5.1, as determined from the calibration curve using the area measured under the  $\text{Ca(OH)}_2$  endotherm.

A microstructural examination of a surface fractured after drying of a 7 - day cured sample was made using the scanning





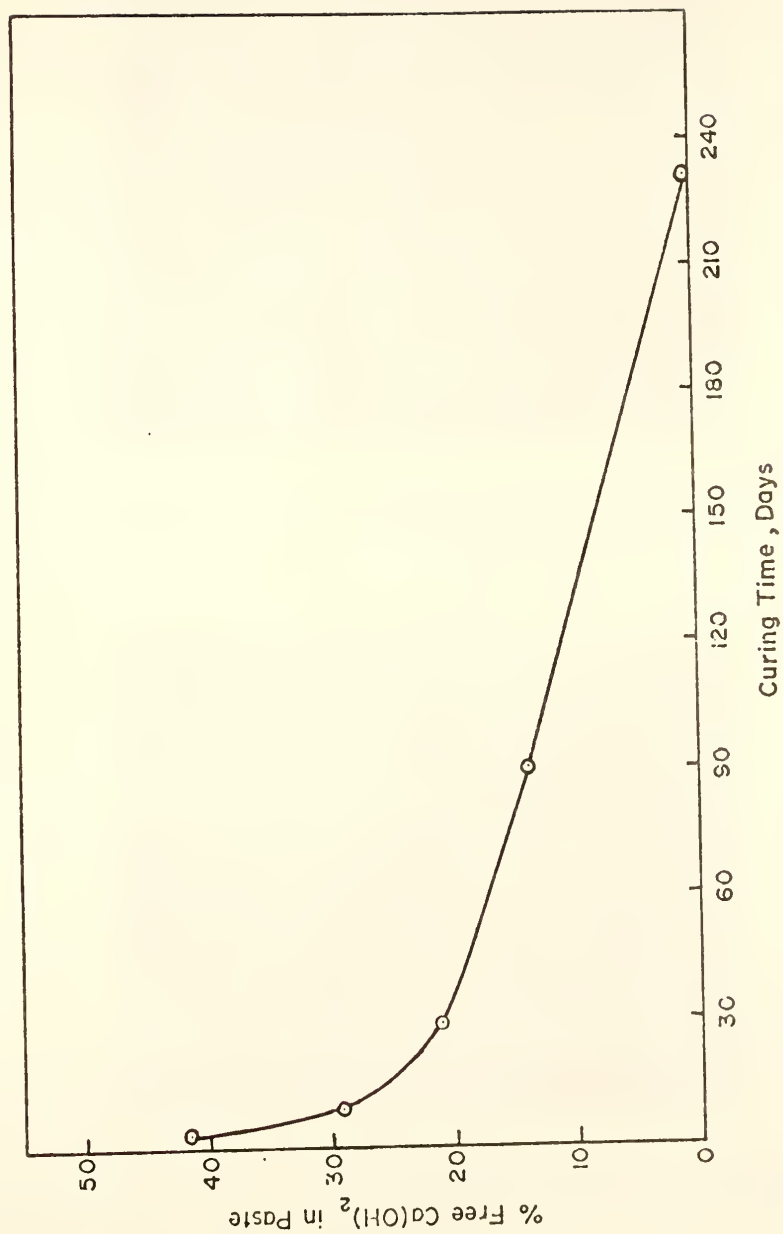


Figure 3.5.2 Reduction of  $\text{Ca(OH)}_2$  with Time in a Fly Ash-CaO Paste





Figure 3.5.3 SEM Micrograph of Fly Ash-CaO Paste,  
w:s = 0.5, at 3 Days (1500X)



Figure 3.5.4 SEM Micrograph of Fly Ash-CaO Paste,  
w:s = 0.5, at 3 Days (10,000X)





Figure 3.5.5 SEM Micrograph of Fly Ash-CaO Paste,  
w:s = 0.5, at 33 Weeks (1500X)



Figure 3.5.6 SEM Micrograph of Fly Ash-CaO Paste,  
w:s = 0.50, at 33 Weeks (3000X)



electron microscope. Two typical micrographs of the surface examined are shown in Figure 3.5.7 and Figure 3.5.8. Interpretation of these micrographs are provided later in section 3.5.6.

### 3.5.5 Study of Pastes of Fly Ash-Bearing Low Porosity Cement Without Admixtures

The same mix proportion of fly ash and low porosity cements and same mixing procedure as described in section 3.5.4 were used to prepare the paste described here, except that plain water, without dissolved admixtures, was used. The water:solid ratio was 0.30. The amount of calcium hydroxide produced in the paste at various ages is given in Table 3.5.1, as determined from the calibration curve, Figure 3.5.1, using the area measured under the  $\text{Ca(OH)}_2$  endotherm.

A plot of the amount of calcium hydroxide produced with time in this paste is shown in Figure 3.5.9 together with the plot of  $\text{Ca(OH)}_2$  produced in the paste which was prepared using the usual low porosity admixtures. The amount of calcium hydroxide produced is higher at all ages for the paste without the usual low porosity admixtures.

A microstructural examination of a surface of a 7-day cured sample fractured after drying was made using the scanning electron microscope. Two typical micrographs of the surface examined are shown in Figures 3.5.10 and 3.5.11 and these are interpreted subsequently in section 3.5.6.





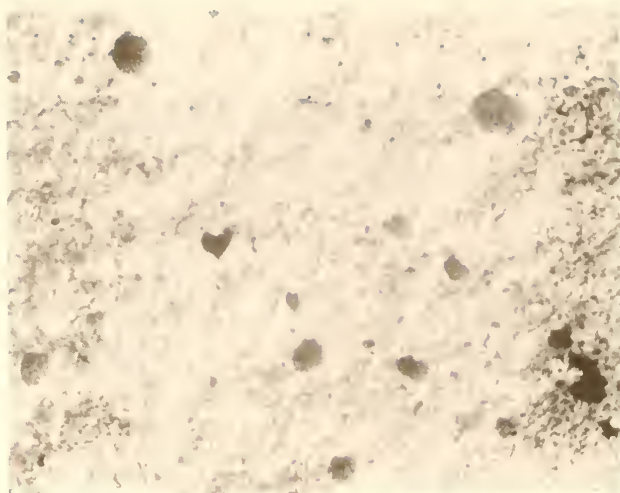


Figure 3.5.7 SEM Micrograph of FALP Paste,  
w:s = 0.24, at 7 Days (150X)

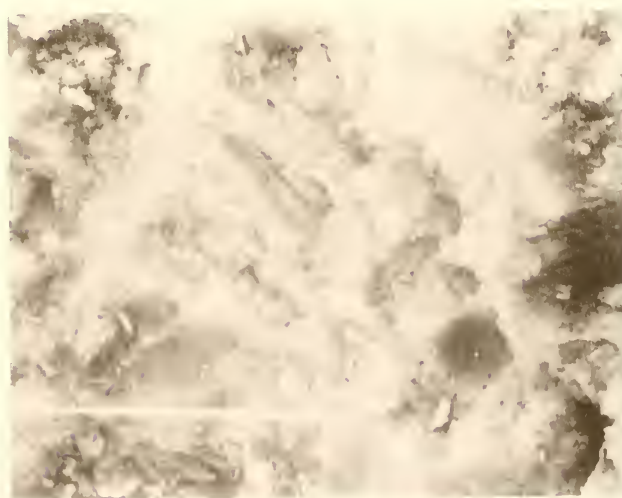


Figure 3.5.8 SEM Micrograph of FALP Paste,  
w:s = 0.24, at 7 Days (2000X)



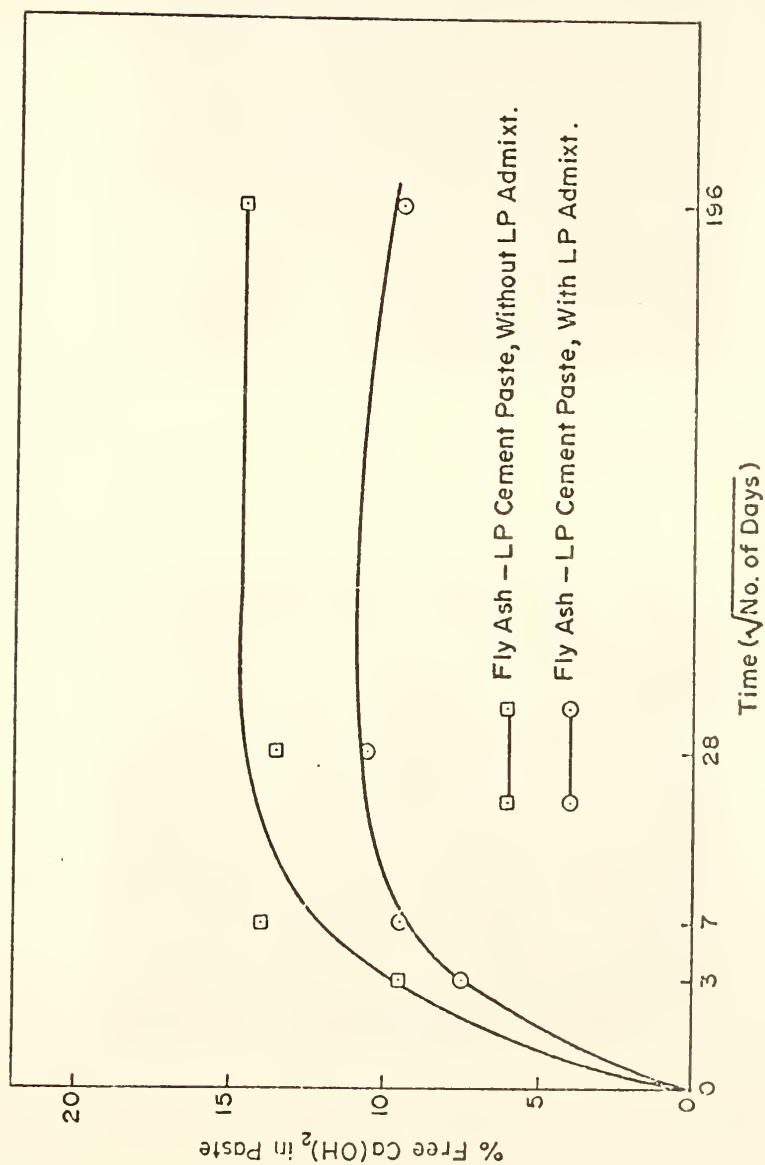


Figure 3.5.9 Generation of  $\text{Ca(OH)}_2$  in Fly Ash-Low Porosity Cement Pastes (With and Without The Usual Admixtures)



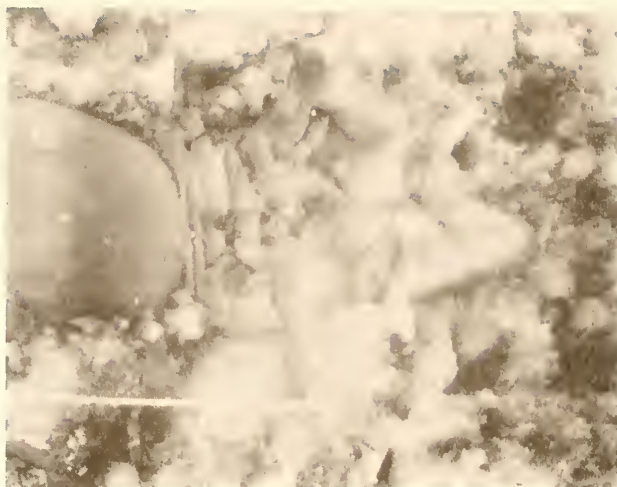


Figure 3.5.10 SEM Micrograph of FALPN Paste,  
w:s = 0.30, at 7 Days (2000X)

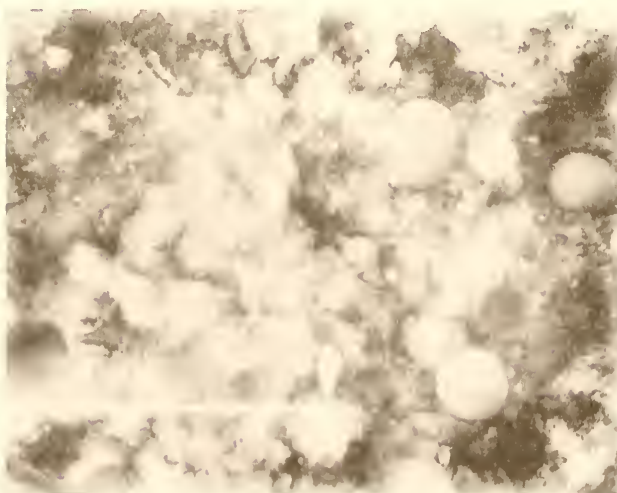


Figure 3.5.11 SEM Micrograph of FALPN Paste,  
w:s = 0.30, at 7 Days (2000X)



### 3.5.6 Results and Discussion

From the chemical analysis of the fly ash used (Table 2.1.2) it is shown that chemically Ca constitutes an unusually large proportion (about 30%) of this type of fly ash. The X-ray diffractogram of the fly ash confirms the presence of crystalline CaO along with other compounds. However, in the study of DTA thermograms of the fly ash-water pastes, no peaks were obtained for  $\text{Ca(OH)}_2$  at 3, 7 or 28 days. The inference from this is that crystalline CaO in the fly ash is not free to form  $\text{Ca(OH)}_2$ .

The X-ray diffractogram of the fly ash-water paste even at 28 days shows the presence of CaO and the absence of  $\text{Ca(OH)}_2$ . In contrast, using the same experimental technique, a 50-50 fly ash-calcium oxide paste at 3, 7 or 28 days show the complete absence of crystalline CaO at all ages and the formation of  $\text{Ca(OH)}_2$  and  $\text{CaCO}_3$  (calcite). Thus, the X-ray and DTA results show that the CaO does not form  $\text{Ca(OH)}_2$  in the fly ash-water pastes, but apparently does so in the fly ash-CaO paste. The inference is that the calcium oxide in the fly ash is unreactive.

The ability of this fly ash to combine with  $\text{Ca(OH)}_2$  in a hydrating low porosity cement paste seems to be questionable as indicated by DTA thermograms of two fly ash-bearing low porosity cement pastes. In one system, the usual admixtures were added to the mix water and in the second mix, plain water was used. In both cases, the amount of calcium hydroxide generally increased with time (up to 28 days), i.e. there was a build up rather than a reduction





with time. In the same period in the fly ash-CaO pastes there was a strong decrease in the  $\text{Ca(OH)}_2$  content of the pastes. Lea (75) has shown that there is a more than proportional reduction in the free lime content in a pozzolanic cement mortar (burnt clay pozzolan), compared to a reference portland cement mortar starting about 7 days and continuing thereafter. Lea's results contrast with those obtained in this study which suggests that a basic difference may exist between the hydration characteristics of the fly ash-bearing low porosity paste on one hand, and the pozzolan bearing portland cement mortar on the other.

The micrograph Figure 3.5.3 of the hydrated fly ash - CaO paste at 3 days does not show much detail at 1,500 magnification. However, clusters of fly ash along with what seems to be calcium oxide or calcium hydroxide are seen. Large intervening pore spaces are apparent and these probably account for the fragile nature of the paste. In Figure 3.5.4, which is a higher magnification view - 10,000X - of the same paste, hexagonal crystals of calcium hydroxide are seen. Some of the plates are parallel to each other, but many have an edge-to-face contact orientation.

The micrograph of the hydrated 33 week old sample, Figures 3.5.5 and 3.5.6, show rods of almost constant thickness throughout their length, and range in thickness from about  $0.2\mu$  to about  $2\mu$ , and in length up to  $10\mu$ . The rods are intermeshed and predominate over all the fields examined. They are almost certainly ettringite. Clusters of fly ash



and possibly calcium hydroxide are interspersed among the rods. A coating of hydration products are seen to cover some of the fly ash particles as in the grain on the left side of Figure 3.5.5.

The micrographs of the fly ash-low porosity cement paste with admixture, FALPA, illustrate the ability of the admixtures (lignosulfonate and  $\text{NaHCO}_3$ ) to entrain air in the paste, as indicated in Figures 3.5.7 and 3.5.8. This observation was previously made in the discussion of fly ash-bearing low porosity concretes. In addition to this effect of the admixture, it also had the effect of reducing the amount of calcium hydroxide formed in the hydrating paste as seen from values of  $\text{Ca(OH)}_2$  obtained by DTA and given in Table 3.5.1. At 3 days the estimated amount of  $\text{Ca(OH)}_2$  was 7.5% in the FALPA samples; it increased to 9.5% at 7 days and again increased to 10.5% at 28 days. The companion samples, FALPN, which had no admixtures, produced higher amounts of calcium hydroxide at each age. In the companion samples, the estimated amounts of  $\text{Ca(OH)}_2$  at 3 days was 9.5%, 14.0% at 7 days, and 13.5% at 28 days.

This difference seems also to be substantiated by SEM examination. There appeared to be somewhat more platy and massive  $\text{Ca(OH)}_2$  in the FALPN samples (e.g., Figure 3.5.10) than in the FALPA samples (e.g., Figure 3.5.8). It is interesting to note a possible decrease in the  $\text{Ca(OH)}_2$  content in the FALPN samples (fly ash-bearing low porosity cement paste without the usual admixtures) from 7 days to 28 days.



### 3.6 STRENGTH CHARACTERISTICS OF LOW POROSITY CONCRETES

#### 3.6.1 Materials and Mixes

The materials used in this investigation (cement, aggregates and admixtures) and the mixing procedure adopted are as described in section 2.1.1 and section 2.2.1 (ii).

Four basic concretes representing variations of the low porosity concrete were prepared and their compressive strengths tested. The mix proportions are given in Table 3.6.1. The concretes are described below.

- (i) a low porosity concrete with no fly ash and no air entraining agent, designated Mix 1.
- (ii) a low porosity concrete with fly ash having no air entraining agent, designated Mix 2.
- (iii) a low porosity concrete with fly ash and 1 oz/100 lb. of cement dosage of vinsol resin, designated Mix 3.
- (iv) a low porosity concrete with fly ash and 2 oz/100 lb. of cement dosage of vinsol resin, designated Mix 4.

The fly ash-bearing low porosity concrete tested had a cement content of 10 bags per cu. yd. (counting both cement and fly ash as cementitious materials; counting only the low porosity cement it was 7.4 bags per cu. yd.). The low porosity concrete without fly ash had a cement content of 8.5 bags per cu. yd. In all concretes, the aggregate:cement ratio was around 4, and the water:cement ratio was 0.30.



Table 3.6.1 Mix Proportions of Low Porosity Concretes for Strength Test

Mix Designation	Cement Content (bags/cu. yd.)	Fly Ash Content (bags/cu. yd.)	Vinsol Resin (oz/100 lb. of cement)	Air Content (%)
1	8.5	-	0	1.5
2	7.4	2.8	0	5.0
3	7.4	2.8	1.0	6.8
4	7.4	2.8	2.0	8.0

Sulfonated Lignin Content. 0.7% by weight of cementitious material.  $\text{NaHCO}_3$  content, 1.2% by weight of cementitious material w:c = 0.30 for all mixes.





The weight of sodium lignosulfonate and sodium bicarbonate expressed as a percentage of the cement was also the same in all the concretes.

The fresh concrete from each mix was cast into fifteen 3 x 6 - in. steel molds immediately after mixing. The samples were compacted by hand rodding. After casting, the specimens were left in the molds covered with plastic sheets for 24 hours. The specimens were then demolded and cured in the fog room for a period of up to one year. At 7 days and 1, 3, 6 and 12 months, three samples of each concrete mix were tested for compressive strength.

### 3.6.2 Test for Hardened Concrete

The ASTM Designation: C 39-72 procedure was followed to determine the compressive strength of the hardened low porosity concretes. A Forney FT40 DR testing machine of capacity 250,000 lb., manufactured by Forney Inc., Newcastle, PA, was used to test the cylinders.

Capping of the samples were done as recommended by ASTM Designation: C 617-73 using sulfur mortar for samples up to 3 months old. Samples older than 3 months were lapped at both ends using a lapping wheel and appropriate powder grits.

The development of strength with time is tabulated in Table 3.6.2. The compressive strength of low porosity concretes at various ages is given in the bar chart in Figure 3.6.1, the relative gain of strength of the same concretes is shown in Figure 3.6.2.



Table 3.6.2 Compressive Strength of Low Porosity Concretes (psi)

Mix Designation	Specimen Number	Age				
		7 days	28 days	3 months	6 months	12 months
1	1	8630	8910	10610	11310	14850
	2	7570	8840	11670	11740	14850
	3	7780	10610	11670	12590	13720
	Avg	7990	9450	11370	11880	14470
	Std Dev	561	1000	611	651	652
2	1	7640	9050	11030	10610	-
	2	7780	8200	9340	8490	-
	3	7140	9120	10610	9900	-
	Avg	7520	8790	10326	9670	-
	Std Dev	336	512	880	1079	-
3	1	6510	8340	8420	-	10750
	2	6930	8630	8130	-	10180
	3	7000	8770	8910	-	-
	Avg	6810	8580	8490	-	10470
	Std Dev	265	219	394		403
4	1	4240	7140	8700	9050	10610
	2	4310	7780	8130	8490	10820
	3	4260	8770	8490	8700	9900
	Avg	4270	7900	8440	8750	10440
	Std Dev	36	821	288	283	482



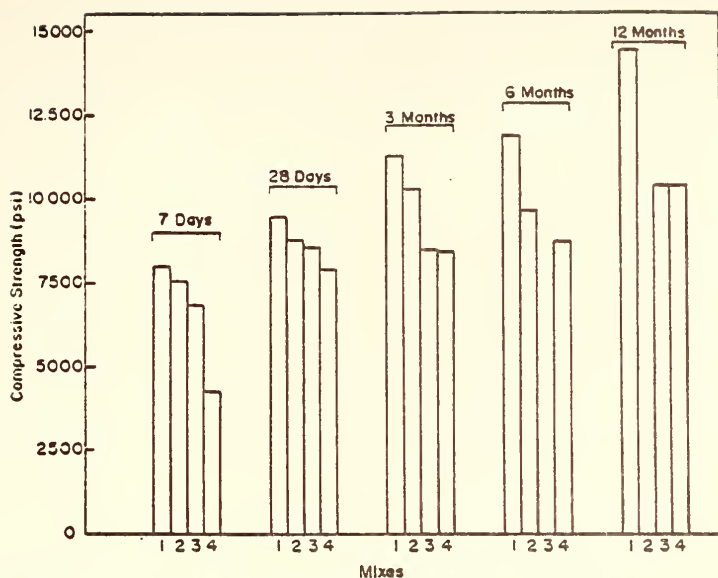


Figure 3.6.1 Compressive Strengths of Low Porosity Concretes at Various Ages

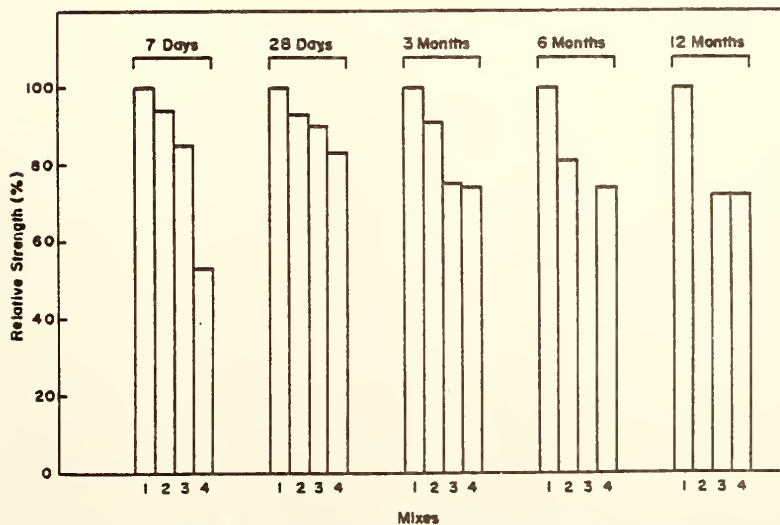


Figure 3.6.2 Strengths of Low Porosity Concretes of Different Compositions at Increasing Ages Relative to Strength of Reference Concrete Without Fly Ash or Admixture at the Same Age



### 3.6.3 Results and Discussion

The results of the compressive strenghts, as indicated in Table 3.6.2, show that the low porosity concrete without fly ash and without air entraining agent achieved strengths in the order of 8000 psi at 7 days, 9,500 psi at 28 days and over 14,500 psi at 1 year.

The results also indicate that the low porosity concrete with fly ash has slightly lesser compressive strength values at all ages than the concrete without fly ash. As can be seen from the histogram of Figure 3.6.2 the decreases were less than 10 per cent for ages up to 3 months, but about 20% at 6 months.

An apparent drop of about 7 per cent in compressive strength for the fly ash-bearing concrete between 3 months and 6 months was recorded. In contrast, the non-fly ash-bearing concrete increased in strength continuously over the first year.

A comparison illustrating the effects of two dosages of an air entraining agent in the development of strength of fly ash-bearing low porosity concretes are available from Table 3.6.2 and specifically illustrated in the bar charts of Figure 3.6.3. This shows that significant reductions in strength occur with air entraining agents at early ages but that the reductions become smaller by 28 days and thereafter (up to 3 months).

A further comparison is available in bar chart form in Figure 3.6.2 in which the effects of the air entraining





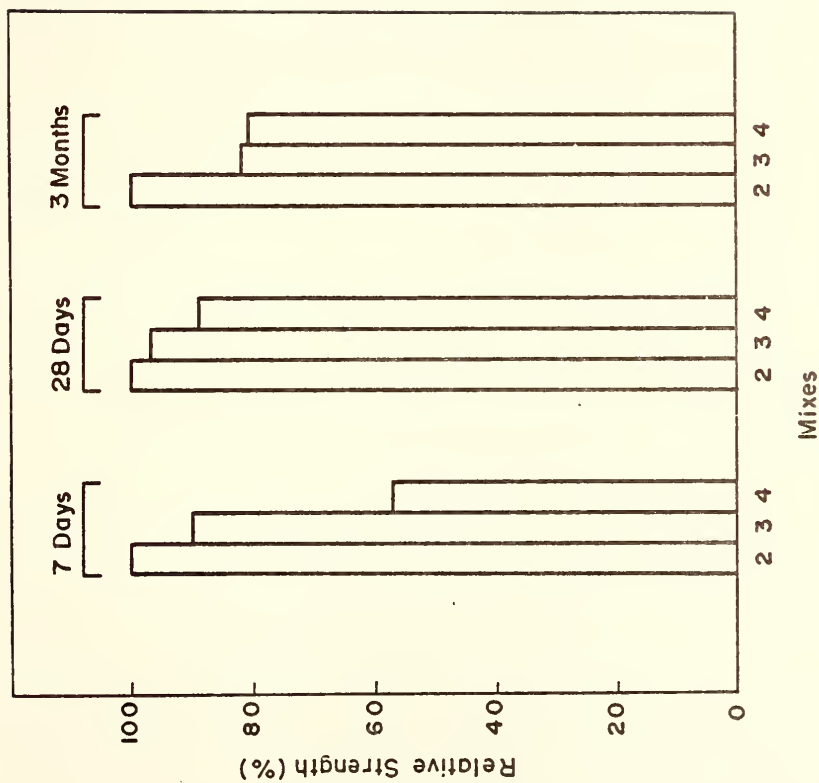


Figure 3.6.3 Strengths at Increasing Age of Fly Ash Bearing Low Porosity Concretes With an Air Entraining Agent Relative to Strength of Reference Concrete Without Air Entraining Agent at the Same Age



agent are compared relative to the strength of the low porosity concrete without fly ash and air entraining agent, the strongest mix series prepared.

In an earlier study (21) it was found that variations in the sulfonated lignin content of the low porosity concrete without fly ash did not affect the compressive strength. Variations in the  $\text{NaHCO}_3$  content influenced the compressive strength at early ages, but the differences disappeared by 7 days. It was further observed that compressive strengths at any age were relatively unaffected by the water:cement ratios between 0.26 and 0.30, but that a significant decrease was obtained when the water:cement ratio was increased to 0.32.

The compressive strength of a typical conventional bridge deck concrete as used in the State of Indiana containing 6 bags per cubic yard of ordinary portland cement is 2800 psi at 3 days; 3370 psi at 7 days, and 4250 psi at 28 days (76). Such concrete is similar to the BD concrete mix used in the main part of this study.

The compressive strength of a typical dense Iowa concrete for resurfacing of bridge decks is 6770 psi at 7 days, 7560 psi at 14 days, and 8300 psi at 28 days (77). Such concrete is similar to the Iowa concrete mix used in the main part of this study.

It is apparent that even with extensive fly ash incorporation, the low porosity concretes are significantly stronger than concretes normally employed in bridge decks.



PART FOUR  
PROPERTIES RELATING TO THE  
COMPACT NATURE OF CONCRETES



## 4.1 PORE SIZE DISTRIBUTION AND POROSITY OF CONCRETES

### 4.1.1 Introduction

The durability of concrete in service is significantly related to its physical and mechanical condition. One of the important properties that affects the physical condition is the permeability of concrete. This property of concrete determines its water-tightness which relates directly to the ease with which a fluid will pass through it. This affects the rate at which calcium hydroxide will be leached from the concrete, the rate of ingress of chloride ions and other deleterious agents into the concrete, the freeze-thaw resistance, the corrosion resistance, the rate of carbonation, and other important concrete properties.

The permeability of concrete depends in part on the distribution of pore sizes. In this study, the method of mercury intrusion was used to determine this characteristic of various concretes. In addition, other properties of the concretes, such as porosity and density were also determined.

### 4.1.2 Materials, Sampling and Testing for Pore Size Distribution Study

Five different concrete formulations were examined in this section of the study. They are:





(i) A formulation representing conventional bridge deck concrete as used in Indiana, designated BD-9.

(ii) A formulation representing the Iowa low-slump concrete for resurfacing bridge decks, designated IWA-2.

(iii) A formulation representing fly ash-bearing low porosity concrete, designated LPF-10.

(iv) A formulation representing low porosity concrete without fly ash, designated LPN-5.

(v) A second formulation representing low porosity concrete without fly ash, but using a greater proportion of sand fines, designated LPN-6.

Some of the details of the formulations of the five different types of concrete are shown in Table 4.1.1

All of five types of concrete were prepared as described in section 2.2.1, and cast into beams in 4 x 3 x 16 in. steel molds. In addition, 6 x 12 in. cylindrical specimens were also prepared for the concrete types BD-9 and LPN-5. The concrete beams were demolded at 1 day and then cured for 14 days in a lime-saturated solution. They were then placed in a controlled atmosphere room at 50  $\pm$  4 per cent relative humidity and a temperature of 23  $\pm$  2°C for 4 months. The concrete cylinders were cured in a saturated lime solution for the same period of 4 months.

Portions of the concrete beams of about 4 x 3 x 3 in. size were sawn off and broken up using a hammer. Mortar pieces were carefully picked from the resulting small pieces of concrete. Mortar was also picked from the



Table 4.1.1 Mix Proportions of Concretes Used for Pore Size Distribution, Porosity and Ingress of Chloride Ions and Shrinkage Studies.

Mix Designation	Cement Content, (bags/cu. yd.)	Fly Ash Content, (bags/cu. yd.)	Water-Cement Ratio	% Air Content	Ratio of Cement: Coarse Aggregate: Fine Aggregate	Slump (in.)
BD-9	6.3	-	0.43	6.0	1.0:3.0:2.1	3.5
IWA-2	8.6	-	0.33	7.3	1.0:1.7:1.7	4.0
LPF-10	7.6	3.0	0.28	5.0	+1.0:1.8:1.2	7.0
LPN-5	10.1	-	0.28	4.0	1.0:1.8:1.2	-
LPN-6	8.3	-	0.27	3.0	1.0:2.4:1.6*	9.0
LPN-4	10.2	-	0.28	2.0	1.0:1.8:1.2	10.5

\* Material passing through #30 sieve and retained on #50 sieve was 49% of the sand used.

+ Values based on weight of low porosity cement alone.



top and bottom 1 in. layers sawn from the concrete cylinders. Small mortar pieces of appropriate size for pore size distribution measurement were oven dried before the pore size distribution determination. The method and instrument used in the pore size distribution measurements are described in Section 2.2.2 (iv).

#### 4.1.3 Results

From the readings of the pressure and intruded volume of mercury obtained in the experiment, the pore diameters and the corresponding intruded volumes were calculated. In addition, the 'unfilled density' (the bulk density, counting voids before filling as part of the solid volume) and the 'filled density' (the apparent density of the solid matter), were also calculated. Cumulative intrusion of mercury versus pore diameter is plotted in Figures 4.1.1 to 4.1.5 for mortar samples taken from the concrete beams and in Figures 4.1.6 to 4.1.9 for mortar samples taken from the concrete cylinders.

In addition, the specific surface, bulk density and the apparent density of the concretes were calculated, and the results are shown in Table 4.1.2.

#### 4.1.4 Discussion

The results of the measurements of the pore size distribution studies are given in Figures 4.1.1 to 4.1.9 and in Table 4.1.2 and are discussed from the standpoints of total volume of mercury intruded per weight of sample;



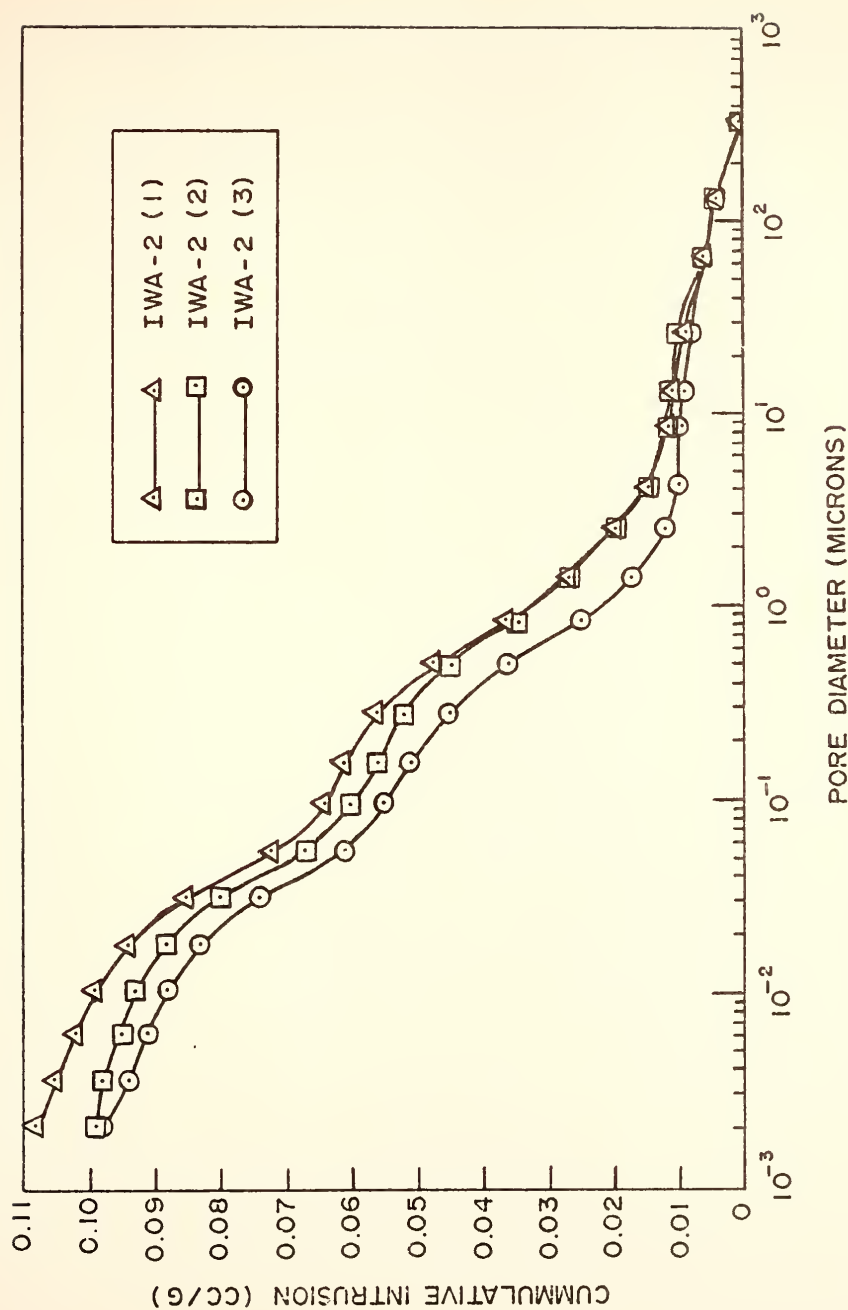


Figure 4.1.1 Pore Size Distribution Curves (By Mercury Porosimetry) of Replicate Mortar Pieces From IWA Concrete





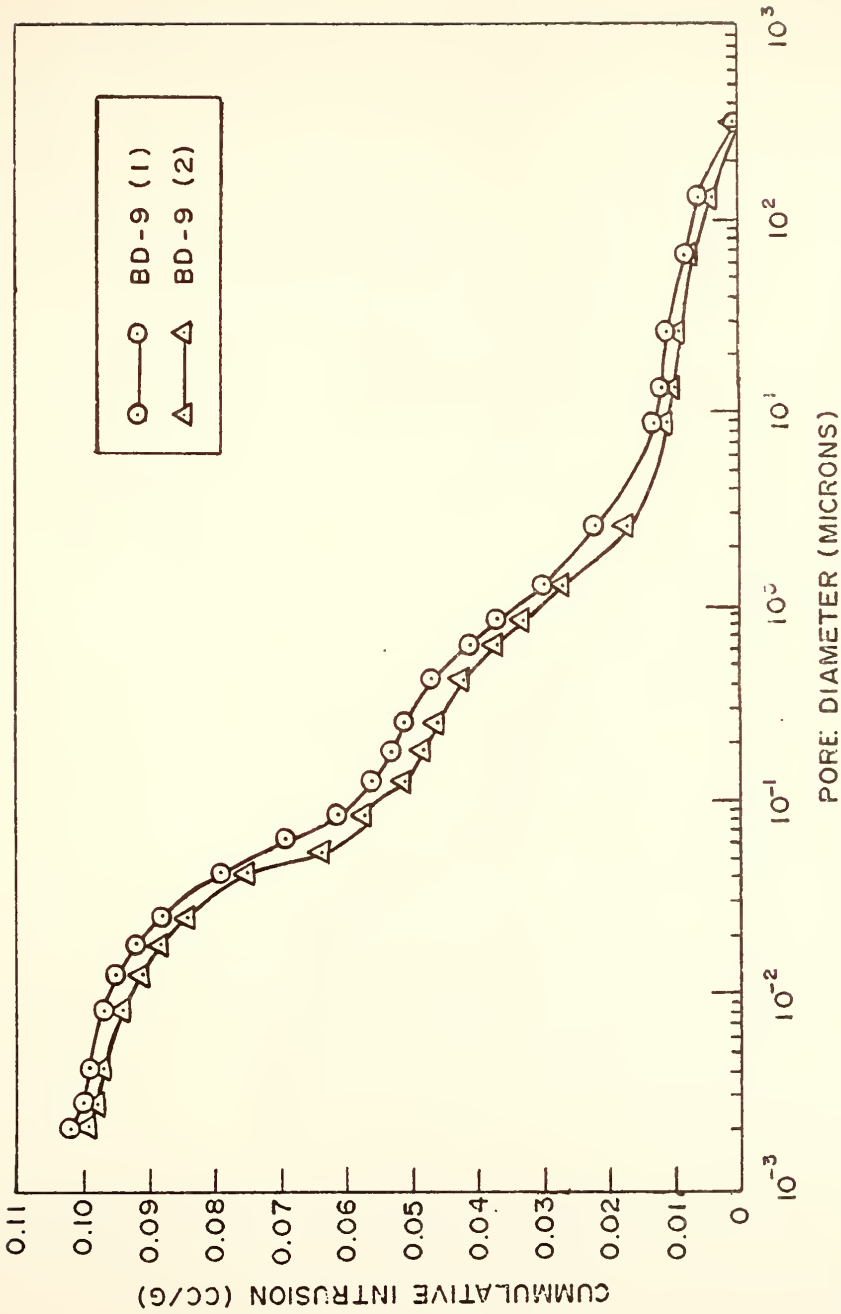


Figure 4.1.2 Pore Size Distribution Curves (By Mercury Porosimetry) of Replicate Mortar Pieces From BD Concrete



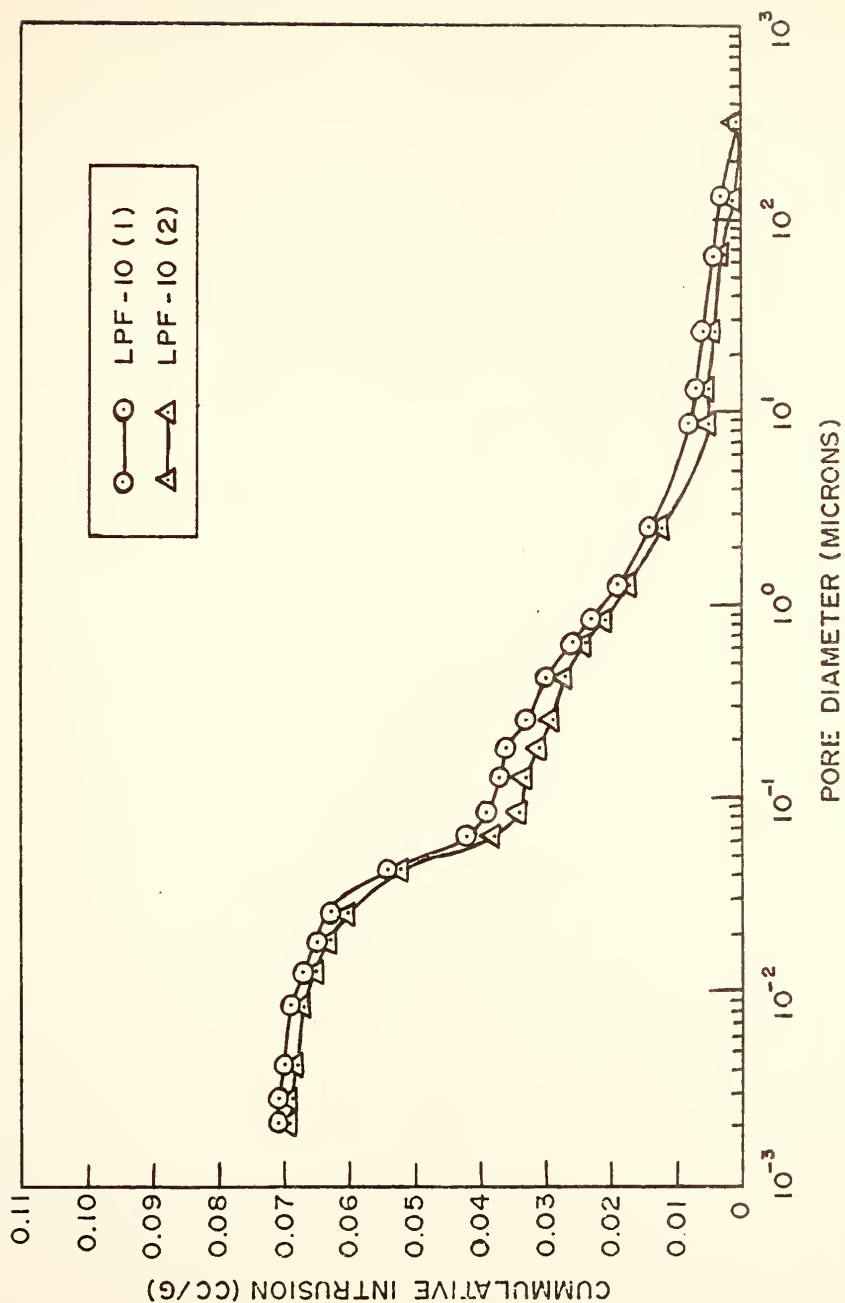


Figure 4.1.3 Pore Size Distribution Curves (By Mercury Porosimetry) of Replicate Mortar Pieces From Fly Ash-Bearing Low Porosity Concrete



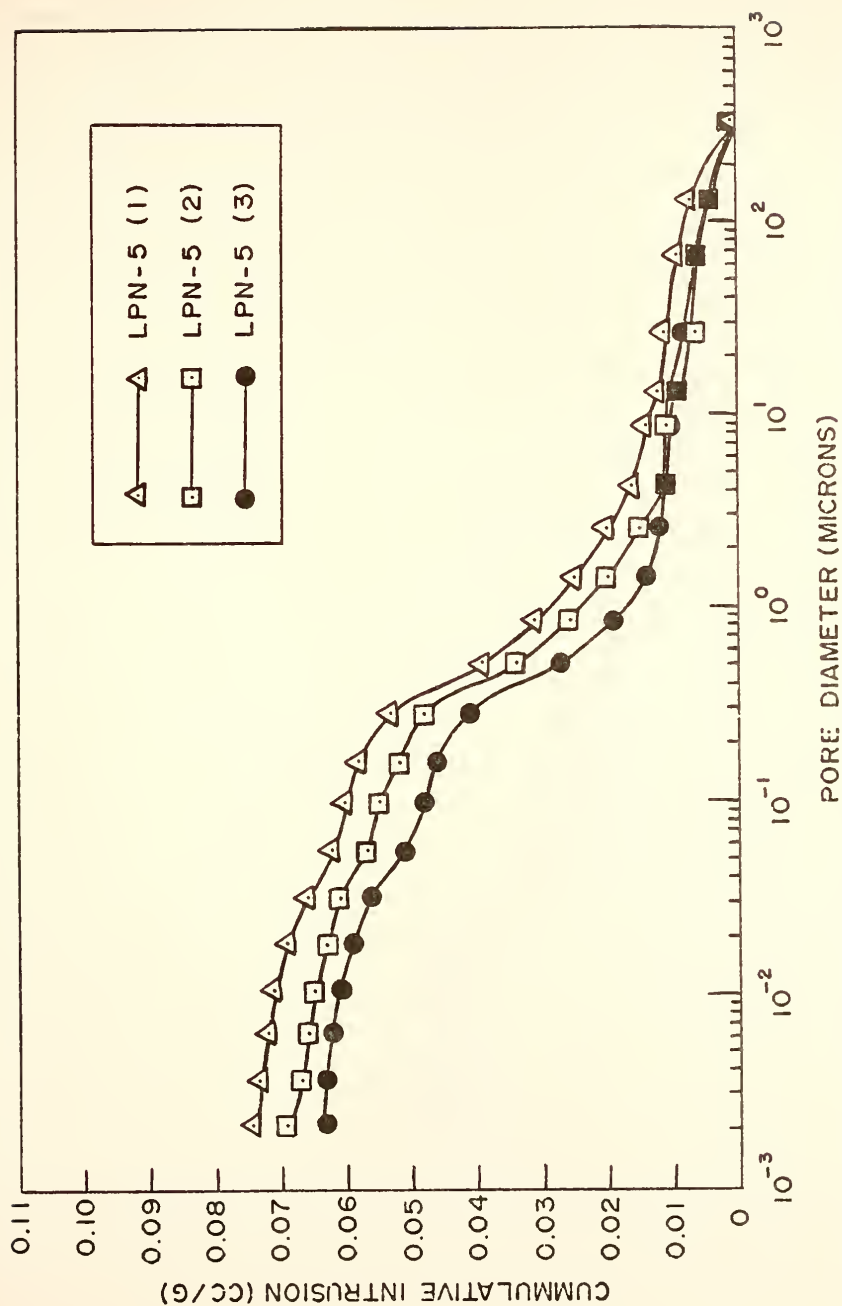


Figure 4.1.4 Pore Size Distribution Curves (By Mercury Porosimetry) of Replicate Mortar Pieces From Low Porosity Concrete Without Fly Ash



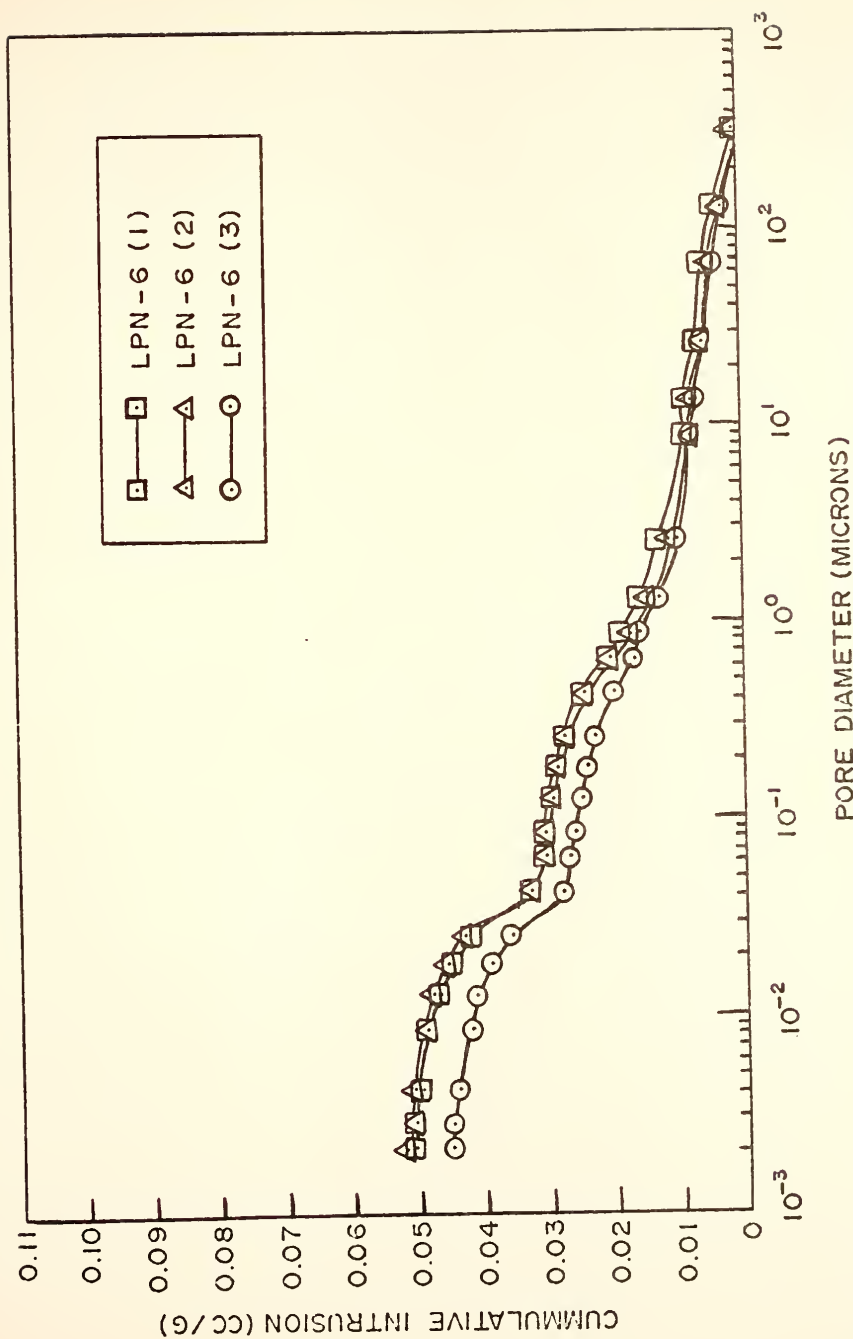


Figure 4.1.5 Pore Size Distribution Curves (By Mercury Porosimetry) of Replicate Mortar Pieces From Low Porosity Concrete Without Fly Ash (Special Sand Gradation)





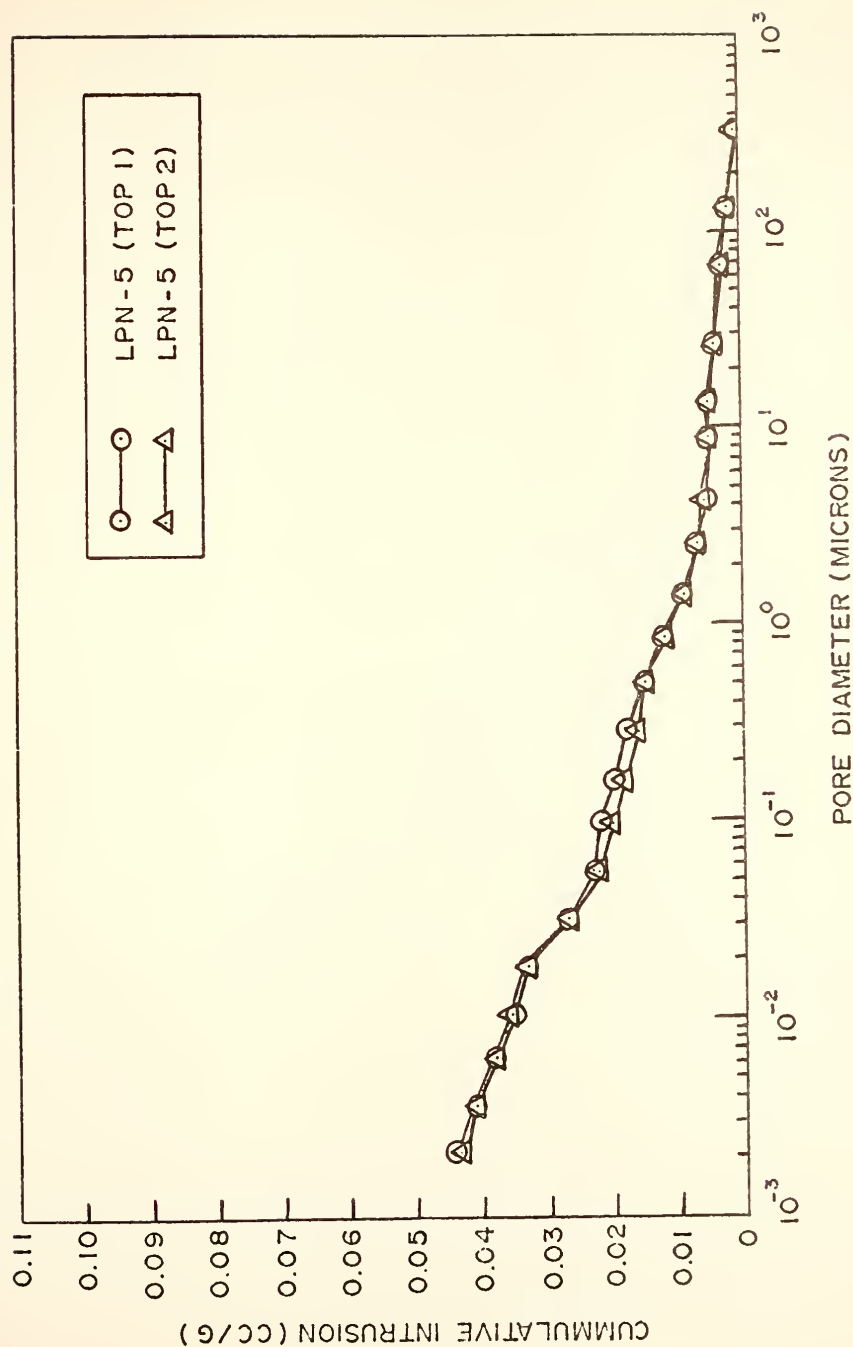


Figure 4.1.6 Pore Size Distribution Curves (By Mercury Porosimetry) of Replicate Mortar Pieces From Top Portion of 6 x 12 in. LPN Concrete Cylinder



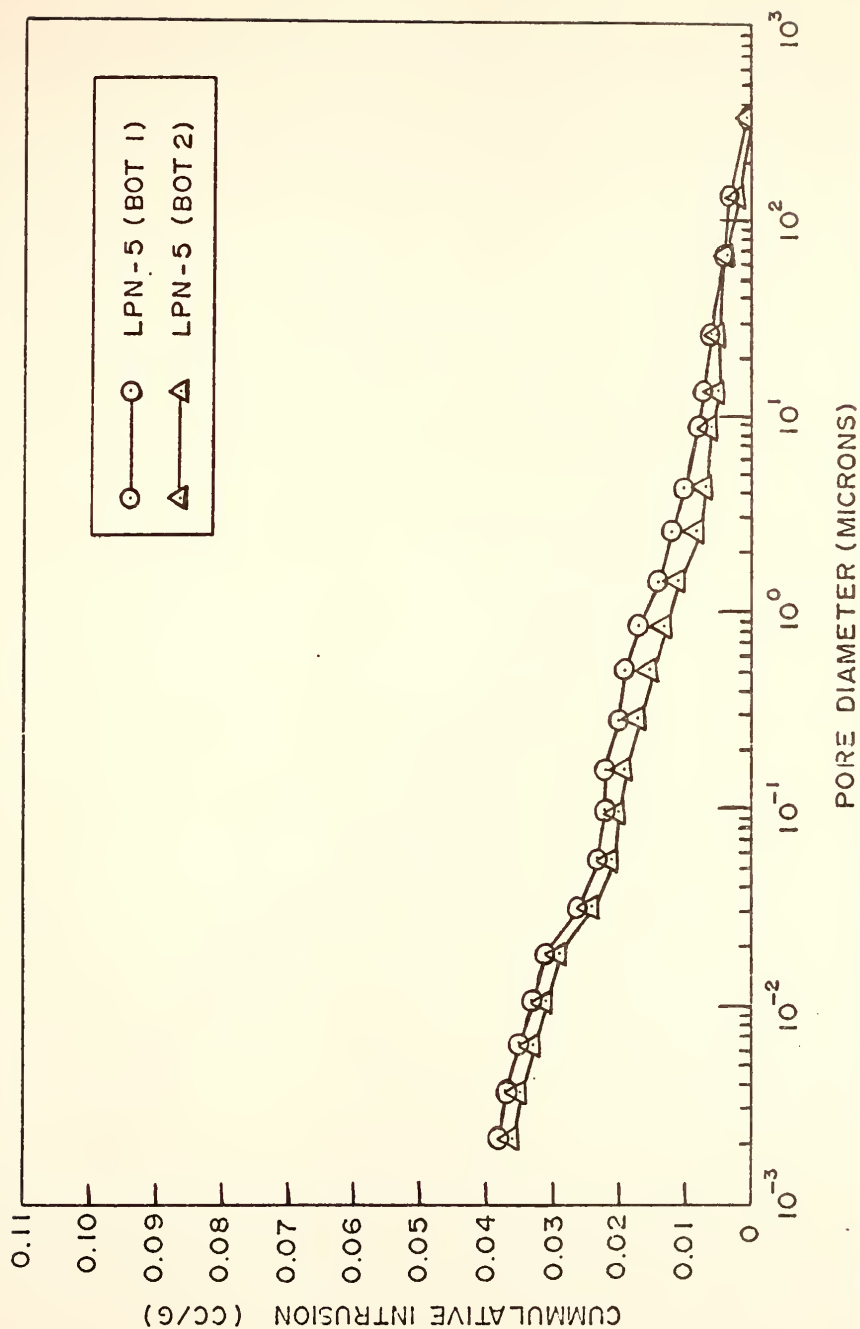


Figure 4.1.7 Pore Size Distribution Curves (By Mercury Porosimetry) of Replicate Mortar Pieces From Bottom Portion of 6 x 12 in. LPN Concrete Cylinder



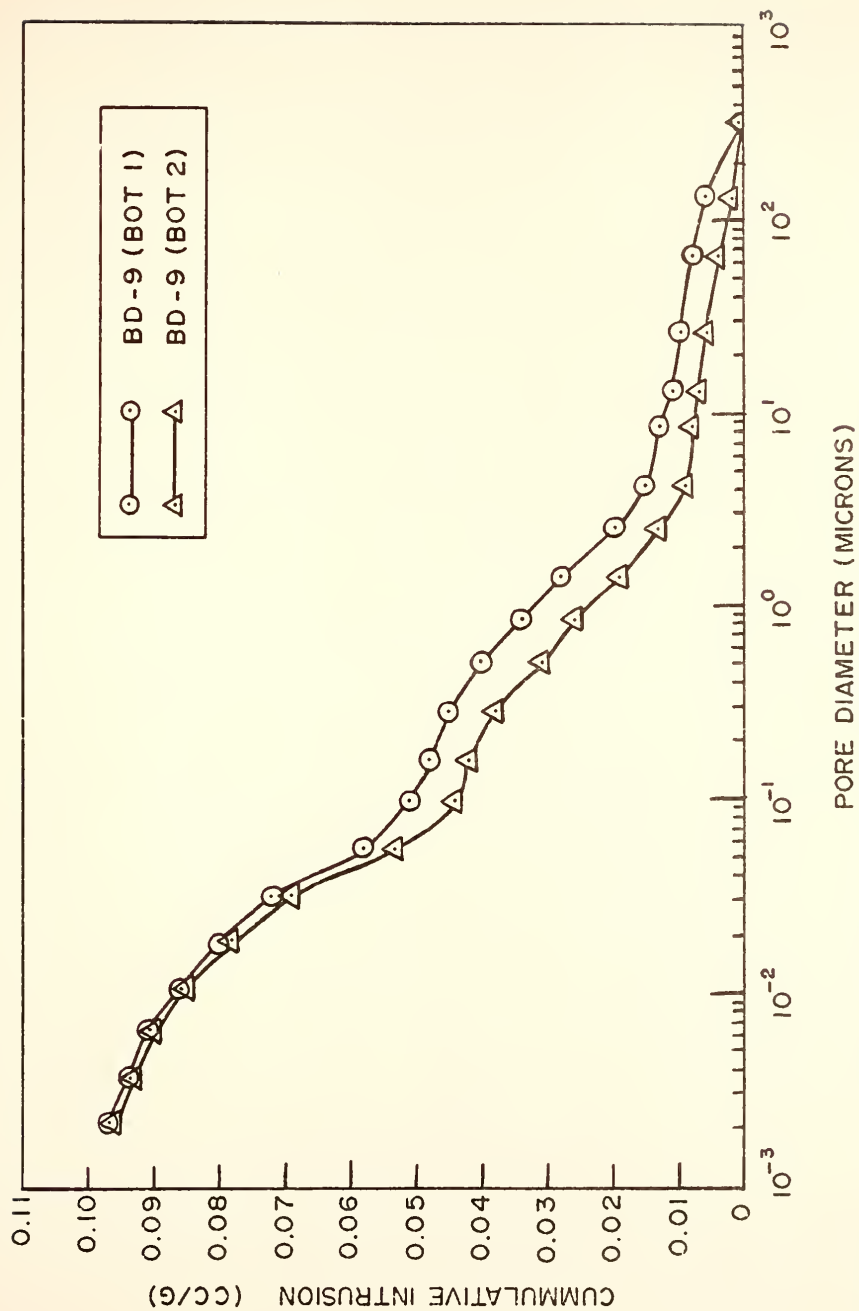


Figure 4.1.8 Pore Size Distribution Curves (By Mercury Porosimetry) of Replicate Mortar Pieces From Bottom Portion of 6 x 12 in. BD Concrete Cylinder



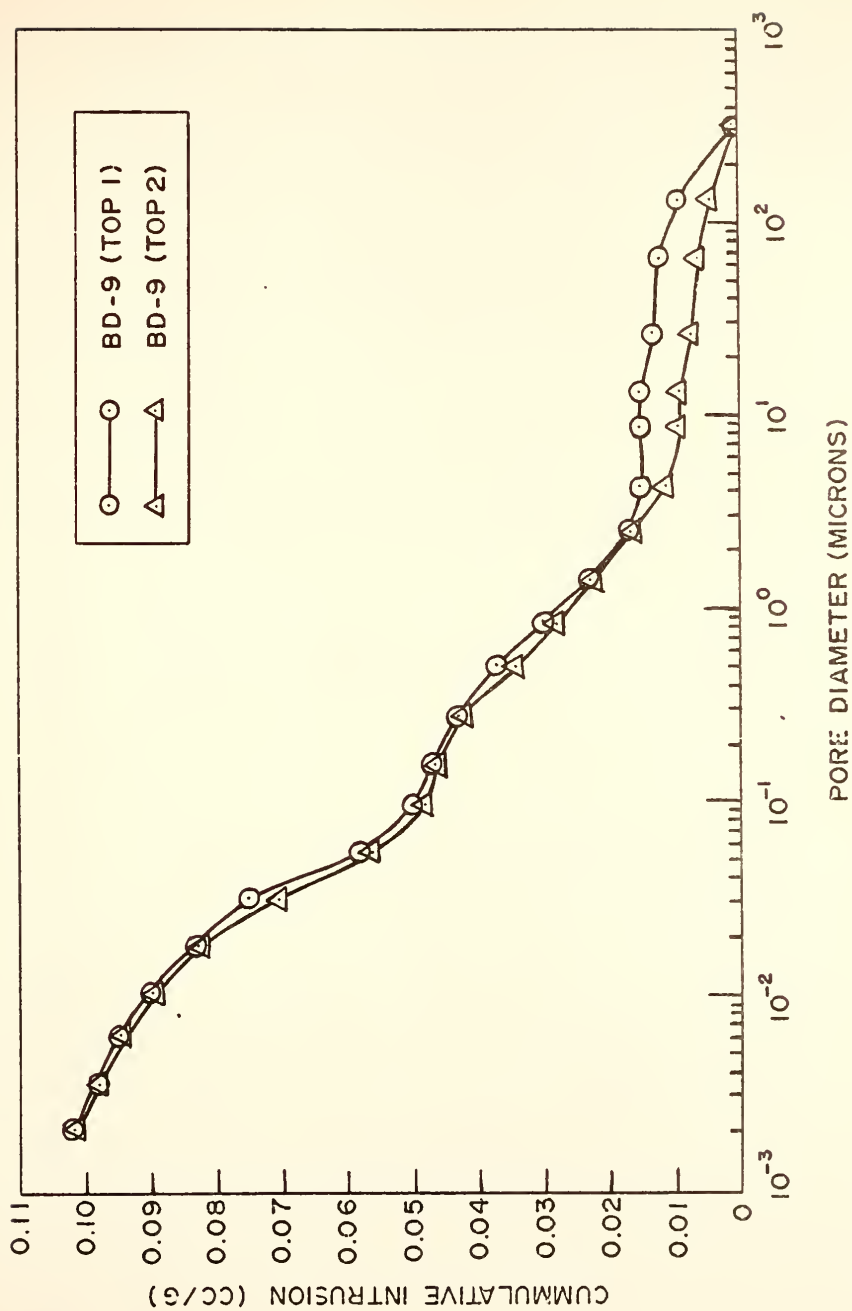


Figure 4.1.9 Pore Size Distribution Curves (By Mercury Porosimetry) of Replicate Mortar Pieces From Top Portion of 6 x 12 in. BD Concrete Cylinder





Table 4.1.2 Measured Specific Surface Areas and Densities of Mortars from Various Concretes

Type of Specimen	Concrete Formulations	Intruded Pore Volume, (ml/g)	Specific Surface ( $\text{m}^2/\text{g}$ )	Measured Density ( $\text{g}/\text{cm}^3$ )	
				Bulk ( $\rho_r$ )	Apparent ( $\rho$ )
Prism	BD-9	0.1005	10.85	2.031	2.526
	IWA-2	0.0990	13.00	2.003	2.494
	LPF-10	0.0650	7.09	2.105	2.464
	LPN-5	0.0673	5.81	2.107	2.445
	LPN-6	0.0493	5.33	2.239	2.502
Cylinder	BD-9 (Bottom)	0.0965	15.10	2.021	2.484
	BD-9 (Top)	0.1015	16.80	1.979	2.448
	LPN-5 (Bottom)	0.0370	6.98	2.259	2.457
	LPN-5 (Top)	0.0435	10.80	2.146	2.347



predominant pore diameter ranges; and measured densities, porosities, and surface areas of the pastes obtained from the different types of concretes. The mercury penetrometer was operated in the pressure range of 22 mmHg (0.43 psi) to 60,000 psi, and measured pore diameters in the range from about 30  $\mu\text{m}$  to about 0.002  $\mu\text{m}$ .

At least two mortar samples were analyzed for each concrete specimen. In the results, as given in Figures 4.1.1 to 4.1.9, the total volume of mercury intruded per gram of sample at the 60,000 psi maximum operating pressure of the penetrometer, gives an indication of the pore volume per unit weight of the sample. A steep rise in the graph indicates that a large volume of mercury is entering the sample per unit pressure increase, which means that a large proportion of pores of the size intrudable at that pressure is present in the sample.

The bulk density of the sample is obtained by dividing the weight of the sample by its volume before filling with mercury. The apparent density of the specimen is obtained by dividing the weight by the volume corrected for the space filled with mercury after pressuring. Porosities are calculated either from the product of the total intruded volume and the bulk density or from the difference between 1 and the ratio of bulk to the apparent density. Both estimates are provided in Table 4.1.3.

A value is also calculated for the specific surface area, based on mercury intrusion results. However, in



Table 4.1.3 Measured Porosities of Mortars from Various Concretes, in Per Cent  
by Volume

Formula Used	Prism Samples					Cylinder Samples		
	BD-9	IWA-2	LPF-10	LPN-5	LPN-6	BD-9	LPN-5	
						Bottom	Top	Bottom Top
$p = V \cdot \rho_r \cdot 100\%$	20.4	19.8	13.7	14.2	11.0	19.5	20.1	8.4 9.3
$p = (1 - \rho_r / \rho) \cdot 100\%$	19.6	19.7	14.6	13.8	10.5	18.6	19.2	8.1 8.6



order for this method to apply, a prerequisite is that all pores should be intruded within the pressuring capacity of the instrument. This condition does not seem to have been met; therefore the validity of the values is questionable.

As indicated in Table 4.1.2, mortar pieces taken from the conventional concrete (BD & IWA) beams have a significantly greater pore volume per unit weight than mortar from the low porosity concrete beams (LPF and LPN). The values being about 0.10 for the former and about 0.07 for the latter.

For concrete in cylinders, it may be expected that the porosity of the mortar at the top of the cylinder may be somewhat greater than that at the bottom. From the results of the porosity calculations of mortar pieces taken from the top and bottom 1-in. sections of 6 x 12 in. cylinders of BD and LPN concretes as shown in Figures 4.1.6 to 4.1.9, it can be seen that indeed the porosities of the mortars taken from the top of the cylinders are slightly higher than those from the bottoms. The effect is presumably attributable to consolidation with depth.

The volume of mercury intruded in the mortars sampled from either the top or the bottom of the 6 x 12 in. cylinders of LPN-5 concrete seems lower than that of mortar taken from the companion concrete beam, being about 0.04 cc/g for the former and 0.07 cc/g for the latter. On the other hand, there was no significant difference between the results of the cylinder and beam specimens for the BD concrete, the





only other variety for which the comparison could be made.

The data of Table 4.1.2 also provide a comparison of the pore volume per unit weight for two different LPN concretes, LPN-5 and LPN-6. The former has a normal content of fine sand; the latter an increased proportion of fine sand. The respective pore volumes intruded were about 0.07 and 0.05 ml/g, indicating that the porosity of a concrete can be significantly reduced by selecting a suitable sand gradation.

From the graphs in Figures 4.1.1 and 4.1.2 it is observed that two distinct regions of steep gradient on the semilog plot are present for the conventional concretes (BD and IWA). The midpoints of these steep gradient portions corresponding to about 1.0  $\mu\text{m}$  and 0.04  $\mu\text{m}$  respectively. For the mortar pieces obtained from the LPF specimen (Figure 4.1.5) the larger diameter region shows a much less steep rise, with a significantly steep gradient occurring only at smaller diameters. The midpoint of this steep gradient region is about 0.03  $\mu\text{m}$ . With the low porosity concrete without fly ash of normal sand gradation (LPN-5), the mortar pieces analyzed also showed a gradual rise with a single steep gradient region, centered at about 0.60  $\mu\text{m}$ , as seen in Figure 4.1.4. As seen in Figure 4.1.5 the low porosity concrete without fly ash of the modified sand gradation (LPN-6), showed a single steep gradient region, but in a significantly lower pore diameter range centered at about 0.02  $\mu\text{m}$ .



The trends for mortar pieces taken from concrete cylinders are essentially the same as those described above for mortar pieces taken from concrete beams.

The pore size distributions observed in this study tend to be bimodal, especially for the conventional concretes, and coarser for these than for the LP concretes. In both BD and IWA concretes, the two modes centered at about  $1.0\text{ }\mu\text{m}$  and about  $0.04\text{ }\mu\text{m}$ . There is a shift into the smaller pore region for the LPN-5 concrete, with the single predominant mode centering at about  $0.60\text{ }\mu\text{m}$ . The shift is much more to the smaller pore region for the LPF and the LPN concrete with special sand gradation, both showing significant volumes of fine pores, with the finer modes centered at about  $0.03\text{ }\mu\text{m}$  for both these concretes.

The bulk density of the low porosity concretes (LPF and LPN) are slightly higher than those of the conventional concretes (BD and IWA). Conversely, the porosities of the LPF and LPN concretes are lower than those of the conventional concretes, being about 12.5% for the low porosity concretes as compared to about 20% for the conventional concretes.



## 4.2 MEASURED SHRINKAGE CHARACTERISTICS OF THE VARIOUS CONCRETES

Five different concrete formulations were used in this portion of the study, being the same as used in the previous section except for LPN-4 which replaced LPN-5. The two latter mixes are essentially the same. The specific mix proportions of these concretes are shown in Table 4.1.1. The method for length change of hardened concrete described in the ANSI/ASTM Designation: C 157-75 was followed in this study.

### 4.2.1 Materials, Specimens and Test

The concrete mixes were prepared as described in 2.2.1 (ii) and cast in 3 x 3 x 11½ in. steel molds. The fresh concrete was placed in the mold in two approximately equal layers, and each layer was consolidated by hand rodding. Consolidation around the gage studs was carefully done with the fingers to avoid damage. Three specimens were prepared for each of the five concrete formulations. After compaction, the fresh concrete in the molds was covered with plastic sheets and allowed to stand under laboratory conditions, at 22°C, for 1 day.

The specimens were demolded and placed in water maintained at 23°C for about 30 minutes. They were then removed



from the water and wiped with a damp cloth. Initial length measurements were taken, after which the specimens were cured in a lime-saturated water for 28 days. At the end of the curing period a second length measurement was taken. The specimens were removed to a controlled-climate room maintained at a relative humidity of  $50 \pm 4\%$  and a temperature of  $23 \pm 2^{\circ}\text{C}$ . Length measurements of each specimen were taken with a length comparator after total periods of air storage of 4, 7, 14 and 28 days, and subsequently of 8, 16, 32 and 64 weeks.

#### 4.2.2 Results and Discussion

The length changes recorded at the indicated times of air storage at  $50 \pm 4\%$  R.H. are plotted in a graph of shrinkage versus age in days, shown in Figure 4.2.1. A list of histograms illustrating the relative shrinkage of the different concretes at various ages are shown in Figure 4.2.2.

The shrinkage of the conventional concrete formulations (BD-9 and IWA-2) were significantly higher at all ages than all of the formulations of low porosity concrete. Of the two conventional mixes, surprisingly, the IWA-2 showed greater overall shrinkage than the BD-9 concrete.

Of the low porosity concrete formulations, the fly ash-bearing mix (LPF-10B) showed rather more shrinkage than the formulations without fly ash. The lowest shrinkage was exhibited by the LPN-4 formulation which had the normal sand gradation.

At 64 weeks the average shrinkage of the conventional concrete formulations was approximately  $600 \times 10^{-6}$ ; the





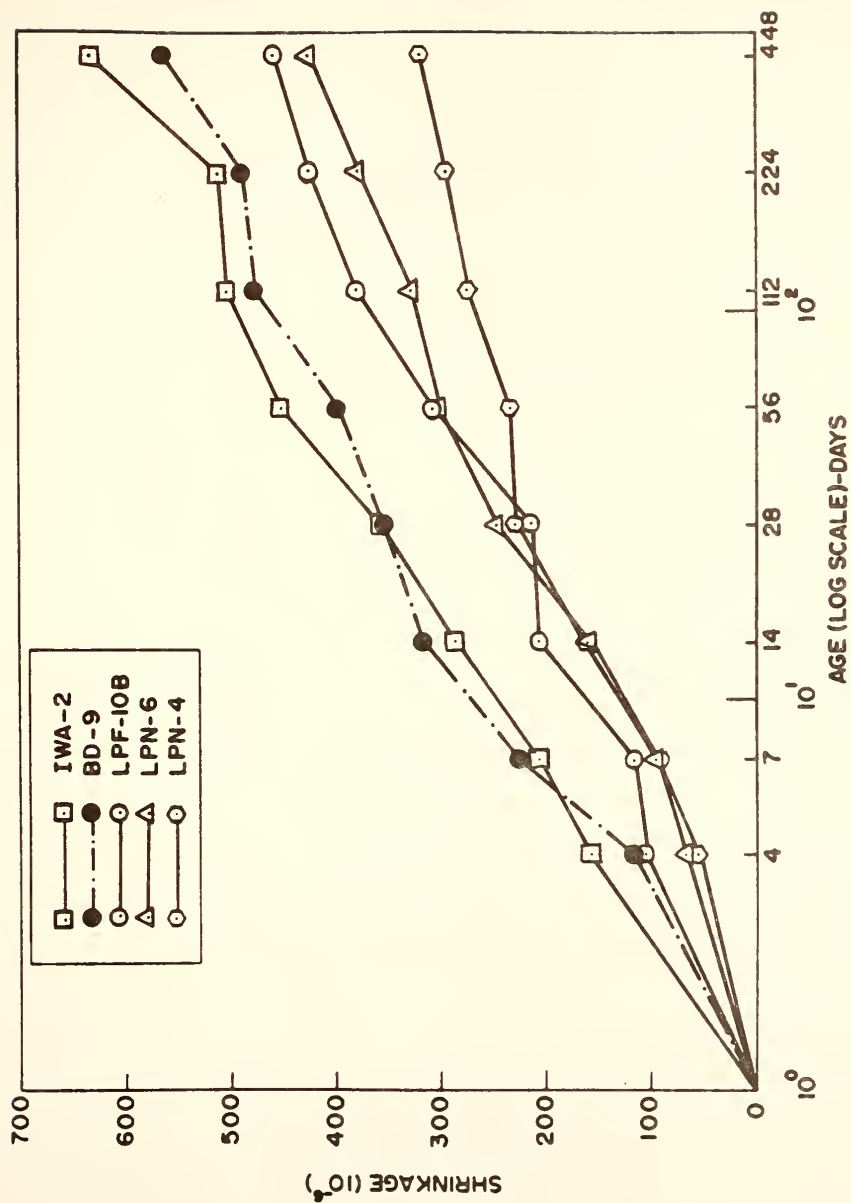


Figure 4.2.1 Shrinkage of Different Concretes at Increasing Ages



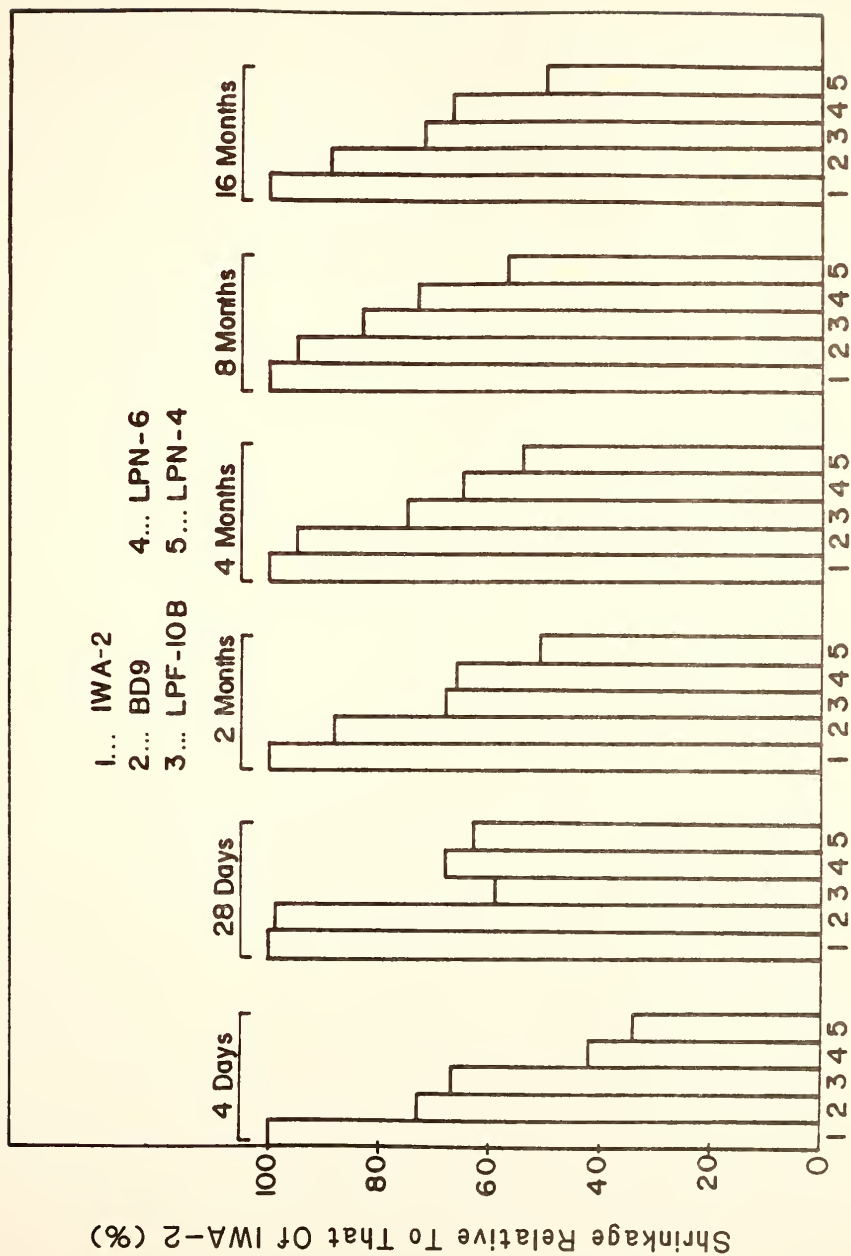


Figure 4.2.2 Shrinkage of Different Concretes at Various Ages Relative to that of IWA-Concrete at the Same Age



corresponding average shrinkage of the low porosity concrete formulations was approximately  $400 \times 10^{-6}$ . These are significant differences. A clear indication of the differences in shrinkage capacity of the several mixes and of the measured relative shrinkages at a number of intermediate ages can be gotten from the histograms of Figure 4.2.2.



### 4.3 CHLORIDE ION PENETRATION INTO CONCRETES

#### 4.3.1 Introduction

The crux of the problem of bridge deck deterioration is the premature corrosion of embedded steel which occurs only after a high concentration of chloride ions has penetrated to the level of the reinforcement. The ingress of chloride ions into concretes depends on several factors, among them the water:cement ratio, the permeability of the concrete, and the type and amount of cement used. This part of the study is concerned with the rate of ingress of chloride ions into the different types of concretes.

#### 4.3.2 Materials, Samples and Tests

Two sets of experiments were carried out in this study. The first involved five different concrete formulations, which were the same as those discussed in section 4.1.2 and shown in Table 4.1.1. The concrete mixes were prepared as described in section 2.2.1 (ii) and cast in three 4 x 3 x 16 in. steel molds. The fresh concrete was placed in the mold in two approximately equal layers and each layer consolidated by hand rodding. The fresh concrete in the molds was then covered with plastic sheets and the concretes stored under ambient laboratory conditions for 1 day. The





specimens were then removed from the mold. Dikes to retain applied solutions were built on two of the beams, and the third concrete beam was left as it was. Each dike ponded an area of about 12 square inches on the 4 x 3 x 16 in. beam. The dikes were made of mortar and were about 0.75 in. high and 0.5 in. wide. The specimens were again covered with plastic sheet and the dikes were allowed to harden for 24 hours. The specimens were then cured in a saturated lime solution for 14 days, removed, and stored until 42 days of age in a controlled climate room having a relative humidity of  $50 \pm 4\%$  and temperature of  $23 \pm 2^{\circ}\text{C}$ .

The upper surface of each of the specimens was abraded with sandpaper prior to being exposed to ponding solutions. The beams with dikes were subjected to continuous ponding of a 0.5 in. deep 3% sodium chloride solution in the controlled climate room ( $40 \pm 4\%$ ;  $23 \pm 2^{\circ}\text{C}$ .) for periods, respectively, of 45 days, 90 days, 6 months and 12 months. The specimens were covered with a plastic sheet to retard evaporation of the solution. At intervals the surfaces of the specimens were flushed with water to remove the build-up of salt on the surface, and then re-exposed to fresh ponding solution.

After the indicated age of exposure, the solution was removed from the dikes and one of the sections isolated by dikes was cut dry from the rest of the beam. The surface of the cut concrete was allowed to dry, and then wire-brushed until all salt crystal build-up was completely



removed. About 3/4-in. of concrete was removed from the sides of each cut specimen to eliminate any salt that might be accidentally introduced to the sides of the concrete in the course of the experiment. One-half inch sections were cut from top of the specimen to a total depth of 2 inches, using a dry laboratory saw. The bottom 1-in. layer was discarded. Slices of concretes cut from the two separate companion specimens were combined and crushed using a small laboratory jaw crusher. This combined crushed sample was quartered, and appropriate portions pulverized to pass a #50 sieve using a laboratory mill. The dummy concrete bar, never exposed to sodium chloride solution, was also sampled and pulverized in a similar manner. The pulverized samples were dried in an oven at 105°C, cooled and analyzed for chloride content.

For the first portion of the specimens analyzed, the analytical method used was that of Clear and Harrigan (78), an updated and revised version of the original silver nitrate potentiometric titration method of Berman (79). However, in view of the large number of chloride determinations that needed to be done in this work, a rapid modified version of the method developed by Prof. W. L. Dolch of Purdue University was investigated and when proven satisfactory, was used for the major portion of these determinations. Five samples were analyzed by both methods and good agreement was found. In Dolch's method a suitable amount of the sample, about 2 to 3 grams, is weighed into a



150 ml beaker and about 10 ml distilled water added to it. One ml per gram of sample weight of concentrated nitric acid is added and swirled for about a minute. The beaker is allowed to stand until the mixture surface became calm, whereupon about 90 ml of distilled water is added to the beaker. The solution is then placed on a magnetic stirring table and titrated with standard silver nitrate solution. No filtration or heating is necessary. The end point is determined using the Gran Plot Method (80).

In all of the analyses, the average of at least two determinations for each of the 1/2 in. sliced sections is reported. The baseline chloride ion content for the test specimen is the average of those determined from the corresponding dummy samples never exposed to sodium chloride solution. The absorbed chloride ion content of each test sample was determined as the difference between the free chloride ion content of that sample and the baseline value determined for the dummy at the same age. The results of these chloride content analysis in concretes are shown in Table 4.3.1.

In the second set of experiments chloride content determinations in four concretes ponded with 4%  $\text{CaCl}_2$  solution and exposed to outdoor conditions were made. The concrete formulations were as previously used, except that the LPN mix with extra fine sand was not included. Details are provided in Table 4.3.2. The concrete mixes were prepared as described in Section 2.2.1 (ii) and cast into



Table 4.3.1 Average Chloride Content (% by Weight) of Concretes Ponded With 3% NaCl

Sample/Age	Depth, in.			
	0-0.5 (I)	0.5-1.0 (II)	1.0-1.5 (III)	1.5-2.0 (IV)
BD-9 (45 days)	0.159	0.018	0	0
" (3 mo.)	0.264	0.053	0.021	0.011
" (6 mo.)	0.339	0.079	0.029	0.023
" (12 mo.)	0.389	0.367	0.409	0.452
IWA-2 (45 days)	0.185	0.055	0.054	0.050
" (3 mo.)	0.182	0.007	0.005	0.005
" (6 mo.)	0.153	0.003	0.001	0
" (12 mo.)	0.249	0.059	0.045	0.025
LPF-10 (45 days)	0.068	0.004	0.002	0
" (3 mo.)	0.074	0.003	0.001	0
" (6 mo.)	0.138	0	0	0
" (12 mo.)	0.258	0	0	0





Table 4.3.1 continued

Sample/Age	Depth, in.				
	0-0.5 (I)	0.5-1.0 (II)	1.0-1.5 (III)	1.5-2.0 (IV)	
LPN-5 (45 days)	0.200	0	0	0	0
" (3 mo.)	0.185	0	0		0
" (6 mo.)	0.325	0.014	0.005		0
" (12 mo.)	0.581	0.003	0		0
LPN-6 (45 days)	0.085	0	0		0
" (3 mo.)	0.144	0	0		0
" (6 mo.)	0.210	0	0		0
" (12 mo)	0.290	0	0		0



Table 4.3.2 Mix Proportions Used in the Second Chloride Ion Penetration Study

Mix Designation	Cement Content, (bags/cu. yd.)	Fly Ash Content, (bags/cu. yd.)	Water-Cement Ratio	Ratio of Cement: Coarse Aggregate: Fine Aggregate	Air Content (%)
IWA-5	8.8	-	0.33	1.0:1.7:1.7	8.5
BD-12	6.3	-	0.43	1.0:2.9:2.1	6.0
LPF-14	7.3	2.7	0.28	+1.0:2.4:1.6	-
LPN-5	10.2	-	0.27	1.0:1.8:1.2	1.5

+ Values based on low porosity cement alone



three 9 x 7 x 3-in. steel molds in which are placed reinforcing steel mats. A sketch of a steel mat used and its dimensions is shown in Figure 4.3.1. The steel mats were supported in the steel molds on four pieces of 1-in. high hardened concrete of the same composition as the fresh mix.

The fresh concrete was consolidated in the mold by hand rodding and covered with plastic sheets. Each of the three replicate specimens were demolded the next day and mortar dikes, about 0.75 in. high and 0.50 in. wide were cast around the edges of the 9 x 7-in. surface. The dikes were covered with plastic sheets and allowed to harden under laboratory conditions for 24 hours. The specimen were then cured in a saturated lime solution for 28 days. The upper surfaces of the specimen were then abraded using sand paper. The specimens were then subjected to continuous ponding for a total of one year. The solution was maintained by periodic addition of fresh  $\text{CaCl}_2$  solution as required. Periodically, the surfaces of the specimens were flushed with water to remove the build up of salt on the surface and then reexposed to fresh ponding solution.

At the end of one year the solution was removed from the specimens and the upper surfaces were allowed to dry. They were then wire-brushed until all salt crystal buildup was completely removed. Two vertical cores, about 1-1/2 in. in diameter, were taken from the middle portion of each of the three specimens. The coring was necessarily done using water as a lubricant. Transverse slices of concrete



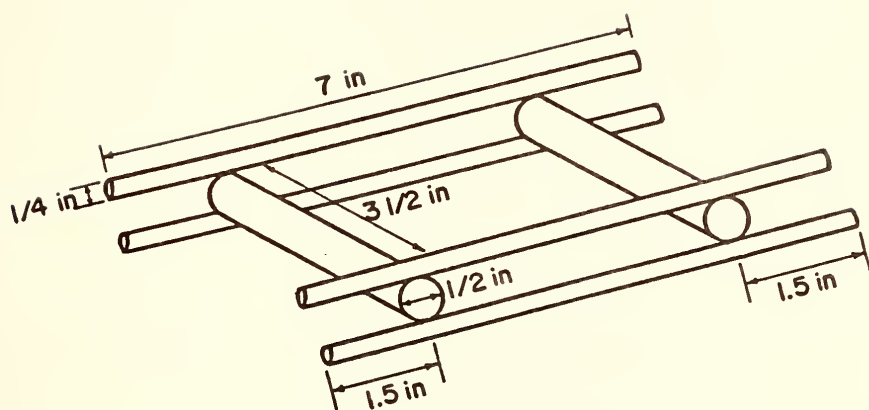


Figure 4.3.1 Sketch of Steel Mat Embedded in Concretes





1/2-in. thick were cut using a small laboratory concrete saw, operated without any lubrication. The first five 1/2-in. slices from the top were separately crushed and milled; the bottom slice was discarded. Thus, five individual depths were sampled from each of two cores from each of the three specimens representing each concrete formulation.

The analysis of this set of samples were carried out at the Materials Testing Laboratories, Indiana State Department of Highways at Indianapolis using the silver nitrate potentiometric method of Clear and Harrigan (78). The courtesy of Mr. P. R. Jackson, Chemist and Mr. R. H. Lowry, Acting Chief is acknowledged with thanks. In these analyses six chloride determinations were made for each depth, and the averages, minus the background chloride determined in the dummy samples, are presented in Table 4.3.3.

#### 4.3.3 Results and Discussion

In presenting the results and the following discussion on the chloride ion penetration into the different types of concretes as evaluated in this work, the conditions under which the two sets of experiments were conducted must be pointed out.

Two different chloride solutions at different concentrations were separately used, respectively a 3% NaCl solution and a 4%  $\text{CaCl}_2$  solution. The chloride ion concentrations in these solutions are obviously different being 18.2 g/l in the 3% NaCl solution, and 25.5 g/l. in



Table 4.3.3 Average Chloride Content (% by Weight) of Concrete in Outdoor Exposed Concretes Bonded for 12 Months Using 4%  $\text{CaCl}_2$  Solution.

Sample	Depth, in.				
	0-0.5	0.5-1.0	1.0-1.5	1.5-2.0	2.0-2.5
BD-12	0.387	0.086	0.093	0.011	0.025
IWA-5	0.320	0.033	0.020	0.020	0.021
LPF-14	0.522	0.023	0.019	0.022	0.015
LPN-9	0.247	0.018	0.014	0.014	0.012



the 4%  $\text{CaCl}_2$  solution. It must also be pointed out that the cation to which the chloride ion is attached may influence the rate of penetration of the two chloride ions into the concrete (71).

The conditions under which the concretes were ponded were also quite different. The 3% NaCl solution exposure was in a controlled-climate room (relative humidity  $50 \pm 4\%$ , temperature  $23 \pm 2^\circ\text{C}$ ). In the controlled room there was air turbulence generated by a continuously operated table fan blowing in the small 7 x 7 x 7 ft. room. The specimens and the ponding solutions on top of them were covered with plastic sheets to check evaporation. The chloride analysis for this set of specimens were done at 45 days, 3, 6 and 12 months. The 4%  $\text{CaCl}_2$  solution was used in ponding specimens which were kept exposed outdoors and subjected to variable changes in wind, temperature and relative humidity.

In the determinations of chloride ion penetration into the different types of concretes using the 3% NaCl solution (specimens kept under controlled climate conditions), parallel chloride ion determinations were made for dummy samples at the same ages as the test samples. The dummy specimens were kept dry throughout the test.

The results of chloride ion content in the dummy samples indicate, within the limits of experimental error, a small but progressive decrease in chloride ion content with age. Since the analysis determines free chloride, it



can be speculated that a portion of the free chloride ions may have been progressively combined with hydrated cement gels (81).

In view of the measurable quantities of chloride ions in the dummy concretes, analyses of the chloride ion contents of the sand and coarse aggregates used were carried out. The chloride ion content of the sand was negligible, about 0.008%; that of the coarse aggregate was somewhat higher, about 0.046%. Essentially all of the chloride ion in the concrete can be shown by calculation to have been contributed by the coarse aggregate.

Analyses reflecting penetration of chloride ions into each of the concretes at 12 months are presented in histogram form in Figure 4.3.2. With either ponding solution it was clear that penetration of  $\text{Cl}^-$  ion beyond the first half inch was negligible for LPF and LPN low porosity concretes. For the IWA concrete significant chloride had penetrated to lower layers, but in progressively decreasing amounts. For the BD concrete ponded with 3% NaCl there was a clear break through of chloride through the entire depth of the specimen (2 in.). Ponding with  $\text{CaCl}_2$  under outdoor conditions resulted in more modest penetration of  $\text{Cl}^-$  into the concrete.

The results generally represent the expected resistance of the low porosity concretes to penetration of  $\text{Cl}^-$  ions, and the partial resistance of the IWA mix. It also points out the extreme penetrability of  $\text{Cl}^-$  ions through the "normal" BD concrete.





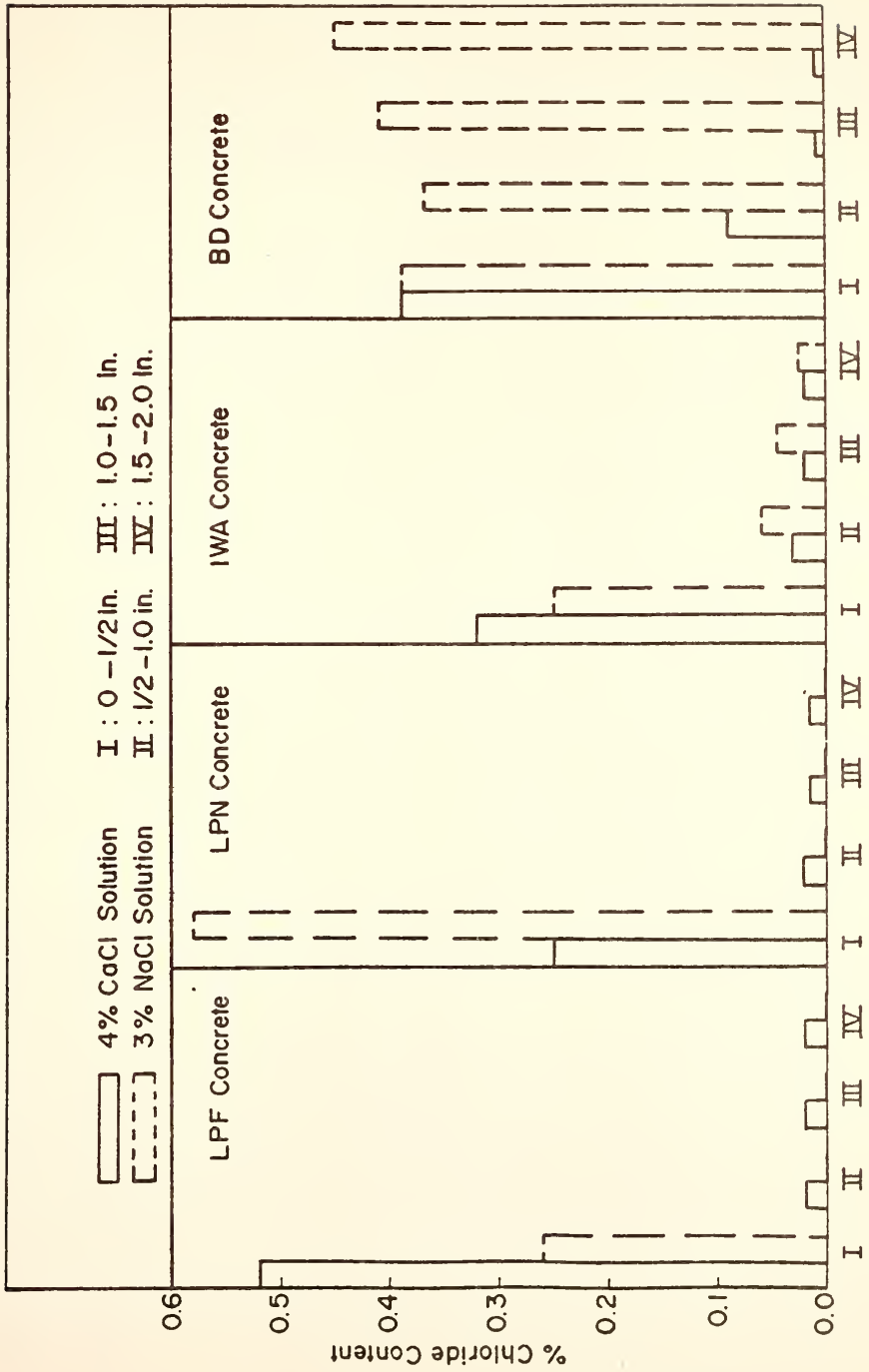


Figure 4.3.2 Chloride Content As a Function of Depth For Different Concretes



## 4.4 CARBONATION OF CONCRETES

### 4.4.1 Introduction

Interest in the study of carbonation of concrete lies principally in the conversion of calcium hydroxide to calcium carbonate which reduces the pH of the pore solution in the concrete. This causes the embedded steel in the concrete to become susceptible to corrosion.

The rate of carbonation depends, among other factors, on the permeability of the concrete to  $\text{CO}_2$  which in turn depends mostly on the water:cement ratio. The relative humidity that prevails also strongly influences the rate of carbonation. Carbonation also causes shrinkage in concretes which may influence cracking.

The objective of this portion of the study is to investigate the depth of carbonation of different concretes under two specified conditions.

### 4.4.2 Materials, Samples and Tests

Two sets of experiments were carried out in this part of the study. The first set involved four different types of concrete under two carbonation conditions. The concretes were:

(i) A formulation representing conventional bridge deck concrete as used in Indiana, designated BD-11.



(ii) A formulation representing the Iowa low slump concrete designated IWA-2.

(iii) A formulation representing the fly ash-bearing low porosity concrete designated LPF-10.

(iv) A formulation representing the low porosity concrete without fly ash designated LPN-5.

The mix proportions of these concretes are given in Table 4.4.1.

The two carbonation conditions are:

(a) A climate room maintained at a relative humidity of  $50 \pm 4\%$  and a temperature of  $23 \pm 2^{\circ}\text{C}$ .

(b) A 6 x 12-in. cylindrical plastic chamber through which carbon dioxide gas, laden with a humidity of 50% was passed at a rate of 2 cubic feet per hour.

The concrete mixes were prepared as described in section 2.2.1 (ii) and cast in three 2 x 4" in. cylindrical steel molds. The methods of compacting the fresh concrete and demolding the hardened concrete after 24 hours were as described in Section 2.2.1 (ii). The demolded samples were cured in a saturated lime solution for 28 days. They were then removed and placed in the climate room ( $50 \pm 4\%$  R.H., at  $23 \pm 2^{\circ}\text{C}$ ) for 7 days and then sawn horizontally into two 2 x 2-in. halves. Of the six half-specimens that resulted, three were placed in the  $\text{CO}_2$  atmosphere and the remaining three in the climate room. At ages 4 and 17 weeks, and at 9 months, samples were removed from the two exposure atmospheres, and sawn vertically in half, thus exposing fresh surfaces.



Table 4.4.1 Mix Proportion of Concretes Used in The Initial Carbonation Test

Mix Designation	Cement Content, (bags/cu. yd.)	Fly Ash Content, (bags/cu. yd.)	Water-Cement Ratio	Ratio of Cement: Coarse Aggregate: Fine Aggregate
BD-11	6.3	-	0.43	1.0:2.9:2.1
IWA-4	8.5	-	0.33	1.0:1.7:1.7
LPF-13	7.4	2.9	0.28	+1.0:1.8:1.2
LPN-8	10.2	-	0.27	1.0:1.8:1.2

+ Values based on low porosity cement alone





The phenolphthalein indicator test was applied to the fresh surfaces. Areas on the concrete surface showing a strong purple coloration indicate no carbonation has occurred in that area. Areas showing diminished purple coloration or no color at all indicate loosely that carbonation has occurred to a limited extent, or has been completed in the area concerned.

In the second set of experiments three different types of concrete cast in 3 x 6 in. cylinders were cured in the fog room for 1 year and were subjected to the two carbonation atmospheres. The three concretes used are approximately of the same composition as the BD, IWA and LPF concretes used in the first carbonation test. No LPN concrete specimen was available for testing in this second experiment.

The mix proportions of these concretes are given in Table 4.4.2. Before exposure, the samples were cut horizontally into three parts, producing three 2 in.- thick slices from each cylinder. Two slices were then placed in the CO<sub>2</sub> atmosphere and the remaining one in the climate room.

At 9 months the samples were removed and sawn vertically into two, exposing fresh surfaces. The phenolphthalein test was then applied.

#### 4.4.3 Differential Thermal Analysis of Mortar Pieces from Concrete

One of the two halves of each 2 x 2 in. cylindrical specimen described previously, which had been kept for 9



Table 4.4.4.2 Second Mix Proportions of Concretes Used in the Carbonation Test Series

Mix Designation	Cement Content, (bags/cu. yd.)	Fly Ash Content, (bags/cu. yd.)	Water-Cement Ratio	Ratio of Cement: Coarse Aggregate: Fine Aggregate
BDS-2	6.6	-	0.41	1.0:2.9:2.1
IWA-1	8.5	-	0.33	1.0:1.7:1.7
LPF-7	7.8	3.0	0.24	+1.0:1.8:1.2

+ Values based on low porosity cement alone.



months in one or the other of the two respective atmospheres, was broken into pieces and the mortar portions carefully hand-picked.

The mortar pieces were milled to pass a No. 100 sieve and differential thermal analysis performed on them as described in Section 2.2.2 (ii). The thermograms of samples BD-11, IWA-4, LPF-13 and LPN-8 kept in the open air, and other samples of the same concrete kept in carbon dioxide atmospheres are presented in Figure 4.4.1.

#### 4.4.4 Results and Discussion

##### (i) Phenolphthalein Test

##### Observations on the Specimens in the First Test Series.

This series comprised 2 x 2 in. specimens cured for 28 days and exposed 4 and 17 weeks, and 9 months in one or the other test atmospheres. None of the specimens placed in either of the atmospheres for 4 weeks showed any carbonation. The same was true for all samples kept for 17 weeks except for specimen BD-11 kept in the enhanced CO<sub>2</sub> atmosphere, in which carbonation was detected on the edges about 4.5 mm deep into the concrete.

Of the samples kept in the respective atmospheres for 9 months, all of those kept in the climate room remained uncarbonated. Samples kept in enhanced CO<sub>2</sub> atmosphere did not show a clear line of demarcation but the intensity of coloration varied depending on the type of concrete, from faint to moderate to intense. The BD concrete showed only



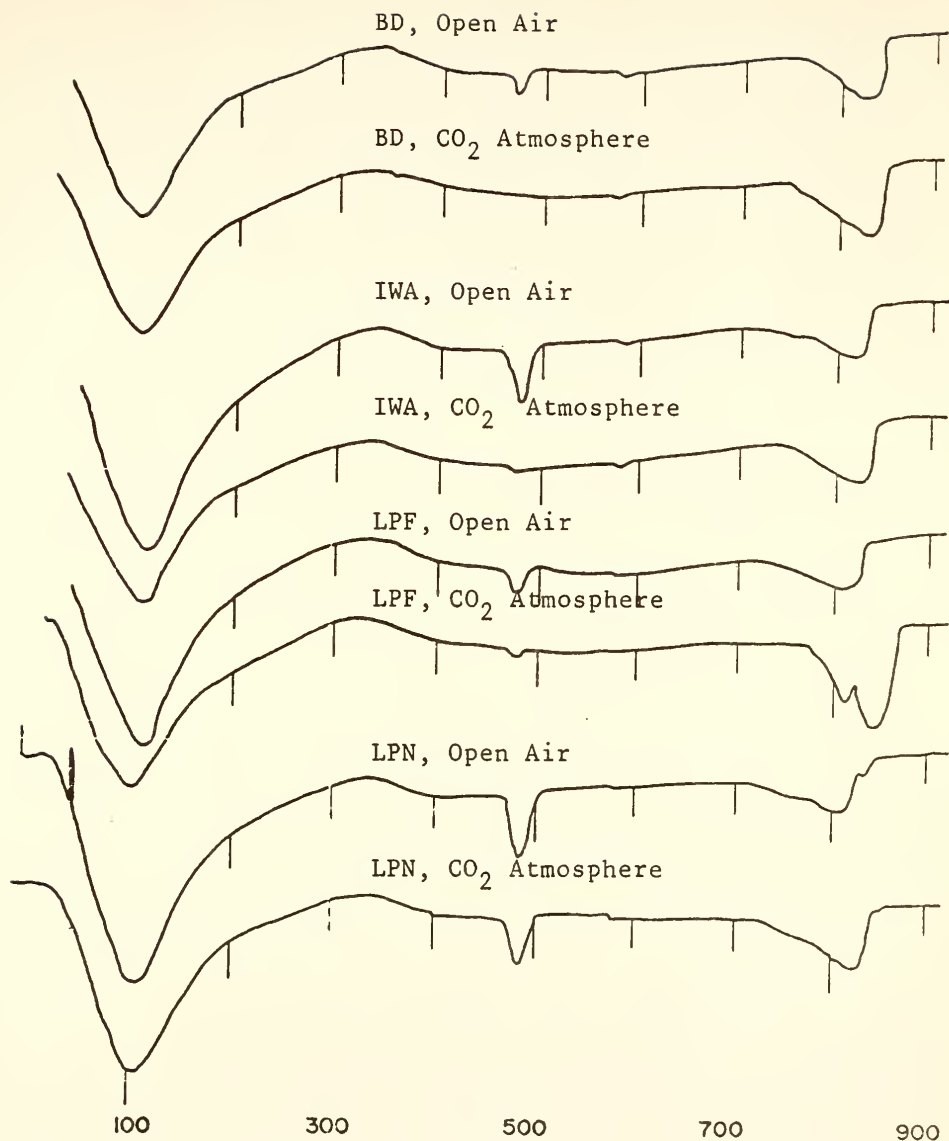


Figure 4.4.1 Differential Thermograms of Powdered Mortar Pieces From Different Concretes Kept in Open Air and in Enhanced CO<sub>2</sub> Atmosphere for 9 Months





faint purple coloration, the IWA concrete showed moderate coloration, and the low porosity concretes LPF and LPN concretes both showed intense coloration. These variations correspond to degrees of carbonation which can be rated as high, moderate and virtually none, respectively. This is a qualitative assessment of the carbonation in the concretes.

A picture of representative specimens of the four types of concretes kept in the enhanced  $\text{CO}_2$  atmosphere for 9 months is shown in Figure 4.4.2

Observations Made on the Specimens in the Second Test Series. This series comprised 3 x 2 in. specimens cured for 1 year and exposed to a  $\text{CO}_2$  atmosphere for 9 months. The IWA and the LPF concretes remained uncarbonated as shown by the intense purple coloration. Carbonation had occurred about 15 mm deep on all sides of the BD concrete, as shown by the faintness of the purple color in that zone. There was no sharp line of demarcation, but an intense purple coloration in the innermost area of the specimen indicate that carbonation had not as yet extended to this area of the concrete. A picture of specimens of the three types of concrete kept in the enhanced  $\text{CO}_2$  atmosphere for 9 months and subjected to the phenolphthalein test is shown in Figure 4.4.3.

#### (ii) DTA Results

DTA thermograms of the mortar portions removed from the concretes are shown in Figure 4.4.1. The results of



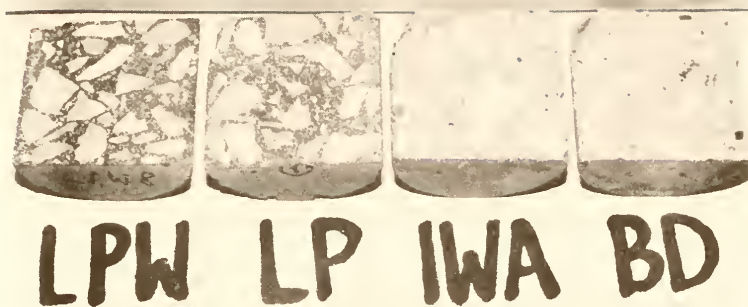


Figure 4.4.2 Extent of Carbonation of Four Different Concretes As Indicated by Phenolphthalein Test

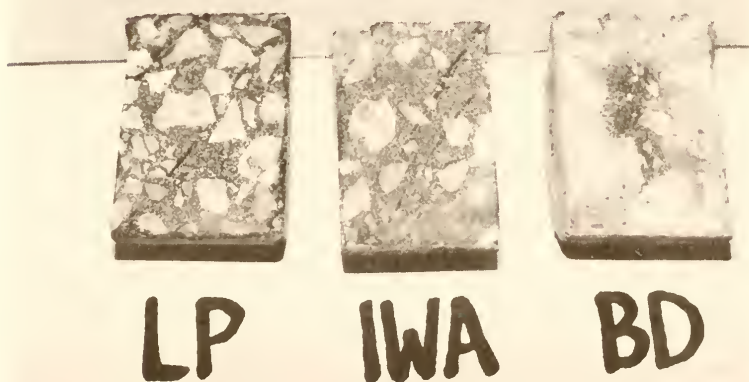


Figure 4.4.3 Extent of Carbonation of Three Different Concretes As Indicated by Phenolphthalein Test



samples cured for 9 months in each of the two different atmospheres are all shown on the same figure.

For all of the specimens kept in the climate room, a significant endotherm for calcium hydroxide was present. The area of the calcium hydroxide endotherm corresponded fairly well with the cement content in the particular mix.

Of the conventional concretes, the BD specimen showed a smaller area than the IWA specimens. The cement content in this BD mix was 6 bags per cubic yard, as compared to 8 bags per cubic yard in this IWA mix. Of the two low porosity formulations of concrete the LPF specimens showed a smaller  $\text{Ca(OH)}_2$  area than the LPN specimens. This may be explained by the known reactivity of fly ash with calcium hydroxide as ascertained in the preliminary studies. However, it is to be noted that the cement content in the LPF concrete is lower than that of the concrete without fly ash. Thus the smaller content of  $\text{Ca(OH)}_2$  in the mortar may be due to either or both of these causes.

All the specimens kept in the enhanced  $\text{CO}_2$  atmosphere for 9 months showed a significant reduction in the area of the calcium hydroxide endotherm compared to the same type of specimen kept in air. The endotherm was completely eliminated in the BD specimen and was almost gone for the IWA specimen, indicating the transformation of  $\text{Ca(OH)}_2$  in these concretes under the enhanced  $\text{CO}_2$  atmosphere exposure.

A small but noticeable endotherm for calcium hydroxide remained for the LPF concrete exposed to the enhanced  $\text{CO}_2$



atmosphere; there was only a slight reduction. The peak for LPN concrete showed only a slight diminution from its reference value. Thus the mortar separated from the LPN concrete was hardly carbonated and that from the LPF concrete only incompletely so. These results substantiate the qualitative inferences made with regard to the degree of carbonation using the phenolphthalein test.

The DTA thermograms also show the expected endotherms for the formation of carbonates at about  $820^{\circ}\text{C}$ . However, as indicated in Figure 4.4.1, the increase in the observed peak area for this peak due to the exposure to the enhanced  $\text{CO}_2$  atmosphere was generally small. It appears that the carbonate endotherm is a much less sensitive indicator of the extent of carbonation than the area of the residual  $\text{Ca}(\text{OH})_2$  peak previously discussed.





#### 4.5 WATER PERMEABILITY OF CONCRETES

##### 4.5.1 Materials, Samples and Test

A study of water permeability in concretes was carried out using four different types of concretes:

(i) A formulation representing conventional bridge deck concrete as used in Indiana, designated BD-9.

(ii) Two formulations representing Iowa low slump concrete for resurfacing bridge decks, designated IWA-2 and IWA-4.

(iii) Three formulations representing fly ash-bearing low porosity concrete designated FPF-10B, LPF10C, and LPF-13.

(iv) Two formulations representing low porosity concrete without fly ash designated LPN-5 and LPN-8.

The compositions of the concretes are shown in Table 4.5.1.

There is no ASTM standard procedure for concrete permeability testing, and the test procedure adopted in this study was patterned after the U.S. Army Corps of Engineers method, CRD-C 48-73.

The samples were mixed as described in Section 2.2.1 (ii) and cast in 6 x 12-in. cylindrical steel molds. They were demolded after 24 hours and cured in a saturated lime solution. As described in Section 2.2.1 (v), 2-in. slices were sawn from the 6- x 12-in. cylinder for testing. The



Table 4.5.1 Concrete Mix Proportions Used in Permeability Studies

Mix Designation	Cement Content, (bags/cu. yd.)	Fly Ash Content, (bags/cu. yd.)	Water-Cement Ratio	Air Content (%)	Ratio of Cement: Coarse Aggregate: Fine Aggregate
BD-9	6.3	-	0.43	6.0	1.0:3.0:2.1
IWA-2	8.6	-	0.33	7.3	1.0:1.7:1.7
IWA-4	8.5	-	0.33	8.5	1.0:1.7:1.7
LPF-10B	7.6	2.7	0.28	5.0	+1.0:2.4:1.6
LPF-10C	7.4	2.6	0.28	-	+1.0:2.4:1.6
LPF-13	8.4	2.9	0.28	-	+1.0:2.4:1.6
LPN-5	10.1	-	0.28	4.0	1.0:1.8:1.2
LPN-8	10.2	-	0.27	-	1.0:1.8:1.2

+ Values based on low porosity cement alone

Amount of lignosulfonate and sodium bicarbonate by weight of cement in all the low porosity concretes in both formulations are 0.56 and 1.2 respectively.



specimens tested ranged in age from 2 months to 7-1/2 months. The procedures for preparation and mounting of the specimens in the compartments of the equipment were described in Section 2.2.2 (vi).

#### 4.5.2 Results and Discussions

It is generally conceded that it is exceedingly difficult to make consistent and reliable experimental measurements of concrete permeability (72, 82, 83). Reproducibility is usually poor, and individual measurements tend to be erratic, even when great care is exercised. Thus relatively large numbers of replicate specimens are needed to establish consistent trends. The difficulties are even greater when the concrete being measured is designed to be dense and as impermeable as possible.

The results obtained in the course of this study are no different from the experience of others in this regard. The measurements secured tended to be erratic and inconsistent, especially when flow was considered on a daily basis. Some of this inconsistency seems to have been the result of uncontrolled temperature fluctuations in the non-air conditioned basement room in which the testing was carried out. Unfortunately also, only a very limited number of specimens could be tested in the time available, probably too few to really establish the differences sought.

Approximately 1-1/2 years was spent in assembling the apparatus and in repeated attempts to remove all leakages and sources of malfunction. The equipment was



capable of testing only two specimens simultaneously. At least two weeks was spent for each run in pre-conditioning a flow regime through each pair of specimens, and from ten to 16 days in daily measurement of flow. Thus the number of specimens that could be tested was in the course of the active portion of this project was quite limited. A total of 16 individual specimens taken from eight different mixes was actually tested, over an aggregate period of over one year. Of these, the results of two mixes were so inconsistent and erratic that they had to be discarded, leaving a total of 12 measurements on six different mixes as listed in Table 4.5.2.

The values in Table 4.5.2 represent permeability as defined by the Darcy coefficient  $K$ , expressed in m/s. Specifically, each value in the table is calculated from the average flow recorded on each of 10 to 16 successive days (depending on the specimen) after 14 to 16 days of prior conditioning flow aimed at achieving a steady state flow regime.

Unfortunately, it was apparent from the daily measurements that steady state flow was not arrived at, with rather large fluctuations being recorded in water transmission from day to day. Nevertheless it is assumed that the average permeability calculated from these measurements does have some validity at least as an indication of the general level of permeability for the concretes involved.





Table 4.5.2 Measured Permeability of Different Types of Concretes

Sample	Age (months)	Permeability, $K$ , $10^{-13} \text{ m/s}$		Number of days Averaged	Average Permeability $10^{-13} \text{ m/s}$	Overall Permeability of Concrete type $10^{-13} \text{ m/s}$
		Bottom Slice	Top Slice			
BD-9	4.5	2.2	4.1	13	3.2	3.2
IWA-2	3	1.5	2.4	14	2.0	1.6
IWA-4	5	1.4	1.0	15	1.2	
LPF-10B	2	0.1	1.0	13	0.6	1.1
LPF-10C	7.5	1.5	1.7	10	1.6	
LPN-8	3	1.0	1.1	14	1.1	1.1



On examining the results recorded in Table 4.5.2 the following generalizations may be obtained:

(a) All the concretes have permeabilities of the same order of magnitude, roughly from 1 to  $3 \times 10^{-13}$  m/s.

(b) Insofar as the data are capable of distinguishing between the permeabilities of the different concrete formulations, it appears as though the low porosity concretes made with and without fly ash tend to have the same permeability, around  $1 \times 10^{-13}$  m/s.

(c) Subject to the same disclaimer, it appears that the permeability of the dense IWA conventional concrete mix is somewhat greater, i.e. about  $1.6 \times 10^{-13}$  m/s, and that of the mix representing the normal Indiana bridge deck concrete formulation (BD) is greater yet, i.e. about  $3 \times 10^{-13}$  m/s.

(d) The measurements recorded for the "top" slices are usually slightly greater than the values recorded for the "bottom" slices of the same concrete, as might be expected because of the tendency toward some bleeding even in low water content concretes.



## 4.6 MICROSTRUCTURE OF CONCRETES

### 4.6.1 Materials, Samples and Test

The scanning electron microscope (SEM) was used to study the microstructural features of mortar portions of the four different concretes.

The concretes were prepared as described in Section 2.2.2 (ii) and the mortar portions examined as described in Section 2.2.2 (iii). The samples from which the mortar specimen were taken were:

- (i) A formulation representing conventional bridge deck concrete as used in Indiana, designated BD-15.
- (ii) A formulation representing Iowa low slump concrete for resurfacing bridge decks, designated IWA-7.
- (iii) A formulation representing fly ash-bearing low porosity concrete, designated LPF-6.
- (iv) A formulation representing low porosity concrete without fly ash, designated LPN-5.

The composition of the different concretes used above is given in Table 4.6.1. SEM micrographs are shown in Figure 4.6.1 to 4.6.10 for 28 day old specimens for all the four samples; in addition, micrographs of one year old specimen of mortars taken from the LPF and LPN concretes are shown in Figures 4.6.11 - 4.6.18.



Table 4.6.1 Concretes Used in SEM Study to Study Microstructure of Mortar Matrix

Mix Designation	Cement Content, (bags/cu. yd.)	Fly Ash Content, (bags/cu. yd.)	Water-Cement Ratio	Air Content (%)	Ratio of Cement: Coarse Aggregate: Fine Aggregate
BD-15	6.4	-	0.43	5.0	1.0:2.9:2.2
IWA-7	8.8	-	0.33	5.0	1.0:1.7:1.7
LPF-6	7.4	2.7	0.26	8.8	+1.0:2.4:1.6
LPN-5	10.1	-	0.28	4.0	1.0:1.8:1.2

+ Values based on LP cement alone





#### 4.6.2 Results and Discussion

Individual specimens of mortars from the respective concretes examined at 28 days show considerable differences in the different small areas being examined; this is in addition to the differences in hydration products and general microstructural features between pastes of the different concretes.

In the Iowa low slump concrete at 28 days, three major areas were distinguished within the paste system. The dominant areas were mostly exemplified by Figures 4.6.1 and 4.6.2. The former shows largely the equant grain structure of C-S-H gel (type III), and in the central pore, long needle-like rods, about 5  $\mu\text{m}$  or more in length, most likely ettringite. A few short fibrous particles attributable to C-S-H gel (type I) are also present in the void. The formation of both types of elongated particle seems to be favored in cavities or voids. In Figure 4.6.2, thin, platy crystals of calcium hydroxide are seen to be formed in a cavity around which is the general mass of hydration products, within which individual particles can be distinguished but with difficulty. Figure 4.6.3 represents a rarely seen morphology; an area showing only what appear to be C-S-H gel (type III) particles.

The microstructure of the paste taken from the BD concrete is somewhat different from that of the paste taken from the IWA concrete and variations occur within the sample



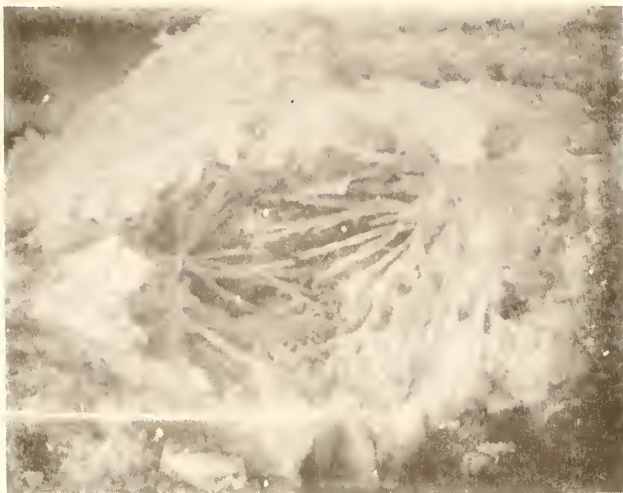


Figure 4.6.1 SEM Micrograph of Mortar From IWA Concrete,  
w:c = 0.33, at 28 Days (2000X)



Figure 4.6.2 SEM Micrograph of Mortar From IWA Concrete,  
w:c = 0.33, at 28 Days (2000X)



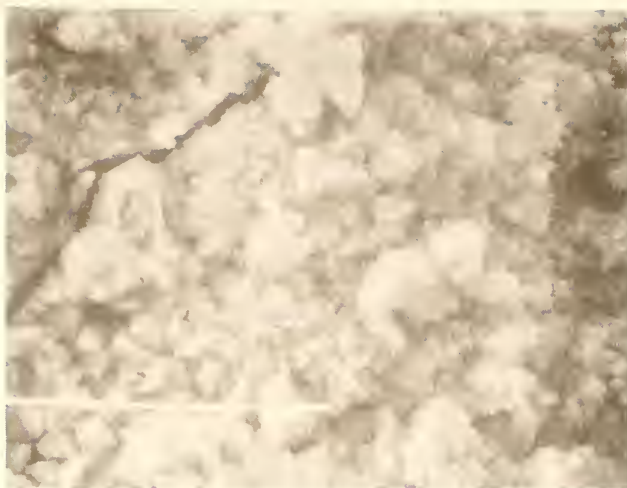


Figure 4.6.3 SEM Micrograph of Mortar From IWA Concrete,  
w:c = 0.33, at 28 Days (2000X)



Figure 4.6.4 SEM Micrograph of Mortar From BD Concrete,  
w:c = 0.43, at 28 Days (2000X)



itself. The structure of the BD paste is more open, probably due to the much higher water:cement ratio, with hydration products not very well fused together. In Figure 4.6.4 hydration products are seen deposited on a piece of aggregate (upper left). There is an incompletely fused structure, in which individual hydration products are discernible. Figure 4.6.5 further show the open structure and individual particles most of which are likely C-S-H gel (type III), although some elongated type I particles and some calcium hydroxide are undoubtedly present.

The fly ash-bearing low porosity samples from concrete at 28 days show areas typified in Figures 4.6.6 and 4.6.7. An almost translucent gelatinous-appearing mass of hydration product seem to cover the area, revealing some fly ash spheres embedded within it. A few isolated equant grain particles typical of type III C-S-H gel are observed within the gelatinous- appearing mass. Unusual regions such as the one represented by Figure 4.6.8 occasionally occur. This represents an area where limited hydration seem to have occurred. The structure is open with hydration product particles and fly ash spheres easily discernible. Here there seems to be a scattered layer of hydration product particles or at least similar appearing particles on the surface of some of the fly ash spheres. It was observed that many small fly ash spheres retain a smooth surface, and hence may be unreactive in this system.







Figure 4.6.5 SEM Micrograph of Mortar From BD Concrete,  
w:c = 0.43 at 28 Days (2000X)



Figure 4.6.6 SEM Micrograph of Mortar From LPF Concrete,  
w:c = 0.26, at 28 Days (2000X)





Figure 4.6.7 SEM Micrograph of Mortar From LPF Concrete,  
w:c = 0.26, at 28 Days (2000X)



Figure 4.6.8 SEM Micrograph of Mortar From LPN Concrete,  
w:c = 0.26, at 28 Days (2000X)



The mortars from the low porosity concrete without fly ash, LPN, showed a "fused" structure typical of LPF fly ash-bearing material except that the hydration product is less translucent and bigger agglomerations of hydration products are found. Such a structure is shown in Figure 4.6.9. An unusual region in this paste is shown in Figure 4.6.10, and also seems to represent an area where the gelatinuous-appearing material is absent and individual hydration product particles are clearly distinguishable. The thin sheet in the center of the micrograph is probably calcium hydroxide.

Mortar samples taken from 1-year old fly ash bearing low porosity concrete, LPF, shows a tighter or more fused structure as compared to the comparable 28 day old mortar. Crystals of calcium hydroxide were observed to be formed in most air voids in the paste. The crystals are about  $0.2\text{ }\mu\text{m}$  thick and lie almost parallel to each other, well packed in the void. This type of microstructure is shown in Figure 4.6.11. Note should also be taken again of the presence of small fly ash spheres which have smooth surfaces and no apparent reaction products on them, even after a year. In Figure 4.6.12 a fused mass of hydration products (C-S-H gel, type III) can also be detected. In the center of the micrograph is a fly ash sphere on which a partial coating - likely a "duplex film" can be observed. Diamond et al (84) have observed duplex films on fly ash spheres in cement-fly ash pastes hydrated for as little as one day. In Figure





Figure 4.6.9 SEM Micrograph of Mortar From LPN Concrete,  
w:c = 0.28, at 28 Days (2000X)



Figure 4.6.10 SEM Micrograph of Mortar From LPF Concrete,  
w:c = 0.28, at 28 Days (2000X)





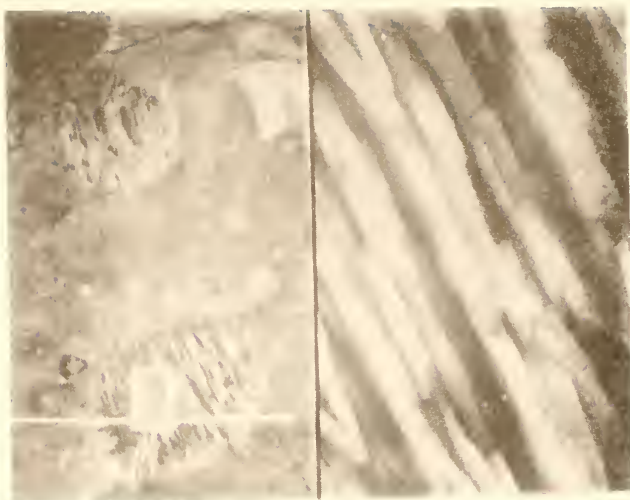


Figure 4.6.11 SEM Micrograph of Mortar From LPF Concrete,  
w:c = 0.26, at 1 Year (1000 and 10,000X)



Figure 4.6.12 SEM Micrograph of Mortar From LPF Concrete,  
w:c = 0.26, at 1 Year (2000X)



4.6.13, again a more fused hydration structure is observed with a few small sharp-edged particles resting on the fracture surfaces of otherwise featureless areas of massive hydration products. The cracks prominent in this micrograph and others are probably due to the fracturing process used to prepare the specimen.

In the mortar taken from the one year old low porosity concrete without fly ash, typical featureless areas of massive hydration products also occur over most of the material observed, as shown in Figure 4.6.14. In a number of areas it was possible to observe the apparent interface between an aggregate grain and the paste. One such area is shown in Figure 4.6.15. The left side of Figure 4.6.15 shows a darker triangular-shaped zone in which a rectangular marker is positioned, and a lighter-textured region surrounding the triangular zone. This triangular zone is apparently an exposed interfacial region between bulk cement paste below the exposed surface and an aggregate grain which was located above the exposed surface and which was removed in the specimen preparation process. Thus the region viewed is that which was directly under the aggregate grain. The right side of Figure 4.6.15 is a somewhat higher magnification view, at 300x, of the area outlined by the rectangular marker and the porosity of the region can be seen. Figure 4.6.16 is an area in the same region at a magnification of 2000x, and a portion of it is further magnified to 10,000x in Figure





Figure 4.6.13 SEM Micrograph of Mortar From LPF Concrete,  
w:c = 0.26, at 1 Year (2000X)



Figure 4.6.14 SEM Micrograph of Mortar From LPN Concrete,  
w:c = 0.28, at 1 Year (2000X)



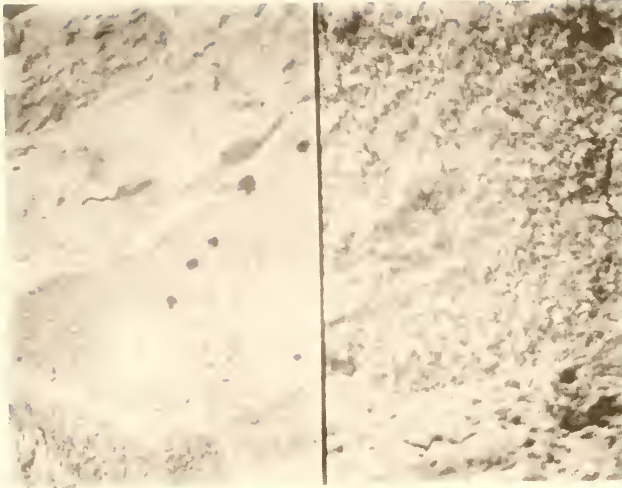


Figure 4.6.15 SEM Micrograph of Mortar from LPN Concrete,  
w:c = 0.28, at 1 Year (30 and 300X)



Figure 4.6.16 SEM Micrograph of Mortar from LPN Concrete,  
w:c = 0.28, at 1 Year (2000X)





4.6.17. In this interfacial zone there occurs an extraordinary volume of unfilled space. The region is characterized by clusters of hydration products which are partly fused equant grained particles for most part (likely C-S-H type III gel) and by rod-shaped products which range in thickness from about 0.1 to 0.3  $\mu\text{m}$  and length to over 2 $\mu\text{m}$ . Such as interface between a paste and sand grain with characteristic open structure has been reported by other workers (32, 82).

Figure 4.6.18, left side, shows the same view as the left side of Figure 4.6.15, except that now the rectangular marker is positioned in a region of bulk cement paste. The right side of the split screen micrograph shows the area within the rectangular marker magnified 10x further, to a total magnification of 300x. This bulk region is obviously more massive in texture than the interfacial zone previously shown in the right side of Figure 4.6.15 at the same magnification. A higher magnification view of this region is found in Figure 4.6.14 which has been previously described.

It is evident from the micrographs of the typical areas of the four different concretes at 28 days that both formulations of the low porosity concretes have a more compact microstructure than their companion conventional bridge deck concretes at the same age.

From the work of Diamond and Gomez-Toledo (22) it was ascertained that by the second day most of the hydration that will occur in low porosity paste had already taken





Figure 4.6.17 SEM Micrograph of Mortar from LPN Concrete,  $w:c = 0.28$ , at 1 Year (10,000X)

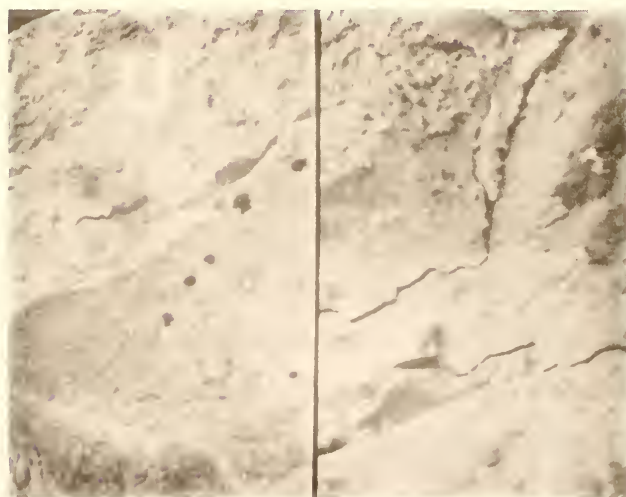


Figure 4.6.18 SEM Micrograph of Mortar from LPN Concrete,  $w:c = 0.28$ , at 1 Year (30 and 300X)



place. About that age the microstructure of the paste had become nearly fused into a massive structure with comparatively little visible residual pore space. Their Figure 10, of the 2 day old low porosity paste at a water:cement ratio of 0.22 bears considerable resemblance to Figure 4.6.9 of the 28 day hydration micrograph of the mortar taken from the LPN concrete.

It is worth pointing out the difference in texture between the hydration product in the mortar taken from the LPF concrete at 28 days, and the hydration product in its companion mortar taken from LPN concrete. In the former the hydration product seems translucent and relatively featureless, as compared to the relatively less translucent and textured appearance of the hydration product in the LPN mix.

Some of the small fly ash spheres of diameters 5  $\mu\text{m}$  or less, possess very smooth and lustrous surfaces. Apparently these do not foster growth of hydration products on them, and this feature persists in samples even up to one year old.

From their characterization studies of the hydrated low porosity pastes, Diamond and Gomez-Toledo (21) concluded that the low porosity paste system gives rise to the same basic hydration products (C-S-H gel and crystalline  $\text{Ca}(\text{OH})_2$ ) that hydration of gypsum bearing cement produces, but that there are differences in: (i) the microstructure which becomes massive at an early stage and, which never develops significant quantities of Type I or Type II C-S-H gel, and



(ii) the fact that no ettringite is formed and very few elongated particles develop. This latter observation is contrary to the observation made in this study for the LPN mortar taken from concrete at one year. Figures 4.6.16 and 4.6.17 show long rods of varying thickness and of the usual dimensions of cement hydration products. In the absence of sulfate in the cement, this hydration product cannot be positively identified as ettringite. However, it may well be a form of ettringite in which the position of the sulfate has been taken by silica. The existence of areas of differing microstructure in the same specimen confirms the non homogeneity of paste systems in concrete and care should be taken in describing microstructural features to distinguish "typical" from "unusual" fields.





## PART FIVE

EVALUATION OF CONCRETES FOR FREEZE-THAW

DURABILITY AND RESISTANCE TO DE-ICER SCALING



## 5.1 INTRODUCTION

The performance of concrete in a freeze-thaw exposure situation depends on the pore sizes and continuity of the pores within the concrete. Pores in concrete may occur in the aggregate as well as in the paste. The aggregate used therefore becomes an important parameter in an evaluation of freezing and thawing performance. In this study the same coarse aggregate, a strong and durable limestone, was used for all the samples.

Concretes mixed at low water:cement ratios are generally strong and relatively impermeable. The pore sizes of the paste component in such concretes may be smaller than usual. However, the range of actual sizes present may be the crucial factor in freezing resistance. It has been suggested (86) that the pore sizes that cause damage to concrete are those that are large enough to admit water but not large enough to permit easy drainage. Kaneuji (87) has established that pores within the diameter range of  $45 \text{ \AA}$  to a little larger than  $1 \text{ }\mu\text{m}$  are responsible for frost damage in coarse aggregates in concrete pavements. This may well be applicable to concretes in general. It has been reported (4) that low porosity concretes are less permeable and therefore would be expected to perform better in a freeze-thaw



condition. This has been substantiated (14).

In the present study the performance of two formulations of low porosity concretes, LPN and LPF were investigated. Comparisons were made also with three types of conventional bridge deck concretes from the standpoint of performance in a freeze-thaw resistance test. The effects of varying proportions of admixtures in the low porosity concretes, and of prolonged curing periods for the fly ash-bearing low porosity concretes were also investigated.

The resistance to the scaling effects of de-icing salts in a freeze-thaw situation for bridge deck concrete and for the two formulations of low porosity concretes was also investigated.



## 5.2 FREEZE-THAW DURABILITY

The following five types of concrete mixes were prepared, cured and subjected to the ASTM Designation: C 666-77, procedure A, rapid freezing and thawing in water test:

- (i) four formulations representing conventional bridge deck concrete as used in Indiana.
- (ii) a formulation representing Iowa low slump concrete for resurfacing bridge decks.
- (iii) a formulation representing conventional bridge deck concrete as used in Illinois.
- (iv) nine formulations representing the fly ash bearing low porosity concrete.
- (v) six formulations representing a low porosity concrete containing no fly ash

The above concrete mixes involved investigation of the effects of a number of variations. These included:

- (a) a properly air-entrained and a non-air entrained BD concrete.
- (b) varying dosages of admixtures in the two formulations of the low porosity concretes (LPF and LPN).





(c) Varying water:cement ratios in the low porosity concretes (LPF and LPN).

(d) Varying cement content in the low porosity concretes (LPF and LPN).

(e) Using different curing times for the fly ash-bearing low porosity concretes, LPF.

The mix proportions of concretes used in the freeze-thaw test is given in Table 5.2.1

#### 5.2.1 Materials, Mixes and Test

The materials and the mixing procedure used in preparing the concretes are the same as were described in Section 2.1 and in Section 2.2.1 (ii). The various mix proportions are given in Table 5.2.1. The fresh concrete was cast into 3 x 3 x 15 in. steel molds and compacted by hand rodding. The freshly cast samples were covered with plastic sheets and left for 24 hours under laboratory conditions. They were then demolded and cured in a saturated lime solution for 2 weeks. Curing times of 3, 7, 8 and 10 weeks were separately provided for some of the fly ash-bearing low porosity concretes. A minimum of three 3 x 3 x 15 in. concrete beams for each concrete mix were tested.

The ASTM Designation: C 666-77, procedure A, rapid freezing and thawing in water test was carried out as described in Section 2.2.2 (vii). A total of about 60 samples were tested.



Table 5.2.1 Mix Proportions of Different Types of Concretes used for Freeze-Thaw Studies

Mix Designation	Water-Cement Ratio	Cementitious Content* (bags/cu. yd.)	Air Content (%)	Curing Time (weeks)	% Ligno-sulfonate +	% NaHCO <sub>3</sub> by weight of cement	Vinsol Resin††	Water†† Reducing-Retarder
LPF-2	0.30	10.1	8.8	10	0.70	1.2	-	-
LPF-3	0.30	10.5	5.0	8	0.48	1.2	-	-
LPF-4	0.30	10.2	7.3	3	0.56	1.2	-	-
LPF-5	0.26	10.4	7.8	7	0.56	1.2	-	-
LPF-6	0.26	10.3	8.8	2	0.56	1.2	-	-
LPF-7	0.24	10.8	4.5	2	0.56	1.2	-	-
LPF-8	0.26	10.3	8.5	2	0.56	1.2	-	-
LPF-9	0.26	10.6	5.5	2	0.56	1.2	-	-
LPF-17	0.24	13.1	-	2	0.54	1.2	-	-
LPN-1	0.26	8.5	1.5	2	0.56	1.2	-	-
LPN-2	0.26	8.5	1.5	2	0.56	1.2	-	-
LPN-3	0.24	10.6	1.0	2	0.56	1.2	-	-
LPN-10	0.30	8.3	2.0	2	0.28	1.2	-	-
LPN-11	0.26	8.5	-	2	0.56	1.2	-	-
LPN-12	0.27	10.4	-	2	0.42	1.2	-	-



Table 5.2.1 continued

Mix Designation	Water-Cement Ratio	Cementitious Content* (bags/cu. yd.)	Air Content (%)	Curing Time (weeks)	% Ligno-sulfonate†	% NaHCO <sub>3</sub> by weight of cement	Vinsol Resin††	Water†† Reducing Retarder
BD-5	0.40	6.2	12.5	8	0.49	-	-	-
BD-6	0.43	6.4	5.5	2	-	-	1.5	8.0
BD-7	0.43	6.6	2.5	2	-	-	-	8.0
BD-8	0.43	6.2	5.0	2	-	-	1.5	8.0
IWA-1	0.33	8.5	8.5	2	-	-	2.0	8.0
ILL-1	0.41	5.9	3.5	2	-	-	1.5	8.0

\* In LPF mixes, fly ash is 35% by weight of total cementitious material. The remaining part is low porosity cement.

In LPN mixes cementitious material is wholly low porosity cement.

In BD, IWA and ILL mixes the cementitious material is wholly portland cement.

† Percentage by weight based on weight of cementitious material.

†† Dosage (oz/100 lb. of cement)



Evaluation of the freezing and thawing resistance of the concretes was carried out in part by measurement of the dynamic modulus of elasticity before freezing and after approximately every 30 cycles of freeze-thaw had been completed. The procedure used was that described by ANSI/ASTM Designation: C 215-76.

Evaluation was also carried out by measuring the weight loss of the specimen before the fundamental transverse frequency readings are taken. This method of evaluation is a variation used by the U.S. Bureau of Reclamation (88). In the test 3- x 6- in. cylinders are used for the evaluation of change in weight of concrete specimens.

As a check on some of the results for the low porosity concrete specimens, pulse velocity measurements were carried out as described in ASTM Designation: C 597-79.

### 5.2.2 Results and Discussion

Measurements of the modulus of elasticity of the specimens before the test and of the relative modulus of elasticity after progressively increasing numbers of freeze-thaw cycles are presented in the Appendix (Tables 1A-1E). The average relative moduli measured for each set of specimen after each increment of freeze-thaw cycles are presented in Table 5.2.2 (A-E). The weights of the specimen before the test and the relative weights at the measured increments of freeze-thaw cycles are presented in the Appendix (Tables 2A-2E). The average relative weights for





Table 5.2.2-A Average Dynamic Modulus and Relative Dynamic Modulus at Different Freeze-Thaw Cycles using the Resonance Frequency Method

Mix Designation	BD-6	BD-7	LPN-1	LPF-6	LPF-4
Elastic Modulus at 0 Cycles (10 <sup>6</sup> psi)	6.3	7.0	7.1	6.1	6.1
No. of Specimens Averaged	3	3	3	3	2
No. of Cycles	0				
32	100.0	100.0	100.0	100.0	100.0
89	97.0	94.4	101.1	101.1	92.0
114	96.6	94.7	99.3	103.0	95.1
142	98.0	96.1	117.4	100.8	97.0
182	95.6	95.8	119.4	99.8	94.7
219	95.4	94.0	117.3	97.5	95.0
287	92.6	91.8	114.3	99.7	93.0
364	93.3	88.4	110.0	95.0	91.6
404	89.8	82.1	105.0	94.6	91.7
476	88.7	77.0	107.0+	94.4	90.2
	84.5	67.5	98.2+	90.4	89.4

+ Avg. of 2 specimens



Table 5.2.2-B continued

Mix Designation	LPN-2	LPN-3	IWA-1	ILL-1	BD-5*
Elastic Modulus at 0 Cycles (10 <sup>6</sup> psi)	8.3	8.1	5.8	6.8	5.3
No of Specimens Averaged	3	3	3	3	1
No. of Cycles					
0	100.0	100.0	100.0	100.0	100.0
39	97.8	98.5	100.4	97.4	95.5
69	96.0	98.1	99.1	95.6	93.4
96	90.7	98.9	100.5	94.5	87.7
167	83.8	95.2	99.7	96.1	86.0
197	74.9	96.7	100.0	95.2	77.6
237	35.7	90.9	98.7	96.6	65.7
287	-	86.0	100.0	92.8	-
350	-	66.1	97.7	87.1	-
409	-	60.5	87.9	71.2	-

\* 9 weeks cured specimen, used as dummy.



Table 5.2.2-C continued

Mix Designation	LPF-2	LPF-3	LPF-5	BD-6*	BD-5
Elastic Modulus at 0 Cycles (10 <sup>6</sup> psi)	6.7	6.9	6.5	5.8	5.6
No. of Specimens Averaged	2	5	3	1	3
No. of Cycles					
0	100.0	100.0	100.0	100.0	100.0
41	96.5	94.0	98.0	106.1	90.3
99	98.0	95.4	98.2	108.0	88.3
158	95.6	94.2	102.2	111.5	78.0
219	87.0	93.2	95.4	104.7	84.0
276	91.3	92.4	97.7	103.6	81.7
332	90.0	92.0	94.0	98.7	75.8+
413	87.7	90.5	93.7	107.0	69.2+

+ Single value

\* 6 weeks cured specimen used as dummy.



Table 5.2.2-D continued

Mix Designation	LPF-7	LPF-8	LPF-9	BD-8
Elastic Modulus at 0 Cycles (10 <sup>6</sup> psi)	7.1	5.1	5.3	5.2
No. of Specimens Averaged	4	4	3	3
No. of Cycles				
0	100.0	100.0	100.0	100.0
35	101.1	101.7	100.6	101.3
92	101.0	101.6	101.0	101.0
165	101.3	101.0	100.6	99.0
211	101.3	100.0	100.2	98.5
265	101.0	99.4	99.6	96.7
323	99.9	98.7	98.0	95.7
363	100.3	98.3	97.6	91.0
422	101.1	98.9	97.6	92.0





Table 5.2.2-E continued

Mix Designation	LPN-12	LPN-10	LPN-11	LPF-17
Elastic Modulus at 0 Cycles (10 <sup>6</sup> psi)	7.7	7.3	7.9	6.6
No. of Specimens Averaged	2	6	4	2
No. of Cycles				
0	100.0	100.0	100.0	100.0
61	99.8	99.4	99.8	98.6
106	96.3	95.2	97.2	96.3
151	95.4	91.3	98.0	96.5
216	92.4	84.6	89.7	97.0
268	82.1	84.4	81.5	96.1
323	79.6	81.4	77.6	95.6
369	76.8	80.5	77.5	98.8
425	78.1	74.6	77.0	95.7



each set of specimens are presented in Table 5.2.3 (A-E). The results of the pulse velocity measurements of some selected specimen before freezing and the relative pulse velocities at different freeze-thaw cycle increments are presented in Table 5.2.4.

The results will be discussed from the standpoint of weight change, of change in physical appearance, of reduction in modulus of elasticity as measured by both the resonance frequency method and the pulse velocity method.

ASTM Designation C 666-77 requires measurements to be carried out to include 300 freeze thaw cycles unless the concrete deteriorates below a specified level before this number has been reached. In the present case, all of the concretes performed well enough that it was decided not to stop at 300 cycles but to continue the test program to at least 400 cycles in all cases.

(i) Weight change in concrete specimens

Initially the average weight of the LPN concrete specimens was significantly higher than that of the other concretes, being about 12.5 lbs., while the other concretes averaged about 11.5 lbs.

In terms of change in weight of concrete specimens at over 400 cycles of freezing and thawing, the LPN concrete performed excellently. None of the several formulations of LPN concretes suffered any loss in weight. Rather, at the end of over 400 cycles of freezing and thawing, most of the specimens had actually gained weight.



Table 5.2.3-A Average Weight and Relative Weight at Different Freeze-Thaw Cycles

Mix Designation	BD-6	BD-7	LPN-1	LPF-6	LPF-4
Wt. at 0 Cycles (lb.)	11.6	12.1	12.6	11.4	11.3
No. of Specimens Averaged	3	3	3	3	2
No. of Cycles					
0	100	100	100	100	100
32	100.10	100.05	100.04	99.90	100.00
89	100.03	99.99	100.04	99.81	100.05
114	100.00	99.84	100.10	99.61	99.95
142	99.71	99.66	100.07	99.42	99.81
182	99.49	99.35	100.07	99.64	99.76
219	99.26	99.12	100.13	99.09	99.64
255	98.80	98.78	100.09	98.79	99.42
287	98.48	98.60	100.16	98.63	99.28
331	98.09	98.02	100.16	98.34	99.13
364	97.40	97.36	100.19	97.84	98.64
404	96.79	96.89	100.22	97.55	98.35
476	95.02	95.72	100.19	97.00	97.29



Table 5.2.3-B continued

Mix Designation	LPN-2	LPN-3	IWA-1	ILL-1	BD-5*
Wt. at 0 Cycles (lb.)	12.6	12.5	11.4	12.0	10.9
No. of Specimens Averaged	3	3	3	3	1
No. of Cycles					
0	100.00	100.00	100.00	100.00	100.00
39	99.92	99.89	100.00	99.94	99.80
69	99.92	99.87	99.97	99.94	99.80
96	99.92	99.89	99.97	99.82	99.70
167	100.06	99.90	99.68	99.48	98.89
197	100.14	99.98	99.55	99.17	98.48
237	100.18	99.95	99.13	99.80	96.46
287	100.26	100.04	98.81	98.13	-
350	-	100.10	98.26	97.55	-
409	-	100.07	97.71	97.00	-

\* 9 weeks cured specimen, used as dummy.





Table 5.2.3-C continued

Mix Designation	LPF-2	LPF-3	LPF-5	BD-6*	BD-5
Wt. at 0 Cycles (lb.)	11.5	11.7	11.5	11.8	10.9
No. of Specimens Averaged	2	5	3	1	3
No. of Cycles					
0	100.00	100.00	100.00	100.00	100.00
41	99.95	100.00	100.00	100.09	99.92
99	99.35	99.74	99.80	99.43	99.33
158	98.88	99.70	99.77	99.34	98.32
219	98.52	99.53	99.64	99.15	97.98
276	98.16	99.40	99.45	98.96	97.45
332	97.56	99.12	99.05	98.42	96.66
413	97.06	98.88	99.05	98.21	95.44

\* 6 week cured specimen, used as dummy.



Table 5.2.3-D continued

Mix Designation	LPF-7	LPF-8	LPF-9	BD-8
Wt. at 0 Cycles (1b.)	12.2	11.1	11.4	11.3
No. of Specimens Averaged	4	4	3	3
No. of Cycles				
0	100.00	100.00	100.00	100.00
35	100.14	100.25	100.22	100.32
92	99.97	99.95	99.88	100.02
165	99.99	99.94	99.96	99.79
211	100.00	99.89	100.03	99.63
263	99.90	99.54	99.84	99.03
323	99.69	99.26	99.24	98.19
363	100.14	99.08	99.44	97.40
422	100.10	99.04	99.31	96.48



Table 5.2.3-E continued

Mix Designation	LPN-12	LPN-10	LPN-11	LPF-17
Wt. at 0 Cycles (1b.)	12.6	12.2	12.5	11.9
No. of Specimens Averaged	2	6	4	2
No. of Cycles				
0	100.00	100.00	100.00	100.00
61	100.14	100.23	100.15	100.16
106	100.15	100.26	100.19	100.16
151	100.25	100.36	100.25	100.15
216	100.31	100.35	100.31	100.14
268	100.33	100.29	100.33	100.11
323	100.36	100.18	100.32	100.10
369	100.37	100.09	100.34	100.07
425	100.38	99.91	100.34	100.03



Table 5.2.4 Dynamic Modulus and Relative Dynamic Modulus at Different Cycles -  
Using Pulse Velocity Method

Mix Designation	LPN-12		LPN-10		LPN-11		LPF-17	
Specimen No.	(1)	(2)	(3)	(5)	(3)	(4)	(1)	(2)
Elastic Modulus at 0 Cycles (psi x 10 <sup>6</sup> )	8.6	8.3	7.8	7.7	8.7	8.6	6.9	6.9
<u>No. of Cycles</u>								
0	100.0	100.0	100.0	100.0	100.0	100.0	100.0	100.0
61	-	-	-	-	-	-	-	-
106	-	-	-	-	-	-	-	-
151	-	-	-	-	-	-	-	-
216	100.2	100.0	100.0	101.3	98.8	100.0	100.0	100.0
268	-	-	-	-	-	-	-	-
323	97.0	97.6	97.4	98.7	97.7	95.3	98.5	99.2
369	95.8	97.6	97.4	98.7	98.8	96.4	100.0	101.4
425	-	-	-	-	-	-	-	-
	86.4	84.3	88.4	88.3	91.9	79.0	100.0	98.5





In all other types of concrete, (LPF, BD, IWA, ILL concretes) weight loss started to occur after about 60 freeze-thaw cycles and the weight loss continued progressively till the end of the experiment.

The weight loss in the LPF concrete was less than in the other three concrete types mentioned above, the average loss after more than 400 cycles being only about 2% for the several formulations of the LPF concretes.

One of the parameters varied for the LPF concretes was the lignosulfonate content, which was varied between a minimum value of 0.48% and a maximum value of 0.70%. The LPF concretes with lower lignosulfonate dosages performed very well with respect to weight loss, there being virtually no loss in weight in such specimens. Specimens made using higher lignosulfonate contents suffered significant weight loss, in the worst case amounting to approximately 3% after more than 400 cycles.

Another parameter varied within the LPF concrete specimens was the length of curing before freezing was begun. Specimens were cured in lime solution for as little as two weeks and as much as ten weeks before starting the freeze-thaw cycles. There was no clear effect of prolonged curing period demonstrated, all weight losses being 3% or less regardless of curing period.

A further variation carried out with the LPF concrete was variation in the water:cement ratios, which ranged from



0.24 to 0.30. The lower water:cement ratio concretes performed better than the relatively higher water:cement ratio concretes, which themselves performed quite well. As an illustration in Tables 5.2.3 D and E it can be seen that concretes of water:cement ratio 0.24 lost no weight and in fact LPF-7 and LPF-17 registered a slight gain in weight at the end of the test, while LPF-2 and LPF-3 concrete of water:cement ratio 0.30 suffered 3% and 1% weight losses, respectively.

From the point of view of weight losses in the freezing and thawing trials, the use of a very high cementitious material factor - 13.1 bags/cu. yd., as the specimens LPF-17 - was not necessary. While there were no weight losses in these specimens after more than 400 freeze-thaw cycles, the same effect was achieved using a lower cementitious material factor of 10.8 bags/cu. yd. at the same water:cement ratio (0.24), in specimens LPF-7.

With respect to the performance of conventional concretes, there was only a limited amount of freeze-thaw data available for the IWA and ILL concrete formulations. Rather more extensive data was available for BD concretes. As indicated in Tables 5.2.2 A, B, C & D, the general range of loss in weight for all of these concretes was about the same, being about 4% after more than 400 cycles. The use of lignosulfonate water reducing admixture in the BD concrete caused the greatest weight loss of all of the specimens tested.



## (ii) Change in Physical Appearance

It was possible to draw distinctions among the concrete formulations in terms of change in physical appearance resulting from the freeze-thaw cycles. Illustrations of the appearance of typical specimens of several formulations after 400 or more cycles are provided in Figures 5.2.1 and 5.2.2. In Figure 5.2.1, the LPN specimen shows no loss in surface cover at all, and this was true for all the other LPN specimens; this concrete was clearly the best of all the formulations in terms of lack of change in physical appearance. Of the two specimens of LPF concrete, one shows comparatively little, the other comparatively much surface erosion. The two BD specimens show considerable surface distress. One of the two, BD-6, on the left, was properly air entrained; BD-7 on the right, was not. Little difference is observed in physical appearance. Figure 5.2.2 shows another LPN specimen, again exhibiting no surface damage, and typical IWA and ILL specimens, each of which shows relatively severe surface exposure of aggregates.

An unusual feature observed in this evaluation was the apparent difference in appearance of the upper (horizontal cast) surfaces of the specimens as compared with the remaining sides. In nearly every case the cast upper surfaces were hardly affected by the repeated freezing and thawing exposure. This was true for all formulations. Examples of the appearance of such surfaces are



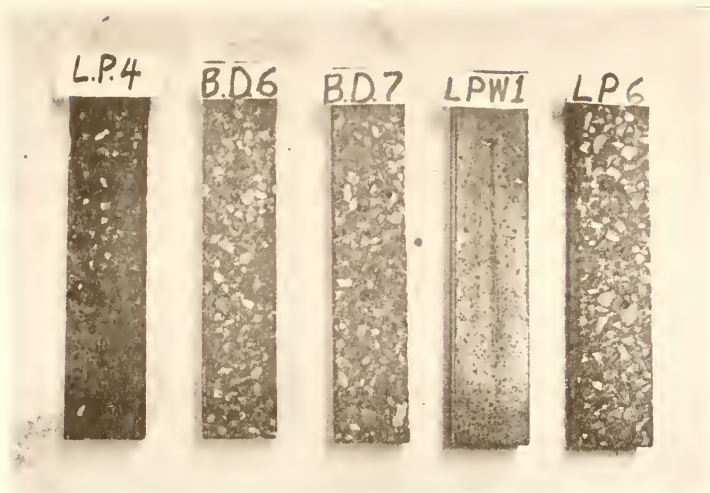


Figure 5.2.1 Physical Appearance of Concrete Specimens After 400 Freeze-Thaw Cycles



Figure 5.2.2 Physical Appearance of Another Set of Concrete Specimens After 400 Freeze-Thaw Cycles





provided in Figure 5.2.3 where the horizontal cast surface is shown for the same specimens already shown in Figure 5.2.1

(iii) Reduction in Modulus of Elasticity

The primary method of evaluation of distress caused by freeze-thaw cycling is reduction in elastic modulus. Differences in the values of the initial modulus of elasticity of the different kinds of concrete before the freeze-thaw test are worth pointing out. The average modulus of elasticity for the LPN concretes is significantly higher than that of the other concrete mixes, being about  $8.0 \times 10^6$  psi. The average value for each of the other concrete types, BD, LPF, IWA and ILL, was about  $6.0 \times 10^6$  psi.

Measurements of the reduction of the dynamic modulus of elasticity due to freezing and thawing showed significant variations among the different concrete formulations.

The fly ash bearing low porosity concretes performed exceedingly well in this regard, the mean reduction in the modulus for all the nine sets of specimens being only about 6% with a standard deviation of about 4.5%, this after more than 400 freeze-thaw cycles. There was some effect of variations of several parameters within the LPF series. In series LPF-2, the combination of a higher dosage of lignosulfonate and a high water:cement ratio (0.30), produced concrete that suffered greatest reduction in



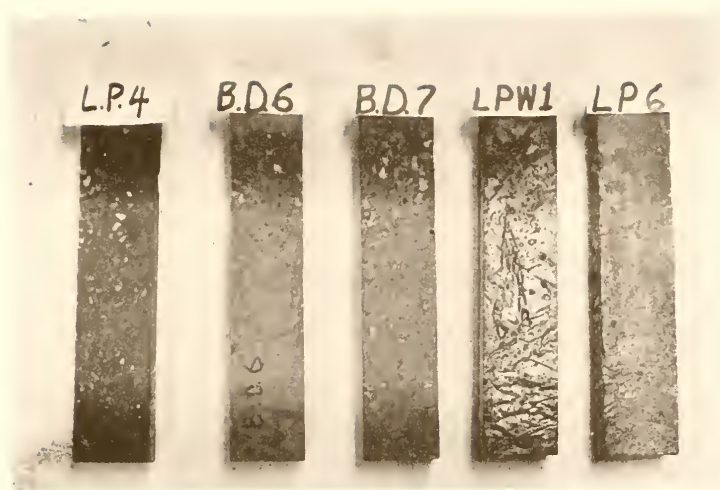


Figure 5.2.3 Physical Appearance of Horizontal Cast Surface of Different Concretes After 400 Cycles of Freezing and Thawing



dynamic modulus, about 13%. Lower dosages of lignosulfonate produced concrete with lesser reductions in the modulus of elasticity, as for example the 10% reductions observed in specimens LPF-3 and LPF-4. The LPF concretes with low water:cement ratios of 0.24 and 0.26 generally performed quite well, reductions being usually 6% or less.

The conventional bridge deck concretes, BD and IWA performed next best to the LPF concretes in terms of retention of the original dynamic modulus. There was a drop of about 12% in dynamic modulus for the IWA concrete, and of about 20% for the BD concretes not counting set BD-5.

The BD-5 concrete incorporated lignosulfonate as a water-reducing admixture and the particular combination entrained an excessive amount of air (about 12.5%). This proved to be incompatible with resistance to freezing and thawing, the weight loss being so excessive that readings made of the fundamental vibrational frequency at later freeze-thaw cycles was rendered inaccurate, and elastic modulus could not be measured.

The reduction of dynamic modulus in the ILL concrete was typically greater than that for the BD concretes, the average reduction being about 25%.

In the low porosity concretes without fly ash, the LPN concretes, variations in the measured response of the modulus to freezing and thawing occurred and some detailed



discussion is appropriate. In the first freeze-thaw test series the LPN specimens did exceptionally well, and it was decided to use this formulation as a standard for the investigations to be carried out in subsequent tests. In these first tests, designated the LPN-1 series, the specimens showed a rather remarkable steady increase (rather than decrease) in the modulus of elasticity, reaching a maximum of about 120% of the starting value at about 150 freeze-thaw cycles. These specimens also showed weight increases rather than decreases as a result of freezing and thawing exposure. The increases in modulus, however, were not sustained on further cycling. Rather, the values started to reduce, and in one of the three specimens went below the initial value after 364 cycles. This prompted a continuation of the test to see the nature of any further reduction. Two of the three replicate specimens did undergo reduction to about 55% and 87% of the initial values while the third retained a modulus over 100% even at 476 freeze-thaw cycles.

In the next set of specimens prepared for the freeze-thaw test, two LPN concretes were prepared. One was formulated using the same proportions of the components as LPN-1 and this was designated LPN-2. A second formulation, LPN-3, had a higher cement content and a lower water: cement ratio. These two new LPN concretes did not perform as well in the second freeze-thaw test series as the LPN-1





did in the first test. There was a steady reduction in the modulus for both LPN-2 and LPN-3 concretes. In the LPN-2 concrete specimens the modulus even dropped below the recommended failure level (60% of the starting value) at about 200 freeze-thaw cycles. On the other hand, the reduction in modulus of the latter, LPN-3, was gradual and it did survive 409 freeze-thaw cycles, retaining about 60% of its original modulus. It should be noted that the initial moduli of the LPN-2 and LPN-3 concretes were both about  $8.0 \times 10^6$  psi and that of the LPN-1 concrete was about  $7.0 \times 10^6$  psi. These are substantially higher than the usual initial modulus for conventional concretes.

In view of the unusually severe reduction in dynamic modulus of elasticity for some of the LPN concretes (LPN-2, LPN-3 specimens) it was considered expedient to perform strength test on some of the specimens which had undergone the freeze-thaw test. Specimen numbers 1 and 2 of the LPN-2 concrete series and specimen number 2 of LPN-3 concrete series were selected for the test. A cube 3 x 3 x 3 in. in. was cut from one end of the 3 x 3 x 15-in. concrete beam and the surfaces smoothed out on a lapping wheel using appropriate powder grits. Additionally a cube of similar size treated in the same way was cut from an LPN concrete beam which had never been subjected to freezing, but had been curing in a saturated lime solution for 1 month. Unfortunately, the specimens that had shown freezing and



thawing-induced reductions in modulus had been stored in a fog room for approximately 5 months between the last freezing cycle and the time of strength test determination. At the time of the strength test these samples were 7 months old. The initial elastic moduli of all four of the specimens tested were close to each other, ranging from  $8.0 \times 10^6$  to  $8.4 \times 10^6$  psi.

The results of the strength tests were as follows:

LPN (1 month cured; as standard)	10,720 psi
LPN-2 (1)	9,170 psi
LPN-2 (2)	12,780 psi
LPN-3 (2)	16,560 psi

In the light of the above results it was felt necessary to check the results of the dynamic modulus determinations using both the pulse velocity method and the resonance frequency method for some selected specimens. Two specimens from each of the three different set of LPN concrete mixes, were tested along with two specimens from one set of LPF (fly ash bearing) concrete. The results for the pulse velocity method shown in Table 5.2.4, indicated a lesser reduction in the dynamic modulus than indicated by the results of the resonance frequency method given in Table 5.2.2.E. The average drop in modulus of elasticity by the pulse velocity method was about 14% as compared with the 25% average drop using the resonance frequency method for the LPN specimens. The drop recorded for the LPF



concrete followed the same trend. However, using the pulse velocity method there was virtually no reduction for the LPF concrete, about 1%, as compared to the 5% reduction indicated using the resonance frequency method.

According to the rating scheme of Guha and Wedpathak (89) the concrete specimens subjected to over 400 freeze-thaw cycles can be considered to be in very good condition. The average initial and final pulse velocity for the LPN concrete were 5.1 km/s and 4.6 km/s respectively. The average initial and final pulse velocity for the LPF concretes were about the same 4.8 km/s. According to the rating, concretes having pulse velocity in excess of 4.0 km/s are in very good condition. In general, the correlation in the modulus of elasticity as measured by the two methods is reasonably good, the differences being 10% or less and the average difference being about 6% overall.

The significant differences in the modulus of elasticity between LPN-1 and LPN-2 using the sonic method remains puzzling, since they were two separate mixes of the same mix proportions. One obvious possible reason for such a difference might be the honey-combing on the top and sides of some of the LPN-2 specimens after casting. However, there was no visible damage done to the material around the honeycomb up to the termination of the test. It should be remarked that subsequent LPN concretes, LPN-3, LPN-10, LPN-11 and LPN-12 showed a consistent and progressive reduction in the modulus of elasticity and all wound up with



approximately the same percentage of reduction of the initial modulus, about 72%, at over 400 cycles. Thus, LPN-1 and LPN-2 can be considered as giving exceptional results, one giving higher than usual LPN results; the other much lower.

In the range of water:cement ratios used, between 0.24 and 0.30, there seems to be no effect of this parameter on the reduction of modulus in the LPN concretes. The use of higher cement content did not exert any favorable influence on the retention of dynamic modulus, as can be seen from the results of LPN-3 and LPN-12 on Tables 5.2.2-B and Table 5.2.2-E respectively.

From the above results and discussion of the freeze-thaw test, the following generalizations can be made:

(a) The low porosity concretes without fly ash, LPN, performed excellently in the test from the standpoint of weight change and physical appearance. However, a somewhat variable and often relatively large loss in dynamic modulus of elasticity was detected. Even so, because of the very high initial modulus of elasticity, at the end of more than 400 freeze-thaw cycles, the LPN concretes wound up with about the same modulus as the LPF concretes, about  $5.7 \times 10^6$  psi. This is as high as the starting modulus of most conventional concretes. It should be emphasized that placing and consolidation of LPN concrete is crucial, and requires great attention.





b) The LPF concrete had typically a lower starting modulus than the LPN concretes, but performed excellently with regard to retention of this lower level of dynamic modulus. However, the results of the weight loss measurements and the physical appearance changes were only fairly good. The latter two characteristics were very much improved by using lower water:cement ratios and higher cementitious material factors up to about 11 bags/cu. yd. of cementitious material.

Longer curing time before the start of the freeze-thaw cycles was found not to exert any significant influence. This is in contrast with results obtained by Kovács (67) who found a beneficial effect of long curing on ordinary gypsum-bearing concrete containing fly ash. It was found that higher dosages of lignosulfonate in these LPF concretes were detrimental in terms of the weight reduction of this concrete in freeze-thaw exposure; low-dosed concretes performed much better in this respect.

(c) The conventional bridge deck concretes, IWA and BD, both performed reasonably well in terms of retention of the initial dynamic modulus, the final values averaging 88% and 80% respectively, of the starting value. Weight loss and physical appearance were about the same for the two concretes, both showing slightly more damage than the LPF concrete,

Entrained air in a BD concrete series did not result in better protection to the concrete, when compared to a



replicate series without any entrained air.

The use of lignosulfonate as a water reducing admixture in the gypsum-based cement was not favorable from the standpoint of weight loss in the freeze-thaw test and also adversely affected the modulus of elasticity of the concrete.

The ILL concrete did not perform well in any of the evaluations.



### 5.3 RESISTANCE TO DE-ICER SCALING

Specimens of the following three different concrete formulation types, with variations in two of them, were prepared, cured and subjected to the de-icing scaling test procedure of ASTM Designation: C 672-76:

- (i) a conventional bridge deck concrete as used in Indiana, BD concrete.
- (ii) a fly ash bearing low porosity concrete, LPF concrete.
- (iii) a low porosity concrete without fly ash, LPN concrete.

Variations in the above concrete mixes include:

- (a) a properly air entrained, and non-air entrained, BD concrete.
- (b) variation in the water:cement ratio of the LPN concrete.
- (c) variation in the cement content of the LPN concrete.

#### 5.3.1 Materials, Mixes and Test

The materials and mixing procedure used in preparing the concretes were the same as described in Section 2.1.1 and Section 2.2.1 (ii). The mix proportions for each concrete is given in Table 5.3.1. The fresh concrete mixes



Table 5.3.1 Mix Proportions of Different Types of Concretes used for De-Icing Scaling Resistance Study

Mix Designation	Water-Cement Ratio	Cementitious Content* (bags/cu. yd.)	Air Content (%)	% Ligno-sulfonate†	% NaHCO <sub>3</sub> †	Vinsol Resin††	Water-Reducer††
LPFS-1	0.24	10.8	-	0.56	1.2	-	-
LPNS-1	0.26	8.5	1.5	0.56	1.2	-	-
LPNS-2	0.28	8.4	1.0	0.56	1.2	2.5	-
LPNS-3	0.30	8.4	1.2	0.56	1.2	2.5	-
LPNS-4	0.28	10.2	2.0	0.56	1.2	5.0	-
BDS-1	0.43	6.4	5.8	-	-	1.5	8.0
BDS-2	0.41	6.6	2.5	-	-	-	8.0
BD-9	0.43	6.3	6.0	-	-	1.5	8.0

\* In LPFS mix, fly ash is 35% by weight of total cementitious material; remaining part is low porosity cement.

In LPN mixes, cementitious material is wholly low porosity cement.

In BDS mixes, cementitious material is wholly portland cement.

† Percentage by weight based on weight of cementitious material.

†† Dosage (oz/100 lb. of cement)





were separately cast in 9 x 7 x 3 in. steel molds and compacted by hand rodding. The freshly cast samples were covered with plastic sheets and left for 24 hours under laboratory conditions. The samples were then demolded and cured in a saturated lime solution for 2 weeks followed by 2 weeks of air curing in a controlled climate room at relative humidity of  $50 \pm 4\%$  and temperature of  $23 \pm 2^{\circ}\text{C}$ .

Two specimens from each concrete mix, were subjected to the test. The upper surface, having an exposed area of 63 sq. in., with no protective coating, had a 4% calcium chloride solution applied after the 4 week curing period. The solutions were retained on the surface by mortar dykes. The specimens were stored in a freezer for 16 to 18 hours each day, and allowed to thaw in laboratory air for the remaining 6 to 8 hours. At every 5-cycle interval for a total of 60 cycles, each specimen was evaluated as per recommendations of ASTM Designation: C 672-76. The total number of cycles applied was in excess of the 50 cycles recommended by the Standard.

### 5.3.2 Results and Discussion

The results of these tests are given in Table 5.3.2. BD concretes with the proper amount of entrained air (BDS-1, BD-9) performed the best. After 60 cycles of freezing and thawing with the de-icing solution on top of the specimen, the broom marks on BDS-1 remained unscathed. The BD-9 specimen showed very slight scaling. Both these concrete mixes contained about 6.4 bags of cement per cubic yard,



Table 5.3.2 Rating of Condition of Specimen Surface per  
Number of Freeze-Thaw Cycle

Mix Designation	No. of Freeze-Thaw Cycles (in presence of de-icing salt, 4% $\text{CaCl}_2$ Solution)						
	0	10	20	30	40	50	60
LPFS-1	0	0	1	1	1	1	1
LPNS-1	0	0	0	1	1	1	1
LPNS-2	0	1	1	2	2	3	3
LPNS-3	0	1	2	3	4	5	5
LPNS-4	0	0	1	1	1	2	2
BDS-1	0	0	0	0	0	0	0
BDS-2	0	1	2	3	4	5	5
BD-9	0	0	1	1	1	1	1

Rating according to ASTM C 672-76

<u>Rating</u>	<u>Condition of Surface</u>
0	No scaling
1	Very slight scaling (1/8 in. depth, max, no coarse aggregate visible).
2	Slight to moderate scaling
3	Moderate scaling (some coarse aggregate visible)
4	Moderate to severe scaling
5	Severe scaling (coarse aggregate visible over entire surface)



and each had a water:cement ratio of 0.43 and an air content of about 6.0%. The other variation of the BD concrete, with about the same cement content and water:cement ratio but with an air content of only 2.5% showed very poor performance. There was significant scaling over all of the surface, exposing some of the coarse aggregates. A picture of a typical BD concrete surface at the beginning of the experiment is shown in Figure 5.3.1. A specimen containing properly entrained air (BDS-1) at the end of the experiment is shown in Figure 5.3.2. The appearance of the BDS-2 specimen with only 2.5% of entrapped air at the end of the experiment is shown in Figure 5.3.3. The difference is apparent.

In the low porosity concretes without fly ash, the water:cement ratio seemed to be significant factor in the scaling resistance. The lower water:cement ratio concrete (w:c 0.26) performed significantly better than the relatively higher water content specimen (w:c 0.30). The lowest water:cement ratio specimen, LPNS-1 showed only slight isolated pitting on the surface at the end of the experiment. A picture of a typical surface before the experiment is shown in Figure 5.3.4. A picture of specimens LPNS-1, at the end of the experiment, is shown in Figure 5.3.5. With a water:cement ratio of 0.28, extensive scaling occurred particularly in specimen LPNS-2 which had a relatively low cement content for low porosity concretes (8.4 bags per cubic yard). A picture of the specimens at the end of the experiment is shown in Figure 5.3.6. Scaling was less severe, as shown





Figure 5.3.1 Appearance of Surface of BD Concrete Specimens Before Scaling Test .



Figure 5.3.2 Appearance of Surface of Air-Entrained BD Concrete After Scaling Test





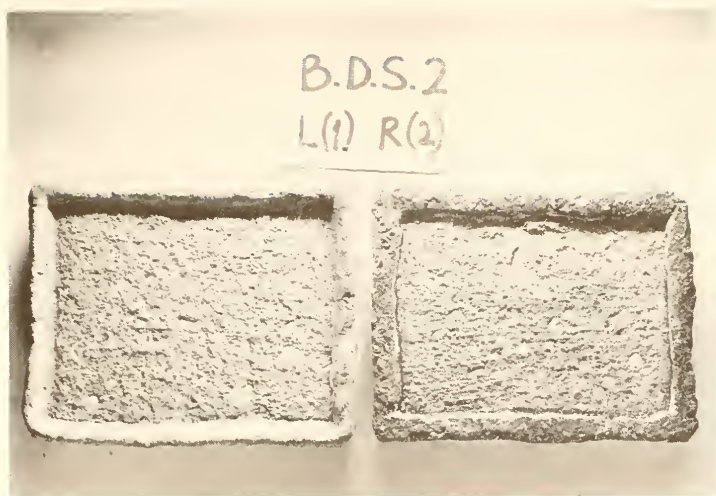


Figure 5.3.3 Appearance of Surface of Non-Air Entrained BD Concrete After Scaling Test



Figure 5.3.4 Appearance of Surface of LP Concrete Before Scaling Test



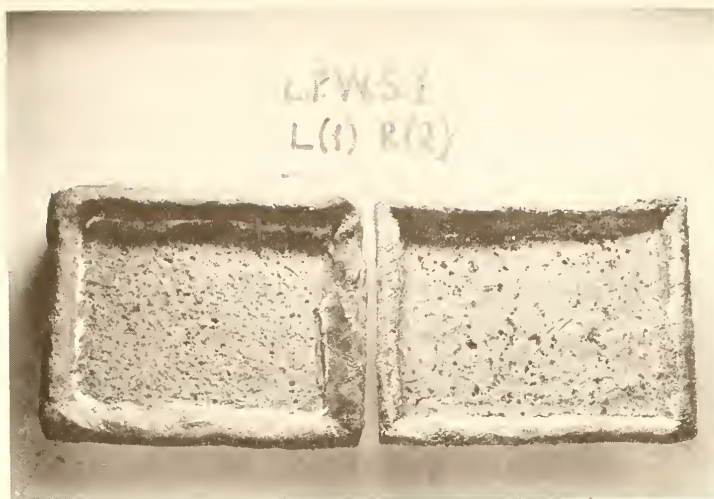


Figure 5.3.5 Appearance of Surface of LPNS-1 Specimen at the End of Scaling Test .

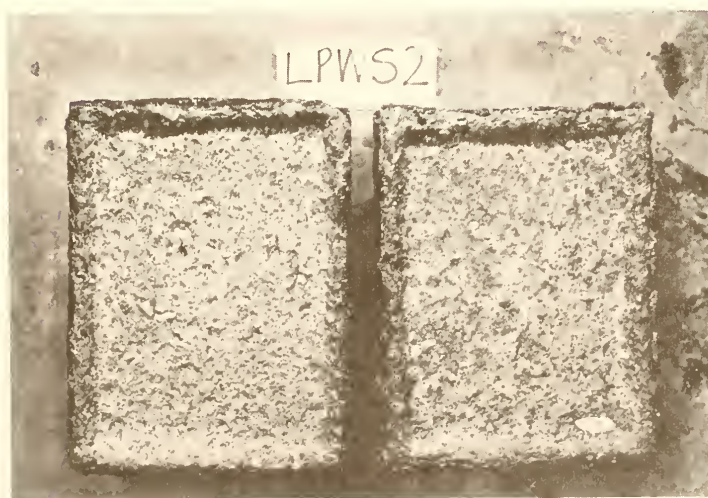


Figure 5.3.6 Appearance of Surface of LPNS-2 Specimens at the End of Scaling Test



in Figure 5.2.7, in the 10.2 bag per cubic yard mix, LPNS-4, at the same water content. At the highest water:cement ratio of 0.30 used in the series, in specimen LPNS-3, the damage observed was the most extensive of all of the concrete specimens tested in this study. The appearance of the specimens after the experiment is shown in Figure 5.2.8, which clearly shows the extensive damage exposing many aggregate surfaces.

The single mix proportion formulated to represent the LPF concrete, LPFS-1, was cast at a water:cement ratio of 0.24. It exhibited only slight scaling and almost no aggregates were exposed, as shown in Figure 5.2.9.

The condition of each specimen surface, as rated according to the standard evaluation scale of ASTM C 672-76 at each 10-cycle interval, is shown in Table 5.3.2. The following generalizations can be made based on the results of the resistance to de-icing salt test:

(a) Properly air entrained conventional bridge deck concrete, provides good resistance to de-icing scaling; non-air entrained BD concretes performed poorly.

(b) The fly ash-bearing low porosity concrete performed quite well in the test.

(c) The poor performance of some of the LPN concrete may be attributed to the presence of vinsol resin. Otherwise the resistance of this concrete in the de-icing test is quite good, comparable to that of the LPF concrete.





Figure 5.3.7 Appearance of Surface of LPNS-4 Specimens at the End of Scaling Test



Figure 5.3.8 Appearance of Surface of LPNS-3 Specimens at the End of Scaling Test





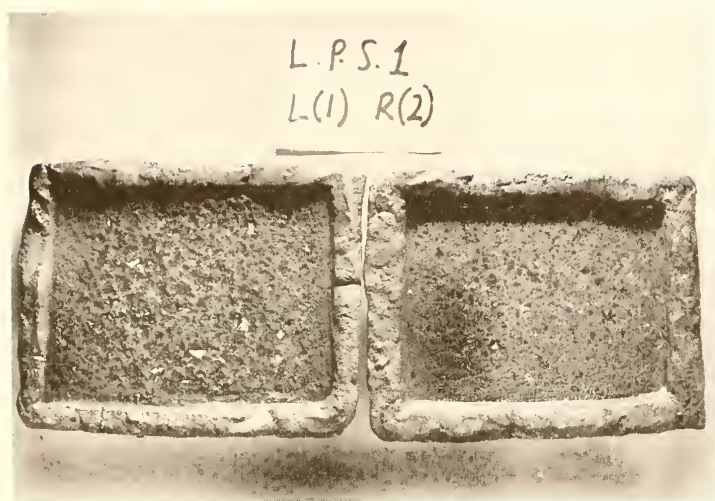


Figure 5.3.9 Appearance of Surface of LPFS-1 Specimens at the End of Scaling Test



PART SIX

CORROSION OF EMBEDDED STEEL IN CONCRETE



## 6.1 INTRODUCTION

The corrosion of embedded steel in concrete occurs when the passivating film around the steel is destroyed. This leads to the formation of ferric hydroxide whose volume is several times larger than metallic iron. Consequently, expansive mechanical pressures as high as 4700 psi (46) are produced, which are many times greater than the tensile strengths of concretes. This expansive pressure causes cracking and spalling of the concrete.

Maintenance of the passivating film is favored by several factors, chief among which are the maintenance of a good watertight cover of concrete and the ability of the concrete pore solution to develop and retain a high pH level in service. These factors are dependent upon the water:cement ratio, the type of cement and admixtures used, and on proper care being taken in the mixing, placing and finishing of the concrete. All of these are important in concrete bridge deck applications, but above all, the service conditions of the concrete in a bridge deck environment are a main determinant of whether corrosion will occur. Factors important here include the adequacy of the bridge deck drainage system, the amount of salt applied, and the number of cycles of freezing and thawing encountered.



In this study the pore fluid in a fly ash bearing-low porosity cement paste series was studied in an attempt to better understand the internal corrosion environment within the concretes. The hydroxide ion concentration in the pore solutions was measured by titration; the concentrations of calcium, sodium and potassium ions were determined by atomic absorption spectroscopy and flame photometry.

Visual estimates of the extent of corrosion that had taken place in concrete specimens were made for specimens that had been exposed to two different simulated service conditions. In the first set of conditions the concrete specimens were kept indoors at constant temperature and relative humidity with a chloride bearing solution kept ponded over the top of the specimens. In the second simulated service condition, similar specimens ponded with a chloride solution were exposed outdoors, and thus subject to daily temperature cycles, wind, and one winter's season of freezing and thawing exposure.

Finally, electrochemical measurements were made to monitor the progress of corrosion of another batch of concrete specimens. These specimens were set up each incorporating two steel mats. In one set of trials the concrete surrounding the upper steel mat was mixed with  $\text{CaCl}_2$  added. In a second set, no calcium chloride was added to the mix.  $\text{CaCl}_2$  solution was ponded on the upper surface of all the specimens after 20 weeks of ponding





with water. Voltage measurements were taken periodically between the two mats to monitor the development of electrochemical corrosion potential. Additionally, an electrochemical measurement of corrosion occurring on each of the two individual steel mats within each specimen was provided by periodic potential measurements made using the  $\text{Cu/CuSO}_4$  half cell as recommended by FHWA (59).

The methods procedures, and results of these tests are presented below.



## 6.2 STUDY OF PORE FLUID OF FLY ASH BEARING LOW POROSITY PASTES

### 6.2.1 Materials, Method of Preparation, and Test Methods

The materials used in the preparation of fly ash-bearing LP cement pastes for pore solution analysis were: a low porosity cement of fineness  $4,500 \text{ cm}^2/\text{g}$  (Blaine); fly ash; and sodium bicarbonate and sodium lignosulfonate (LP admixtures) as previously described in section 2.1.1

A low porosity cement paste was made with the usual LP admixtures  $\text{NaHCO}_3$  and sodium lignosulfonate, and 35% fly ash (by weight of cement) incorporated. The mix proportion of the paste is given in Table 6.2.1. The paste was prepared as described in section 2.2.2 (i) and poured into four 120 ml (4 oz.) plastic containers. They were compacted by striking each one several times on the laboratory bench, and then covered and stored under laboratory conditions. At 12 hours and at 1, 4, and 7 days the pore fluid in the paste was expressed. The paste set after 1 day. The 12-hour and 24-hour old pastes were expressed using a filtration device. The pore fluid in the 4-day and 7-day samples were expressed using a special apparatus described by Barneyback and Diamond (90).



The amount of fluid expressed ranged from about 5 ml at 12 hours to about 1 ml at 7 days. An aliquot of the expressed fluid was taken and titrated with standard HCl to determine the  $\text{OH}^-$  ion concentration. Appropriate dilutions were prepared for determinations of Na and K by flame photometry and for Ca by atomic absorption spectroscopy, using standard methods.

The non-evaporable water content was determined from the difference between the bound water retained between  $105^\circ\text{C}$  and the ignited condition at  $1050^\circ\text{C}$ . A similar paste series was prepared using low porosity cement without fly ash addition. However, due to unknown reasons, these pastes failed to set even by 7 days, and the results have not been included in this work.

#### 6.2.2 Results and Discussion

The measured  $\text{OH}^-$  ion concentrations of the pore fluids expressed from the various pastes are given in Table 6.2.2. In this table also are the pH values calculated from the measured  $\text{OH}^-$  concentrations using the original Sørensen pH definition of pH as the base 10 logarithm of the reciprocal of the  $\text{H}^+$  ion concentration. The concentrations of  $\text{Ca}^{++}$ ,  $\text{Na}^+$  and  $\text{K}^+$  ions are also presented in this table.

The values of pH obtained from the pore fluid of the fly ash bearing low porosity paste were in excess of 14 after the paste had set. Such high pH values are favorable from the standpoint of corrosion resistance of steel in concrete. Analysis of the pore fluid indicated that the



total alkali concentration ( $\text{Na}^+$  and  $\text{K}^+$ ) ranged between 1.2 M and 1.7 M. This high concentration of alkali cations in the pore fluid is in part due to the  $\text{NaHCO}_3$  added, and in part to the particular fly ash used, which itself has a high total alkali content (about 4.7% as  $\text{Na}_2\text{O}$  equivalent).

The results of the non-evaporable water determinations are presented in Table 6.2.3. There is a gradual increase in the non-evaporable water from 4.0% at 12 hours to 10.5% at 7 days.





Table 6.2.1. Mix proportion of Fly Ash Bearing-Low Porosity Paste

Low Porosity Cement	1000g
Fly Ash	350g
Sodium Lignosulfonate	7.6g
Sodium bicarbonate	16.2g
Water	330 ml

Table 6.2.2. pH Values and Ion Concentrations in Pore Fluids of LPF Paste

Sample	Age	Ion concentration, Molarity				Calculated pH
		Ca <sup>++</sup>	Na <sup>+</sup>	K <sup>+</sup>	OH <sup>-</sup>	
Fly Ash-Bearing	12 hr.	0.008	1.14	0.084	0.151	13.2
Low Porosity	24 hr.	0.019	1.11	0.087	0.187	13.3
Paste, LPF	4 days	0.004	1.12	0.142	1.18	14.1
	7 days	0.002	1.52	0.204	1.51	14.2



Table 6.2.3 Non-evaporable Water in Fly Ash Bearing -  
Low Porosity Paste

Age	Non-evaporable Water %
12 hours	4.0
24 hours	6.1
4 days	9.5
7 days	10.5

Table 6.3.1 Mix Proportions of Different Types of Concretes  
Used in Indoor Corrosion Study

Mix Designation	Cement Content (bags/cu. yd.)	Fly Ash Content (bags/cu. yd.)	Water- Cement Ratio	Air Content (%)
IWA-2	8.6	-	0.33	7.3
LPF-10B	7.6	2.7	0.28	-
LPF-10D	7.8	2.7	0.28	3.5
LPN-5	10.1	-	0.28	4.0
LPN-6	8.3	-	0.27	3.0



### 6.3 VISUAL EVALUATION OF CORROSION OF STEEL EMBEDDED IN CONCRETE

#### 6.3.1 Steel Mats Embedded in Concrete Specimens Kept Indoors

Three basic mixes were used in this portion of the study. They are:

- (i) a formulation representing Iowa low slump concrete, designated IWA-2.
- (ii) two formulations representing the fly ash-bearing low porosity concrete, designated LPF-10B and LPF-10D.
- (iii) two formulations representing low porosity concrete without fly ash designated LPN-5 and LPN-6.

The materials for the concrete mixes and the mix procedure used are the same as described in sections 2.1.1 and 1.1.1 (ii). The mix proportions are given in Table 6.3.1. The 3200 cm<sup>2</sup>/g fineness low porosity cement was used for preparing the low porosity concretes. The fresh concrete was cast into three steel molds having the following dimensions: length 9 in.; breadth 7 in.; depth 3 in. Two 8 in. long, 1/4-in. diameter steel bars were embedded in each specimen 2 in. below the upper surface, except for LPF-10D which had only 1 in. of concrete cover above the steel. The specimens were demolded 24 hours later and cured in a saturated Ca(OH)<sub>2</sub> solution for 28 days. A 4% calcium chloride



solution was then applied to the surface, and the samples were kept in a controlled climate room at relative humidity  $50 \pm 4\%$  and temperature of  $23 \pm 2^{\circ}\text{C}$  for 4, 8, and 12 months. Plastic sheets were used to cover the specimens to check evaporation of the solution. Periodically, the specimens surface were flushed with water to remove the build up of salt. At the indicated ages specimens were broken and the steel reinforcing bars removed for visual examination. A rating has been developed to estimate the distribution of rust occurring on individual segments of the steel reinforcing bars and of the overall extent of rust occurring on them. The rating scheme is presented in Table 6.3.2-A and in the sketch accompanying it. The results of the examinations are given in Table 6.3.2-B. The specimens described in Table 6.3.2-B have been ponded for 12 months. Steel bars in concrete specimens ponded for 4 and 8 months were also examined and showed extents of rusting almost proportionate to the length of exposure.

#### 6.3.2 Steel Mats Embedded in Concrete Specimens Exposed Outdoors

The specimens used in the second set of experiments for chloride penetration into concretes, described in section 4.3.1, were also as used for this portion of the study. Details of specimen preparation were given in the above mentioned section. At 12 months of 4%  $\text{CaCl}_2$  solution ponding under outdoor conditions, two 1-1/2 in. cores were taken from the middle of each specimen for the chloride





Table 6.3.2-A Details of Rating Scheme For Recording Corrosion Extent on Individual Segments of Steel Bars as Delineated in Sketch Below

Rating	Area of Surface Corroded
0	no rust
1	very slight, $1/8$ or less of surface corroded
2	slight to moderate, $1/8 - 1/4$ of surface corroded
3	moderate, $1/4 - 1/2$ of surface corroded
4	moderate to severe, $1/2 - 3/4$ of surface corroded
5	severe, $3/4 -$ of surface corroded

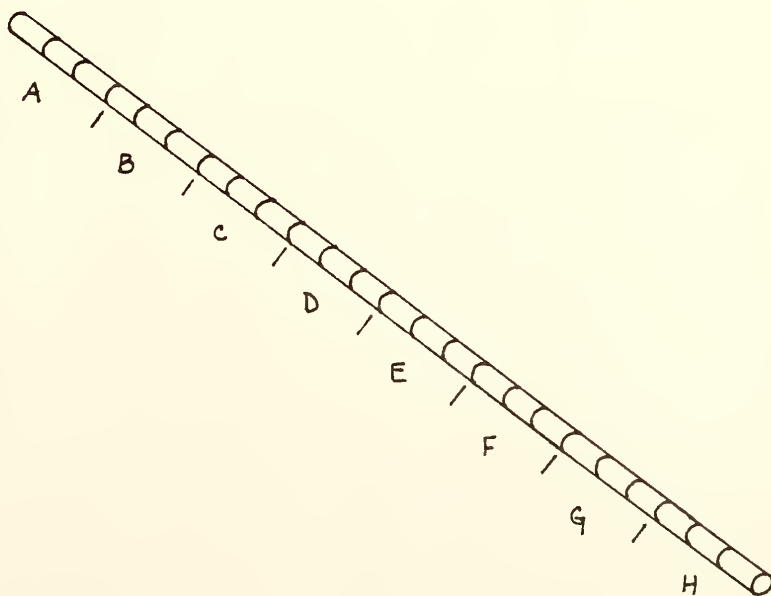




Table 6.3.2-B Results of Visual Estimation of Corrosion on Steel Bars Embedded in Different Types of Concretes After 12 Months Ponding With 3% NaCl Solution

Sample	Individual Corrosion Rating of 1" Long Segments								Estimate of Percentage of Total Area Corroded	Average Percentage of Total Area Corroded
	A	B	C	D	E	F	G	H		
IWA-2	(1)	1	1	1	1	1	1	1	3	4
	(2)	3	2	1	1	1	1	1	5	
LPF-10B	(1)	2	2	1	1	2	1	1	8	9
	(2)	3	2	1	1	1	1	1	10	
LPN-5	(1)	0	0	0	0	0	0	1	1	1.5
	(2)	1	0	0	0	0	1	0	2	
LPF-10D	(1)	1	1	1	1	1	0	1	4	4.5
	(2)	2	2	1	1	1	1	1	5	
LPN-6	(1)	1	1	1	1	1	1	1	4	3.5
	(2)	1	1	1	1	1	1	1	3	



content determination described earlier. The ends of the concrete specimens were then chipped off to expose the ends of the embedded steel mat, and the corrosion potential of the steel mat was determined using the  $\text{Cu/CuSO}_4$  half cell, described in Section 6.4.2 (iii). The specimens were then broken and the steel mat removed for visual examination. The same rating scheme used in the previous section was applied here.

### 6.3.3 Results and Discussion

#### (i) Steel Bars Embedded in Concrete Specimens Kept in Controlled Room

The results of the visual observations made on the steel reinforcing bars taken from the different concretes after 12 months of treatment with a 3% NaCl solution in a controlled atmosphere are given in Table 6.3.2-B. The LPN concrete showed only a little corrosion, being only about 1.5% of the steel surface. For the LPF concrete, greater amounts were found, up to about 9% in the case of one of them.

The data are somewhat inconsistent for the LPF concretes in that paradoxically a greater extent of corrosion was observed on the reinforcing steel bars with a 2-in. concrete cover (embedded in LPF-10B) compared to the bars with only a 1-in. concrete cover (in LPF-10D). The latter concrete had the same mix proportion as LPF-10B, except for the gradation of the coarse aggregates. Within the



various LPN concretes, a reasonable relationship was shown between results for the two concretes used in the test specimens: LPN-5, with higher cement content showed much better corrosion resistance than LPN-6, of lower cement content.

The IWA concrete offered corrosion protection to the reinforcing steel comparable to that given by the LPF concrete.

Unfortunately, a representative BD concrete was not included in this test series, and thus no comparison for this material is available.

(ii) Steel Mats Embedded in Concrete  
Specimens Kept Outdoors

In Table 6.3.3 results of the observation of the physical condition of the concrete specimens, the visual corrosion rating of the steel mat and its corrosion potential measurements are presented.

(a) Physical Condition of Concrete Specimens

The concrete specimens of the two types of low porosity concretes, LPF and LPN, showed no sign of distress; all concrete specimens were intact. The IWA concrete specimens showed scaling at the ends, but no rust spots. All the BD concrete specimens showed a typical rust stain or stains on one end of the specimens. The rust stains first appeared on the specimens after about 6 months of ponding. Figure 6.3.1 show representative concrete specimens after 12 months of outdoor exposure to 4%  $\text{CaCl}_2$  solution. There were cracks





Table 6.3.3 Physical Condition of Concrete Specimens and the Corrosion of Steel Mats in the Different Types of Concretes Ponded for 12 Months in Outdoor Conditions

Sample	Physical Condition of Concrete Specimen at End of Ponding Period (12 months)	Corrosion Potential of Embedded Steel Referenced to Cu/CuSO <sub>4</sub> Half-Cell (V)	Visual Corrosion Rating of Each End of Steel Mat*								Estimate of % of Total Area Corroded	Average of Total Area Corroded (%)
			1	2	3	4	5	6	7	8		
LPN-9 (1)	Excellent, intact	-0.25	0	0	0	0	1	1	1	1	3	
" (2)	"	-0.20	1	0	0	1	1	1	1	1	2	2
" (3)	"	-0.15	1	1	0	0	0	0	1	0	1	
LPF-14 (1)	Excellent, intact	-0.26	0	1	1	0	1	1	0	0	3	
" (2)	"	-0.20	0	0	0	0	1	0	1	0	2	3
" (3)	"	-0.23	1	0	1	1	0	0	0	0	3	
IWA-5 (1)	Scaling on sides of concrete	-0.23	1	1	0	0	1	1	1	0	3	
" (2)	Same as (1) above	-0.30	1	1	3	0	2	1	1	0	10	7
" (3)	Same as (1) above	-0.28	1	2	1	1	1	1	1	0	8	
BD-11 (1)	Rust on surface, cracks, scaling	-0.33	1	2	0	0	3	3	3	3	21	
" (2)	Same as (1) above	-0.35	1	1	1	2	2	3	2	4	25	24
" (3)	Same as (1) above	-0.38	2	1	1	1	3	3	2	2	27	

\* See Figure 6.3.3



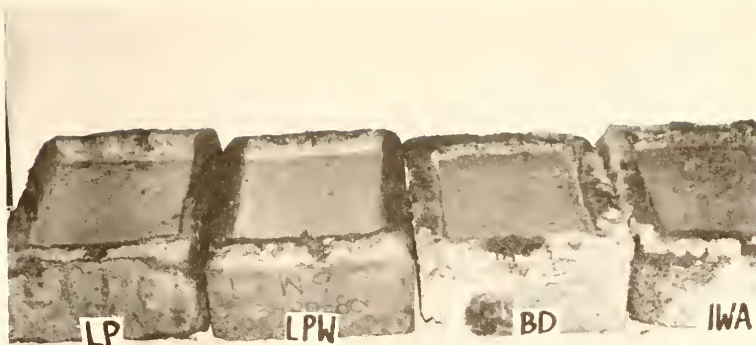


Figure 6.3.1 Appearance of Concrete Specimens  
Ponded with 4%  $\text{CaCl}_2$  Solution After  
Being Exposed Outdoors for 12 Months



Figure 6.3.2 Close-Up Picture of Damaged BD Concrete  
Specimen



and scaling on the BD concrete specimens, as shown by a closeup picture of one such specimen in Figure 6.3.2.

(b) Corrosion of Steel Mat  
in Concrete Specimens

A sketch of the physical layout of the steel mats embedded in these specimens is shown in Figure 6.3.3. In all of these specimens signs of corrosion were visible only at the 1-1/2 in. ends projecting beyond the cross bars indicated by numbers in the Figure. No corrosion was seen on the remaining parts of the mats. Thus, the corrosion ratings were given only in terms of the areas of the eight projecting ends of the steel mat. From the results of the average estimated percentage of area showing corrosion of the ends of the mats embedded in the different types of concretes, it is apparent that the performance of the steel in BD concrete was the poorest. About 24% of the end area was covered with rust. Resistance was much better in the IWA concrete, the percentage area covered with rust being about 7%. The resistance in both formulations of low porosity concretes were much superior, estimated corroded areas of the steel being only about 3%.

(c) Electrochemical Potential of Steel Mat

The electrochemical potential readings of the steel mats correlated quite well with the visual corrosion observations. The average corrosion potential readings recorded with reference to the  $\text{Cu/CuSO}_4$  half-cell for the steel mats



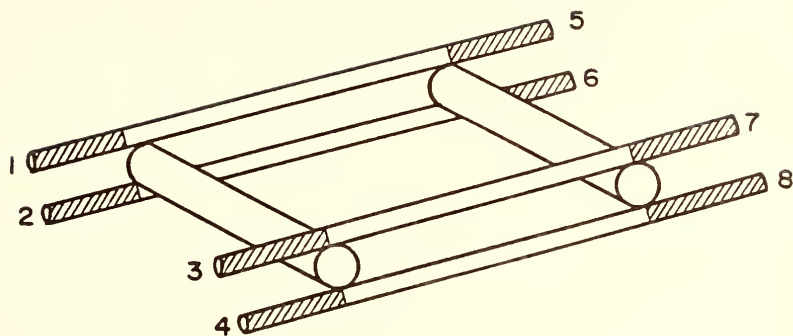


Figure 6.3.3 Sketch Showing Physical Layout of Steel Mat





embedded in the following types of concretes were as follows: -0.35V for BD concretes; -0.28V for IWA concretes; -0.23V for LPF concretes; -0.20V for LPN concretes. These readings may be referred to the expressed relationship between potential readings with respect to  $\text{Cu}/\text{CuSO}_4$  half-cell and probability of corrosion occurring in steel embedded in concrete as given by the FHWA (59). In that relationship a reading of -0.35 volts or more was taken as an indication of 95% probability that active corrosion is occurring.



## 6.4 ELECTROCHEMICAL MEASUREMENTS OF ONGOING CORROSION

### 6.4.1 Introduction

Corrosion is an electrochemical process. It is initiated with the formation of anodic and cathodic areas on the reinforcing bars. Electron flow through the metal occurs from the anodic areas to the cathodic areas. A potential difference, or voltage, is set up between the anodic half cell and the cathodic half cell areas, which may be measured by a voltmeter.

The electrical activity of these half cells change seasonally and with changes in the electrolyte such that the difference in measured voltage between two unstable half cells is not a good measure of corrosion activity in a concrete bridge deck. For this reason the electrical potential of the corrosion half cells in bridge decks are usually referred to a standard reference half cell which has a known electrical potential.

Earlier studies used calomel cell as the reference cell, but this has since been replaced by the copper/copper/sulfate cell (59), which is sturdier and easier to use. The  $\text{Cu/CuSO}_4$  half cell is essentially a copper



rod immersed in a saturated copper sulfate solution and it represents a half cell of constant electrical potential of + 0.316V. with reference to the standard hydrogen electrode. To compare the electrical potential of the standard cell to that of the steel embedded in the concrete, the two must be connected through a high impedance voltmeter. This is done by making a positive connection to the mat of the reinforcing steel and providing a moisture path through the concrete between the standard cell and the point at which the potential is being measured. Potentials are reported as negative values by convention.

In this section two sets of potential measurements were taken, both on steel mats embedded in concrete bars parts of which have been exposed to external environments.

The first set of measurements represents voltage readings between the two steel mats embedded in a concrete specimen. The upper mat is positioned at the same distance from the upper surface (1-1/2 in.) as the lower mat is from the bottom surface. The mats are separated by a distance of 3 in., and are not electrically connected.

The second set of measurements involved the FHWA method (59) of determining the rate of corrosion of reinforcing steel in concrete bridge decks by measurement of electrical potential against a  $\text{Cu/CuSO}_4$  half-cell. These potential measurements were made independently for the upper and lower steel mats.



#### 6.4.2 Equipment, Concrete Mixes and Voltage Measurements

##### (i) Equipment and Materials

Equipment for the measurement of corrosion potential of steel embedded in concrete bridge decks was originally loaned to this project by the Research and Training Center of the Indiana State Department of Highways at West Lafayette, Indiana. This equipment consisted of a copper/copper sulfate half cell (CSE) and a modified Sencore FE 160 multimeter.

Subsequently a replacement  $\text{Cu}/\text{CuSO}_4$  half-cell was specially fabricated at Purdue University and the multimeter was replaced by a high impedance digital voltmeter (Keithley Instruments, Cleveland, Ohio).

Steel mats were fabricated in accordance with Figure 6.4.1 in which five parallel 1-1/2 in. diameter reinforcing bars, four of them 14 in. long; and one 18 in. long were connected by five 1/4 in. diameter, 14 in. long cross bars.

A wooden mold 18 x 18 x 6-in. with two perforated holes was fabricated, the holes being designed to allow the middle rods of both top and bottom mats to project out of the concrete specimen.

##### (ii) Concrete Mixes

Four basic concrete types were prepared for this part of the study with variations as follows:





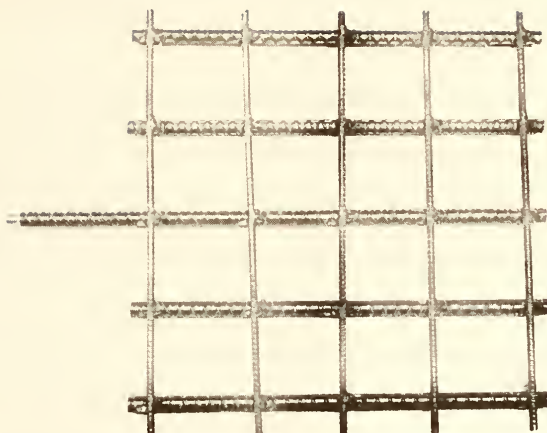


Figure 6.4.1 Photograph of Steel Mat of the Kind  
Embedded in 18 x 18 x 6 in. Concrete  
Specimens



(i) three formulations representing conventional bridge deck concrete as used in Indiana, designated BD-13, BD-14 and BD-15.

(ii) three formulations representing Iowa low slump concrete designated IWA-6, IWA-7 and IWA-8.

(iii) three formulations representing the fly ash-bearing low porosity concrete, designated LPF-16, LPF-18, LPF-19.

(iv) a formulation representing low porosity concrete without fly ash, designated LPN-12.

The materials for the concrete mixes and the mix procedure used are the same as described in sections 2.1.1 and 2.2.1 (ii). The low porosity cement of fineness 3200  $\text{cm}^2/\text{g}$  was used for the preparation of LPF & LPN concretes. The mix proportions are given in Table 6.4.1. Two types of specimens were prepared. In the first type, the concrete was cast in two equal layers. The bottom 3-in. layer was chloride-free concrete. The top 3-in. layer contained 0.6% by weight of cement of chloride ions added as dissolved  $\text{CaCl}_2$  in the mix water. The chloride free concrete was first placed around a previously positioned lower steel mat, and well compacted. The top layer was then carefully placed (while the bottom layer was still fresh) around the top steel mat, which was well secured by a steel wire and wooden rod arrangement attached to the top of the mold. In the second type of specimen, the concrete specimens were cast in one single operation and the concretes were wholly chloride-free.



Table 6.4.1 Mix Proportions of Different Types of Concretes  
Used in Outdoor Corrosion Study

Mix Designation	Cement Content (bags/cu. yd.)	Fly Ash Content (bags/cu. yd.)	Water- Cement Ratio	Air Content (%)	Chloride Content in Top 3 in.-Layer (% by wt. of Cement)
BD-13	6.7	-	0.43	5.3	0.6
BD-14	6.4	-	0.43	5.5	0.6
BD-15	7.4	-	0.43	5.0	0.0
IWA-6	8.8	-	0.33	5.1	0.6
IWA-7	8.8	-	0.33	5.0	0.0
IWA-8	8.8	-	0.33	5.0	0.6
LPF-16	9.4	3.3	0.26	-	0.6
LPF-18	9.5	3.3	0.24	4.7	0.0
LPF-19	9.5	3.3	0.24	4.7	1.2
LPN-12	10.4	-	0.27	-	0.6



Each of the specimens of both types was covered with plastic sheets and allowed to stand under laboratory conditions for 24 hours. They were then demolded and mortar dikes built around the perimeter of the upper surface to hold the ponding solution. One day later, water was poured to the upper surfaces. The specimens were kept under laboratory conditions for one week, then taken outdoors and placed on 6 in. brick supports. The projecting ends of the steel bars exposed outside of the concrete were protected with tape. The specimens were continuously ponded with water for the first 20 weeks. Thereafter a 4%  $\text{CaCl}_2$  solution was used. Six of the specimens prepared and exposed outdoors in the summer of 1980 were investigated for a period of 56 weeks; the remaining four prepared and exposed outdoors in the spring of 1981 were investigated for only about 20 weeks, mainly to check the reproducibility of the measurements previously obtained.

(iii) Electrical Potential Measurements

a) Direct Potential Readings Between the Two Steel Mats. The digital multimeter (Keithley-Instruments) was adaptable to read low currents (of the order of  $\mu\text{A}$ ), as well as potentials, and it was originally used to monitor corrosion currents, starting about 30 minutes after casting of the concrete specimens. However, there were severe fluctuations in the readings of the currents which continued for periods up to about 2 weeks. Because of this





instability of current readings voltage measurements were resorted to and fairly stable readings were obtained. The voltage measurements were originally made by simply making the appropriate connections between the digital voltmeter (multimeter) and the two projecting steel rods, and a minute or two was allowed for a stable voltage reading to be obtained. Later, it was observed that often significant voltage fluctuations were occurring with some of the specimens. Several individual readings were therefore taken over a period of 24 hours and the average taken to represent a voltage reading. A weekly average of such voltage readings is given in Table 6.4.2.

b) Measurement of Electrical Potential  
Using Copper/Copper Sulfate (CSE) Half Cell

A schematic diagram of the electrical potential reading set-up is given in Figure 6.4.2. A connection was made between one of the two projecting steel rods and the negative lead of the voltmeter. The copper sulfate half cell was then connected to the positive side of the voltmeter. Cotton wool was used to plug the end of the CSE half cell. The ponding solution on the specimen surface was removed and the porous end of the CSE half cell placed sequentially at each of twelve points on the 18 x 18 in. specimen surface. Contact was maintained until a stable voltmeter reading was obtained (usually only a few seconds). The average potential reading taken from the twelve readings represents the electrochemical corrosion potential on the steel mat at



Table 6.4.2-A Weekly Average Voltage Reading of Embedded Steel Mats in Different Concretes

Week	Voltage, (mV)					
	BD-13	IWA-6	LPN-12	LPF-16	LPF-18	LPF-19
1	191	197	-	-	26	9
2	124	123	21	22	15	1
3	293	110	13	13	11	2
4	230	102	17	11	4	5
5	200	92	-	16	4	10
6	251	185	-	12	37	44
7	187	-	-	18	33	61
8	211	283	-	-	-	-
9	205	233	-	66	-	-
10	188	228	63	50	-	-
11	234	202	66	52	3	43
12	-	-	64	47	-3	56
13	-	-	-	-	-	54
14	-	-	-	-	-5	53
15	-	181	-	-	-7	54
16	231	251	56	35	-6	52
17	-	-	47	28	-6	25
18	220	-	56	35	-1	38
19	169	172	55	30	-19	49
20	150	172	54	33	-19	29
21	180	291	79	80	-13	-
22	197	194	20	72	-	-
23	315	247	18	68	-	-
24	289	178	13	83	-	-
25	115	244	-1	90	-	-



Table 6.4.2 continued

Week	Voltage, (mV)					
	BD-13	IWA-6	LPN-12	LPF-16	LPF-18	LPF-19
26	-	-	1	-	-7	-
27	-	-	-	-	-	37
28	-	-	-	-	-	50
29	-	-	-	-	-73	-
30	-	-	-	-	-71	40
31	-	-	-	-	5	40
32	171	63	-	-	-	-
33	249	-	17	26	10	50
34	-	110	10	62	-	-
35	356	-	33	58	-	-
36	323	82	-	-	-	-
37	373	-	83	48	4	-
38	-	-	58	-	-6	66
39	-	-	-	-	-	66
40	335	-	-	100	-12	-
41	-	64	-	-	-	59
42	280	-	-	-	-	-
43	298	72	-	67	-15	-
44	-	-	-	-	-	60
45	347	123	-	34	-4	-
46	-	-	-	89	-	36
47	-	150	57	-	-	-
48	333	-	-	-	-	-
49	-	135	-	70	-	-
50	320	-	32	-	-29	47
51	-	210	-	84	-	-
52	250	-	12	93	8	59
53	-	170	-	70	-7	54
54	270	-	-	-	-	56
55	-	155	-	70	-	-
56	280	-	60	-	-	-



Table 6.4.2-B Average Weekly Readings of Embedded Steel Mats in Different Concretes

Week	Voltage, mV			
	IWA-7	IWA-8	BD-14	BD-15
1	20	118	-	-
2	-	-	-	-
3	63	105	-	-
4	-	-	108	-
5	60	136	-	69
6	-	-	118	63
7	77	120	-	-
8	-	-	125	64
9	77	130	-	-
10	-	-	140	58
11	77	140	-	-
12	-	-	-	70
13	77	145	110	75
14	-	-	100	-
15	89	126	-	60
16	-	-	95	120
17	78	134	-	-
18	-	-	90	105
19	75	-	-	-
20	-	120	80	50





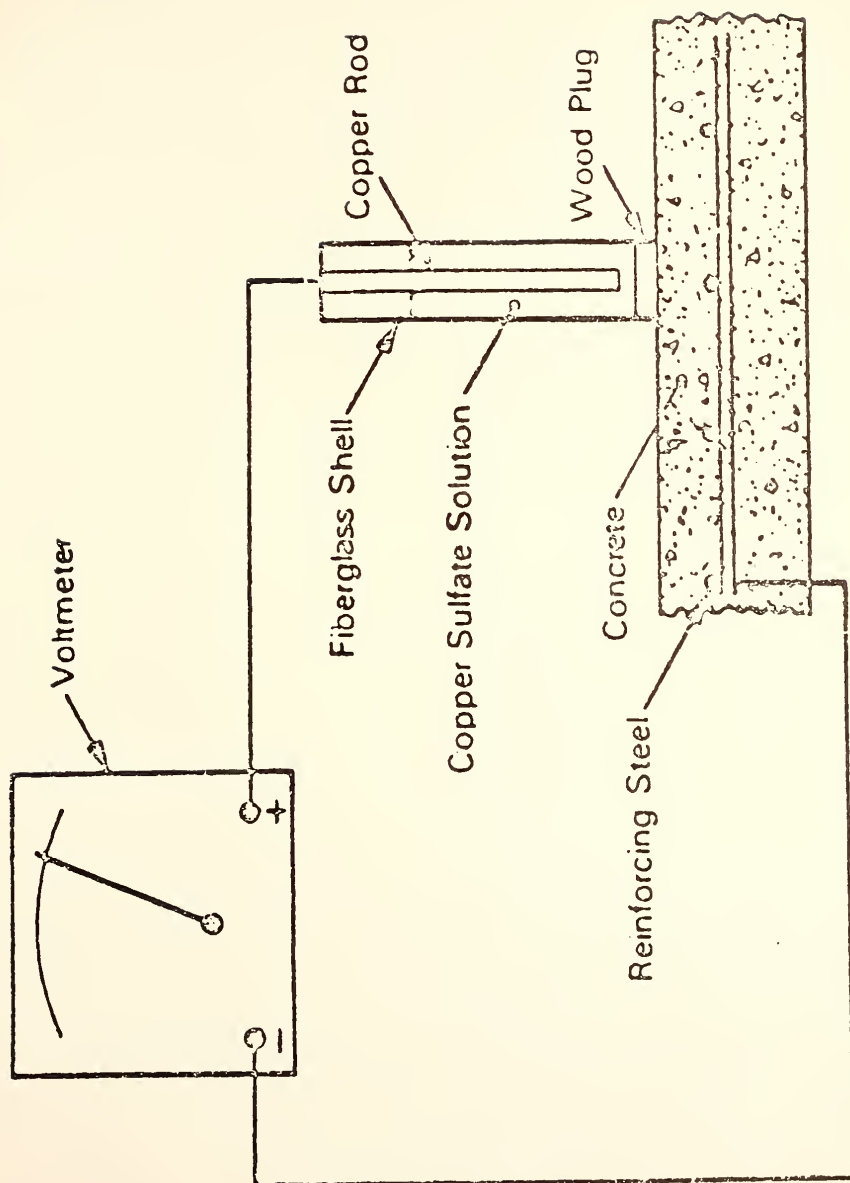


Figure 6.4.2 Scheme For Measuring Electrical Potential of Embedded Steel Using Copper/Copper Sulfate Half Cell



the specified age. Readings were taken for both the top and bottom steel mats. The results of the potential readings are all shown in Table 6.4.3

#### 6.4.3 Results and Discussion

##### (i) Potential Measurement Across the Two Steel Mats

Potential readings between the two steel mats were taken, using the high impedance voltmeter. These readings were obtained approximately twice weekly from the first week after casting until the 56th week for the first six specimen exposed outdoors, in the summer, of 1980, and over the first 20 weeks for the subsequent four specimens exposed outdoors in the spring of 1981.

Results for the conventional concretes will be discussed first. The potential readings measured between the mats were all positive, indicating that the upper mat was at a higher potential. The range of potentials was from a maximum of about 370 mV to values as low as 20 mV. In the conventional concretes with 0.6% chloride ion content in the top 3-in. layer (BD-13 and IWA-6) high readings of about 190mV were obtained in the first week. The readings kept fluctuating but remained generally in the 150-250 mV range for the BD-13 specimen up to about the 33rd week. Thereafter, readings of over 300 mV were often recorded.

Voltage readings in the IWA-6 specimens also kept fluctuating and were mostly in the 100-250 mV range



Table 6.4.3 Voltage Readings With Respect to  $\text{Cu}/\text{CuSO}_4$  Half Cell  
of Steel Mats Embedded in Different Concretes

Specimen (Exposed during Summer 1980)	Age (weeks)	Chloride Content in Top 3 in. Layer (% by wt. of Cement)	Voltage, V (CSE)	
			Top Mat	Bottom Mat
BD-13	38	0.6	-0.47	-0.20
BD-13	41		-0.49	-0.16
BD-13	56		-0.47	-0.20
IWA-6	38	0.6	-0.40	-0.14
IWA-6	41		-0.32	-0.15
IWA-6	56		-0.36	-0.21
LPN-12	39	0.6	-0.17	-0.08
LPN-12	42		-0.17	-0.14
LPN-12	56		-0.23	-0.22
LPF-16	39	0.6	-0.17	-0.06
LPF-16	42		-0.16	-0.10
LPF-16	56		-0.18	0.10
LPF-19	34	1.2	-0.14	-0.08
LPF-19	37		-0.19	-0.10
LPF-19	56		-0.21	-0.05
LPF-18	34	0.0	-0.07	-0.07
LPF-18	37		-0.11	-0.11
LPF-18	56		-0.05	-0.05
Exposed during Spring 1981				
BD-14	2	0.6	-0.24	-0.10
BD-14	21		-0.06	-0.02
BD-15	2	0.0	-0.18	-0.13
BD-15	21		0.12	-0.01
IWA-7-	1	0.0	-0.18	-0.20
IWA-7	20		-0.06	-0.02
IWA-8	1	0.6	-0.28	-0.19
IWA-8	20		-0.12	-0.01



throughout the 56 week monitoring period. The readings thus recorded higher potential developing between the two steel mats for the BD specimens as compared to the IWA specimen.

Another set of the same kind of specimens prepared as a check and exposed outdoors in the spring of 1981 (BD-14 and IWA-8) developed potentials between the two steel mats only half as large as those recorded for the original specimens (BD-13 and IWA-6) that had been exposed outdoors during the warm months of the previous summer. There were no significant differences between the voltages measured for the two spring 1981 specimens, both generally being in the 100-140 mV range.

Two other conventional concrete specimens were exposed during the same spring, (IWA-7 and BD-15). These were both completely free of added chloride. Measured potentials between the upper and lower mats were only about half as much as for companion specimens with chloride ions in the top 3-in. layer, these voltage readings being generally in the range 50-90 mV. Specimen BD-15 showed higher readings from the 16th week, about 120mV.

The corresponding results for the low porosity concretes will next be discussed. The potential readings measured between the mats were again all positive, indicating that the upper mat was at a higher potential, except in one case. The range of potential observed was from a maximum of 100 mV to values as low as zero mV. In the





exceptional case (LP) potentials ranged from about +40 mV to typically -20 mV.

Voltage readings between the steel mats in specimens LPF-16 and LPN-12 with 0.6% chloride ion content in the top layer and LPF-19 with double the chloride ion dosage in this layer were all in the same range, 10-100 mV.

Voltage readings between the steel mats in specimen LPF-18, a chloride-free specimen, were very low, about 40 mV or less in the first seven weeks. Subsequently, small negative voltage readings were recorded typically of the order of -20 mV. This is the only instance in which the bottom mat was indicated to be at a higher potential than the top mat.

(ii) Potential Readings Measured with Respect to the  $\text{Cu/CuSO}_4$  Half Cell (CSE Electrode)

As stated before, it is generally accepted that potential readings in excess of -0.35V with respect to the CSE Electrode indicate a 95% probability that corrosion is occurring; readings lower than -0.20V indicate a 95% probability that corrosion is not occurring. There is uncertainty about the state of corrosion between -0.20V and -0.35V.

Three voltage readings with respect to the CSE electrode were recorded for both the top and bottom steel mats for the first six specimens exposed during the summer of 1980. The readings were taken between the 34th and 56th week. Two readings were also obtained in the 20



week exposure period of the four specimens exposed in the spring of 1981. The readings were taken separately for the top and bottom steel mats.

Results for the conventional concretes (BD-13 and IWA-6) as shown in Table 6.4.3 indicate that potentials of approximately  $-0.48\text{V}$  for the BD concrete and  $-0.35\text{V}$  for the IWA concrete occur in the top steel mats. Since potentials in excess of  $-0.35\text{V}$  indicate active corrosion, it appears that active corrosion was underway in the BD concrete even prior to the start of the measurements at 38 weeks. Results of visual evaluation of corrosion in Section 6.3 support this view insofar as the BD concrete is concerned, rust first appearing in these specimens at about 24 weeks.

The lower steel mats with a 4-1/2 in. concrete cover, generally showed voltage readings of about  $-0.20\text{V}$  or lower, indicating that active corrosion was probably not occurring.

For the low porosity concretes, potentials recorded for the top steel mats for LPN-12 and LPF-16 with 0.6% chloride ion in the top layer were about  $-0.20\text{V}$  or less. Even doubling the concentration of the chloride ion from 0.6% to 1.2% as was the case in LPF-19 did not result in any higher potential being recorded, the same range of about  $-0.20\text{V}$  or less, being observed. The bottom steel mats for these specimens also showed much lower readings; here these readings were generally below  $-0.14\text{V}$ .



The entirely chloride-free low porosity concrete, LPF-18, showed identical and low voltage readings for both the top and bottom steel mats, all being between  $-0.05\text{V}$  and  $-0.11\text{V}$ .

Potential readings for the four conventional concrete specimens exposed during the spring of 1981 will next be discussed. Two of these specimens, BD-14 and IWA-8, with 0.6% chloride ion in the top layer, showed relatively high values within the first two weeks, about  $-0.25\text{V}$ , and dropped to about  $-0.10\text{V}$  by the 20th week. The same trend, but at reduced voltages, is shown for the lower steel mats. Voltage readings for steel mats in the chloride-free concrete specimens, BD-15 and IWA-7, showed a similar trend with the voltage measured for the top mats within the first two weeks being lower, about  $-0.18\text{V}$ , instead of about  $-0.25\text{V}$ . It should be recalled that these specimens were only exposed for a 20-week period.

There seems to be a correlation between the two separate kinds of readings recorded in this section of the study. Specifically the conventional concretes showed generally high voltage readings, 200-300 mV, between the two steel mats, and gave the "95% probable corrosion" voltage readings for the top steel mats as measured with respect to the CSE electrode. On the other hand, voltage readings between the two steel mats in the low porosity concretes showed relatively low values, generally 50-100 mV, and these concretes gave potential readings with the



CSE electrode indicating that active corrosion was not likely to be occurring in either the top or bottom steel mat.

On a daily basis there was no significant influence of temperature fluctuations on the voltage readings between the steel mats using the high impedance voltmeter. However, there was an influence of the season on the readings as is apparent from Tables 6.4.2 A and B.

In addition, the surface conditions of the first six specimens which were exposed outdoors starting during the summer of 1980, with water ponding for 20 weeks, and 4%  $\text{CaCl}_2$  ponding thereafter, were as follows. There was very little scaling on the top of all the three of the LPF concrete specimens. There was slightly more widespread, but still isolated scaling on the concrete specimen of the LPN concrete. In contrast, almost all the top layer of the upper surfaces of the BD and IWA concrete specimens were scaled off, with the scaling extent being visibly greater with BD concrete than with the IWA concrete. A photograph of the surface condition of these specimens are provided in Figures 6.4.3 to 6.4.6.

Summarizing from the visual evaluation and the electrochemical results in this section, it is apparent that the conventional concrete as used in Indiana, BD, offers only poor protection to steel bars embedded in them, thus causing corrosion of the bars to occur







Figure 6.4.3 Appearance of Surface Condition of BD Concrete Ponded With 4%  $\text{CaCl}_2$  Solution After Being Exposed Outdoors for 56 Weeks

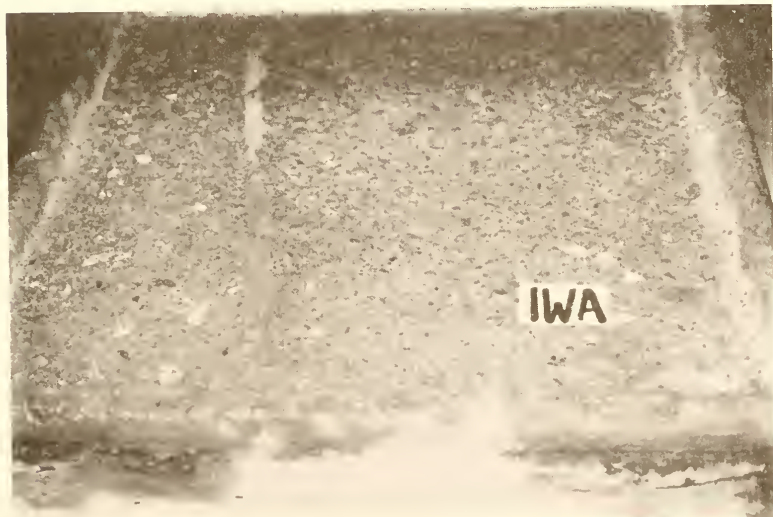


Figure 6.4.4 Appearance of Surface Condition of IWA Concrete Ponded With 4%  $\text{CaCl}_2$  Solution After Being Exposed Outdoors for 56 Weeks





Figure 6.4.5 Appearance of Surface Condition of LPF Concrete Ponded with 4%  $\text{CaCl}_2$  Solution After Being Exposed Outdoors for 56 Weeks



Figure 6.4.6 Appearance of Surface Condition of LPN Concrete Ponded With 4%  $\text{CaCl}_2$  Solution After Being Exposed Outdoors for 56 Weeks



rapidly on chloride exposure and resulting in the deterioration of the concrete cover. The IWA concrete was much better, but from the electrochemical results with the CSE electrode, active corrosion had started to occur at the latter stage of the monitoring period. All of the low porosity concretes offered very good protection to the steel. Active corrosion was not indicated with the electrochemical (CSE Electrode) method, and observed corrosion was minimal in the visual evaluation of corrosion study.



PART SEVEN

BRITTLE FAILURE BEHAVIOR OF LOW POROSITY CONCRETE





## 7.1 INTRODUCTION

A topic of considerable concern in contemplating the potential use of low porosity concrete for highway bridge decks is potential brittleness of the concrete in a possible failure situation. This report provides the results of investigations aimed at assessing the failure characteristics of this very high strength material, based on experimental investigations and current state of the art as reviewed in the literature.

It is now generally agreed that the stress-strain curve for concrete in compression does have a valid descending branch when tests are conducted in properly instrumented testing equipment (1).

It is also generally agreed that the descending portion will be steeper with increasing strength of the concrete. When the concrete strength is high enough, the descending portion will be vertical. There is disagreement on the limiting value of strength required for a vertical descending branch. Nilson and Slate (2) have suggested that the descending branch for all practical purposes is vertical for concretes with strengths above about 50 MPa (7,000 psi). On the other hand, Wang, Shah, and Naaman (3) have demonstrated non-vertical descending branches for concretes as strong as 90 MPa (13,000 psi), although at such high strengths the descending branch slope is very steep. Reasons for the disagreement were discussed by Ahmad and Shah (4).

Increasing brittleness of concrete in a concrete structure is usually looked on as a disadvantage, due to the possibility that a failure might propagate rapidly through the structure without prior warning. The problem is serious for high-strength plain concrete but is much less so for reinforced



concrete, because of the ductility of the reinforcing steel. It should be noted that bridge decks are highly reinforced structures with large percentages of reinforcing steel.

In comparing expected behavior of reinforced concrete structures, it is natural to suppose that a structure made of high strength reinforced concrete will be more brittle than a similar structure using normal strength concrete. While in fact it is not possible at this time to quantify the failure characteristics of reinforced high strength concrete very well, and current research is underway in the area, there are indications that under some circumstances high strength reinforced concrete can show higher ductility than ordinary reinforced concrete. The percentage of reinforcing steel is clearly an important factor. Tognon, Ursella, and Copetti (5) have shown that reinforced beams of high strength concrete have higher ductility (in terms of ratio of ultimate curvature to yield curvature of the beam) than reinforced beams of normal strength concrete when the percentage of reinforcement in each case is at its optimum.

In the present work, the brittleness characteristics of plain concretes have been investigated. The tests have included specimens of low porosity concrete with and without flyash, concrete formulated to represent ordinary bridge deck concrete as normally specified by the Indiana Department of Highways, and dense concrete as specified for repair of deteriorated bridge decks by the Iowa State Highway Department. These concretes were prepared and cast at Purdue University and tested with the kind assistance of Prof. S. P. Shah, at the University of Illinois at Chicago Circle.



## 7.2 CONCRETES

The concretes tested were representative of four different formulations whose properties were being compared in a larger study. Specimens coded LPN were formulated from a relatively rich mix using low porosity cement as the sole cementitious component. Specimens coded LPF contained flyash with a somewhat reduced amount of low porosity cement. Specimens coded BD were conventional Portland cement concrete as specified for highway bridge decks in Indiana, and finally, specimens coded IWA was representative of Iowa dense concrete as designed for bridge deck repair.

The aggregates used were the same in all of the concretes: a high-quality crushed limestone coarse aggregate, and a rather heterogeneous glacial sand of fineness modulus 2.71. The flyash used in the LPF specimens was a high-calcium flyash with a rather significant content of sulfate.

Mix proportions used are given in Table 7.2.1 for all of the concretes.

The specimens were cast in the form of 3 x 6 in. cylinders, demolded at one day, and cured for several months in a fog room. Prior to testing each cylinder was lapped to insure that the end faces were flat, parallel to each other, and perpendicular to the axis of the cylinder. The specimens were not capped. All of them were wet at the time of testing.

## 7.3 INSTRUMENTATION AND TESTING PROCEDURE

The testing machine used in this work was a fully servo-controlled MTS testing machine of 200,000 lb. capacity. A closed loop servo system was used to control the rate of loading to a high degree of accuracy. With this instrument either axial deformation or circumferential deformation could be used to provide the feedback control signal. In seven of the eight trials carried out in the present work, axial deformation control was used, and



TABLE 7.2.1

Mix Proportions of Concretes

<u>Constituent and Basis</u>	<u>Concrete Designation</u>			
	<u>LPN</u>	<u>LPF</u>	<u>BD</u>	<u>IWA</u>
Cement ( $\text{kg}/\text{m}^3$ )	620	450	390	530
Flyash ( $\text{kg}/\text{m}^3$ )	---	160	---	---
Coarse Aggregate ( $\text{kg}/\text{m}^3$ )	1110	1070	1150	895
Fine Aggregate ( $\text{kg}/\text{m}^3$ )	740	720	830	895
Water ( $\text{kg}/\text{m}^3$ )	170	181	167	173
Lignosulfonate LP Admix. (wt. % of cement)	0.28	0.69	---	---
$\text{NaHCO}_3$ LP Admix. (wt. % of cement)	1.20	1.20	---	---
Vinsol Resin AEA ( $\text{l}/\text{m}^3$ )	2.0	---	0.4	0.4
MB 122 WR Admix. ( $\text{l}/\text{m}^3$ )	---	---	2.0	2.8
Water:Cem. Solids Ratio	0.27	0.30	0.43	0.33





the strain rate was maintained equal to  $30 \times 10^{-6}$  (30 microstrain units) per second. On one specimen of low porosity concrete (LPN-1 (2)) circumferential deformation was used to provide the feedback control signal, although the readout recorded was in terms of axial deformation. The axial deformations were measured over the total lengths of the 3 x 6 in. specimens. The measurements were made by inductive transducers, and the resulting load-deformation curves were recorded automatically on an x-y plotter, and converted to plots of stress vs. strain.

#### 7.4 RESULTS

Traces of the original stress-strain curves of the eight specimens tested (two replicates of each of the four concrete types) are given in Figs. 7.4.1-7.4.4. It is apparent that reproducibility between replicates is excellent.

##### 7.4.1 Compressive Strength Levels

It is clear from the figures that the concretes fall into two very different groups as far as strength is concerned, with the conventional concretes being in the 6,000 - 7,000 psi range and the low porosity concretes in the 11,000 - 13,000 psi range. Actual values for compressive strength are provided in Table 7.4.1.

##### 7.4.2 Strain at Maximum Load

Values for measured strain at maximum load are also provided in Table 2. They were uniformly about  $2,500 \times 10^{-6}$  for the conventional concretes and only a little higher, averaging  $2,700 \times 10^{-6}$ , for the low porosity concretes.

##### 7.4.3 Young's Modulus

Examination of the curves of Figs. 1-4 shows that the early portion of the ascending branch of the stress-strain curve is not linear, but slightly



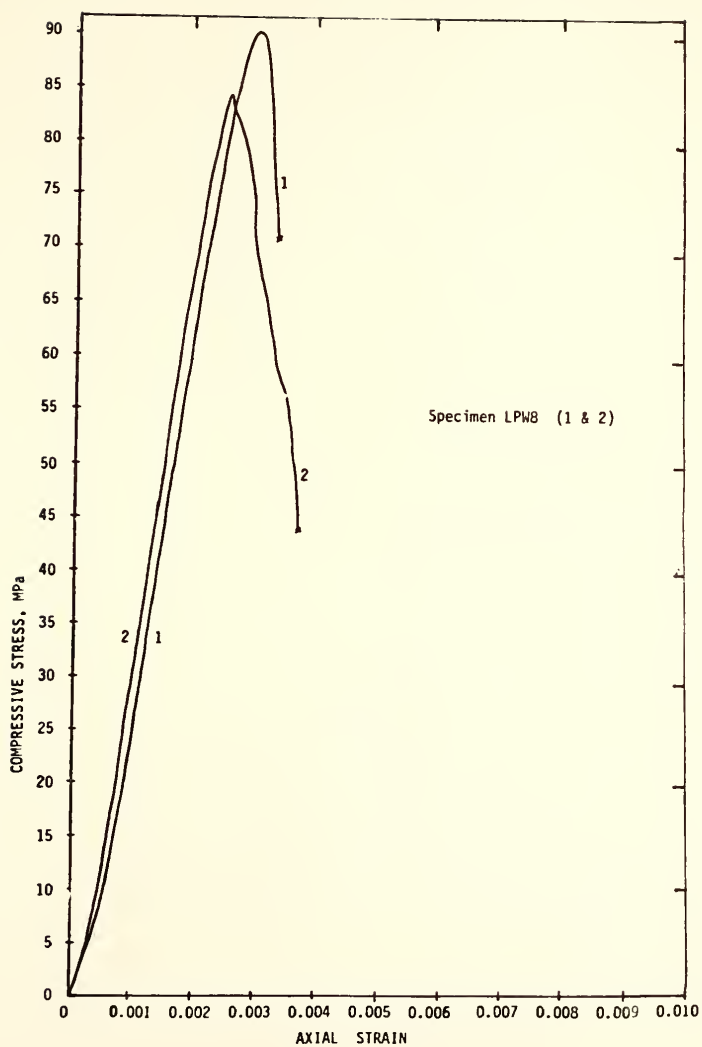


Fig. 7.4.1. Stress-Strain Curve for LPN-8 Low Porosity Concrete Specimens.(Originally Coded LPW8).



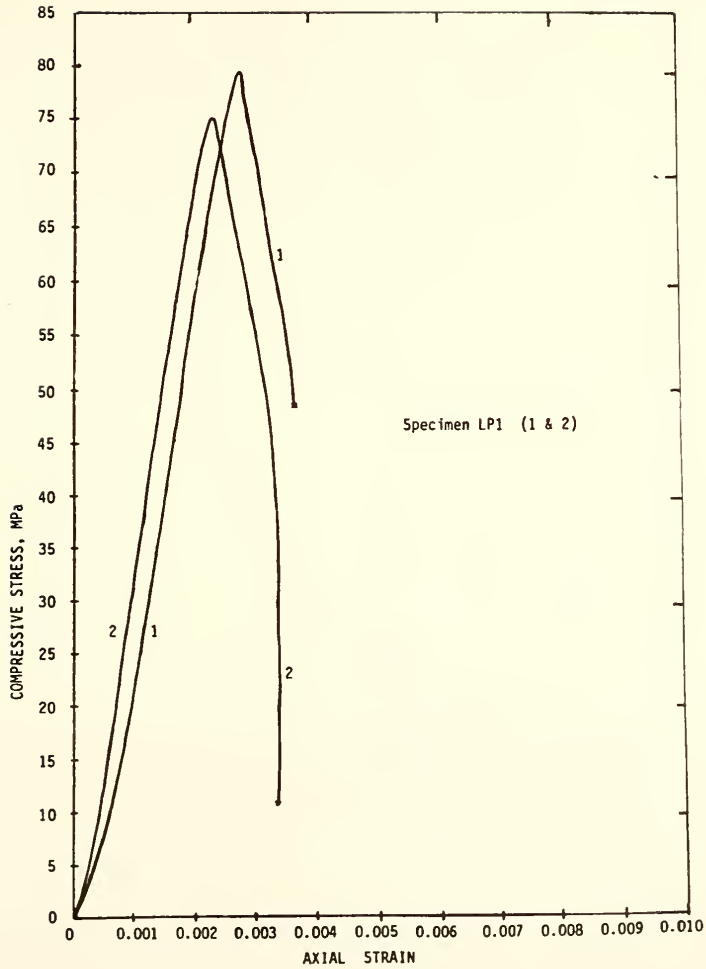


Fig. 7.4.2. Stress-Strain Curves for LPF-1 Flyash-Bearing Low Porosity Concrete Specimens. (Originally Coded LP1).



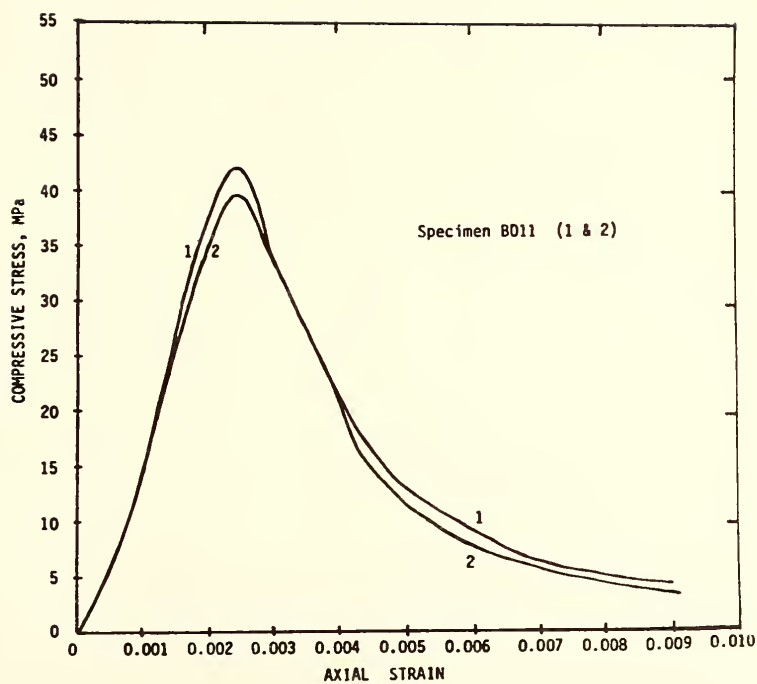


Fig. 7.4.3. Stress-Strain Curves for BD-11 Conventional Bridge Deck Concrete.





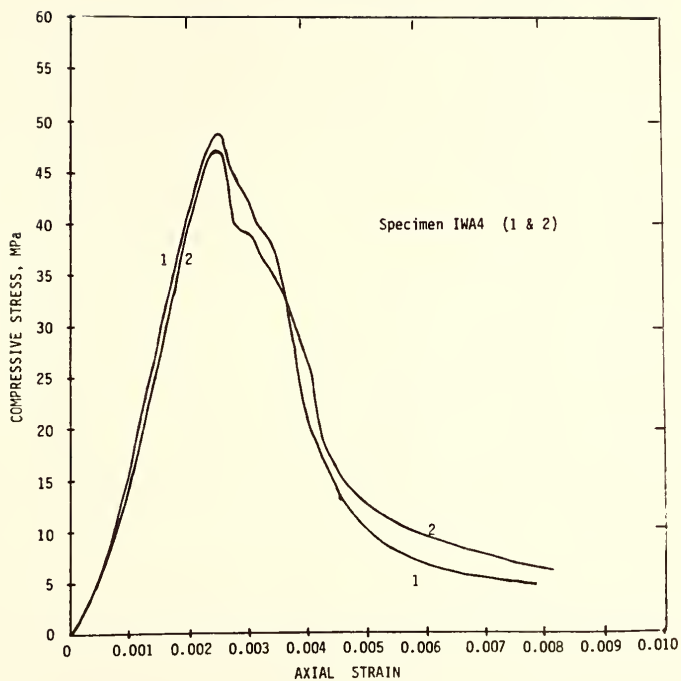


Fig. 7.4.4. Stress-Strain Curves for IWA-4 Iowa Dense Concrete.



TABLE 7.4.1

Measured Properties of the Concrete Specimens

<u>Specimen</u>	<u>Compressive Strength</u>		<u>Strain at Max. Load x 10<sup>-6</sup></u>	<u>Young's Mod.</u>		<u>Ductility Ratio</u>
	<u>psi</u>	<u>MPa</u>		<u>psi x 10<sup>6</sup></u>	<u>MPa x 10<sup>4</sup></u>	
LPN-8 (1)	13160	90.4	3100	6.09	4.21	0.19
LPN-8 (2)	12310	84.6	2600	6.09	4.21	0.73
LPF-1 (1)	11600	79.7	2800	5.77	3.99	0.53
LPF-1 (2)	11030	75.8	2300	6.08	4.20	0.67
BD-11 (1)	6080	41.8	2500	3.63	2.51	1.84
BD-11 (2)	5770	39.7	2500	3.13	2.16	1.62
IWA-4 (1)	7090	48.7	2500	3.61	2.49	1.44
IWA-4 (2)	6890	47.3	2600	3.61	2.49	1.99



curved, and in the direction opposite to the usual subsequent curvature at higher stress levels. Several factors seem to be involved, but the primary one is that the deformation was measured not over a portion of the length of the specimen, but rather over the full distance between the cross heads of the testing machine. This, combined with the fact that these are all virgin loading curves, means that the seating of the specimen will be recorded as a small amount of excess deformation at low stress. Trials indicated that if the loading was stopped at low stress and the specimen unloaded and reloaded, the early part of the second stress-strain curve were indeed linear.

This effect, however, interferes with the usual measurement made for Young's modulus in concrete. Initially, Young's modulus was calculated as suggested in ASTM C 469-65, which specifies a chord modulus measured between an initial point at a  $50 \times 10^{-6}$  axial strain and a second point corresponding to 40 percent of the ultimate stress level. Values of the order of  $2.3 \times 10^6$  psi for the conventional concretes, and  $4.2 \times 10^6$  psi for the low porosity concretes were calculated using this procedure. These are clearly unreasonable and reflect the initial curvature of the stress-strain plot.

In order to get around this difficulty, Young's modulus was simply estimated from the slope of the linear portion of the ascending branch in each case, and the results are provided in Table 1. The values obtained are on the order of  $3.5 \times 10^6$  psi ( $2.4 \times 10^4$  MPa) for the conventional concretes, and  $6.0 \times 10^6$  psi (4.2 MPa) for the low porosity concretes.

#### 7.4.4 Brittle Behavior

Examination of the stress-strain curves provided in Figs.7.4.1-7.4.4 show the qualitative difference in the post-maximum load behavior of the low porosity



as compared to the conventional concretes. The descending branch for the BD and IWA concretes shows relatively modest slopes, with strain measurements extending to more than 3 times the strain at maximum load. In contrast, the descending branches for the LPN and LPF low porosity concretes are very much steeper. Maximum strains recorded before the onset of instability were on the order of only  $3,500 \times 10^{-6}$ , i.e., only about 30 percent in excess of the strain at maximum load.

In order to try to quantify the brittleness, or conversely, the ductility of the various concretes an arbitrary definition of ductility was adopted, patterned after a suggestion by Naaman (6). The ductility of a concrete is here defined as the ratio of the area under the "post-peak" portion of the stress-strain curve to that of the "pre-peak" portion. This definition has the advantage of providing a relative measure independent of the system of units in use. The definition suffers from the usual one of deciding how far one takes the upper limit of strain for the post-peak area. Here it was arbitrarily decided that if the descending portion of the stress-strain curve was stable all the way, the upper limit of strain was set at the strain at which the stress dropped to 10 percent of the peak value. If the descending portion of the curve was unstable, the upper limit of strain was the point where the instability began. This is the point at which the record terminates in Figs. 3 and 4.

The results of analysis according to this criterion of ductility of concrete are provided in Table 1. The ductility ratio of the conventional concretes averaged approximately 1.7. In contrast, that of the low porosity concretes averaged only about 0.5. There was little apparent difference between the BD and the IWA conventional concretes, and also little to distinguish the flyash-bearing LPF concrete from the low porosity concrete without flyash.





#### 7.4.5 Relationship Between Strength and Brittleness

Fig. 7.4.5 indicates the relationship between the ductility ratio and the strength level for the eight specimens tested in this study. A reasonable linear fit is obtained by the usual least squares procedure, the correlation coefficient being -0.951. The line of best fit intercepts the strength axis at almost exactly 100 MPa (14,550 psi), this being the "intrinsic limit" (6), the strength level at which the concrete would be expected to be "perfectly brittle", i.e., have a completely vertical descending branch.

Failure behavior of high strength concrete is strongly conditioned by the nature of the aggregate, since the mode of failure involves direct crack propagation through the aggregate rather than around it as is the case with normal strength concretes. Thus, so-called "intrinsic limit" should not be considered a universal limiting value, but one restricted to concretes with coarse aggregate similar to the limestone aggregate used in the present concrete. Indeed, the intrinsic limit value reported by Naaman (6) for concrete made with calcareous aggregate is 105 MPa, in quite good agreement with the 100 MPa estimate from Fig. 7.4.5.

### 7.5 DISCUSSION

It appears that low porosity concrete, made with or without flyash, is a high-strength material with significantly brittle intrinsic character. For the concretes tested, maximum load is reached at strains of approximately  $2,700 \times 10^{-6}$ ; the descending branch is short and steep, but not quite vertical.

This is precisely the behavior expected from any high-strength concrete. Furthermore, the concordance between the estimated "intrinsic limit" of strength found here for low porosity concrete with limestone aggregate and that found by Naaman (1) for high-strength conventional Portland cement



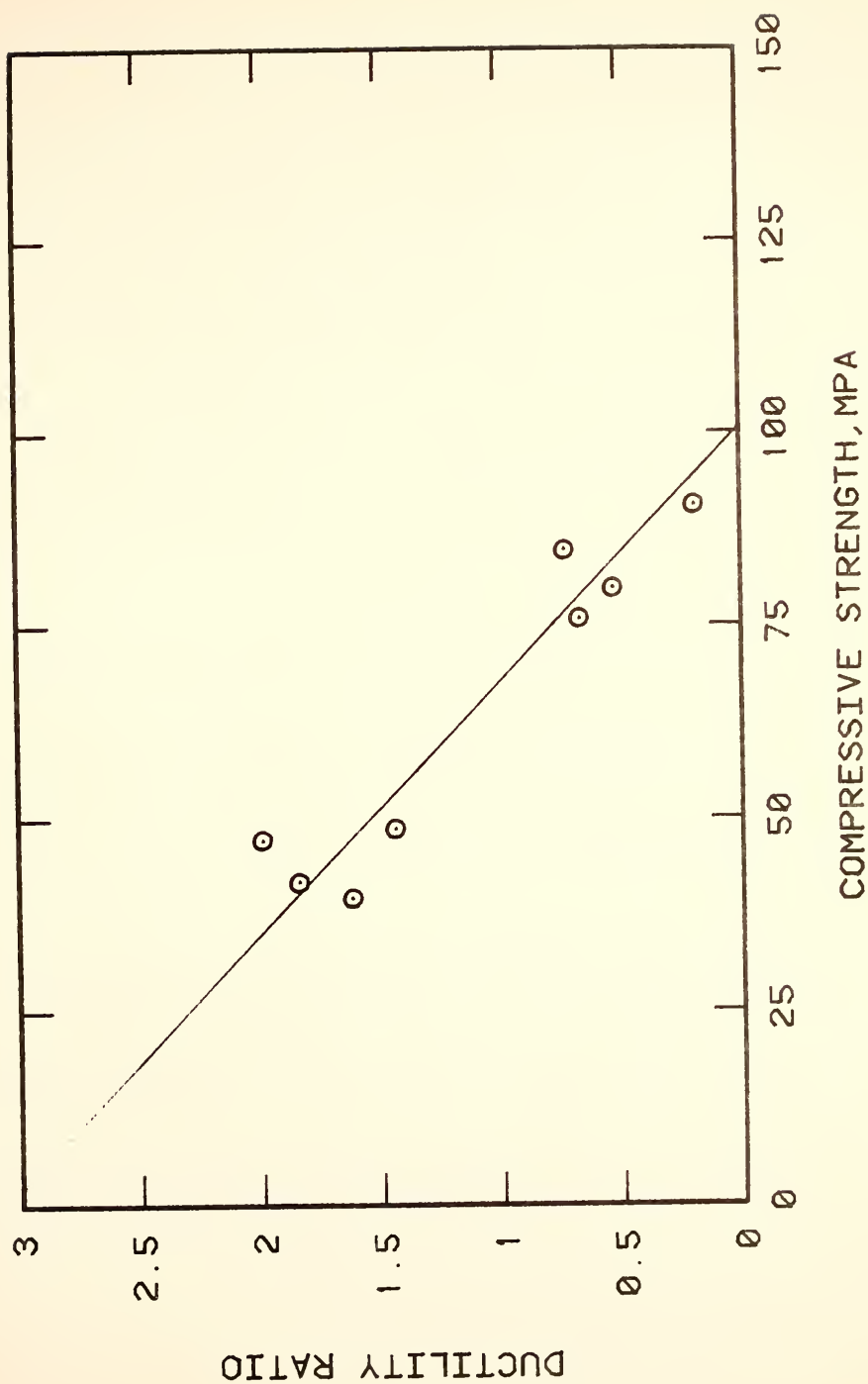


Fig. 7.4.5. Linear Regression Between Ductility Ratio and Compressive Strength



concrete with limestone aggregate suggests that low porosity concrete behaves exactly as would be expected for any concrete of equivalent strength level made with the same kind of aggregate.

A reasonable implication from this finding is that the experimental results and analyses of Tognon, Ursella, and Copetti (5) for the ductility of reinforced high-strength concretes should apply to reinforced low porosity concrete as well. Thus, properly reinforced low porosity concrete bridge decks may be expected to have as great or greater ductility under extreme deformation as decks made from conventional reinforced concrete, despite the brittle behavior of the low porosity concrete itself.

## 7.6 REFERENCES

1. Proc. Workshop on High Strength Concrete, Dec. 1979, S. P. Shah, ed., 226 pp. Univ. of Illinois at Chicago Circle (1980).
2. A. H. Nilson and F. O. Slate, "Properties of Very High Strength Concrete," Second Progress Report, Department of Structural Engineering, Cornell Univ., Ithaca, N.Y., 62 pp. (1979).
3. P. T. Wang, S. P. Shah, and A. E. Naaman, "Stress-Strain Curves of Normal and Lightweight Concrete in Compression," J. Amer. Concr. Inst. 75 (11) 603-611 (1978).
4. S. Ahmad and S. P. Shah, "Compressive Stress-Strain Curve of Concrete and Nonlinear Design," Proc. CSCE-ASCE-ACI-CIB Intl. Symp. on Nonlinear Design of Concrete Structures, Univ. of Waterloo, Ontario, Canada (1979).
5. G. Tognon, P. Ursella, and G. Copetti, "Design and Properties of Concretes with Strength Over 1500 kgf/cm<sup>2</sup>," J. Amer. Concr. Inst. 77 (3) 171-178 (1980).
6. A. E. Naaman, "Structural Design Considerations for High Strength Concrete," in Proc. Workshop on High Strength Concrete, S. P. Shah, ed., Univ. of Illinois at Chicago Circle, 194-216 (1980).



PART EIGHT  
COST COMPARISONS





## 8.1 INTRODUCTION

In this section an attempt is made to provide a potential cost comparison between conventional bridge deck concrete and the low porosity concrete formulations with and without flyash that have been the subjects of the testing program.

As in any economic formulation, costs must be expected to vary with time, especially in a prevailing inflationary period. Costs of engineering materials are also unusually sensitive to the specific location contemplated, since transportation costs form so large a proportion of the whole. The estimates provided here are for mid-1982, and the location contemplated is central Indiana.

In this comparison current costs of Portland cement, crushed limestone coarse aggregate, natural sand air-entraining agent were estimated with the assistance of a local concrete supplier. These individual concrete component costs were then applied to the normal bridge deck (BD) mix design formulation used throughout this study. The difference between the estimated delivered cost of ready-mix bridge deck concrete as estimated by the supplier and the cost of the components was allocated to costs of mixing, transportation, administration (including labor), and profit.



In calculating the estimated costs of the two low porosity concrete formulations the same approach was used. The individual costs of the components were tallied and added, and the same allowance was made for the mixing, transportation, administration, and profit costs. In these calculations the cost of the sulfonated lignin admixture was estimated at \$0.50 per lb., which is thought, after consultation with the Westvaco Corporation, to be a reasonably conservative figure. The actual cost would depend on the size of the potential market, and might be somewhat lower than the assumed figure if a large enough market were developed. The cost of the sodium bicarbonate, \$0.16 per lb., is taken from a current issue of the Chemical Market Reporter.



## 8.2 COST ESTIMATES

### 8.2.1 Conventional Bridge Deck Concrete (BD)

The mix design for this material as given, for example, in Table 4.1.1 involves a cement factor of 6.3 bags/cu. yd. and weight ratios of cement:coarse aggregate:sand of 1.0:3.0:2.1. Expressed on a tons per cubic yard basis, the quantities are: portland cement-0.296 tons, coarse aggregate-0.888 tons, and sand-0.622 tons. Six ounces (0.047 gal.) of air-entraining agent would normally be used. The individual materials cost estimates for these concrete components are provided in Table 8.2.1. In this table we have included the estimated delivered price of the concrete (\$50.00), with the difference between the total materials costs and the delivered price allocated to mixing, transportation, administration, and profit. The total cost of the materials is seen to be \$22.94 per cubic yard of concrete, leaving an estimate of \$27.06 for the non-material costs.

### 8.2.2 Flyash-Bearing Low Porosity Concrete (LPF)

The mix design for this type of concrete, also provided in Table 4.1.1 calls for a ground clinker factor of 7.6 bags/cu.yd. supplemented by a flyash factor equivalent to 3.0 bags/cu.yd. The weight ratios of ground clinker:coarse aggregate:sand are 1.0:1.8:1.2. The low porosity admixtures used are REAX LP sulfonated lignin at 0.7% of



Table 8.2.1 Cost Calculations for Conventional BD Concrete

<u>Item</u>	<u>Content per Cu. Yd.</u>	<u>Cost per Unit</u>	<u>Cost per Cu. Yd.</u>
Portland cement	0.296 tons	\$50.00 per ton	\$14.80
Coarse aggregate	0.888 tons	\$ 6.50 per ton	\$ 5.77
Sand	0.622 tons	\$ 3.50 per ton	\$ 2.18
Air-entraining agent	0.047 gal.	\$ 4.00 per gal.	\$ 0.19
<hr/>			
Total materials			\$22.94
<hr/>			
Estimated delivered cost of concrete			<div style="border: 1px solid black; padding: 2px;">\$50.00</div>
<hr/>			
Allocation for costs of mixing, transportation, administration, and profit			\$27.06
<hr/>			





the combined weight of ground clinker and flyash, and sodium bicarbonate at 1.2% of that combined weight.

The individual materials contents are recalculated on a tons per cubic yard basis (or lbs. per cubic yard for the admixtures), and cost estimate calculations are provided in Table 8.2.2

In these calculations the cost of the ground clinker is assumed to be the same as that of Portland cement. This is a reasonable assumption for routine production costs, since the extra cost of the finer grinding required would be offset by the savings stemming from the absence of gypsum normally interground with the clinker. Gypsum is substantially more expensive than the ground clinker component of portland cement.

The results of the calculations show that the total materials cost for the flyash-bearing low porosity concrete is \$30.26 per cu. yd., as compared to \$22.94 for the BD concrete. When the allowance for non-material costs is added, the estimated delivered cost of the LPF concrete is \$57.70 per cu. yd., which is 15% higher than the corresponding figure for BD concrete.

### 8.2.3 Low Porosity Concrete Without Flyash (LPN)

The usual mix design for this type of concrete, as provided also in Table 4.1.1 calls for a ground clinker factor of 10.1 bags/cu. yd., although smaller factors have been used successfully. The ground clinker:coarse aggregate:sand ratio is 1.0:1.8:1.2, and the admixture dosages are



Table 8.2.2 Cost Calculations for Flyash-Bearing Low Porosity Concrete (LPF)

<u>Item</u>	<u>Content per Cu. Yd.</u>	<u>Cost per Unit</u>	<u>Cost per Cu. Yd.</u>
Ground Clinker	0.357 tons	\$50.00 per ton	\$17.85
Flyash	0.141 tons	\$12.00 per ton	\$ 1.69
Coarse aggregate	0.643 tons	\$ 6.50 per ton	\$ 4.18
Sand	0.428 tons	\$ 3.50 per ton	\$ 1.50
Sulfonated lignin	7.0 lbs.	\$ 0.50 per lb.	\$ 3.50
Sodium bicarbonate	12.0 lbs.	\$ 0.16 per lb.	\$ 1.92
<hr/>			
Total materials			\$30.64
<hr/>			
Mixing, transportation, administrative, and profit*			\$27.06
<hr/>			
Estimated delivered cost of concrete			\$57.70
<hr/>			

\*Assumed to be the same as that for conventional BD concrete as calculated in Table 8.2.1.



0.7% of the weight of the ground clinker for the sulfonated lignin and 1.2% for the sodium bicarbonate. The calculations for the contents of individual components per cubic yard and the cost estimate calculations stemming from them are provided in Table 8.2.3.

The results of the calculations show that the total materials cost for the low porosity concrete without flyash is \$36.43 per cu. yd., the most expensive of the alternatives. Nevertheless even for this concrete, adding the allowance for non-material costs brings the estimated total delivered cost of the concrete to only \$63.49 per cu. yd., a value only 27% higher than that of the conventional concrete.



Table 8.2.3 Cost Calculations Low Porosity Concrete  
Without Flyash (LPN)

<u>Item</u>	<u>Content per Cu. Yd.</u>	<u>Cost per Unit</u>	<u>Cost per Cu. Yd.</u>
Ground clinker	0.475 tons	\$50.00 per ton	\$23.75
Coarse aggregate	0.855 tons	\$ 6.50 per ton	\$ 5.56
Sand	0.570 tons	\$ 3.50 per ton	\$ 2.00
Sulfonated lignin	6.6 lbs.	\$ 0.50 per lb.	\$ 3.30
Sodium bicarbonate	11.4 lbs.	\$ 0.16 per lb.	\$ 1.82
<hr/>			
Total materials			\$36.43
<hr/>			
Mixing, transportation, administrative, and profit*			\$27.06
<hr/>			
Estimated delivered cost of concrete			\$63.49
<hr/>			

\*Assumed to be the same as that for conventional BD  
concrete as calculated in Table 8.2.1.





### 8.3 EVALUATION OF COST COMPARISONS

The preceding sections have indicated that the total delivered costs of concrete to a bridge deck site in central Indiana in mid-1982 would be \$50.00 per cu. yd. for conventional bridge deck concrete, \$57.70 per cu. yd. for flyash-bearing low porosity concrete, and \$63.49 per cu. yd. for low porosity concrete without flyash.

On the basis of technical factors, primarily workability and delay of slump loss, the flyash bearing formulation would be a clearly superior choice to the unmodified low porosity concrete. Use of this formulation would thus involve a 15% increase in cost of the delivered concrete.

Balanced against this, even on an initial cost basis, is the likelihood of more efficient production and thus lower cost in the operations of placing, compacting, and finishing the flyash-bearing low porosity concrete. The high initial slump, the flowing character, and the essentially self-consolidating characteristics of this material should provide considerable economy in the difficult job of placing the concrete around the relatively closely spaced steel reinforcement elements usual in bridge decks, and the finishing characteristics are excellent. Thus much of the extra cost of the delivered concrete might be made up in the processes of placing and finishing the material.



It should be borne in mind that the comparisons here are initial-cost comparisons. While no attempt has been made to estimate life-cycle cost comparisons, it is clear that the vastly increased service life to be expected from the low porosity formulation far outweighs whatever modest initial cost disadvantage it might show in practice.

One caution must be specifically mentioned, however. The low porosity concrete formulation has as its major component ground portland cement clinker, without the gypsum normally interground with it in the manufacture of portland cement. While every cement plant in the world is capable of producing such material, it is not presently an article of commerce. Thus special arrangements need to be made to procure a supply of such ground clinker adequate to any given project contemplated. The cost comparisons due not include any allowance for extra cost attendant on making such special arrangements, and indeed such extra costs cannot easily be estimated. It is reasonable to assume that should use of low porosity concrete become an accepted practice, manufacture and sale of non-gypsum-bearing ground clinker would develop on the same basis and essentially at the same cost as that of portland cement.



PART NINE

TECHNICAL FINDINGS, CONCLUSIONS,  
AND RECOMMENDATION



## 9.1 TECHNICAL FINDINGS

In view of the large amount of detailed information presented in this study, individual sections labelled "Results and Discussion" have been appended to sections of each part of the report. The reader is directed to these individual sections for detailed statements of individual findings.

In general, the findings of this study were as follows:

- (i) Low porosity cements (type I clinker ground without gypsum) of finenesses of 3200, 4500 and 5400  $\text{cm}^2/\text{g}$  Blaine, all produced pastes and concretes of similar rheological properties in the fresh state when mixed with low porosity admixture ( $\text{NaHCO}_3$  plus lignosulfonate). The pastes were all of the "flowing" type even when mixed at water:cement ratio as low as 0.20. The concretes all had high slumps (6-10 in.) using water:cement ratios in the range of 0.24 to 0.30. The relatively coarser ground cements performed quite well in the portions of the study in which they were used, including the corrosion studies. It appears that LP cement of fineness between 3200-4000  $\text{cm}^2/\text{g}$  can be used for low porosity concrete without difficulty.





- (ii) Low porosity concrete mixes without flyash produced high slump concrete when mixed at water:cement ratios in the range of 0.24 to 0.30, but despite the high slump, the fresh concretes were hard to work with. In general, such concrete had a short working life of about 60 minutes or less. It was difficult to entrain air in this type of concrete even when large doses of an air entraining agent were used. The fresh concrete had a high unit weight, about 155 lb/ft<sup>3</sup>. The hardened concrete had excellent durability properties, specifically, good resistance to carbonation, low permeability, low porosity, high compressive strength, and high resistance of embedded steel to corrosion. However, attempted usage of an air-entraining agent resulted in severe scaling problems.
- (iii) Low porosity concrete batched with a high-calcium fly ash in the proportion of 35%, by weight of the cement, showed much better fresh concrete properties. Specifically, the working life of such concrete was prolonged to about 2 hours, and the concrete was much more easily workable. The desirable high slump at low water content feature of the low porosity concrete was retained for these concretes as well. These concretes entrained a suitable amount of air, 5% to 8% depending on the amount of sodium lignosulfonate used, without added air entraining agent. Fly



ash incorporation reduced the unit weight to about 160 lb/ft<sup>3</sup>, still a unit weight higher than most conventional concretes. These hardened concretes had durability properties quite similar to those of low porosity concrete without fly ash. The compressive strengths were slightly lower than for non-fly ash-bearing low porosity concretes, but they were still much higher than those of the conventional concretes. Some slight loss in weight and some damage to the physical appearance occurred for fly ash-bearing low porosity concrete specimens in the extended freeze-thaw test. In contrast, the low porosity concrete without fly ash showed no damage to the physical appearance, and even recorded weight gain.

For both formulations, a problem may arise from the fresh concrete when concrete slumps higher than 6 in. are placed on slopes about 5° or more (i.e., about 1 in. to 1 foot) in that the fresh concrete tended to flow out of the forms.

- (iv) Conventional concrete formulations were distinctly inferior in most measured characteristics to the low porosity concretes tested. In general, the dense Iowa mixes performed much better in an all-round evaluation than the concrete mixes representing normal bridge deck concrete except in the shrinkage characteristics studies where both performed about



the same. Specifically, a number of the difficulties that give rise to deterioration of concrete bridge decks were found to be severe with the conventional bridge deck concrete. For example, the rate of ingress of chloride ions into such concrete was the highest recorded and was high enough to rapidly initiate corrosion of embedded steel mats. Such concretes were found to have relatively high permeability and porosity, and relatively low compressive strength.

- (v) Some difficulties were found with the setting behavior of low porosity pastes in that prolonged set times were sometimes observed. This was never observed with low porosity concretes and should not be a practical problem. Addition of fly ash to the pastes removed any such difficulty with the pastes. From heat evolution studies it was found that the heat evolution maximum occurred much earlier when fly ash was added.
- (vi) The microstructure of mortar from the low porosity concretes was studied and was shown to be more compact than that of mortar from conventional concretes. Fly ash particles in low porosity concrete were found to be incompletely reacted and some hardly reacted, even after one year in the concrete.



## 9.2 CONCLUSIONS

From the results obtained in this study, the following conclusions have been drawn:

- (i) The current concrete mix design specified for bridge decks in Indiana, using a cement factor of 6 bags/cu. yd., is clearly inadequate to ensure durability of bridge decks under conditions of winter salting.
- (ii) Low porosity concrete is shown to have highly superior durability characteristics for such service. There may be a problem with a relatively short working time and the peculiar rheological character that renders the fresh concrete difficult to work with despite its high slump.
- (iii) The rheological behavior of low porosity concrete and the working time are very much improved by addition of fly ash in suitable proportion, without such addition interfering significantly with the highly superior durability and strength properties of low porosity concrete.
- (iv) Dense conventional concrete mixes patterned after those developed by the Iowa State DOT show considerable superiority to conventional bridge deck





concrete but are very much inferior to low porosity concretes in most measured characteristics.

- (v) One important characteristic of low porosity concretes is the high alkalinity of their pore solutions. This promotes excellent corrosion resistance of embedded steel. However, aggregates used in low porosity concretes must be tested to ensure lack of susceptibility to any potential alkali-aggregate reaction.
- (vi) Low porosity concrete, with or without flyash, is a much higher strength material than conventional concrete (10,000-13,000 psi as compared to 4,000-6,000 psi). In consequence, it is a brittle material and fails in the same brittle mode that other high strength concretes show. However, properly reinforced high strength concrete is actually more ductile than reinforced conventional concrete. In highway bridge decks sufficient reinforcement is usually present that brittle failure should not constitute a problem.
- (vii) Cost comparisons suggest that the delivered cost of flyash-bearing low porosity concrete would be about 15% higher than that of conventional concrete. Some or all of this premium may be recoverable in terms of decreased costs of placing, compacting, and finishing the concrete, since the low porosity concrete is of flowing character, is essentially self-compacting, and finishes easily. Low porosity concrete without flyash is somewhat more expensive, the cost estimate being about 27% higher than that of conventional concrete.



### 9.3 RECOMMENDATION AND PROPOSED FIELD TRIAL

It is clear from the great mass of evidence presented in this report that some form of low porosity concrete appears to be a possible solution to premature degradation of bridge decks.

The testing and study of the characteristics of low porosity concrete with and without flyash have shown the clear superiority of the flyash-bearing formulation in practical terms. The advantages of much better workability, delay of slump loss, and lower cost make it the obvious choice of the two for practical application, despite the slightly lower strengths developed. The differences in other durability characteristics were thought to be of minor importance, in view of the great superiority of both forms of the low porosity concrete over conventional bridge deck concrete and even over the Iowa dense concrete formulation.

It is thus recommended that initial field trials be carried out using the low porosity concrete formulation with flyash.

While the design and carrying out of such trials are beyond the scope of this project, the writers are very



much interested in seeing such field evaluations take place as the next logical step in the development process. In June 1982 the Indiana Department of Highways listed a proposal to include a field structure incorporating low porosity concrete as part of a study plan for "Long Term Evaluation of Selected Bridge Deck Protection Systems" as part of a NEEP 12 plan. If this project is approved informal collaboration and assistance will be provided to the Department of Highways throughout the evaluation project.



## BIBLIOGRAPHY





## BIBLIOGRAPHY

1. Lukyanova, O. I., Segalova, E. E. and Rehbinder, P. A. "The Effect of Hydrophilic Plastifier Additions on the Properties of Concentrated Suspensions", *Kolloid Zhurnal* 19, pp. 82-89, 1957.
2. Brunauer, S., "A Research Proposal for the Investigation of Hardened Portland Cement Pastes of Low Porosity", Division of Research, Clarkson College of Technology, Potsdam, New York, Dec. 1965.
3. Yudenfreund, M., Odler, I. and Brunauer, S., "Hardened Portland Cement Paste of Low Porosity", I. Materials and Experimental Methods. *Cement and Concrete Research*, Vol. 2, No. 3, pp. 313-330, 1972.
4. Yudenfreund, M., Skalny, J., Mikhail, R. and Brunauer, S., "Hardened Portland Cement Pastes of Low Porosity. II. Exploratory Studies Dimensional Changes", *Cement and Concrete Research*, Vol. 2, No. 3, pp. 331-348, 1972.
5. Odler, I., Yudenfreund, M., Skalny, J. and Brunauer, S., "Hardened Portland Cement Pastes of Low Porosity, III. Degree of Hydration. Expansion of Paste. Total Porosity", *Cement and Concrete Research*, Vol. 2, No. 4, pp. 463-480, 1972.
6. Odler, I., Hagymassy, J., Jr., Yudenfreund, M. and Brunauer, S., "Hardened Portland Cement Pastes of Low Porosity, IV. Surface Area and Pore Structure". *Cement and Concrete Research*, Vol. 2, No. 5, pp. 577-589, 1972.
7. Yudenfreund, M., Hanna, K., Skalny, J., Odler, I. and Brunauer, S., "Hardened Portland Cement Pastes of Low Porosity, V. Compressive Strength", *Cement and Concrete Research*, Vol. 2, No. 6, pp. 731-741, 1972.
8. Brunauer, S., Yudenfreund, M., Odler, I. and Skalny, J., "Hardened Portland Cement Pastes of Low Porosity, VI. Mechanism of the Hydration Process". *Cement and Concrete Research*, No. 3, No. 2, pp. 129-147, 1973.



9. Brunauer, S., Skalny, J., Odler, I. and Yudenfreund, M., "Hardened Portland Cement Pastes of Low Porosity, VII. Further Remarks about Early Hydration. Composition and Surface Area of Tobermonite Gel". Cement and Concrete Research, Vol. 3, No. 3, pp. 279-293, 1973.
10. Brunauer, S., U.S. Patent No. 3,689,294. Sept. 1972.
11. Stryker, J. L., U.S. Patent No. 3,959,004. May 26, 1976.
12. Ball, F. J., Braddon, D. V. and Stryker, L. J., U.S. Patent No. 3,960,582. June 1, 1976.
13. Wills, M. H., Jr. U.S. Patent No. 4,019,918. Apr. 26, 1977.
14. Skalny, J., Philips, J. C. and Cahn, D. S., "Low Water to Cement Ratio Concretes", Cement and Concrete Research, Vol. 3, No. 1, pp. 29-40, 1973.
15. Milestone, N. B., "The Effect of Lignosulfonate Fractions on the Hydration of Tricalcium Aluminate", Cement and Concrete Research, Vol. 6, No. 1, pp. 89-102, 1976.
16. Odler, I., Duckstein, V. and Becker, T., "On the Combined Effect of Water Solubles Lignosulfonates and Carbonates on Portland Cement and Clinker Pastes", I. Physical Properties", Cement and Concrete Research, Vol. 8, No. 4, pp. 469-480, 1978.
17. Odler, I., Schonfeld, R., and Dorr, H., "On the Combined Effect of Water Soluble Lignosulfonates and Carbonates on Portland Cement and Clinker Pastes - II. Mode of Action and Structure of the Hydration Products", Cement and Concrete Research, Vol. 8, No. 5, pp. 525-538, 1978.
18. Skalny, J. and Odler, I., "Use of Admixtures in Production of Low Porosity Pastes and Concretes", Transportation Research Records, Vol. 564, pp. 27-38, 1976.
19. Hanna, K. M., and Taha, A., "Rheological Properties of Low Porosity Cement Pastes", Zement-Kalk-Gips, Vol. 30, pp. 293-295, 1977 (in German).
20. Hanna, K. M., "Application of Experience With Low Porosity Cement Paste and Mortar", Zement-Kalk-Gips, Vol. 30, pp. 140-142, 1977 (in German).
21. Diamond, S. and Gomez-Toledo, C., "Studies on Cement Paste and Concrete Both Made with Low Porosity Cement",



Joint Highway Research Project, No. JHRP-77-10, July 1977.

22. Diamond, S. and Gomez-Toledo, C., "The Microstructure of Low Porosity Portland Cement Paste", *Il Cemento*, 75, 1978, pp. 189-194.
23. Diamond, S., "An Alternative to Gypsum Set Regulation for Portland Cements", *World Cement Technology*, pp. 116-121, April 1980.
24. Collepardi, M., Monosi, S. and Moriconi, G., "Combined Effect of Lignosulfonate and Carbonate on Pure Portland Clinker Compounds Hydration. I. Tetracalcium Alumino-ferrite Hydration". *Cement and Concrete Research*, Vol. 10, No. 3, pp. 455-462, 1980.
25. Škavára, F., Kolář, K., Novotný, J. and Zadák, Z., "Cement Pastes and Mortars with Low Water-to-Cement Ratio", *Cement and Concrete Research*, Vol. 10, No. 2, pp. 253-262, 1980.
26. Škvára, F., Zadák, Z., and Kolář, K., "Gypsum-Free Portland Cement", *Silikáty XXV*, pp. 251-261 (1981) (in Czech).
27. Lukjanova, O. I., Segalova, E. E. and Rehbinder, P. A., *Doklady Akad. Nauk. S.S.S.R.* 117, 1034 (1957).
28. Scripture, E. W., Jr., "Cement Dispersion and Concrete Quality", *Engineering News Record*, Vol. 127, pp. 82-85, Dec. 1941.
29. Powers, T. C., "Should Portland Cement be Dispersed?" *Proceedings of the American Concrete Institute*, Vol. 42, pp. 117-140, Nov. 1945.
30. Ernsberger, F. M., and Wesley, G. Rance, "Portland Cement Dispersion by Adsorption of Calcium Lignosulfonate", *Industrial and Engineering Chemistry*, Vol. 37, No. 6, pp. 598, June 1945.
31. Daimon, M. and Roy, D. M., "Rheological Properties of Cement Mixes: I. Methods, Preliminary Experiments, and Adsorption Studies", *Cement and Concrete Research*, Vol. 8, No. 6, pp. 753-764, 1978.
32. Škvára, F., Kolář, K., Novotný, J., Zadák, Z., and Bazantová, Z., "Hydraulic Binder Setting at Low Temperatures", *Silikáty XXIII*, pp. 217-231, 1979.



33. Arup, Hans, (Editor), "New Super-Strength Grout May Find Interesting Application in Fighting Corrosion" Steel in Concrete. Electrochemistry and Corrosion Newsletter. No. 7, January 1981, pp. 3-4.
34. Feature: "Concrete Overlays Cuts Paving Costs", Engineering News Record, pp. 40, December 1980.
35. Gowda, V. K., Shater, M. A. and Mikhail, R. Sh., "Corrosion of Steel Reinforcement Versus Pore Structure of the Paste Matrix", Cement and Concrete Reserach, Vol. 5, No. 2, pp. 99-102, 1975.
36. Cady, P. D., "Corrosion of Reinforcing Steel in Concrete - A General Overview of the Problem", Chloride Corrosion of Steel in Concrete, ASTM Publication STP 629, 1976, pp. 3-11.
37. Sanding, L. D., Highway Building, 42, pp. 16-17, Nov. 1974
38. Fontana, M. G. and Greene, N. D., "Corrosion Engineering", McGraw-Hill, New York, 1967.
39. Hausmann, D. A., "Steel Corrosion in Concrete", Materials Protection, pp. 19-23, Nov. 1967.
40. Clear, K. C., "Time-To-Corrosion of Reinforcing Steel in Concrete Slabs", Report No. FHWA-RH-76-70, April, Washington, D.C., 1976.
41. Stratful, R. F., Jurkovich, W. J., Spellman, D. L., "Corrosion Testing of Bridge Decks". Presented at the 54th Annual Meeting of the Transportation Research Board. Washington, D.C. 1975.
42. Clear, K. C., "Evaluation of Portland Cement Concrete for Permanent Bridge Deck Repair", Report No. FHWA-RD-74-5, Federal Highway Administration, Washington, D.C. 1974.
43. Kilareski, W. P., "Epoxy Coatings for Corrosion Protection of Reinforcement Steel", Chloride Corrosion of Steel in Concrete, ASTM Publication SPT 629, 1976, pp. 82-88.
44. GjØrv, O. E. and Vennesland, Ø., "Diffusion of Chloride ions from Seawater into Concretes", Cement and Concrete Research, Vol. 9, No. 2, pp. 229-238, 1979.
45. Manning, D. G. and Ryell, J., Durable Bridge Deck. Report RR 203. Ministry of Transportation and Communication Research and Development Division. Ontario, Canada 1976.





46. Peterson, P. C., "Concrete Bridge Deck Deterioration in Pennsylvania", Chloride Corrosion of Steel in Concrete, ASTM Publication SPT 629, pp. 61-68, 1976.
47. Carrier, R. E. and Cady, P. D., "Factors Affecting the Durability of Concrete Bridge Decks", Durability of Concrete, ACI Publication SP-47-7, 1975.
48. Neville, A. M., Properties of Concrete, Pittman Publishing Co., London, 1975.
49. Leber, I. and Blakey, F. A., "Some Effects of Carbon Dioxide on Mortars and Concrete", J. Amer. Concr. Inst. 53, pp. 295-308, Sept. 1956.
50. Berger, R. L., "Stabilization of Silicate Structures by Carbonation", Cement and Concrete Research, Vol. 9, No. 5, pp. 649-651, 1979.
51. Verbeck, G. J., "Carbonation of Hydrated Portland Cement", ASTM Sp. Tech. Publicn. No. 205, pp. 17-36, 1958.
52. Pihlajavaara, S. E. and Pihlman, E., "Effect of Carbonation on Microstructural Properties of Cement Stone", Cement and Concrete Research, Vol. 4, No. 2, pp. 149-154, 1974.
53. Litvan, G. G., "Frost Action in Cement in the Presence of De-icers", Cement and Concrete Research, Vol. 6, No. 3, pp. 351-356, 1976.
54. Dolch, W. L., Purdue University, Private Communication.
55. Diamond, S., Symposium on Alkali-Aggregate Reaction. Reykjavik, Aug. 1975.
56. Spellman, D. L. and Stratfull, R. F., "Laboratory Corrosion Test of Steel in Concrete Research, Report M & R 635116-3. Materials and Research Department. California Division of Highways, September, 1968.
57. Lankard, D. R., Slater, J. E., Hedden, W. A. and Niesz, D. E., "Neutralization of Chloride in Concrete", Report No. FHWA-RD-76-60, Federal Highway Administration, Washington, D.C. 1975.
58. Demonstration Project No. 33: Bridge Deck Evaluation Techniques. Federal Highway Administration, U.S. Department of Transportation, undated.
59. Clear, K. C., and Hay, R. E., "Time-To-Corrosion of Reinforcing Steel in Concrete Slabs", Vol. 1, Report FHWA-RD-73-32. Federal Highway Administration



U.S. Department of Transportation, 1973.

60. Berry, E. E. and Malhotra, V. M., "Fly Ash Use in Concrete - A Critical Review", ACI Journal Technical Paper Title No. 77-8, pp. 59-73, March-April 1980.
61. Pasko, T. J. and Larson, T. D., "Some Statistical Analysis of the Strength and Durability of Fly Ash Concrete", Proceedings, ASTM, V. 62, pp. 1054-1067, 1962.
62. Price, G. C., "Investigation of Concrete Materials for the South Saskatchewan River Dam", Proceedings, ASTM, V. 61, pp. 1155-1179, 1961.
63. Compton, F. R. and MacInnis, C., "Field Trial of Fly Ash Concrete", Ontario Hydro Research News (Toronto) Jan.-Mar. 1952, pp. 18-21.
64. Davis, R. E., Culson, R. W., Kelly, J. W. and Davis, H. E., "Properties of Cements and Concretes Containing Fly Ash", ACI Journal, Proceedings, V. 33, No. 5, May-June 1937, pp. 577-612.
65. Rehisi, S. S., "Studies on Indian Fly Ashes and Their Use in Structural Concrete", Proceedings, Third International Ash Utilization Symposium (Pittsburgh Mar. 1973). Information Circular I.C 8640 U.S. Bureau of Mines. Washington, D.C. pp. 231-243, 1973.
66. Elfert, R. J., "Bureau of Reclamation Experiences with Fly Ash and Other Pozzolanas in Concrete", Proceedings, Third International Ash Utilization Symposium (Pittsburgh Mar. 1973). I.C. 8640 U.S. Bureau of Mines, Washington, D.C. pp. 80-93, 1973.
67. Kovács, R. "Effects of the Hydration Products on the Properties of Fly Ash Cements", Cement and Concrete Research, Vol. 5, No. 1, pp. 73-82, 1975.
68. Ryan, J. R., "Relationship of Fly Ash and Corrosion", ACI Journal, Proceedings, V. 47, No. 6, Feb. 1951, pp. 481-484.
69. Larsen, T. J., McDaniel, W. H. Jr., Brown, R. P. and Sosa, J. L., "Corrosion-Inhibiting Properties of Portland and Portland-Pozzolan Cement Concrete", Transportation Research Record No. 613, pp. 21-29, 1976.
70. Washburn, E. W., "Note on a Method of Determining the Distribution of Pore Sizes in a Porous Material" Proc., National Academy of Sciences, Vol. 7, p. 115, 1921.



71. Gjølrv, O. E. and Loland, K. E., "Effect of Air on the Hydraulic Conductivity of Concrete", Report, Cement and Concrete Research Institute, Report No. STF. 65 A78010, Trondheim, Norway.
72. Robson, R. A., "Mobility of Water in Porous Media of High Surface Area", Rilem Symposium 1964 on Transfer of Water in Porous Media.
73. Davis, R. E., "Permeability and Triaxial Tests of Lean Mass Concrete", A Report to the Office, Chief of Engineers, Corps of Engineers, U.S. Army, Washington, D.C., April 1950.
74. Sweet, H., "Research on Concrete Durability as Affected by Coarse Aggregate", Proc. ASTM, Vol. 48, pp. 988, 1948.
75. Lea, F. M., "The Chemistry of Cement and Concrete, Third Edition, Chemical Publishing Company, New York 1970.
76. Smutzer, R.K., Indiana State Department of Highways, Materials Testing Division, Indianapolis, Private Communication, 1981.
77. Briston, R., Iowa Department of Transportation, Ames, Private Communication, 1981.
78. Clear, K. C. and Harrigan, E. T., "Sampling and Testing for Chloride Ions in Concrete", Report No. FHWA-RD-77-85, Federal Highway Administration, August 1977.
79. Berman, H. A., "Determination of Chloride in Hardened Portland Cement Paste, Mortar, and Concrete", Journal of Materials JMLSA Vol. 7, No. 3, September 1972, pp. 330-335.
80. Clemena, G. G., Reynolds, J. W. and McCormick, R., "Gran Method of Endpoint Determination of Chloride Analysis by Potentiometric Titration", Transportation Research Record 651, 1, 1977.
81. Ramachandran, V. S., Materiaux et Constructions, Vol. 4, No. 19, 1971, pp. 3-12 (NRC Canada Building Research Paper 483).
82. Ruettgers, A., Vidal, E. N. and Wing, S. P., "An Investigation of the Permeability of Mass Concrete With Particular Reference to Boulder Dam", Proc. ACI, Vol. 31, 1935, p. 382.



83. Tyler, I. L. and Erlin, B., "A Proposed Simple Test Method for Determining the Permeability of Concrete", Bulletin 133, Research and Developmental Laboratory Portland Cement Association, Chicago.
84. Diamond, S., Ravina, D. and Jovell, J., "The Occurrence of Duplex Films on Fly Ash Surfaces", Cement and Concrete Research, Vol. 10, No. 2, pp. 297-300, 1980.
85. Barnes, B. D., Diamond, S. and Dolch, W. L., "Hollow Steel Hydration of Cement Particles in Bulk Cement Paste", Cement and Concrete Research, Vol. 8, pp. 263-272, 1978.
86. Lewis, D. W., Dolch, W. L. and Woods, K. B., "Porosity Determinations and the Significance of Pore Characteristics of Aggregates", Proceedings, ASTM, V. 53, 1953, pp. 949-962.
87. Kaneuji, M., "Correlation Between Pore Size Distribution and Freeze Thaw Durability of Coarse Aggregate in Concrete", Ph.D. Thesis. Purdue University, 1978.
88. Cordon, W. A., Freezing and Thawing of Concrete - Mechanisms and Control, American Concrete Institute Monograph No. 3, 1966.
89. Guha, S. K. and Wedpathak, A. V., "The Practical Use of Ultrasonic Pulse Velocity Measurements in the Assessment of Concrete Quality", (Discussion on a paper published in Magazine of Concrete Research, Vol. 32, No. 110, March 1980) Magazine of Concrete Research, Vol. 33, No. 114, March 1981.
90. Barneyback, R. S., Jr. and Diamond, S., "Expression and Analysis of Pore Fluids from Hardened Cement Pastes and Mortars", Cement and Concrete Research, Vol. 11, pp. 279-285, 1981.





## APPENDIX



Table 1A Dynamic Modulus and Relative Dynamic Modulus at Different Freeze-Thaw Cycles using the Resonance Frequency Method.

Mix Designation	BD-6			BD-7			LPN-1			LPF-6			LPF-4		
Specimen No.	(1)	(2)	(3)	(1)	(2)	(3)	(1)	(2)	(3)	(1)	(2)	(3)	(1)	(2)	(3)
Elastic Modulus at 0 Cycles (10 <sup>6</sup> psi)	6.2	6.4	6.4	6.9	7.1	7.1	7.1	7.1	7.1	6.2	6.0	6.0	6.2	6.0	6.0
No. of Cycles															
0	100.0	100.0	100.0	100.0	100.0	100.0	100.0	100.0	100.0	100.0	100.0	100.0	100.0	100.0	100.0
32	96.0	95.8	99.3	98.7	91.3	93.1	101.0	101.2	101.1	101.6	102.8	98.4	91.8	92.1	92.1
89	99.3	95.5	95.0	95.5	94.2	94.4	98.3	99.5	100.0	101.2	104.0	104.0	90.8	99.4	99.4
114	99.1	93.7	101.0	94.4	99.0	96.2	118.0	116.2	118.1	101.8	99.5	101.2	97.7	96.2	96.2
142	86.5	86.3	103.0	93.0	99.6	94.9	113.6	120.5	124.0	101.4	98.4	99.6	96.1	93.3	93.3
182	96.2	88.8	101.3	95.5	97.7	88.9	112.0	119.3	120.5	97.7	96.6	98.1	93.0	97.0	97.0
219	94.4	83.7	99.7	94.0	93.0	88.4	108.2	115.4	119.4	98.8	100.4	100.0	92.3	93.7	93.7
287	92.6	88.8	98.5	90.2	90.0	85.1	101.2	111.7	117.0	94.4	97.1	93.6	91.0	92.2	92.2
364	86.6	87.3	95.5	86.9	86.0	73.3	90.3	110.7	116.2	95.5	94.2	94.2	91.0	92.5	92.5
404	87.2	82.4	96.6	86.3	83.1	61.4	66.5	99.6	114.3	94.2	95.3	93.8	90.5	89.8	89.8
476	76.6	79.5	97.3	84.8	62.0	55.7	56.9	87.4	109.0	91.0	90.2	90.1	88.7	90.0	90.0



Table 1-B continued

Mix Designation	LPN-2			LPN-3			IWA-1			ILL-1			BD-5*
Specimen No.	(1)	(2)	(3)	(1)	(2)	(3)	(1)	(2)	(3)	(1)	(2)	(3)	(1)
Elastic Modulus at 0 Cycles (10 <sup>6</sup> psi)	8.4	8.2	8.2	8.1	8.0	8.1	5.9	5.8	5.6	6.7	6.8	7.0	5.3
No. of Cycles	100.0	100.0	100.0	100.0	100.0	100.0	100.0	100.0	100.0	100.0	100.0	100.0	100.0
0	96.9	99.6	96.8	99.1	98.5	98.0	99.1	101.0	101.2	98.2	94.8	99.2	95.5
39	94.2	96.3	97.6	98.9	98.5	97.0	99.1	98.7	99.5	97.8	94.6	94.5	93.4
69	84.8	89.6	97.8	98.3	97.4	101.0	100.6	103.6	102.2	96.3	93.2	94.0	87.7
96	74.2	88.4	88.8	96.1	95.8	93.6	97.7	102.1	99.4	101.0	96.0	91.3	86.0
167	72.3	75.7	76.7	96.4	94.1	99.7	101.6	98.7	100.5	102.4	95.0	88.2	77.6
197	21.0	36.2	49.8	95.3	88.2	89.1	98.6	99.0	98.4	101.4	93.0	95.5	65.7
237	-	32.6	32.2	93.0	81.0	83.7	103.0	96.0	101.2	91.3	96.9	90.1	-
287	-	-	-	78.1	65.5	54.8	99.5	93.1	100.6	87.0	88.5	85.7	-
350	-	-	-	64.2	65.0	52.4	100.0	81.4	82.2	73.0	70.6	69.9	-
409													

\* 9 week's cured specimen, used as dummy



Table 1-C continued

Mix Designation	LPF-2		LPF-3					LPF-5			BD-6*	BD-5		
Specimen No.	(1)	(2)	(1)	(2)	(3)	(4)	(5)	(1)	(2)	(3)	(1)	(2)	(3)	
Elastic Modulus at 0 Cycles (10 <sup>6</sup> psi)	6.7	6.4	7.1	7.1	7.3	7.0	6.4	6.1	7.0	6.5	5.8	5.3	5.8	
<u>No. of Cycles</u>														
0	100.0	100.0	100.0	100.0	100.0	100.0	100.0	100.0	100.0	100.0	100.0	100.0	100.0	
41	95.4	97.5	94.1	91.3	89.2	96.2	99.0	103.0	91.5	99.4	106.1	87.0	94.0	
99	99.1	96.8	93.1	92.4	91.6	96.0	104.0	105.5	88.6	100.5	108.0	84.5	94.0	
158	95.7	95.4	87.5	96.1	94.0	92.8	100.6	112.5	95.0	99.1	111.5	77.3	84.6	
219	85.7	88.2	89.2	94.2	93.5	89.8	99.4	99.8	92.0	94.4	104.7	78.1	95.6	
276	89.2	93.3	89.6	91.4	92.5	86.1	102.3	103.2	91.8	98.3	103.6	77.6	92.0	
332	89.0	91.0	88.1	90.2	91.5	87.8	102.1	97.7	89.3	94.8	98.7	75.8	-	
413	85.8	89.6	84.8	89.1	90.8	86.3	101.4	96.8	89.3	94.9	107.0	69.2	-	

\* 6 week-old cured specimen used as dummy





Table 1-D continued

Mix Designation	LPF-7			LPF-8			LPF-9			BD-8		
Specimen No.	(1)	(2)	(3)	(4)	(1)	(2)	(3)	(4)	(1)	(2)	(3)	(4)
Elastic Modulus at 0 Cycles (10 <sup>6</sup> psi)	7.1	7.2	7.0	7.3	5.1	5.1	5.3	5.0	5.4	5.3	5.3	5.3
No. of Cycles												
0	100.0	100.0	100.0	100.0	100.0	100.0	100.0	100.0	100.0	100.0	100.0	100.0
35	103.0	100.3	102.1	99.0	102.4	101.9	102.2	100.4	102.2	99.6	100.0	101.0
92	103.0	100.6	101.2	99.4	101.8	101.2	102.2	101.2	101.1	101.2	100.5	100.4
165	100.0	105.4	100.5	99.5	101.3	98.7	101.9	102.0	102.1	100.3	99.3	98.2
211	103.0	102.2	100.5	99.7	101.6	97.8	101.0	99.6	101.2	101.4	98.1	96.8
263	105.0	102.0	100.1	97.0	100.0	98.0	-	100.1	-	101.0	98.2	94.4
323	102.0	100.5	100.0	97.0	99.3	96.3	99.0	100.0	98.5	97.4	98.2	93.8
363	101.0	101.6	101.1	97.5	98.1	99.3	97.0	98.8	96.1	99.0	97.7	86.2
422	101.0	101.0	104.8	97.4	98.1	98.1	99.2	100.0	96.8	98.4	-	-



Table 1-E continued

Mix Designation	LPN-12		LPN-10						LPN-11				LPF-17	
Specimen No.	(1)	(2)	(1)	(2)	(3)	(4)	(5)	(6)	(1)	(2)	(3)	(4)	(1)	(2)
Elastic Modulus at 0 Cycles (10 <sup>6</sup> psi)	7.8	8.1	7.2	7.5	7.1	7.2	7.3	7.3	8.0	7.7	7.8	8.1	6.6	6.6
No. of Cycles														
0	100.0	100.0	100.0	100.0	100.0	100.0	100.0	100.0	100.0	100.0	100.0	100.0	100.0	100.0
61	100.0	99.6	100.0	100.5	97.2	103.2	99.0	96.6	98.4	101.4	100.0	99.3	98.7	98.4
106	96.7	95.8	98.0	90.8	96.5	96.0	96.0	94.6	94.2	100.0	98.8	95.8	96.6	96.0
151	96.0	94.7	88.0	83.4	94.3	96.2	95.0	91.1	75.4	100.5	100.0	93.6	97.0	96.0
216	96.0	88.7	82.5	79.6	88.0	87.7	-	85.4	78.3	96.7	-	82.7	97.0	96.8
268	82.0	82.1	83.2	77.4	84.2	92.6	85.6	83.2	74.0	75.8	97.4	78.8	97.3	94.8
323	82.2	77.0	83.8	76.4	79.4	89.7	80.0	78.8	54.3	78.3	78.5	76.1	94.6	96.5
369	79.2	74.4	79.0	78.8	82.2	82.8	82.5	77.6	-	82.5	76.8	73.2	99.4	98.2
425	78.8	77.3	70.1	76.2	78.5	78.4	77.7	66.5	-	78.6	77.5	74.8	94.6	96.8



Table 2-A Weight and Relative Weight at Different Freeze-Thaw Cycles

Mix Designation	BD-6			BD-7			LPN-1			LPF-6			LPF-4		
Specimen No.	(1)	(2)	(3)	(1)	(2)	(3)	(1)	(2)	(3)	(1)	(2)	(3)	(1)	(2)	(3)
Wt. at 0 Cycles (lb.)	11.6	11.5	11.8	12.1	12.2	12.1	12.6	12.6	12.5	11.5	11.4	11.3	11.4	11.2	
<u>No. of Cycles</u>															
0	100.00	100.00	100.00	100.00	100.00	100.00	100.00	100.00	100.00	100.00	100.00	100.00	100.00	100.00	
32	100.10	100.10	100.19	100.00	100.07	100.09	100.00	100.04	100.09	99.90	99.91	100.00	100.00	100.00	
89	100.00	100.00	100.09	100.00	99.89	100.09	100.00	100.04	100.09	99.90	99.52	100.00	100.00	100.10	
114	99.90	100.00	100.09	99.91	99.80	99.82	100.09	100.04	100.18	99.90	99.03	99.90	99.90	100.00	
142	99.52	99.71	99.91	99.73	99.62	99.64	100.09	100.04	100.09	99.62	98.84	99.81	99.71	99.90	
182	99.24	99.43	99.81	99.45	99.35	99.24	100.09	100.04	100.09	99.58	98.74	99.61	99.61	99.90	
219	98.86	99.20	99.72	99.27	99.17	98.91	100.18	100.12	100.09	99.33	98.55	99.38	99.42	99.86	
255	98.48	98.47	99.44	99.09	98.89	98.36	100.09	100.04	100.14	99.00	98.45	98.93	99.13	99.71	
287	98.10	98.08	99.25	99.91	98.71	98.18	100.18	100.11	100.18	98.75	98.41	98.73	98.94	99.61	
331	97.52	97.70	99.06	98.27	98.35	97.45	100.18	100.12	100.18	98.46	98.26	98.34	98.74	99.51	
364	96.67	96.93	98.59	97.63	97.72	96.73	100.18	100.21	100.18	97.88	97.87	97.76	98.35	98.92	
404	95.52	96.55	98.31	97.26	97.35	96.00	100.26	100.21	100.18	97.50	97.67	97.47	98.06	98.63	
476	92.00	95.40	97.65	96.44	95.99	94.73	100.18	100.21	100.18	96.92	96.90	97.17	97.48	97.10	



Table 2-B continued

Mix Designation	LPN-2			LPN-3			IWA-1			ILL-1			BD-5
Specimen No.	(1)	(2)	(3)	(1)	(2)	(3)	(1)	(2)	(3)	(1)	(2)	(3)	(1)
Wt. at 0 Cycles (lb.)	12.6	12.6	12.5	12.5	12.4	12.5	11.5	11.4	11.2	12.0	11.9	12.1	10.9
<u>No. of Cycles</u>													
0	100.00	100.00	100.00	100.00	100.00	100.00	100.00	100.00	100.00	100.00	100.00	100.00	100.00
39	99.95	99.86	99.96	100.04	99.82	99.82	100.00	100.00	100.00	99.94	99.87	100.00	99.80
69	99.95	99.86	99.96	100.04	99.82	99.74	99.90	100.00	100.00	99.94	99.87	100.00	99.80
96	99.95	99.86	99.96	100.04	99.91	99.74	99.90	100.00	100.00	99.85	99.78	99.82	99.70
167	100.09	99.95	100.14	100.04	99.91	99.74	99.62	99.61	99.80	99.49	99.22	99.73	98.89
197	100.17	100.12	100.14	100.12	100.00	99.82	99.62	99.52	99.51	99.03	99.13	99.36	98.48
237	100.26	100.04	100.23	100.04	100.00	99.82	99.24	99.03	99.12	98.57	98.85	98.98	96.46
287	100.35	100.12	100.32	100.12	100.18	99.82	98.95	98.75	98.82	98.29	98.11	97.99	-
350	-	-	-	100.21	100.18	99.91	98.38	98.07	98.33	97.74	97.74	97.17	-
409	-	-	-	100.21	100.09	99.91	97.99	97.39	97.75	97.29	97.19	96.53	-





Table 2-C continued

Mix Designation	LPF-2		LPF-3					LPF-5			BD-6	BD-5		
Specimen No.	(1)	(2)	(1)	(2)	(3)	(4)	(5)	(1)	(2)	(3)	(1)	(1)	(2)	(3)
Wt. at 0 Cycles (lb.)	11.5	11.5	11.6	11.7	11.8	11.7	11.8	11.3	11.5	11.6	11.8	10.9	10.9	10.9
<u>No. of Cycles</u>														
0	100.00	100.00	100.00	100.00	100.00	100.00	100.00	100.00	100.00	100.00	100.00	100.00	100.00	100.00
41	100.00	99.90	100.00	100.00	100.99	100.00	100.00	100.00	100.00	100.00	100.09	100.00	99.90	99.86
99	99.56	99.13	99.62	99.72	99.81	99.72	99.81	99.75	99.81	99.85	99.43	99.76	98.89	99.35
158	98.90	98.85	99.53	99.72	99.81	99.62	99.81	99.75	99.71	99.85	99.34	98.04	98.79	98.14
219	98.52	98.56	99.24	99.72	99.72	99.44	99.53	99.55	99.81	99.56	99.15	97.93	98.69	97.33
276	98.04	98.27	99.05	99.62	99.63	99.34	99.34	99.45	99.43	99.47	98.96	97.53	98.59	96.22
332	97.26	97.86	98.84	99.47	99.42	99.00	99.86	99.14	99.08	98.92	98.42	96.64	98.16	95.19
413	96.67	97.44	98.41	99.36	99.25	98.70	98.69	98.87	98.83	98.33	98.21	95.44	-	-



Table 2-D continued

Mix Designation	LPF-7				LPF-8				LPF-9			BD-8		
Specimen No.	(1)	(2)	(3)	(4)	(1)	(2)	(3)	(4)	(1)	(2)	(3)	(1)	(2)	(3)
Wt. at 0 Cycles (lb.)	12.3	12.2	12.1	12.3	11.0	11.1	11.3	10.9	11.4	11.3	11.4	11.3	11.2	11.2
<u>No. of Cycles</u>														
0	100.00	100.00	100.00	100.00	100.00	100.00	100.00	100.00	100.00	100.00	100.00	100.00	100.00	100.00
35	100.13	100.11	100.18	100.13	100.26	100.26	100.19	100.30	100.21	100.25	100.21	100.37	100.31	100.29
92	100.04	99.91	100.02	99.89	100.08	99.70	100.19	99.82	99.61	99.90	100.12	100.23	99.80	100.04
165	100.04	99.82	100.15	99.95	99.78	99.98	99.96	100.02	100.06	100.04	99.77	99.96	99.69	99.71
211	100.04	99.95	99.98	100.02	99.86	99.84	99.96	99.88	100.02	100.14	99.94	99.86	99.37	99.67
263	100.04	99.75	99.85	99.95	99.48	99.40	99.55	99.72	99.75	100.10	99.67	99.38	98.80	98.92
323	99.82	99.57	99.65	99.73	99.18	98.93	99.55	99.38	99.21	99.16	99.36	98.63	98.21	97.74
363	100.13	100.20	100.13	100.09	98.76	99.01	99.28	99.26	99.32	99.84	99.15	98.13	97.61	96.46
422	100.13	100.20	100.04	100.00	98.76	99.01	99.22	99.15	99.32	99.84	98.76	97.83	97.21	94.41



Table 2-E continued

Mix Designation	LPN-12		LPN-10						LPN-11				LPF-17	
Specimen No.	(1)	(2)	(1)	(2)	(3)	(4)	(5)	(6)	(1)	(2)	(3)	(4)	(1)	(2)
Wt. at 0 Cycles (1b.)	12.5	12.7	12.3	12.2	12.1	12.3	12.3	12.2	12.5	12.6	12.5	12.5	11.9	11.9
No. of Cycles														
0	100.00	100.00	100.00	100.00	100.00	100.00	100.00	100.00	100.00	100.00	100.00	100.00	100.00	100.00
61	100.13	100.13	100.25	100.24	100.16	100.25	100.20	100.27	100.18	100.16	100.14	100.12	100.17	100.15
106	100.14	100.16	100.34	100.27	100.16	100.23	100.22	100.31	100.28	100.14	100.18	100.14	100.17	100.15
151	100.23	100.26	100.52	100.38	100.22	100.32	100.29	100.40	100.41	100.18	100.23	100.19	100.17	100.13
216	100.32	100.30	100.50	100.42	100.22	100.40	100.16	100.38	100.44	100.23	100.28	100.28	100.15	100.13
268	100.32	100.33	100.47	100.34	100.15	100.36	100.05	100.34	100.49	100.25	100.28	100.28	100.15	100.07
323	100.34	100.38	100.38	100.24	99.93	100.32	99.96	100.24	100.46	100.26	100.28	100.28	100.17	100.02
369	100.35	100.38	100.31	100.18	99.80	100.29	99.80	100.16	100.49	100.28	100.28	100.32	100.17	99.96
425	100.37	100.38	100.05	99.96	99.67	100.14	99.59	100.07	100.46	100.32	100.25	100.34	100.11	99.94





COVER DESIGN BY ALDO GIORGINI